Deciphering CXCR4 and ACKR3 interactomes reveals an influence of ACKR3 upon Gap junctional intercellular communication

Amos Fumagalli

THÈSE POUR OBTENIR LE GRADE DE DOCTEUR DE L'UNIVERSITÉ DE MONTPELLIER

En Biologie Santé

École doctorale École doctorale Sciences Chimiques et Biologiques pour la Santé (CBS2)

Unité de recherche Institut de Génomique Fonctionnelle (IGF)

Deciphering CXCR4 and ACKR3 interactomes reveals an influence of ACKR3 upon Gap Junctional Intercellular Communication

Présentée par Amos FUMAGALLI

Le 22 Novembre 2018

Sous la direction de Philippe MARIN et Séverine CHAUMONT-DUBEL

Devant le jury composé de

Gwendal LAZENNEC, Directeur de Recherches, Sys2Diag, Montpellier	Président
Christian GIAUME, Directeur de Recherches, CIRB, Paris	Rapporteur
Marc MESNIL, Professeur des Universités, STIM, Poitiers	Rapporteur
Eric REITER, Directeur de Recherches, BIOS, Nouzilly	Examinateur
Jean-Luc GALZI, Directeur de Recherches, BSC, Illkirch	Examinateur
Philippe MARIN, Directeur de Recherches, IGF, Montpellier	Directeur de thèse
Séverine CHAUMONT-DUBEL, Maitre de Conférences, IGF, Montpellier	Co-directeur de thèse

UNIVERSITÉ DE MONTPELLIER

to my family and zia Nives

SUMMARY

The Atypical Chemokine Receptor 3 (ACKR3) and CXCR4 are two G protein-coupled receptors (GPCR) belonging to the CXC chemokine receptor family. Both receptors are activated upon CXCL12 binding and are over-expressed in various tumours, including glioma, where they have been found to promote proliferation and invasive behaviours. Upon CXCL12 binding, CXCR4 activates canonical GPCR signalling pathways involving $G\alpha_i$ protein and β-arrestins. In addition, CXCR4 was found to interact with several proteins able to modify its signalling, trafficking and localization. In contrast, the cellular pathways underlying ACKR3-dependent effects remain poorly characterized. Several reports show that ACKR3 engages β-arrestin-dependent signalling pathways, but its coupling to G proteins is restricted to either specific cellular populations, including astrocytes, or occurs indirectly *via* its interaction with CXCR4. ACKR3 also associates with the epidermal growth factor receptor to promote proliferation of tumour cells in an agonist-independent manner. These examples suggest that the extensive characterization of ACKR3 and CXCR4 interactomes might be a key step in understanding or clarifying their roles in physiological and pathological contexts. This thesis addressed this issue employing an affinity purification coupled to high-resolution mass spectrometry proteomic strategy that identified 19 and 151 potential protein partners of CXCR4 and ACKR3 transiently expressed in HEK-293T cells, respectively. Amongst ACKR3 interacting proteins identified, we paid particular attention on the gap junction protein Connexin-43 (Cx43), in line with its overlapping roles with the receptor in the control of leukocyte entry into the brain, interneuron migration and glioma progression. Western blotting and BRET confirmed the specific association of Cx43 with ACKR3 compared to CXCR4. Likewise, Cx43 is co-localized with ACKR3 but not CXCR4 in glioma initiating cell lines, and ACKR3 and Cx43 are co-expressed in astrocytes of the sub-ventricular zone and surrounding blood vessels in adult mouse brain, suggesting that both proteins form a complex in authentic cell or tissue contexts. Further functional studies showed that ACKR3 influences Cx43 trafficking and functionality at multiple levels. Transient expression of ACKR3 in HEK-293T cells to mimic ACKR3 overexpression detected in several cancer types, induces Gap Junctional Intercellular Communication (GJIC) inhibition in an agonist-independent manner. In addition, agonist stimulation of endogenously expressed ACKR3 in primary cultured astrocytes inhibits Cx43-mediated GJIC through a mechanism that requires activation of $G\alpha_i$ protein, and dynamin- and β-arrestin2-dependent Cx43 internalisation. Therefore, this thesis work provides the first functional link between the CXCL11/CXCL12/ACKR3 axis and gap junctions that might underlie their critical role in glioma progression.

Key words: chemokine, ACKR3, interactome, Connexin 43, Gap Junction, glial cell.

RÉSUMÉ

Le récepteur atypique ACKR3 et le récepteur CXCR4 sont des récepteurs couplés aux protéines G appartenant à la famille des récepteurs CXC des chimiokines. Ces deux récepteurs sont activés par la chimiokine CXCL12 et sont surexprimés dans de nombreux cancers comme les gliomes, dont ils favorisent la prolifération et le caractère invasif. Le récepteur CXCR4 active des voies de signalisation qui dépendent de la protéine Gi et des β-arrestines et s'associe à plusieurs protéines impliquées dans la transduction du signal, le trafic et la localisation cellulaire du récepteur. Par contre, les mécanismes de signalisation impliqués dans les effets d'ACKR3 restent mal connus. Le récepteur déclenche une signalisation dépendant des β-arrestines, mais son couplage aux protéines G dépend du type cellulaire ou se fait par un mécanisme indirect *via* son association au récepteur CXCR4. Le récepteur ACKR3 s'associe également au récepteur de l'EGF pour induire la prolifération cellulaire par un mécanisme indépendant de sa stimulation par un agoniste. Ces données illustrent l'intérêt de caractériser de façon systématique l'interactome de ces récepteurs pour comprendre leurs rôles physiologiques et pathologiques. Cette thèse a poursuivi cet objectif grâce à la mise en œuvre d'une approche protéomique combinant la purification des partenaires des deux récepteurs par affinité suivie de leur identification par spectrométrie de masse. J'ai ainsi identifié respectivement 19 et 151 partenaires protéiques potentiels des récepteurs CXCR4 et ACKR3 exprimés dans les cellules HEK-293T. Parmi les protéines recrutées par ACKR3, nous nous sommes focalisés sur la connexine 43 (Cx43, une des protéines constituant les jonctions Gap) du fait de la similitude des effets du récepteur et de la Cx43 dans la pénétration des leucocytes dans le parenchyme cérébral, la migration des interneurones et la progression des gliomes. J'ai confirmé par Western blot et par BRET l'association spécifique de la Cx43 à l'ACKR3 et non pas au CXCR4. De la même façon, j'ai montré une co-localisation de la Cx43 et de l'ACKR3 dans des cellules de gliome humain, ainsi que dans les astrocytes de la zone sous-ventriculaire et les pieds astrocytaires entourant les capillaires cérébraux chez la souris, suggérant que les deux protéines forment un complexe protéique dans un contexte biologique authentique. Des études fonctionnelles ont révélé que l'ACKR3 module les fonctions de la Cx43 par différents mécanismes. L'expression de l'ACKR3 dans les cellules HEK-293T (mimant la surexpression du récepteur dans les tumeurs), induit par elle-même une inhibition de l'activité jonctionnelle de la Cx43. De même, la stimulation du récepteur par un agoniste réduit l'activité jonctionnelle de la Cx43 par un mécanisme impliquant l'activation d'une protéine Gi, la β-arrestine2 et l'internalisation de la Cx43. Cette thèse établit donc pour la première fois un lien fonctionnel entre le système constitué par les chimiokines CXCL11, CXCL12 et leur récepteur ACKR3 d'une part et les jonctions Gap d'autre part qui pourrait jouer un rôle critique dans la progression des gliomes.

Mots clés : chimiokine, ACKR3, interactome, connexine 43, jonction gap, cellule gliale.

ACKNOWLEDGEMENTS

It is a strange sensation to be here writing my PhD acknowledgments 10 years after almost dropping out school for trying to be a professional football player.

In these regards, I would like to thank Prof. Corrado Lodovico Galli and Prof. Johanna Fink-Gremmels for instilling in me the passion of science that motivated the choice to pursue a PhD here in Montpellier at IGF.

Heartfelt thanks go to my thesis supervisor Dr. Philippe Marin. Your scientific guidance has been essential for all the results obtained in these three years. Furthermore, your dedication and passion for this work, your attention to the details, your scientific and logic reasoning will be forever an example for me.

My sincere thanks to my other thesis supervisor Dr. Severine Chaumont-Dubel. Despite your hectic agenda (thanks to your enviable organization) you were always there when I needed you.

In addition to my supervisors, I would like to thank the rest of my thesis committee: Prof. Marc Mesnil, Dr. Christian Giaume, Dr Eric Reiter, Dr. Jean-Luc Galzi and Dr. Gwendal Lazennec. I am looking forward to hearing your comments, suggestions and criticisms and I am eager, besides being a little anxious, to be engaged in a scientific discussion with such renowned experts in the field.

My deepest gratitude goes out to all the current and former members of Philippe Marin's team. Dr. Claeysen, Dr. Becamel, Dr. Thouvenot, Prof. Bockaert, Simon, Caroline, Vincent, Lucile, Coralie, Camille, Samy, Hugo, Emilie, Angelina, Bérénice, Geoffrey and Patrizia. Thank you all for your constant support and encouragement. Special thanks go to Dr. Vandermoere for finding the time to read and correct this manuscript.

I am grateful to all the ONCORNET members. Thanks to Prof. Martine Smit and Prof. J.E. van Muijlwijk-Koezen for coordinating this amazing network. Thanks to all the students: Ilze, Birgit, Vladimir, Marta, Joyce^2, Cristina, Maria, Davide, Aurelién, Ali, Carmen, Sebastian and Angeliki. It has been an immense pleasure to share such an amazing experience with you. Special mention goes to my "bench-mate" and roommate Vladimir. You cheered me up and helped me chilling out when I needed it the most.

A very special gratitude goes to Dr. Françoise Bachelerie and Dr Géraldine Schlecht-Louf for hosting me in their laboratory and for giving me the opportunity to perform very interesting experiments. Needless to say that I could not even find a pipette without the continuous help of Joyce and Carmen.

I would also like to dedicate few lines to express my immense gratitude towards Dr. Nathalie Guérineau and Enora. Both of you believed in my work and both of you helped me performing experiments that I would not have been able to carry out alone. Thank you again. Just a little disclaimer…I will still need your help.

A special thank goes to all the members of the Functional Proteomic Platform of Montpellier and in particular to Dr Martial Seveno. Despite the initial "Triton" problems we managed to finalize what was planned. That would not have been possible without your help.

Impossible not to include in my acknowledgments Dr. Bienvenue, Dr. Decorsière and Maëva who have been my office neighbours, companions of coffee breaks and lunch at the RU, scientific counsellors and audiences for evening singing shows (Yeah, sometimes I sing in my office and for this I need to apologize also to Edith and David). My gratitude also goes to Julien that I encountered only few years ago but that I feel to have known since a lifetime.

Finishing up the IGF Sud tour I would like to thank Laia, Laura and Emma for accepting my incursions in their office and for their continuous support and help in my existential crisis.

I am also thankful to Dr. Thierry Durroux. Your scientific honesty, work ethics and altruism will always be an inspiration for me.

My sincere thanks to Joyce. Rarely in my life I found a person with your optimism and enthusiasm. Thank you for reading and correcting this manuscript for helping me in my experiments, in keeping a decent body shape and in all the bureaucratic issues I encountered. Keep this sprit and attitude and life will keep smiling at you!!

With my entire heart I have to admit that my research would have been impossible without the aid and support of Elisabeth. You have been my technical-supervisor and my French teacher and now I am very pleased to call you friend.

A general thank you to all the IGF community. Forgive me if I have not mentioned you. Yet, all little attentions that you have dedicated me have not been unnoticed.

With this I once again thank you all and wish you all the best for your future!

P.S. I apologise but in the next part I will write in Italian for thanking my family.

Per terminare questi ringraziamenti vorrei prendermi qualche riga per ringraziare la mia famiglia.

Grazie a tutti, niente di tutto ciò che ho fatto sarebbe stato possibile senza di voi. Grazie a mamma e papà per avermi insegnato i valori chiave per uno scienziato quali perseveranza, coraggio e onestà. Grazie alla nonna e a zia Patrizia per dimostrarmi che bisogna sempre avere fede. Grazie ad Asia per ricordarmi che la vita è bella. Grazie a Siria che mi testimonia che non bisogna avere paura nel fare la scelta più difficile. Grazie a Giona che con la sua fantastica famiglia mi aiuta a capire che a seguire il cuore non si sbaglia mai.

Un grazie speciale al mio amico Giulio che con la sua incredibile tenacia mi stimola a non abbandonare mai i sogni in cui si crede.

Un grazie a Valentina mia compagna di vita e per la vita.

Un abbraccio a zio Marino, Enea, Loris e Bianca e un bacio a Zia Nives.

LIST OF ABBREVIATIONS

5-HT2A, 5-hydroxytryptamine receptor 2A

5-HT6, 5-hydroxytryptamine receptor 6

7TM, Seven Transmembrane

AC, adenylyl cyclase

ACKR, Atypical ChemoKine Receptor

ADP, Adenosine Diphosphate

AIP4, Atrophin Interacting Protein 4

AKT, RAC-alpha serine/threonine-protein kinase

AP, Affinity Purification

arr, arrestin

ATP, Adenosine TriPhosphate

BBB, Blood Brain Barrier

BRET, Bioluminescence Resonance Energy Transfer

cAMP, Cyclic adenosine monophosphate

CBX, CarBeneXolone

Cdk, Cyclin-dependent kinase

CDNA, complementary DeoxyriboNucleic Acid

CFP, Cyan Fluorescent Protein

cGMP, cyclic Guanosine MonoPhosphate

CNS, Central Nervous System

Co-IP, Co-ImmunoPrecipitation

Cx, Connexin

Cx43, Connexin 43

DMSO, Dimethyl sulfoxide

DNA, DeoxyriboNucleic Acid

EGF, Epidermal Growth Factor

EGFP, Enhanced Green Fluorescent Protein

EGFR, Epidermal Growth Factor Receptor

ERK, Mitogen-activated protein kinase

FRAP, Fluorescence Recovery After Photobleaching

FRET, Fluorescence Resonance Energy Transfer

Fsk, Forskolin

GABA, Gamma-AminoButyric Acid

GAG, glycosaminoglycan

GBM, GlioBlastoma Multiforme

GDP, Guanosine DiPhosphate

GFAP, Glial Fibrillary Acidic Protein

GFP, Green Fluorescent Protein

GIP, G protein-coupled receptor Interacting Protein

GJ, Gap Junction

GJIC, Gap Junctional Intercellular Communication

GLAST, Glutamate Aspartate Transporter

GPCR, G Protein-Coupled Receptor

GRK, G protein-coupled Receptor kinase

GTP, Guanosine TriPhosphate

HA, Hemagglutinin

HEK, Human Embryonic Kidney

HIV, Human Immunodeficiency Virus

HSC, Hematopoietic Stem Cells

IHC, ImmunoHistoChemistry

IL, InterLeukin

IP, ImmunoPrecipitation

IP_3, Inositol Trisphosphate

LFQ, Label-Free Quantification

LY, Lucifer Yellow

MAPK, Mitogen-Activated Protein Kinases

MEK, Mitogen-activated protein kinase

$mGlu_2$, Metabotropic Glutamate receptor 2

mi-RNA, micro- RiboNucleic Acid

MIF, macrophage Migration Inhibitory Factor

mRNA, messenger RiboNucleic Acid

MS, Mass Spectrometry

mTOR, mammalian Target Of Rapamycin

MYTH, The Membrane Yeast Two Hybrid assay

NF-kB, nuclear factor kappa-light-chain-enhancer of activated B cells

NLuc, Nano Luciferase

NPC, Neuronal Progenitor Cell

ODDD, autosomal dominant occulodentodigital dysplasia

PFA, paraformaldehyde

PI3K, phosphoinositide 3 kinases

PKC, Protein Kinase C

PLA, Proximity Ligation Assay

PLC, PhosphoLipase C

PTM, Post-Translational Modification

PTX, Pertussis ToXin

RLuc, Renilla-luciferin 2-monooxygenase

RNA, RiboNucleic Acid

S phase, synthesis phase

SEM, Standard Error of the Mean

siRNA, Short interfering RiboNucleic Acid

Src, Proto-oncogene tyrosine-protein kinase Src

STAT, signal transducer and activator of transcription

SVZ, Sub Ventricular Zone

TGF, Tumour Growth Factor

TLR2, Toll Like Receptor 2

TMZ, Temozolomide

UV, UltraViolet

vs., versus

WHO, World Health Organization

Y2H, Yeast two-Hybrid

YFP, Yellow Fluorescent Potein

ZO-1, Zonula occludens-1

1. INTRODUCTION

1.1 G PROTEIN-COUPLED RECEPTORS

G protein-coupled receptors (GPCRs) are seven-transmembrane receptors (7TM) that form the largest family of membrane receptors targeted by more than one third of the drugs present on the market[1]. Based on structural and functional similarities, GPCRs can be divided in six different classes: class A (rhodopsin family), class B (secretin family), class C (glutamate family), class D, class E and class F (frizzled family)[2]. GPCRs can signal through several parallel pathways simultaneously such as activation of heterotrimeric G proteins, β-arrestins, GRKs or non-canonical interacting proteins.

1.1.1 G PROTEINS

GPCRs were originally thought to operate in a “two dimensional” system exclusively interacting with heterotrimeric G protein complexes composed of three G protein subunits α, β and γ. Upon receptor stimulation by an agonist, conformational changes lead to the coupling[6] (**BOX 1**) and activation of heterotrimeric G protein.

BOX 1 PRE-COUPLING

Though the main paradigm asserts that heterotrimeric G proteins couple with the receptor only upon receptor activation, an opposing view hypothesizes that G protein might couple to the receptor in the absence of an agonist (pre-coupled GPCR). The pre-coupling of G protein would overcome the rate-limiting step of GPCR and G proteins diffusion that is necessary in the classical view. Already in 1988, using radioligand binding assay in human platelet membranes, it has been postulated that three different populations of α_2-adrenergic receptor exist: a first one, unable to couple to G proteins, the second pre-coupled to G-proteins and the last one coupled only upon agonist stimulation[3]. FRET microscopy in transiently transfected HEK-293 cells revealed that G proteins might be pre-coupled to the α_2-adrenergic receptor. In addition the authors also observed pre-coupling of the M4 muscarinic receptor, the D2 dopamine receptor, the adenosine A1 receptor and the prostacyclin receptor[4]. In a more recent publication the pre-coupling of $G\alpha_q$ to the M_3 muscarinic acetylcholine receptor (M3R) was shown using Fluorescence Recovery After Photobleaching (FRAP) methods[5]. HEK-293T cells were transfected with cDNA encoding M3R-CFP and YFP tagged $G\alpha_q$. The receptor was then immobilized into the membrane by avidin cross-linking. The lateral diffusion of $G\alpha_q$ was measured quantifying the recovery of signal after photobleaching. M3R receptor was able to slow down the lateral diffusion of $G\alpha_q$ suggesting a pre-coupling of the G protein to the receptor. Agonist and inverse agonist did not have effects on the pre-coupling.

Activated GPCRs function as guanine nucleotide exchange factors catalysing the exchange of GDP with GTP on the Gα subunit that in turn triggers the dissociation of the Gα subunit from the Gβγ complex[7]. Subsequently, the intrinsic GTP hydrolysis of the Gα will lead to the re-association of the αβγ complex.

Gα subunits are divided in four principal families: $G\alpha_s$, $G\alpha_i$, $G\alpha_q$ and $G\alpha_{12/13}$[8]. $G\alpha_s$ family is characterized for its ability to stimulate adenylyl cyclase (AC) (enzyme catalysing the transformation of ATP in cAMP). Stimulation of adenylyl cyclase results in elevated cAMP levels that in turn trigger the activation of several effectors such as protein kinase A, cyclic nucleotide-gated channels, and the exchange protein directly activated by cAMP (EPAC)[9]. On the other hand, $G\alpha_i$ proteins inhibit adenylyl cyclase. The $G\alpha_q$ family activates the β-isoform of phospholipase C (PLC) that catalyses the cleavage of phosphatidylinositol 4,5-bisphosphate into inositol triphosphate (IP_3), which opens IP_3-sensitive calcium channels present in the endoplasmic reticulum, and membrane-bound diacylglycerol, which activates the protein kinase C (PKC) family[9] (**Figure 1**). $G\alpha_{12/13}$ family is responsible for the activation of a plethora of effectors such as Rho proteins, Btk family tyrosine kinases, Gap1, rasGAP and cadherins[8].

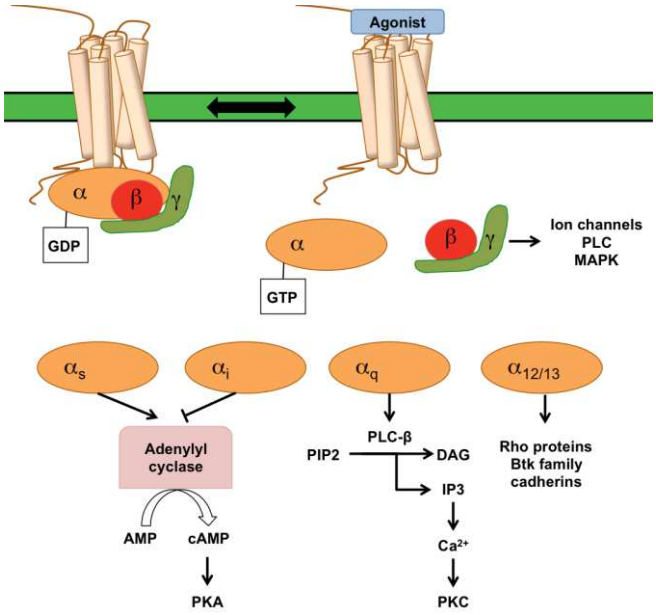

Figure 1 Schematic representation of G protein activation and G protein-activated pathways. Agonist binding to GPCR triggers conformational changes in the receptor that catalyze the exchange of GDP with GTP on the Gα subunit that in turn triggers the dissociation of the Gα subunit from the Gβγ complex. These two subunits are then able to activate the available downstream signalling pathways.

The βγ units were originally accounted only for the inactivation of the Gα unit. However, purified βγ units have been shown to activate a cardiac potassium channel in 1987[10]. From this study, accumulating evidence has been showing that βγ complexes activate several other effectors such as PLC, AC, voltage-gated calcium channels, phosphoinositide 3 kinase (PI3K) and Mitogen-Activated Protein Kinases (MAPKs)[11].

1.1.2 GRKs and β-arrestins

Researchers rapidly realized that G proteins are not the only proteins interacting with GPCRs. In fact, almost simultaneously G protein coupled-receptor kinases (GRKs)[12] and β-arrestins[13] (especially the ubiquitously expressed β-arrestin1 and 2 [14]) were identified as GPCR interacting proteins (GIPs) involved in the desensitization process. Ligand-induced activation of the GPCR promotes conformational changes that trigger the recruitment of GRKs, which phosphorylate the receptor leading to the recruitment of β-arrestins. β-arrestins impair receptor coupling to G proteins through steric hindrance and therefore receptor-operated signal transduction. Further studies revealed that β-arrestin roles are not limited to signal transduction termination. They in fact actively participate in the receptor endocytosis by clathrin coated pits, functioning as adaptor protein for the recruitment of clathrin and its adaptor protein AP2[15]. Recent evidence showed that they are also essential scaffold proteins for the recruitment and activation of proteins of the MAP kinase ERK1/2 pathway [16]. As for β-arrestins, GRKs have been involved in the activation of others effectors such as phosducin, AKT and Mitogen-activated protein kinase MEK[17].

1.1.3 Non canonical G Protein-Coupled Receptor Interacting Proteins

A special class of GIPs is constituted by GPCRs themselves. In fact, accumulating evidence, principally collected in heterologous systems, has been showing that GPCRs can interact forming hetero and homomers[18]. Heteromers are formed by at least two different GPCRs, whereas in homomers the monomers are the same receptor. Therefore, when engaged in heteromers, one GPCR can be considered as a GIP of the other. GPCRs may have a pharmacologically-distinct profile as a monomer, homomer and heteromer. Exemplificative is the case of the chemokine receptor ACKR3. ACKR3 is not coupled to G proteins in HEK-293 cells as monomer or homodimer but it is able to modify CXCR4 G protein activation and Ca^{2+} mobilization when engaged in the ACKR3/CXCR4 heterodimer[19]. Another example is

the cross talk between the 5-HT_{2A} and $mGlu_2$ receptor. Activation of the $5HT_{2A}$ receptor was shown to mediate the phosphorylation of $mGlu_2$ at Ser^{843} and to promote its receptor-operated $G\alpha_{i/o}$ signalling[20].

In addition to canonical GIPs (G proteins, β-arrestins and GRKs), and GPCRs themselves, GPCRs have been found to specifically interact with a large number of proteins that modulate their activity[21], trafficking[22], and signal transduction properties[23]. GIPs can even open a new vista of signalization. For instance, the AT1 angiotensin receptor was thought to signal only *via* its coupling to $G\alpha_q$ proteins. Yet, upon stimulation it can recruit Jak2 that in turn will phosphorylate a member of the STAT family of transcription factors[24]. Another case is the agonist-dependent recruitment of the Na^+/H^+ exchange regulatory factor 1 (NHERF-1) to the C-terminal domain of the β_2-adrenergic receptor[25]. This association allows the β_2-adrenergic receptor to control the Na^+/H^+ exchange in the kidney in a G protein-independent way. A more recent example is the interactions between the serotonin6 (5-HT_6) receptor and the cyclin-dependent kinase (Cdk) 5. Cdk5 bound to the receptor constitutively phosphorylates its Ser^{350}, a necessary step in the activation of the Cdc42 pathway to promote neuronal differentiation[26]. In addition, the 5-HT_6 receptor was found to physically interact with several proteins of the mammalian target of rapamycin (mTOR) pathway, including mTOR itself. Correspondingly, activation of the receptor increases mTOR signalling through a mechanism requiring physical interaction between the receptor and mTOR. Conversely, inhibition of mTOR by rapamycin prevented cognitive deficits induced by 5-HT_6-receptor agonists[27].

However, interactions with GIPs can also tune the canonical signalling pathways such as G protein and β-arrestin activation. For instance, the association of GPCRs with proteins of the regulator of G protein signalling (RGS) family regulates the amplitude and time course of GPCR signalling by increasing the GTPase activity of the activated Gα subunit[28]. Another example is the association of Calmodulin with the $5HT_{2C}$ receptor that is critical for G protein-independent, but arrestin-dependent receptor signalling[29].

In addition GIPs can both modify GPCR targeting by clustering and anchoring the receptors[30] and modify GPCRs trafficking as in the case of dynein light chain component that facilitates the rhodopsin trafficking to the membrane or the case of GASP proteins which increase the trafficking of the D_2 dopamine, CB_1 cannabinoid and δ opioid receptors[21] to the lysosomes.

1.1.4 GPCR PHARMACOLOGY: BALANCED *VS.* BIASED AGONISM

GPCRs can therefore signal through parallel pathways simultaneously. Agonists that have different efficacy for these different pathways are defined as "biased" (**Figure 2**). Whereas "balanced" agonists have equal efficacy to available downstream pathways, "biased" agonists will preferentially or selectively activate specific pathways[31]

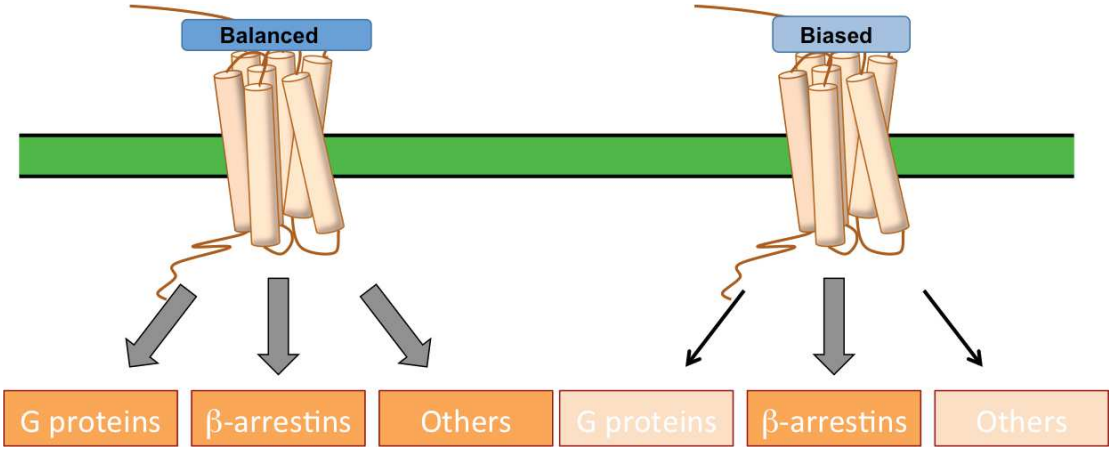

Figure 2 Balanced *vs.* biased agonism. "Balanced" agonists have equal efficacy to available downstream pathways associated with the GPCR activation. On the other hand, "biased" agonists preferentially activate only specific pathways, β-arrestin-dependent pathways in this case.

1.1.5 METHODS FOR THE IDENTIFICATION OF GPCR-INTERACTING PROTEINS

As earlier reported considerable evidence has been accumulating supporting that GPCRs recruit a number of proteins called G receptor interacting proteins (GIPs)[32]. This prompted numerous investigations aimed at identifying GIPs and at characterizing GPCR-GIP interactions, using either blind or targeted approaches. In blind methods no beforehand knowledge of the GIP is required and the GPCR of interest is used as bait for fishing GIPs, while targeted methods are devoted to the validation and characterization of a previously identified GPCR-GIP interaction. Methods for identifying GIPs or characterizing GPCR-GIP interactions can be divided into three major classes: genetic, biophysical and proteomic ones.

1.1.5.1 GENETIC METHODS

The first method belonging to this class is the Yeast two-Hybrid (Y2H) assay[33]. In Y2H, the protein of interest (bait protein) is expressed in yeast as a fusion to the DNA-binding domain of a transcription factor lacking the transcription activation

domain. To identify partners of this bait, a plasmid library that expresses cDNA-encoded proteins fused to a transcription activation domain is introduced into the yeast strain. Interaction of a cDNA-encoded protein with the bait protein results in the activation of the transcription factor and expression of a reporter gene, enabling growth on specific media or a colour reaction and the identification of the cDNA encoding the target proteins. A first disadvantage is the loss of spatio-temporal localization of the interaction; in fact, Y2H only captures a snapshot of potential interaction in an artificial biological system. A second disadvantage is the impossibility to investigate membrane-anchored proteins since the two proteins must cross the nuclear membrane for carrying the reconstituted transcriptional factor to the DNA. The Membrane Yeast two Hybrid assay (MYTH)[34] has been developed for overcoming this limitation. In this assay, the ubiquitin protein is split into two fragments, which are fused to the two proteins of interest. The ubiquitin C-terminal fragment is conjugated to a transcription factor that is released when the interaction occurs and the ubiquitin protein is reformed. However, as in Y2H, the spatio-temporal localization of the interaction is lost. A second limitation is that the ubiquitin C-terminus carrying the transcription factor cannot be fused to soluble proteins because they could diffuse into the nucleus. Recently, a mammalian version of the assay, Mammalian membrane two-hybrid (MaMYTH)[35], has been developed. The Kinase substrate sensor (KISS)[36] assay, using STAT3 as transcriptional factor, can also be used for investigating protein-protein interactions implicating both cytosolic and membrane proteins in mammalian cells, but not for studying GPCR interaction with proteins involved in the STAT cascade.

1.1.5.2 BIOPHYSICAL METHODS

Energy transfer-based methods such as Bioluminescence and Fluorescent Resonance Energy Transfer (BRET[37] and FRET[38]) assays, are generally targeted methods used to investigate previously reported interactions. Both are based on the transfer of energy from a donor to a nearby acceptor (<100 Å) and their high sensitivity allows the study of weak and transient interactions. The high spatial-temporal resolution permits accurate kinetic studies for investigating interaction dynamics.

Proximity Ligation Assay (PLA)[39] is an other powerful targeted fluorescent method. In the direct PLA technique a couple of DNA oligonucleotide conjugated antibodies against the proteins of interest are used. In the indirect PLA technique secondary DNA conjugated antibodies are used after targeting the proteins of interest with the

appropriate primary antibody. If the two conjugated antibodies are close enough (30-40 nm) they can bind together with the addition of two connectors. The DNA connecting the two probes is then amplified and hybridized with fluorophores that allows the visualization of the interaction in the place where it occurs, at a single molecule resolution. Main disadvantages are the high costs and the necessity of specific antibodies that are not always available. In the bimolecular fluorescent complementation (BiFC)[40] assay, a fluorescent protein is divided into two non-fluorescent fragments that are fused to the proteins of interest. Interaction reconstitutes the entire fluorescent protein. This method allows the direct visualization of the interaction and can be used for soluble or membrane-bound proteins. In addition, several interactions can be investigated in parallel using different fluorescent proteins. Since there is a delay in fluorescence formation upon reconstitution of the fluorescent proteins and the fluorophore formation is irreversible, these methods are not well suited for kinetic studies.

1.1.5.3 PROTEOMIC METHODS

Proteomic methods consist in the identification of GIPs interacting with a receptor of interest by mass spectrometry (MS) after an Affinity Purification (AP) selection phase and are therefore often named AP-MS. AP-MS is usually employed as a blind method for screening virtually all the GIPs of a GPCR of interest. Targeted versions of the method also exist and rely on GIP identification by Western Blotting. However, the requirement of specific antibodies seriously limits their applications. Several strategies can be used for the affinity purification step. In Co-IP specific antibodies against the protein of interest are used for precipitating the bait from a protein lysate. As specific GPCR antibodies providing high IP yields are rarely available, epitope-tagged versions of the receptor of interest are often expressed in the cell type or the organism of interest and precipitated using antibodies against the tag. The main advantages of Co-IP are the purification of proteins interacting with the entire receptor (whenever possible the native receptor) in living cells or tissues and its ability to purify the entire associated protein complex. The main limitations are the necessity of specific antibodies for precipitating GPCRs, the loss of spatio-temporal information and the use of detergents for cell lysis that might disrupt weak interactions. Alternatively, pull-down assays using the receptor (or one of its domains) fused with an affinity tag (e.g. Glutathione S-transferase) and immobilized on beads as baits, can be performed to purify GPCR partners from a cell or tissue lysate. Such *in vitro* binding assays can also be used to prove the direct physically

interaction between two protein partners. In that case, the bait is incubated with a purified protein instead of a cell or tissue lysate. Two-step versions of AP called Tandem Affinity Purification (TAP)[41] have also been reported[42] and apply to both co-IPs or pull-downs. Although TAP methods drastically reduce the number of false-positive identifications, they require larger amounts of starting material.

In the proximity-dependent biotin identification (BioID)[43] method, the ‘‘bait’’ protein is fused to a prokaryotic biotin ligase molecule that biotinylates proteins in close proximity once expressed in cells. BioID can detect weak and transient interactions occurring in living cells and detergents do not affect the results. However, the fusion of biotin ligase to the bait might alter its targeting or functions.

1.2 Chemokine and chemokine receptor network

Chemokines and 7TM receptors form the chemokine signalling system. Approximately, fifty chemokines and twenty chemokine receptors are encoded by the mammalian genome (**Table 1**). The complexity of this network is increased by the promiscuity of the chemokine-receptor binding: different chemokines can bind to the same receptor and different receptors can recognize the same chemokine. The intricacy is further enhanced by the ability of chemokines and chemokine receptors to form homo- and hetero-oligomers. This multi-level network tuning allows to accurately control the biological processes regulated by chemokines and chemokine receptors such as cell movement, cell-cell adhesion, embryonic development and immune cell development.

Chemokine	Other name	Receptor	Chemokine	Other name	Receptor
CXC class					
CXCL1	Groα	CXCR2,CXCR1	**CXCL9**	MIG	CXCR3, CXCR3B
CXCL2	Groβ	CXCR2	**CXCL10**	IP-10	CXCR3, CXCR3B
CXCL3	Groγ	CXCR2	**CXCL11**	I-TAC	CXCR3, CXCR3B, ACKR3
CXCL4	PF4	CXCR3B	**CXCL12**	SDF-1α/β	CXCR4, ACKR3
CXCL4V1			**CXCL13**	BLC, BCA-1	CXCR5
CXCL5	ENA-78	CXCR2	**CXCL14**	BRAK, Bolekine	Unknown
CXCL6	GCP-2	CXCR1,CXCR2	**CXCL16**		CXCR6

Chemokine	Other name	Receptor	Chemokine	Other name	Receptor
CXCL7	NAP-2	Unknown	**CXCL17**	DMC	Unknown
CXCL8	IL-8	CXCR1,CXCR2			
CC class					
CCL1	I-309	CCR8	**CCL15**	HCC-2	CCR1, CCR3
CCL2	MCP-1	CCR2	**CCL16**	HCC4- LEC	CCR1, CCR2, CCR5, HRH4
CCL3	MIP-1α	CCR1, CCR5	**CCL17**	TARC	CCR4
CCL3L1	LD78β		**CCL18**	PARC	Unknown
CCL3L3	LD78β		**CCL19**	MIP3β	CCR7
CCL4	MIP-1β	CCR5	**CCL20**	MIP3α	CCR6
CCL4L1	AT744.2		**CCL21**	SLC	CCR7
CCL4L2			**CCL22**	MDC	CCR4
CCL5	RANTES	CCR1, CCR3, CCR5	**CCL23**	MPIF-1	CCR1, FPRL-1
CCL7	MCP-3	CCR1, CCR2, CCR3	**CCL24**	Eotaxin 2	CCR3
CCL8	MCP-2	CCR1, CCR2, CCR3, CCR5	**CCL25**	TECK	CCR9
CCL11	Eotaxin	CCR3	**CCL26**	Eotaxin 3	CCR3
CCL13	MCP-4	CCR1, CCR2, CCR3	**CCL27**	CTACK	CCR10
CCL14	HCC-1	CCR1	**CCL28**	MEC	CCR10, CCR3
Other classes					
XCL1	Lymphotactin	XCR1	**CX3CL1**	Fractalkine	CX3CR1

Table 1 **List of known human chemokines with the associated receptors.** Adapted from[44].

1.2.1 CHEMOKINES

Chemokines are small proteins classified by the arrangement of conserved cysteine residues in their primary amino acid sequence. Chemokines are divided in four subfamilies: CC chemokines where the two cysteine residues are next to eachother, CXC whose cysteines are separated by one variable amino acid, CX_3C chemokines have three amino acids separating the cysteine residues and XC chemokines lack the first and third cysteine of the motif. A systematic nomenclature named the chemokines based on their subfamily followed by the letter L (standing for “ligand”) and a number indicating when the gene was first isolated [45].

BOX 2 CHEMOTAXIS

Chemotaxis is defined as *"the directional locomotion of cells towards a source of a chemical gradient"*[46]. Chemokines are shaped in a chemoattracting gradient by immobilization on GAGs, heparane sulfate and extracellular matrix[47,48] and by sequestration by chemokine receptor[49]. Cells, such as leukocytes, migrate towards higher chemokine concentrated areas. The migration can be divided in three steps: gradient sensing, polarization and cell-mobility[50]. After interaction of the chemokine with its receptor the cell undergoes cytoskeletal rearrangements forming a leading and a trailing edge enabling its movement along the gradient.

Approximately fifty chemokines are encoded by the mammalian genome and several polymorphisms have been identified in chemokine genes[51]. For example, a single point polymorphism (G801A) has been reported for CXCL12 and homozygotes for this polymorphism have shown protection against the acquired immunodeficiency syndrome (AIDS) caused by the retrovirus known as human immunodeficiency virus (HIV)[52]. Once translated, chemokines must undergo deep rearrangements for exerting their biological functions. In fact, chemokines, due to their high affinity, bind to small linear polysaccharides consisting in repeated disaccharide subunits present on the cell surfaces of most cells called glycosaminoglycans (GAGs). GAGs promote the formation of the chemotactic gradient (**BOX 2**) anchoring chemokines and avoiding that they are washed out by the blood flow. In addition, GAGs are engaged in oligomerization that improves chemokine solubility[53]. The vital role played by GAGs in chemokine activity is exemplified by CCL2, CCL4 and CCL5 that were found to be inactive *in vivo* when their binding site for GAGs is mutated[54].

Furthermore, after their translation, chemokines can be deeply modified by post-translational modifications (PTMs). Specifically, chemokines can be citrullinated[55], nitrated[56], glycosylated[57] and cleaved[58]. The paramount importance of PTMs for chemokine activity is clearly illustrated by CXCL7 and CCL14 that are active only after proteolytic processing[59,60].

Modified and GAG-bound chemokines are ready for binding with their receptor. Early works on CXCL8 showed that the N-terminal domain of the chemokine is necessary for the activation and that binding and activation are un-coupled. Mutations on the 30s-loop of CXCL8 (N-terminal domain) were found to have a little effect on the affinity but a drastic effect on the activity[61]. On the receptor side, it was observed that the N-terminal domain is necessary for the binding of the chemokine into the receptor[62]. These observations have been later generalized into a two site model (**Figure 3**) where the site 1 (N-terminal domain of the receptor) is responsible for the recognition and the binding of the chemokines; after the binding, the flexible N-

terminal part of the chemokine (site 2) is free to “enter” the chemokine receptor and to trigger the structural rearrangements necessary for its activation [63].

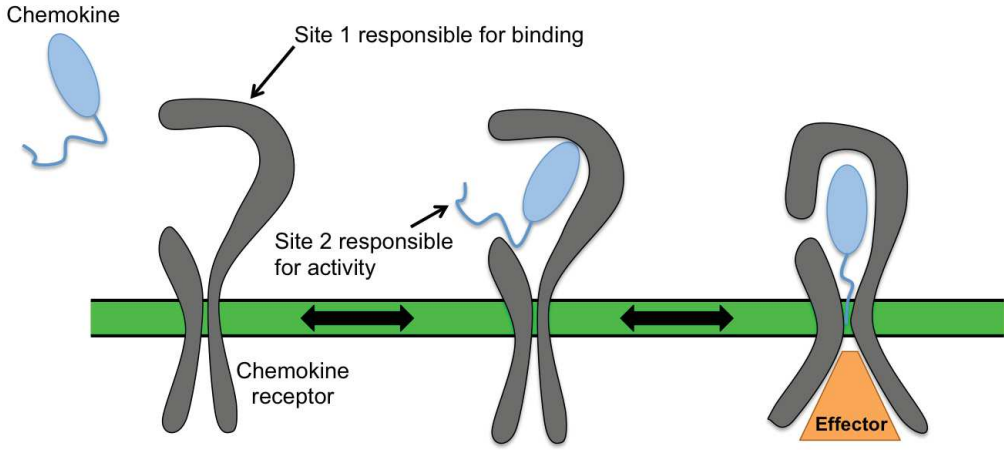

Figure 3 Two binding site model. Site 1 present in the N-terminal domain of the receptor is needed for the binding of the chemokine to its receptor. After binding the receptor N-terminal wrap the chemokine. The flexible N-terminal domain of the chemokine (site 2) is then free to activate the receptor.

1.2.1.1 CXCL12

CXCL12 was initially thought to transduce signals exclusively through its binding to CXCR4[64]. However, in 2005 it has been discovered that CXCL12 can also bind to another chemokine receptor named ACKR3[65]. In order to be biologically active the pro-CXCL12 precursor needs to be cleaved, resulting in the elimination of the 21 amino acid signal peptide present at the N-terminal region. Six and three different CXCL12 isoforms have been identified in human and mice, respectively. CXCL12 isoforms are generated by alternative splicing[66]. CXCL12α (major isoform) is highly conserved among species[67], suggesting an essential role in developmental processes. Accordingly, CXCL12$^{-/-}$ mice are lethal (half the embryos die at E18.5 and neonates die within one hour after birth)[68]. CXCL12 plays pivotal roles in hematopoietic and germ cell development, cardiogenesis and vascular formation, immune-response as well as neurogenesis[66]. It is highly expressed in homeostatic conditions in lymph nodes, lung, liver and bone marrow. Lower expression levels have been shown in small intestine, kidney, skin, brain and skeletal muscle[69].

1.2.1.2 CXCL11

As CXCL12, CXCL11 was originally thought to bind only to one chemokine receptor (CXCR3)[70]. However, as CXCL12, CXCL11 also binds ACKR3[71]. CXCL11 is

primarily found in leukocytes, pancreas, liver, thymus, spleen and lung. It has been found at lower level in the small intestine, placenta and prostate[69]. CXCL11, as CXCL12, plays a pivotal role in the immune response, mediating the T-cell polarization and migration (*via* activation of STAT3 and STAT6)[72], as well as the migration of macrophages[73].

1.2.2 CHEMOKINE RECEPTORS

Chemokine receptors were originally named only according to the chemokine subfamily recognized, followed by the capital letter R (standing for "receptor") and a number according to their order of discovery[74]. However, in 2014, a new functional nomenclature divided the chemokine receptor family into two subfamilies: conventional chemokine receptors G protein-coupled and atypical chemokine receptors unable to activate G proteins[75]. The first group, that structurally shares the DRLYAIV motif at the end of transmembrane domain 3, follows the original nomenclature. The atypical receptors were named ACKR (standing for Atypical ChemoKine Receptor) followed by an identifier number. In spite of this different nomenclature all chemokine receptors are classified as Class A GPCRs.

Conventional chemokine receptors are able to activate G proteins upon chemokine binding. This subfamily includes ten CCR receptors (CCR1-10), six CXCR receptors (CXCR1-6), CX_3C1 and XCR1[75].

The atypical chemokine receptor family contains 7TM receptors highly homologous to typical chemokine receptors that binds chemokines but do not signal trough G proteins. Before 2014 they were called scavengers, decoys, interceptors or chemokine-binding proteins[75]. ACKR1 (previously Duffy Antigen Receptor for Chemokines), ACKR2 (formerly D6 or CCBP2), ACKR3 (alias CXCR7), ACKR4 (formerly CCRL1 and CCX CKR), CCRL2 (ACKR5, reserved, pending confirmation; aliases CKRX, HCR, and CRAM), PITPNM3 (also known as the CCL18/PARC Receptor; new name: ACKR6, Reserved) and C5L2 belong to this family.

1.2.2.1 CXCR4

CXCR4 belongs to the conventional chemokine receptor family and it was identified for the first time in leukocytes. It is now appreciated that CXCR4 is expressed in several cellular types such as endothelial cells, lymphocytes, fibroblasts and hematopoietic stem cells[76]. As for CXCL12, the CXCR4 knock out is lethal[77]. Its crystal structure, in complex with its antagonist IT1t, has been resolved in 2010[78].

Upon binding to its endogenous agonists CXCL12, CXCR4 activates $G\alpha_i$ proteins that subsequently inhibit adenylyl cyclase activity[79]. This leads to the activation of the Src tyrosine kinase family that stimulates the Ras/Raf/MEK/ERK pathway. In addition, CXCR4 can also activate PI3K by both the α and βγ subunits of $G\alpha_i$ proteins, leading to Ca^{2+} mobilization and activation of PKC and MAPK. CXCR4 can also signals through GRKs and β-arrestins. CXCL12 stimulation triggers activation of GRK2, GRK6, GRK3, β-arrestin1 and 2. GRK2 and 6 as well as β-arrestin2 negatively regulate Calcium mobilization. GRK3 and 6 as well as β-arrestin1 increased ERK1/2 activation whereas GRK2 negatively regulates ERK1/2 activation[80].

1.2.2.1.1 CXCR4 NON CANONICAL INTERACTING PROTEINS

Beside canonical interacting proteins, CXCR4 has been shown to interact with additional proteins that modulate CXCR4 trafficking, subcellular localization and signalling and proteins whose functions are still unknown. The CXCR4 interacting proteins, the methods used for the identification, the site of their interaction in the receptor sequence and their functional impact are indicated in **Table 2**.

1.2.2.1.1.1 PROTEINS CONTROLLING CXCR4 LOCALIZATION OR TRAFFICKING

Filamin A directly interacts with CXCR4 and stabilizes the receptor at the plasma membrane by blocking its endocytosis[81]. The association of the E3 Ubiquitin Ligase Atrophin Interacting Protein 4 (AIP4) has opposite consequences: ubiquitination of CXCR4 by AIP4 targets the receptor to multi-vesicular bodies, which is followed by receptor degradation. In addition, agonist treatment increases CXCR4/AIP4 interaction, as assessed by Co-IP and FRET experiments[82], indicating that this interaction is dynamically regulated by the conformational state of the receptor. Reticulon3 (RTN3) is another CXCR4 interacting protein that constitutively promotes its translocation to the cytoplasm[83].

1.2.2.1.1.2 PROTEINS MODULATING CXCR4 SIGNALLING AND FUNCTIONS

CD74, a single-pass type II membrane protein sharing with CXCR4 the ability to bind to the Macrophage migration inhibitory factor (MIF), was also shown to interact with CXCR4[84]. The CXCR4/CD74 complex is involved in AKT phosphorylation. In fact, blocking either CXCR4 or CD74 inhibits MIF-stimulated AKT activation. Using FRET, an interaction between CXCR4 and the Toll Like Receptor 2 (TLR2) was observed in

human monocytes upon activation by Pg-fimbria (fimbriae produced by the major pathogen associated with periodontitis named *Porphyromonas gingivalis*). Analysis of a possible crosstalk between the two receptors showed that Pg-fimbria, directly binds to CXCR4 and inhibits TLR2-induced NF-κB activation by *P. gingivali*. [85,86]. In Jurkat cells, CD164 co-precipitates with CXCR4 in presence of CXCL12 presented on fibronectin[87]. CXCR4-CD164 interaction participates in CXCL12-induced activation of AKT and PKC isoform zeta ***(***PKCζ***).*** Down-regulation of CD164 reduces the activation of both kinases measured upon exposure of Jurkat cells to CXCL12. CXCR4/CD164 interaction has been detected in additional cell lines, such as primary human ovarian surface epithelial **(**hOSE***)*** cells stably expressing CD164 [88].

The ability of CXCR4 to promote cell migration requires deep cytoskeletal rearrangements that can be modulated by CXCR4 interacting proteins. In J77 T cells, CXCR4 constitutively associates with Drebrin[89], a protein known to bind to F-actin and stabilize actin filaments. Drebrin is also involved in CXCR4- and CD4-dependent Human immunodeficiency virus (HIV) cellular penetration[90]. CXCR4 interacts with Diaphanous-related formin-2 (mDIA2). This interaction induces cytoskeletal rearrangements that lead to non-apoptotic blebbing. The mDIA2-CXCR4 interaction is only detected during non-apoptotic amoeboid blebbing and is confined to non-apoptotic blebs upon CXCL12 stimulation[91], suggesting a fine spatio-temporal regulation of the interaction. CXCR4 also constitutively associates with the motor protein non-muscle myosin H chain (NMMHC) *via* its C-terminal domain[92]. The authors showed hat NMMHC and CXCR4 are co-localized in the leading edge of migrating lymphocytes, suggesting that this association might have a role in lymphocyte migration. The PI3-kinase isoform p110γ co-precipitates with CXCR4 in CXCL12-stimulated human myeloid cells. This interaction contributes to receptor-operated integrin activation and chemotaxis of myeloid cells[93]. Finally, CXCR4 was found to be part of a junctional mechano-sensitive complex through its interaction with PECAM-1[94].

1.2.2.1.1.3 Proteins with unknown functions

Other potential CXCR4-interacting proteins have been identified using blind methods. These include the lysosomal protein ATP13A2[95] and the nuclear protein Myb-related protein B that is involved in cell cycle progression[96]. In a study aimed at characterizing the human interactome by Co-IP of 1,125 GFP-tagged proteins and

MS analysis, CXCR4 was found to co-precipitate with the potassium channel subfamily K member 1, the CSC1-like protein 2 and the Vesicle transport protein GOT1B[97].

1.2.2.1.2 CXCR4 FUNCTIONS IN HEALTH AND DISEASE

Blood cells are generated in the bone marrow from hematopoietic stem cells. CXCR4 plays a pivotal role in the colonization of the bone marrow by hematopoietic stem cells (HSCs), as well as in HSCs homeostasis. In fact, the hematopoietic stem cell niche is maintained by the high CXCL12 concentration in the bone marrow[98]. In addition, CXCR4 negatively regulates the proliferation of hematopoietic stem cells[99]. Similarly to its effect upon hematopoietic stem cells, CXCR4 also controls lymphocyte and myeloid cell homeostasis[100,101]. Besides regulating bone marrow homeostasis, CXCR4 is essential for coordinating both adaptive and innate immune responses. It controls leucocyte dissemination and trafficking, contributes to the organization of lymph nodes[99] and, finally, sustains T cell priming[102].

CXCR4 involvement in severe diseases including immunodeficiencies, autoimmunity and cancer has been largely confirmed. During HIV infection, CXCR4 functions as a co-receptor (together with CD4) for viral entry into T cells[103]. An heterozygous mutation of CXCR4, consisting in the truncation of the C-terminal domain and leading to a gain of function of the receptor, was identified as the genetic basis of the Warts, Hypogammaglobulinemia, Infections and Myelokathexis (WHIM) syndrome[104]. CXCR4 involvement in cancer has first been suggested by its overexpression in more than 23 types of different cancers including kidney, lung, brain, prostate, breast, pancreas, ovarian, and melanomas and its involvement in tumour growth, angiogenesis, metastasis, and therapeutic resistance[105] is now well established.

Protein	Method of identification	Cellular context	Direct	Constitutive / induced	Site of interaction	Role	Ref
Filamin A	Pull-Down Co-IP	HEK-293 cells Recombinant protein	Yes	Constitutive and CXCL12-induced. The ROCK inhibitor Y27632, reverses CXCL12-induced increased interaction	C-terminal tail and third loop of CXCR4	Stabilize CXCR4 at the surface	81
E3 Ubiquitin Ligase Atrophin Interacting protein 4 (AIP4)	Pull Down Co-IP FRET	HEK-293 cells	Yes	Constitutive and CXCL12-induced.	CXCR4 C-tail serines and WW domains of AIP4. Serine 324 and 325 when phosphorylated increase interaction	Increase CXCR4 degradation	82
Reticulon3	Y2H Co-IP	HEK-293 cells	NA	Constitutive, induction not tested	Carboxyl terminal of RTN3	Increase cytoplasmic localization of CXCR4	83
CD74	Co-IP Co-localization	HEK-293 and MonoMac6 cells	NA	Constitutive, induction not tested	NA	Phosphorylation of AKT	84
Toll-like receptor 2 (TLR2)	FRET Co-IP	Human monocyte and HEK-293 cells	NA	Induced by Pg-fimbria	NA	CXCR4 inhibits TLR2-induced NF-kB activation. In addition CXCR4 found to be receptor of the pattern-recognition receptor complex	85,86

Protein	Method of identification	Cellular context	Direct	Constitutive / induced	Site of interaction	Role	Ref
Motor protein non muscle myosin H chain (NMMHC)	Pull-Down Co-IP Co-localization	Jurkat T and Peer T cells lymphocytes	NA	Constitutive and not induced by CXCL12	CXCR4 C-terminal domain	Lymphocytes migration	92
Drebrin	Pull Down Co-IP FRET	J77 T, HEK293T and HIV-infected T cells	YES	Constitutive and induced by superantigen E which also re-localize that interaction to the leading edge of migrating lymphocytes.	CXCR4 C-terminal domain. Drebrin N-terminal region positively regulates interaction whereas the C-terminal region seems to negatively regulate it.	Drebrin affects key physiological processes during antigen presentation. HIV entry	90,106
Endolyn (CD164)	Co-IP Co-localization	Jurkat and Ovarian surface epithelial cells	NA	Only CXCL12 induced. CXCL12 was presented on fibronectin.	NA	CD164 participates to the CXCL12 mediated AKT and PKC-ζ phosphorylation.	87,88
Diaphanous-related formin-2 (mDIA2)	Co-IP Co-localization	MDA-MB-231 cells	NA	Constitutive (very weak) and CXCL12 induced.	NA	Cytoskeletal rearrangement necessary for non-apoptotic blebbing	91
ATP13A2	MYTH	Yeast	YES	Constitutive	NA	NA	95
PI3-kinase isoform p110g	Co-IP	Human myeloid cells	NA	Only CXCL12 induced	NA	Integrin activation and chemotaxis	93
PECAM-1	PLA	Human Coronary Artery Endothelial Cells (HCAEC)	NO	Constitutive, induced not studied	NA	CXCR4 part of a junctional mechano-sensitive complex	94
Myb-related protein B	2HY	Yeast	Yes	NA	NA	NA	97

Protein	Method of identification	Cellular context	Direct	Constitutive / induced	Site of interaction	Role	Ref
Potassium channel subfamily k	Co-IP	HeLa cells	NA	NA	NA	NA	[97]
CSC1-like protein 2	Co-IP	HeLa cells	NA	NA	NA	NA	[97]
Vesicle transport protein GOT1B	Co-IP	HeLa cells	NA	NA	NA	NA	[97]

Table 2 **CXCR4 interacting proteins described in the literature.**

1.2.2.2 ACKR3

ACKR3 belongs to the atypical chemokine receptor family and it was identified for the first time in 1990 as the orphan receptor RDC1[107]. It was deorphanized in 2005[65] when CXCL12, originally identified as the exclusive ligand of CXCR4, was found to bind to ACKR3. Only one year later, CXCL11, originally exclusive ligand of CXCR3, was identified as the second ligand of ACKR3[108]. Interestingly, CXCL12 has a 10-fold higher affinity for ACKR3 than CXCL11 (Kd = 0.4 nM vs. 4 nM, respectively)[65,108].

A recent study has investigated the structural basis of the interaction between ACKR3 and its endogenous ligand CXCL12[109]. Consistent with the previously described two-step model (see page 11), the N-terminal domain of the receptor binds to the N-loop and 40s loop of the chemokine, then the N-terminus of the chemokine interacts with the second extracellular loop and trans-membrane domain pocket of the receptor. Additionally, the authors showed that the conformational changes of ACKR3 upon activation are strikingly similar to those observed for other GPCRs.

Partial proofs of a possible binding of adrenomedullin to ACKR3 have also been obtained[110]. Although a possible cross-talk between both proteins has been shown[111], further and more precise binding studies are needed before adding adrenomedullin to the ACKR3 ligand list. Likewise, though a functional link between ACKR3 and Macrophage migration-Inhibitory Factor (MIF)[112], the ligand of CD74, has been suggested, further studies are needed for confirming the direct binding of MIF to ACKR3.

Some ACKR3 ligands were also synthetized such as CCX773, CCX771, CCX451 and CCX754. Originally they were all classified as antagonists[71,113,114]. However, when these molecules were tested, ACKR3 was thought to be a silent receptor. Not surprisingly, at least one of them, CCX771, was later identified as a potent agonist for β-arrestin recruitment[115]. Despite this agonistic effect the CCX771 compound can also be considered as a functional antagonist[116] due to its ability to inhibit CXCL12 induced CXCR4 mediated chemotaxis. Further experiments should be conducted with the other molecules for assessing their actual pharmacological profile. However, in this manuscript all “antagonists” will be considered as antagonists when no proof of agonism is provided.

1.2.2.2.1 ACKR3 EXPRESSION

The first pioneering study aimed at mapping ACKR3 expression showed that ACKR3 is expressed in astrocytes, neutrophils, kidney, spleen and heart of mice[117]. ACKR3 mRNA expression in kidney was confirmed using *in situ* hybridization[118]. The receptor is expressed in the ureter, the region of the renal capsule, immature/mature glomeruli of kidneys from E12.5 and E14.5 mice. ACKR3 expression in the heart was confirmed using ACKR3$^{-/-}$ mice. Although the gene deletion was lethal for more than the 95% of the new-born mice, the survivors exhibited severe abnormal heart formation[119]. In wild type mice, the expression of ACKR3 in the endothelial layer of the forming heart (E=9.5) and in the microvasculature of the myocardium and valves (from E=14.5) was confirmed using *in situ* hybridization[119].

Consensus on the expression of ACKR3 in spleen has not yet been reached. In fact, immunohistochemistry on mouse, rat and human spleen revealed that ACKR3 is expressed only in B cells of the marginal zone of the rat and not in human or mouse. These results were confirmed by flow cytometry and by β-galactosidase enzymatic staining of spleen sections from ACKR3$^{+/lacZ}$ mice[120]. In contrast with these results, Wang *et al*[114] and others[121,122] observed ACKR3 expression in mouse splenic marginal zone B cells. These different results might be due to the different protocols used in cell *ex vivo* isolation that could have affected ACKR3 expression.

Contrasting results were obtained regarding ACKR3 expression by peripheral blood cells. In fact, ACKR3 was found in primary T cells[65,123] and B cells[124]. On the other hand, other studies failed to detect ACKR3 in T cells[125] or human lymphocytes[126]. However, in the latter study the authors failed to detect CXCR4 expression on leukocytes, which express high CXCR4 levels, raising doubts on the quality of the data. In addition to B and T cells, platelets isolated from healthy volunteers and patients suffering from both acute coronary syndrome and stable coronary artery disease express ACKR3, as shown by Western Blot, immunofluorescence and flow cytometry[127,128].

ACKR3 was also detected in human placenta[129], normal endometrial stromal cells[130], marmoset and human testes[131], human umbilical cord venous endothelial cells[132] and mouse limb muscles[133].

1.2.2.2.1.1 ACKR3 EXPRESSION IN THE CENTRAL NERVOUS SYSTEM

After the pioneering study that detected ACKR3 in astrocytes[117], additional groups of investigators identified the receptor in several areas of the Central Nervous System (CNS) both during development and in adulthood, suggesting an important role of this receptor for the development and functions of the CNS (see Table 3 for detailed information on ACKR3 expression in different species and different ages). ACKR3 expression was found to increase between E14 to E18 in rat and then to dramatically decrease after birth[134]. Different groups have consensually found ACKR3 in several cellular populations, namely neurons, astrocytes, endothelial, neuronal and oligodentrocyte progenitor cells[134–137]. Regarding the neuronal sub-populations Cajal-Retzuis neurons, GABA-ergic neurons, interneurons and olfactory tubercle neuron precursors express ACKR3. GLAST-positive as well as GFAP-positive and Bergmann glial cells were also found to express ACKR3. Immunohistochemistry performed on human brain slices showed that 89% of the cells positive for ACKR3 in both cortex and hippocampus were mature neurons[138]. However, the remaining 11% of the population was not investigated.

Species	Stage	Quantification	Structures	Cell Type	Ref
Rat	Adult	mRNA	Dentate gyrus, CA3 pyramidal cell layer, cortex, ventral striatum thalamus hypotalamaus	Neurons (pyramidal and GABAergic)	135
			Blood vessels	Endothelial cells	135
			Choroid plexus, wall lateral ventricle	Non neuronal (GLAST-positive astrocytes)	135
	E14-E18	mRNA	Marginal zone	Cajal-Retzius neurons	134
	E15-E17	mRNA	Appearance in the cortical plate (lateral and medial part)	Cortical plate neurons	134
	E18	mRNA	Appearance in the ventricular and subventricular zone		134
	Late-embryonic and postnatal	mRNA	Telencephalon (germinative zone, medial ganglionic eminences and caudate putamen)	Migrating GABA-ergic precursors	134
			Scattered throughout brain. Intense staining in the subventricular zone, granular layer of the dentate gyrus and hippocampal subfield CA3	GABAergic (high expression) and pyramidal (low expression) neurons.	134
			Corpus callosum, cortex, striatum.	GLAST-positive astrocytes	134
			Cerebellum	Bergmann glial cells	134
Mouse	E11.5	mRNA	Medial ganglionic eminence (ventricular and subventricular zone), lateral ganglionic eminence (ventral part)	Cajal-Retzius neurons	136
	E12.5	mRNA	Ganglionic eminence and ventral pial surface	Cortical interneurons and olfactory tubercle neuron precursors (Cajal-Retzius and subplate)	136
		mRNA	Subventricular an marginal zone	Immigrating cortical interneurons	136
	Postnatal	mRNA	Striatal subventricular zone		136
		Protein	Blood vessels	Endothelial cells	137
	Adult	Protein	Ventral striatum (nucleus accumbens), basal ganglia (globus pallidus), cerebral cortex (layer IV-V of the parietal cortex), hippocampus (subgranular layer, molecular layer, pyramidal layer, oriens layer and the hilus), hypothalamus (ventromedial hypothalamic and supraoptic nucleus), cerebellum (Purkinje cell layer).	Neurons, astrocytes and neuronal stem cells	137
		Protein	Subventricular zone	Cells morphologically resembling migrating oligodendrocyte progenitors	137
Human	Adult	Protein	Cortex and hippocampus	89% (MAP2-positive neurons), 11% remaining not investigated	138

Table 3 **Table summarizing the ACKR3 expression profile in the CNS.**

1.2.2.2.2 ACKR3 SIGNALLING: FROM A "SILENT" TO A "TALKATIVE" RECEPTOR

Since the discovery of ACKR3, its signal transduction properties and functions have been animatedly discussed. Although ACKR3 has been tainted with the reputation of being merely a decoy and silent receptor[49], undisputable and accumulating evidence have shown that this receptor activates intra cellular signalling pathways and plays key roles in several important physiological processes, such as cell migration, proliferation and trans-endothelial migration.

1.2.2.2.2.1 ACKR3 AS SILENT DECOY RECEPTOR

Although ACKR3 expression was found to be essential for *in vivo* migration of zebrafish primordial germ cell[49] the receptor was originally described as a silent receptor unable to activate any downstream signalling upon CXCL12 or CXCL11 binding (**Figure 4**). This idea rose from two early studies where the authors failed to observe any ACKR3-operated calcium mobilization[108] or PIK3 activation[49].

ACKR3 function was limited to the shaping of the chemokine gradient by binding with CXCL12 or CXCL11 and concomitant internalisation[124] (**BOX 3**). Repression or inhibition of ACKR3 would lead to an absence of gradient, which would result in the disruption of CXCR4-dependent migration.

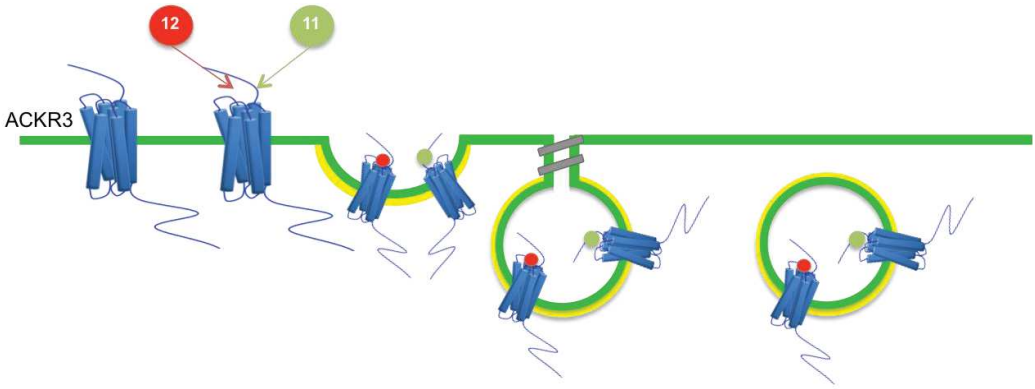

Figure 4 ACKR3 as decoy receptor. ACKR3 was originally described as decoy receptor, able only to bind CXCL12 and CXCL11 and internalise without activating any intracellular signalling cascade. This agonist-dependent internalisation would result in a lower extracellular chemokine concentration.

1.2.2.2.2.2 ACKR3 AS ATYPICAL CHEMOKINE RECEPTOR

The simplistic view of ACKR3 as a silent receptor was overcome with the discovery that the receptor signals through β-arrestins[139]. Using co-localization techniques ACKR3 was found co-localizing with β-arrestin-2 upon stimulation with CXCL12 and

11 in transfected HEK-293 cells. In the same study down-regulation of either β-arrestin-1 or 2 inhibited CXCL12 and CXCL11 induced ACKR3- dependent migration. Since ACKR3 was unable to trigger calcium mobilization, as in the aforementioned studies, it was concluded that ACKR3 signals only through β-arrestins and not G proteins. In later studies it has been shown that β-arrestins are recruited to the C-terminal domain of the receptor[140–142] that is de-ubiquinated upon stimulation[142].

BOX 3 ACKR3 internalisation

ACKR3 C-terminal domain was shown to be involved in its internalisation since two C-terminal truncating mutants, lacking the last 16 and 40 AA, were characterized by lower constitutive and ligand-induced internalisation[141]. In addition, expression of chimera ACKR3 whose C-terminal domain is switched with the CXCR4's one diminished internalisation[140]. Internalisation that is dynamin-dependent since ACKR3 does not internalise in HEK-293T cells expressing dominant negative K44A dynamin[141] or cells treated with the dynamin inhibitor Dynasore[143]. In addition, both mutants also displayed less interaction with β-arrestin2. Another article from the same group showed that ACKR3 internalisation is dependent on β-arrestin2 and not β-arrestin1[143]. In the same article ACKR3 co-localized with Rab7 and lysosomes after 30 min challenges with CXCL12, indicating that the receptor is trafficked to late endosomes, leading to its subsequent degradation[143]. The pivotal role played by β-arrestins in ACKR3 internalisation was confirmed by a work from a different group where simultaneous suppression of both β-arrestin1 and 2 completely inhibited CXCL12-mediated ACKR3 internalisation[142]. Inhibition of clathrin with sucrose also inhibited ACKR3 internalisation[142,143]. Both phosphorylation[140] and de-ubiquitination[142] of the receptor regulate ACKR3 internalisation.

Consistent with engagement of β-arrestin-dependent signalling by ACKR3, subsequent studies showed ACKR3 and β-arrestin-dependent ERK1/2 phosphorylation upon receptor activation in melanocytes[144], transfected HEK-293 cells[141,142] and microglia[145].

CXCL12 dose-dependently stimulates AKT and ERK1/2 phosphorylation as well as PKCζ/λ in primary cultures of postnatal rat cortical astrocytes[146]. On the other hand, it fails to activate p38 and PKCα/β. Inhibition of either CXCR4 (by AMD3100) and ACKR3 (by CCX754) completely impairs engagement of all these pathways suggesting that both receptors are involved in the CXCL12 responses. Furthermore, invalidation of ACKR3 using RNA interference abrogates CXCL12 signalling. Interestingly, CXCL12 triggers only phosphorylation of AKT and ERK1/2 in embryonic mouse primary cultures, whereas PKCs were not activated. Since ACKR3 was expressed at comparable levels to that measured in rat cultures, it suggests inter-species or age differences in ACKR3 signalling. In addition, ACRK3 activation was linked to higher expression of the proliferative marker Ki67 in both cultures.

GRK2 but not GRK3, 5 or 6 was found to play a pivotal role in CXCL12-mediated activation of ACKR3 in astrocytes[147].

Expanding the signalling pathways activated by the receptor, ACKR3 increases the expression of Cyclin D1, D3 and E1 and decreases the expression of p27 in $CD34^+$ cells, thus altering cell cycle and increasing cell proliferation[148] (**Figure 5**). In addition to triggering ERK1/2 phosphorylation, ACKR3 increases the expression of Vascular endothelial growth factor A in endothelial cells[149].

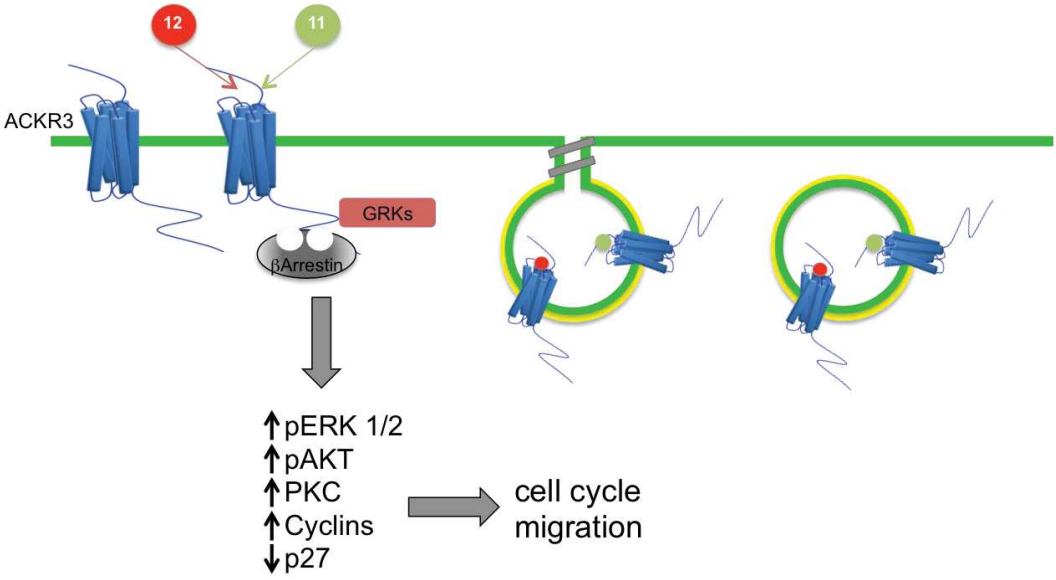

Figure 5 ACKR3 signals trough β-arrestins and GRKs. It is well recognized that ACKR3 is able to interact with GRKs and β-arrestins leading to increase phosphorylation status or altered expression level of downstream proteins involved in the control of migration or cell proliferation.

1.2.2.2.2.3 ACKR3 AND G PROTEINS: A CLOSED STORY?

Although several groups of investigators have shown that ACKR3 is unable to activate G proteins, few studies showed that the receptor might directly or indirectly interact with and activate G proteins. In fact, ACKR3 was found to constitutively recruit, but not to activate, $G\alpha_i$ proteins[150]. In addition, ACKR3 influences CXCR4-operated G protein activation when engaged in the CXCR4/ACKR3 heterodimers[119,150,151]. Furthermore, ACKR3 induces cAMP production after adrenomedullin activation,[110] suggesting a possible $G\alpha_s$ coupling of the receptor.

BOX 4 Pertussis Toxin (PTX)

Pertussis toxin (PTX) is the toxin produced by the whooping cough causing bacterium *Bordetella pertussis*. It is used in the investigation of $G\alpha_{i/o}$-dependent signalling pathways engaged by GPCRs due to its ability of irreversible ADP-ribosylate the $G\alpha_{i/o}$ subunits[152]. This does not preclude the coupling of G proteins with the receptor[150] but it avoids the dissociation of the $G\alpha i_{/o}$ subunit from the βγ complex and therefore the activation of the G protein.

In this context, astrocytes have been identified as a specific cell population where ACKR3 might activate G proteins. Specifically, ACKR3 activation by CXCL12 (40ng/ml) in membrane prepared from wild type rat and $CXCR4^{-/-}$ mouse primary astrocytes increased [^{35}S]-GTPγS binding. This increase was lost after the inhibition of ACKR3 expression by siRNA. CXCL12 induced a Calcium mobilization that was inhibited by CCX771, ACKR3 invalidation by RNA interference, Pertussis Toxin (**BOX 4**) and the PLC inhibitor U73122 suggesting that ACKR3 activation by CXCL12 induces a $G\alpha_{i/0}$ and PLC-dependent cytosolic Ca^{2+} increase. Inhibition of $G\alpha_{i/0}$ proteins also hindered the ACKR3-mediated phosphorylation of AKT and ERK1/2. CXCL12 mediates ACKR3-dependent migration, proliferation and internalisation that are also dependent of $G\alpha_{i/o}$ proteins. Although CXCL11 was unable to activate G proteins, it triggers β-arrestin2-dependent AKT and ERK1/2 phosphorylation via ACKR3 and not CXCR3 in rat cortical astrocytes[153], suggesting that ACKR3 can engage different signal transduction mechanisms upon activation by its cognate chemokine agonists CXCL12 and CXCL11.

These results do not pretend to overlook all the literature classifying ACKR3 as an atypical chemokine receptor in most of the cellular contexts. However, they raise the interesting possibility that in specific cellular contexts, where not yet identified specific and necessary partners are expressed, ACKR3 might activate G proteins.

1.2.2.2.2.4 ACKR3 AS A TALKATIVE RECEPTOR

Discovered as a silent receptor unable to activate any intracellular signalling, ACKR3 later became an atypical chemokine receptor unable to activate G proteins but capable of recruiting β-arrestins and activating their downstream signalling cascades. The evolution continued when ACKR3 was shown to interact with other proteins including the other CXCL12 chemokine receptor CXCR4.

ACKR3 and CXCR4 interconnection might not only be limited to the sharing of CXCL12 binding but also involves physical interaction between both receptors. First evidence of a possible constitutive hetero-dimerization between the two receptors

was provided in 2007 by FRET and co-precipitation techniques performed in transfected HEK-293 cells. The distinct signalling profile of the dimer was evidenced by the fact that it evokes a larger Ca^{2+} increase and a slower ERK phosphorylation, compared with CXCR4 alone[119]. These first pieces of evidence of heterodimerisation were elegantly confirmed[150] using BRET approaches in transfected HEK-293 cells where ACKR3 forms constitutive and ligand-modulated heterodimer with CXCR4 as well as a homo-dimer with itself. In addition, although ACKR3 on itself is unable to activate calcium mobilization in HEK-293 cells, it reduces the potency of CXCL12 to trigger calcium mobilization upon activation of CXCR4. Accordingly, ACKR3 expression modifies the ability of CXCR4 to recruit and activate $G\alpha_i$ proteins. The possible cross talk between ACKR3 and CXCR4 to activate G protein was confirmed by experiments showing that ACKR3 expression reduces the potency of CXCL12 to inhibit cAMP production[154]. In addition, the ACKR3/CXCR4 heterodimer interacts more efficiently with β-arrestin (with or without CXCL12 stimulation) than ACKR3 alone. Corroborating these findings, the co-expression of CXCR4 and ACKR3 leads to more sustained ERK, Stress-activated protein kinase and p38 constitutive phosphorylation (only ERK phosphorylation was induced by CXCL12) compared to that measured in cells expressing each receptor alone. Silencing of β-arrestin2 expression reversed this effect. Although the existence of ACKR3/CXCR4 heterodimers is well proven in transfected cell lines, their identification in cells or tissues endogenously expressing the two receptors is still lacking.

CXCR4 is not the only protein able to interact with ACKR3. Using PLA and co-localization strategies, ACKR3 was shown interacting with the Epithelial Growth Factor Receptor (EGFR) in breast cancer cell lines but not in normal tissues[155]. β-arrestin2 is involved in this interaction. ACKR3 phosphorylates EGFR and participates in the EGFR mediated ERK phosphorylation via a β-arrestin2-dependent mechanism. A subsequent study showed that β-arrestin2 is a negative regulator of ACKR3-mediated EGFR activation and nuclear translocation[156].

EGFR is not the only receptor interacting with ACKR3 as also the MIF receptor CD74 weakly interacts with ACKR3[112]. Moreover, ACKR3 co-localizes with PECAM-1, the cell adhesion molecule required for leukocyte transendothelial migration in human coronary artery endothelial cells[157]. Using a Membrane Yeast two Hybrid assay (MYTH) screen, ATP13A2 was identified as a putative ACKR3 interacting protein[95]. In a study aimed at characterizing the human interactome of 1,125 GFP-tagged proteins by Co-IP followed by MS analysis, ACKR3 was found to interact with the gap junction beta-2 protein GJB2, the probable E3 ubiquitin-protein ligase HECTD2,

the 54S ribosomal protein L4, mitochondrial MRPL4, different ATP synthases (ATP5H, ATP5B, ATP5A1, ATP50), ACKR3 itself, the caspase Separin ESPL1 and the Putative E3 ubiquitin-protein ligase UBR7[97].

1.2.2.2.3 ACKR3 PHYSOLOGICAL ROLES

The paramount importance of ACKR3 in life became clear with the discovery that 95% of mice ACKR3$^{-/-}$ die only one day after birth[119]. Consistent with its expression pattern, ACKR3 has been recognized to participate to the cardiovascular, reproductive, renal and neuron physiology[158].

In addition to the aforementioned role of ACKR3 in the migration of primordial germ cell[49] ACKR3 also influences the migration of T cells[65], vascular smooth muscle cells (in response to CXCL11)[139], human epidermal melanocytes (NHEM)[144], B-cells[159], microglia (in Experimental autoimmune encephalomyelitis)[145] and neurons. In 2011, two articles showed that ACKR3 expressed by migrating interneurons plays a pivotal role in their migration during embryonic brain development. Wang and colleagues[160] showed that conditional knock-out of ACKR3 in interneurons leads to neuronal laminar positioning defects similar to the ones observed in CXCR4$^{-/-}$ mice (migrating interneurons express also CXCR4). In both ACKR3 and CXCR4 conditional mutants more interneurons were found in the cortical plate and less are present in the marginal zone and sub-ventricular one *in vivo.* In the cortical plate, movements of interneurons from the two mutants exhibited opposite phenotypes compared to the wild type. ACKR3$^{-/-}$ interneurons were much less motile with a shorter leading process, whereas CXCR4-deficient neurons were highly motile with longer and complicated processes. *In vitro*, CXCL12 mediated migration was inhibited by the ACKR3 functional antagonist CCX771 and by the CXCR4 antagonist AMD3100 suggesting that both CXCR4 and ACKR3 are required for the correct migration. Importantly, AMD3100 did not exacerbate the ACKR3$^{-/-}$ phenotype *in vivo* indicating that the receptors have different functions. Using PTX the CXCR4$^{-/-}$ *in vivo* phenotype was mimicked. On the other hand, ACKR3 but not CXCR4 triggered phosphorylation of ERK1/2 in interneurons.

Also another study[161] confirmed that ACKR3 is necessary for correct migration of cortical interneurons. The authors suggested that ACKR3 is necessary for the fine tuning of CXCL12 concentrations (as confirmed in a following article[162]). Not only interneurons but also Cajal-Retzius neuron localization strongly depends on ACKR3 since in ACKR3$^{-/-}$ E14.5 mice Cajal-Retzius cells are detected in the lateral and

dorsal parts of the dorsal pallium instead of being in the subpial zone as in control animals[163]. These results were also reproduced by pharmacological inhibition of ACKR3 in wild type animals. ACKR3 also mediates neurogenesis of glutamatergic neurons including granule neurons, elicited by CXCL12[164].

ACKR3 functions are not limited to promoting migration but include transendothelial migration and adhesion of renal multipotent progenitors[165] and human brain microvascular endothelial cells[166], oligodendrocyte maturation[167,168], transvascular entry of leukocytes into the central nervous system[169] and proliferation of $CD34^+$ cells of the hematopoietic system[148].

Therefore regarding the CNS, ACKR3 has been linked with both neuronal and microglial migration as well as oligodentrocyte maturation. However, its functions in astrocytes are still poorly characterized.

1.2.2.2.4 ACKR3 PATHOLOGICAL ROLES: RELEVANCE IN CANCER

The prominent role of ACKR3 in pathological contexts was immediately clear since the discovery that the receptor is a co-receptor for the HIV entry[170]. Paradoxically, this was the first “function” attributed to the receptor.

After this first discovery, AKCR3 expression was found to be up-regulated during inflammation, infection, ischemia and neoplasia. ACKR3 expression is increased in inflammatory bowel disease, encephalitis rheumatoid arthritis, acute renal failure, Epstein-Barr virus type I infection, permanent middle cerebral artery occlusion and cancer[69].

ACKR3 has been detected in more than 15 cancer types, namely hepatocellular carcinoma[171,172], renal cancer[173], ovarian cancer[174], papillary thyroid carcinoma[175–177], osteosarcoma[178], brain mestastases[179], lung cancer[180,181], prostate cancer[182,183], lymphoma[184,185], gastric cancer[186], breast cancer[187–190], melanoma[191], esophageal[192] and cutenous[193] squamous cell carcinoma, pancreatic cancer[194], colon cancer[195], cervical cancer[196], bladder cancer[197] and glioma (detailed in the next chapter).

ACKR3 expression is induced by the pro-inflammatory cytokines TGFβ1[181], IL-8[183] and IL-6[192] as well as by the Zinc finger protein GLI1[198] and oestrogen (E2)[199]. Since IL-8 can also be induced by ACKR3[197], a possible positive loop might exist between the two proteins in cancer context. miRNA100 suppressed ACKR3 expression[177,186].

In contrast to its induction by pro-inflammatory cytokines, ACKR3 was not induced by hypoxia in colon cancer[200].

Although the heterogeneity of cancer models used in these studies produced heterogeneous results, there is consensus on few ACKR3-regulated signalling pathways. In fact, ACKR3 principally regulates two pathways: the MAPK ERK1/2 pathway [155,173,174,183,193,197] and the mTOR[173,178,193,194] pathway, leading to the phosphorylation of P38, AKT, JNK and PI3K. In addition, ACKR3 induces and activates metalloproteinase-9 (MMP-9)[174,178], to modulate the expression of proteins involved in the regulation of cell cycle (cyclin A and B1, Cdk2 and 4, p21 and p57)[155,183,201] as well as to induce N-cadherin and repress E-cadherin expression[181,197]

Through the activation of these pathways ACKR3 has been linked with increased invasion, adhesion and tumour growth of several cancer types.

Both expression and activation of ACKR3 have been correlated with cancer progression. In fact, its genetic suppression inhibited tumour growth invasion and adhesion in several studies [171,178,181,183,184,202,203]. In addition, its pharmacological inhibition by CCX771 (biased agonist but functional antagonist[115]) reduced CXCL12- and CXCL11-mediated ERK1/2 phosphorylation[178,204] (also in CXCR4$^{-/-}$ cells [205]) and AKT phosphorylation[148] resulting in lower proliferation[187,206,207], invasion [160,184,185,187,206,208], adhesion[175] of cancer cells.

1.2.2.2.5 ACKR3 PATHOLOGICAL ROLES: FOCUS ON GLIOMA

The term glioma encloses a variety of intrinsic Central Nervous System (CNS) tumours. These tumours were traditionally classified based on the presumed cells of origin (astrocytoma, oligodendroglioma, oligoastrocytoma) and the extension of infiltration (diffuse or non diffuse glioma). Regardless of the sub-classification, gliomas are divided in three malignancy grades (II, III and IV) considering their mitotic activity, necrosis and florid microvascular proliferation. Glioblastoma is the most malignant one (grade IV) and it is categorized in either “secondary” or “primary” depending on whether there are evidence of a progression from a lower grade glioma. However, in 2016, the WHO introduced a genotypic classification based on the presence of recurrent point mutation in isocitrate dehydrogenase 1 and 2 (IDH1/IDH2), dividing glioblastoma in glioblastoma-IDH-wild type and glioblastoma-IDH-mutant. Interestingly, the majority of “secondary” glioblastoma are IDH-mutants, whereas “primary” glioblastoma are typically IDH-wild type[209]. Recently, it was

proposed that ACKR3 also influences the prognosis of human glioma[210] depending on the IDH classification. In fact, ACKR3 expression in tumour-associated vessels improves the prognosis in IDH1-WT glioma whereas it has opposite consequences in the IDH1-mutant. In addition, mRNA as well as protein levels of ACKR3 were found to be up-regulated[211] and to positively correlate with WHO grade in several studies[210,212–214].

Not only ACKR3 expression levels change accordingly with WHO grades but also its localization. In fact, in grade II glioma, ACKR3 is mainly expressed in cancer cells. In grade III, it is present primarily in tumour vascular endothelial cells and only marginally in cancer cells. In glioblastoma, ACKR3 was found in cancer cells in pseudo-palisades near necrotic areas and in the tumour endothelium[214].

Overall, an increasing body of evidence has been accumulating showing high ACKR3 expression in gliomas and glioma cell lines. Although its role in cancer progression has not yet been fully characterized, some studies have been correlating ACKR3 with glioma drug/radio resistance, glioma cell proliferation and angiogenesis.

1.2.2.2.5.1 DRUG/RADIO RESISTANCE

Standard care for the treatment of WHO grade III and IV gliomas consists in surgery followed by chemotherapy using the alkylating agent temozolomide (TMZ) that can be combined with intermediate-frequency alternating electric fields[215]. However, glioma exhibit both radio[216] and drug resitance[217] making the current therapies completely ineffective with a median survival ranging from 12 to 16 months[218] after diagnosis. Few studies observed a role of ACKR3 in these acquired resistances. In fact, CXCL12 (1 nM) reversed the anti-proliferative effect of non-toxic concentrations (20-100 µg/ml) of TMZ in C6 rat cells isolated from murine glioma. Accordingly, CXCL12 (1 nM) also reduces TMZ-induced apoptosis[219]. Inhibition of ACKR3 by CCX771 after irradiation (IR) provokes tumour regression in nude mice injected with U251 glioma cells. In addition, treatment with the ACKR3 antagonist CCX662 was shown to extend the survival of rats with ethylnitrosourea (ENU)-induced brain tumours after irradiation[213]. In a more aggressive model, consisting in the injection of C6 glioma cells in rats, only irradiation in conjunction with CCX662 extended survival[213]. Although CXCL12 did neither influence proliferation nor migration of glioma A764 and U343 cells, it decreases apoptosis after exposure to camptothecin and temozolomide[212].

1.2.2.2.5.2 PROLIFERATION AND ANGIOGENESIS

Gliomas are characterized by extensive vascularization[220] and they are composed of cells with high proliferative state. Contradictory results are emerging regarding the role of ACKR3 in the proliferation of glioma cells. In fact, in the U373 GBM cell line and human foetal astrocytes, its activation by CXCL12 (200 ng/ml for 48 hours) was found to promote cell proliferation[211]. On the other hand, CXCL12 did not influence proliferation nor migration of A764 and U343 cells[212]. Moreover in co-cultures of U87 with HBMEC, the receptor was found to have no trophic effect, in contrast to CXCR4[113].

Long non-coding RNAs (lncRNAs) X-inactive-specific transcript (XIST) is up-regulated in glioma endothelial cells[221]. Down-regulation of XIST represses expression of ACKR3 and tight junctions (ZO-1 and 2) resulting in less angiogenesis and increased blood-tumour barrier permeability.

1.3 CONNEXINS

Gap Junctions (GJs) ensure intercellular communication by forming a channel that allows exchange of small molecules or ions between two adjacent cells. In vertebrates, these channels are formed by connexins (Cxs). As summarised in

Table 4 twenty-one human genes and twenty mouse genes encoding for connexins have been identified[222]:

Human		Mouse	
Gene symbol	Protein name	Gene symbol	Protein name
GJB1	CX32	Gjb1	Cx32
GJB2	CX26	Gjb2	Cx26
GJB3	CX31	Gjb2	Cx26
GJB4	CX30.3	Gjb4	Cx30.3
GJB5	CX31.1	Gjb5	Cx31.1
GJB6	CX30	Gjb6	Cx30
GJB7	CX25	-	-
GJA1	CX43	Gja1	Cx43
GJA3	CX46	Gja3	Cx46
GJA4	CX37	Gja4	Cx37
GJA5	CX40	Gja5	Cx40
-	-	Gja6	Cx33
GJA8	CX50	Gja8	Cx50
GJA9	CX59	-	-
GJA10	CX62	Gja10	Cx62
GJC1	CX45	Gjc1	Cx45
GJC2	CX47	Gjc2	Cx47
GJC3	CX30.2/31.3	Gjc3	Cx29
GJD2	CX36	Gjd2	Cx36
GJD3	CX31.9	Gjd3	Cx30.2
GJD4	CX40.1	Gjd4	Cx39
GJE1	CX23	Gje1	Cx23

Table 4 Table summarizing the connexin genes identified. The genes are identified starting with "GJ" (for Gap Junction), whereas the most common nomenclature uses "Cx" (for connexin) followed by a number indicating the predicted molecular mass in kDa of the protein.

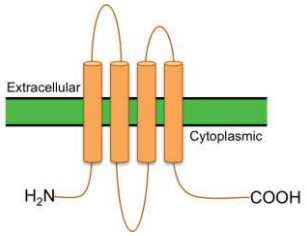

Figure 6 General Cx schematic topology.

Although differing in molecular weight, all connexins share the same topology consisting in two highly conserved extracellular and one cytoplasmic loops, four transmembrane domain and cytoplasmic N- and C-terminal domains[223] (Figure 6). Six connexins

oligomerize together to form a hemichannel called connexon. After oligomerization of connexins, the hemichannels are inserted into the plasma membrane. When two hemichannels present on adjacent cells come to proximity they can dock head-to-head together to form a gap junction. Cx belonging to the β-family (GJB1-7) oligomerize in hexameric channels prior to transport from the endoplasmic reticulum to the Cis-Golgi apparatus, whereas the other connexins oligomerize only in the trans-Golgi apparatus[224]. Gap junctions are divided in two classes: homotypic and heterotypic Gap junctions (**Figure 7**). In the former, the same types of connexins form the channels while in the latter the connexins are different. The hemichannels formed by different connexin types are defined as heteromeric in contrast to hemichannels formed by the same connexin that are homomeric[225].

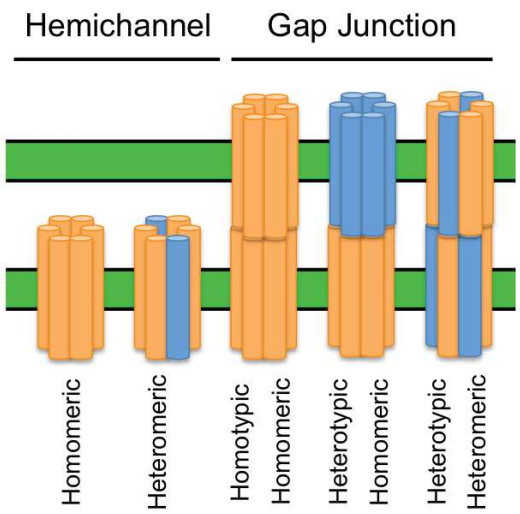

Figure 7 Homomeric vs. heteromeric connexins. In blue and orange two different Cx subtypes are illustrated.

The channel's central pore allows the diffusion of small molecules between interconnected cells that are coupled both electrically and chemically. Four models have been proposed for the opening and closure of the channel (represented in **Figure 8**):

A. In the subunit rotation model, the twelve connexin subunits simultaneously rotate for the opening and closure of the channel[226]. This model has been proposed based on the conformational changes following Calcium treatment that leads to Cx closure.
B. In the plug-gating model, the N-terminal domains of the assembled connexins form a gate in the pores. The pores are opened by conformational changes of the N-terminal domains of both hemichannels. This mechanism is involved in the gating of connexin channels by transjunctional voltage[227].
C. Another model is the loop-gating one that is primarily involved in the closure of unopposed hemichannels. The closure of the channels is achieved by narrowing the channel pore size with a movement of the transmembrane domain and extracellular loop 1[228].

D. The particle-receptor model was proposed based on the evidence that the C-terminal domain of Cx43 is necessary for the closure of the channel at low pH. In fact, truncation of the C-terminal domains completely hindered the acidification-induced channel closure. The authors suggested that the C-terminal domain forms a gating particle that closes the channel trough its interaction with the second half of the cytoplasmic loop in response to pH changes[229].

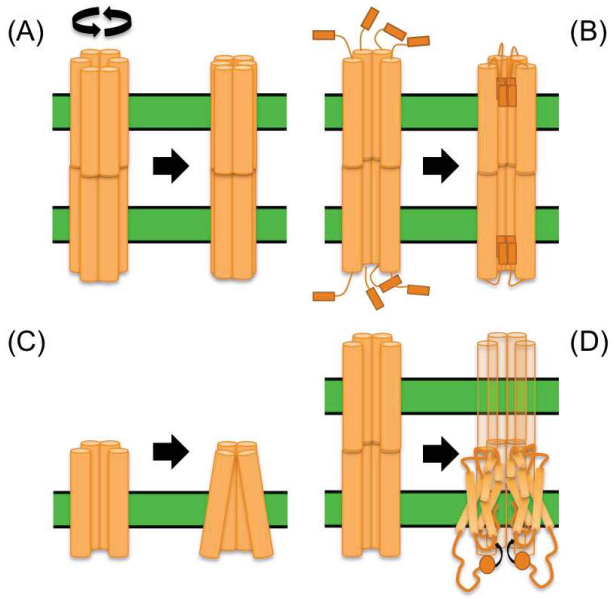

Figure 8 Mechanisms of Cx closure. (A) Subunit rotation model. (B) Plu-gating model. (C) Loop-gating model. (D) Particle-receptor model.

Opening and closure will determine the passage of ions and small molecules (<1KDa) from one cell to the other. Connexins are differently permeable to monovalent ions including Rb^+, Cs^+, K^+, Na^+ and Li^+[230] as well as second messengers and other cytoplasmic molecules such as ATP, ADP, AMP, Adenosine, Aspartate, cAMP, cGMP, Ca^{2+}, Glucose, Glutamate, Glutathione, IP3, NAD^+, Prostaglandin E2 and miRNA[231]. Interestingly, there are dramatic connexin-specific differences in the channel permeability for different molecules. For example, there is a 3.4-fold difference between ADP/ATP and glutamate in Cx43 junctional channels and a 33-fold difference between Cx43 and Cx36 junctional channels in the permeability to cAMP.

As earlier reported, connexins are transported to the plasma membrane as hemichannels. Originally, hemichannels were thought to remain closed. This notion started to be challenged by the discovery that Cx hemichannels could be opened either following lowering the extracellular calcium concentration[232] or a large

depolarization[233]. Recent studies have demonstrated a functional activity of hemichannels in different cell types such as glial cells where they mediate the release of ATP, glutathione, glutamate and aspartate in the extracellular space[234] even if the opening probability at resting membrane potential and normal concentration of the extracellular divalent cations is low[235].

Diffusion of molecules between adjacent cells is not the only role of connexins, which can also influence cell growth and migration in a channel-independent fashion. In fact, studies focusing principally on Cx43 have shown that its expression inhibits cell growth even in the absence of gap junctional communication[236]. These channel-independent effects were later attributed to the Cx43 C-terminal domain as its sole expression inhibited cell growth of neuroblastoma as efficiently as the entire Cx43 protein[237]. Cx43 C-terminal domain also increased cell migration *via* the activation of P38[238] and cytoskeletal rearrangements[239]. Taken together, these results indicate that the Cx43 C-terminal domain alone decreases cell growth and promotes migration. However, other studies challenged these results, suggesting that the situation might be more complex than initially imaginated[240].

1.3.1 Connexin mutations and pathology

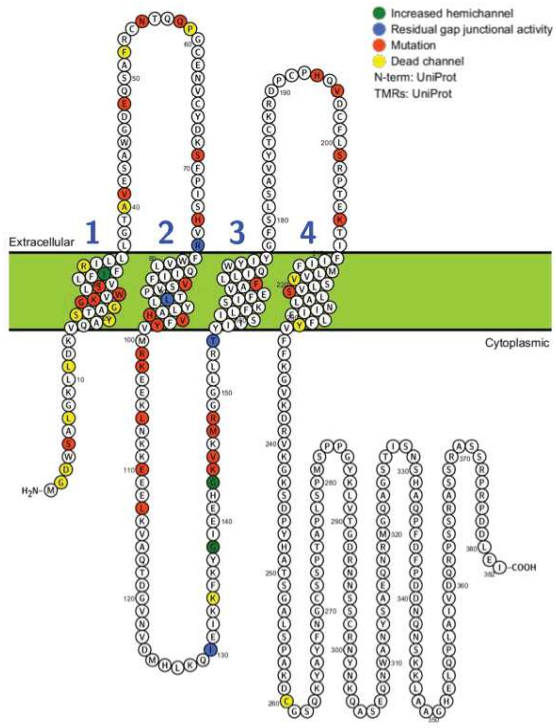

Figure 9 Cx43 mutations involved in ODDD occurrence. Adapted from [242].

Mutations in ten different connexin genes have been connected with twenty-eight different diseases (connexinopathies)[241]. Eight of these diseases have been linked with mutations in the Cx26 gene that cause non-syndromic and syndromic deafness as well as skin disease. Mutations in Cx30 and Cx31 genes provoke non-syndromic hearing loss or skin disease. Cx30.3 mutations are associated with skin disease. Cx32 mutations cause peripheral neuropathy. Cx40 mutations cause atrial fibrillation or standstill. Cx46 and Cx50 mutations cause

cataract, whereas Cx47 mutations cause leukodystrophy, spastic paraplegia, or lymphedema.

Seventy-three Cx43 mutations cause autosomal dominant oculodentodigital dysplasia (ODDD)[242], a developmental disorder characterized by webbing of skin between fingers, small eyes and craniofacial and dental abnormalities. The most severe is a non-sense mutation in position 33 of Cx43. Curiously, although patients do not have Cx43 hemichannels or channel function, the mutation is not lethal[243]. One Cx43 mutation (Arginine to Glutamine in position 239)[244] causes the autosomal recessive craniometaphyseal dysplasia (CMDR) characterized by progressive thickening of bones in the skull and abnormalities at the ends of the long bones of the limbs. The substitution of Glutamic acid with Lysine in position 42 was found to be lethal in infants[245]. Finally, Cx43 mutations were also associated with hearing loss and skin disorders[242]. Surprisingly there was no consensus between diseases and loss or gain of function of Cx43. In fact, ODDD-linked mutations are correlated with loss of as well as increased Cx43 hemichannel activity or Cx43 with residual gap junctional communication activity (see **Figure 9**). Accordingly, Cx43 does not tolerate virtually any change for preserving all its functions since different single-point mutations widespread along the Cx43 all have a severe impact on connexin functionality and health.

1.3.2 Methods for studying gap junctions and hemichannels

Since gap junctions are permeable to ions and small molecules, their activity can be investigated measuring the passage of current or tracer between coupled cells.

1.3.2.1 Electrophysiological measurement of the Junctional Current

The first recording of the current passing between cells coupled through gap junctions was made using the dual whole-cell patch clamp method between rat lacrimal gland isolated cells. In that case, each cell was implanted with two microelectrodes[246]. Nowadays, the most widely used electrophysiological method to record junctional current is the double whole-cell voltage-clamp with one patch pipette positioned on each coupled cell. In this case, the two cells are voltage-clamped at a potential close to the average resting membrane potential (source VA and VB). A junctional current (Ij) is triggered by applying a step-wise increasing transjunctional voltage in one of the two cells (referred as cell C1 in the **Figure 10**). If the two cells are electrically coupled, a current (I2) is recorded in cell C2. It is of

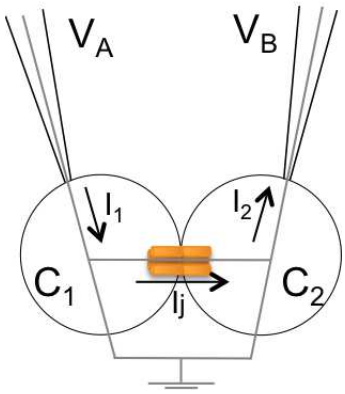

Figure 10 Schematic representation of double whole-cell voltage clamp. VA & VB = source, I1 & I2 = electric current, C1 & C2 = cellule, Ij = junctional current.

equal magnitude but opposite sign of the junctional current (Ij), in order to maintain constant the cell potential. The junctional conductance (Gj) can be calculated by simply dividing the junctional current by the amplitude of the voltage step applied to C1[247]. The main advantage of this technique is its exquisite sensitivity, which even allows the recording of activity down to a single channel level[248]. The main disadvantage is that analysis of electrical conductance is a time and labor-intensive technique.

Electrophysiological recordings can also be used for investigating hemichannel activity using voltage-clamp in the whole-cell configuration. In this case the goal is to record total and single channel current of isolated cells[249]. In addition hemichannels were found to have approximately twice the conductance of the corresponding gap junction channels[235].

1.3.2.2 TRACER DIFFUSION

Six techniques have been developing for assessing gap junctional communication using the diffusion of a tracer. Three of them differ in the way that the tracer is introduced into the cells. These are the scrape loading, microinjection and electroporation (**Figure 11**).

A. The most widely used method for assessing the gap junctional activity is the scrape loading technique. In this approach a confluent monolayer of cells is scraped in the presence of a membrane-impermeable, but gap junctional permeable, tracer. The tracer will enter the damaged cells and then diffuse to neighbouring cells trough gap junctions. The magnitude of the diffusion reflects the gap junctional activity. One of the most used tracers is the fluorescent Lucifer Yellow (LY) dye[250]. Gap junctional impermeable dyes, such as rhodamine-dextran, can be used for assessing the unspecific diffusion of Gap junctional permeable dyes. For the quantification of the diffusion, several methods have been used, including measurement of the area of diffusion[251], the diffusional distance[252] and the distance at which the

fluorescence is halved[253]. The scrape loading technique has the advantage to be fast and convenient to study the gap junctional activity in a cell population. Intuitively, it is not appropriate for studying cells at low confluence and for studying connexins impermeable to dyes such as Cx45 that is impermeable to LY[254].

B. The microinjection is a more suitable technique for investigating the coupling of cells at low density. In this case, the tracer is injected in one single cell using a micropipette[255]. The dye then diffuses from one cell to the other and the number of neighbouring cells receiving the dye is quantified. Compared to the scrape loading technique, its lower invasiveness makes its suitable for studies of intact tissues[247]. Its main limitation is the possible bias introduced by visually counting dye-positive cells. In fact, cells could have a very different morphology and in addition the dye becomes more diluted the more it is diffusing.

C. The tracer can also be introduced into the cells via electroporation as proposed by Raptis *et al*[256]. A glass slide, half covered with an electric conductive material, is used for this experiment. Cells are grown on the glass slide in order that half of them are in contact with the conductive part. Then, an electric pulse is applied in the presence of the tracer. This transient pulse generates “pores” on the cellular membrane of the cells growing on the conductive part. The tracer penetrates the cells through these “pores” and then diffuses to the half of the cells growing on the non-conductive part of the glass slide. This method has the advantage to study gap junctional activity in a cell population as the scrape loading. Compared to the latter, it is less invasive. However, it is not suitable for cells, which poorly adhere on glass.

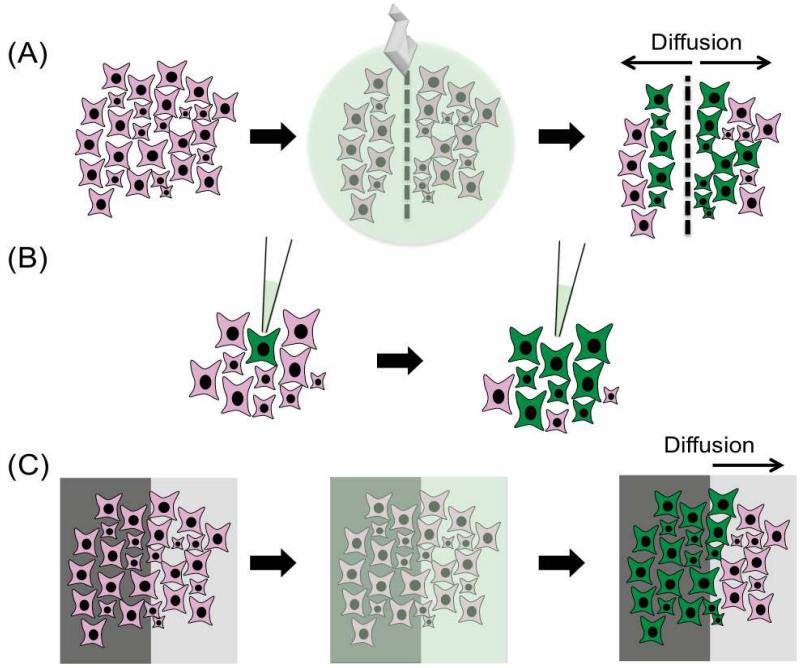

Figure 11 Tracer-based methods for the study of Cx activity. (A) Scrape loading method. (B) Microinjection. (C) Electroporation where the conductive surface is represented in dark grey.

Three other techniques employing a dye for the investigation of gap junctional activity are the Gap-FRAP, the preloading assay and the LAMP (Local Activation of Molecular Fluorescent Probe) (**Figure 12**). For all these assays cells are preloaded with the tracer.

A. In the former, cells forming a confluent monolayer are equally loaded with the tracer. A cell is then photobleached by a laser. After photobleaching, the tracer of a non-bleached neighbouring cell diffuses into the bleached one through Gap junctions. Monitoring the redistribution of the tracer as a function of time will give the gap junctional activity of the cells[256].
B. In the preloading assay, different from the Gap-FRAP where all cells are equally preloaded with the tracer, only a portion of cells are preloaded with the tracer[257]. These cells are then plated with unloaded cells. Again the passage of tracer from pre-loaded to unloaded cells is used as surrogate for quantifying gap junctional activity. This method is well suited for studying gap junctional communication between homogenous cell populations.
C. The LAMP is the most recent technique using a specific type of tracer defined as caged tracers[258]. These tracers have the characteristic to become fluorescent only upon irradiation with an UV beam. For this experiment cells are equally loaded with a caged tracer. Using an UV lamp the cage is removed and the tracer becomes fluorescent. The diffusion of the tracer is

then analysed. The advantage of this technique is its non-invasiveness and the ability of repeated measures on the same cells. In fact, after the diffusion reaches equilibrium, more tracer can be un-caged from the same cell and the measurement can be repeated.

Cx hemichannel activity can also be studied using tracers. In this case, cells are exposed to a solution of ethidium bromide. Its uptake by hemichannels is then registered using a fluorescence microscope and quantified[259].

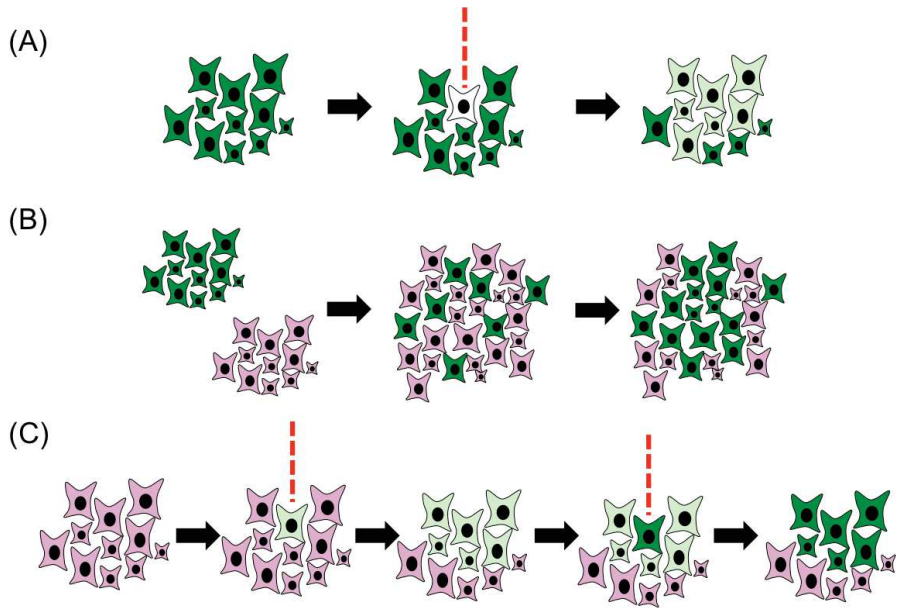

Figure 12 Preloaded tracer-based methods for the study of Cx activity. (A) GAP-FRAP method. (B) Pre-loading assay. (C) LAMP method.

1.3.3 Pharmacological tols

Generating specific pharmacological tools to modulate specific connexin subtypes and distinguish between gap junctional and hemichannel activity has been stimulating scientists for a long time. Since gap junctions are formed by two hemichannels the major difficulty was first to specifically target only hemichannel and not gap junction. The second major obstacle was then to specifically target a subtype of connexin that is structurally similar to the others. In the 80s, connexins were blocked using long-chain alcohols, volatile anaesthetics or glycyrrhetinic acid derivatives. However, all of them turned out to be unspecific. Nowadays, the most frequently used connexin inhibitor is carbenoxolone (CBX) that was shown to be a

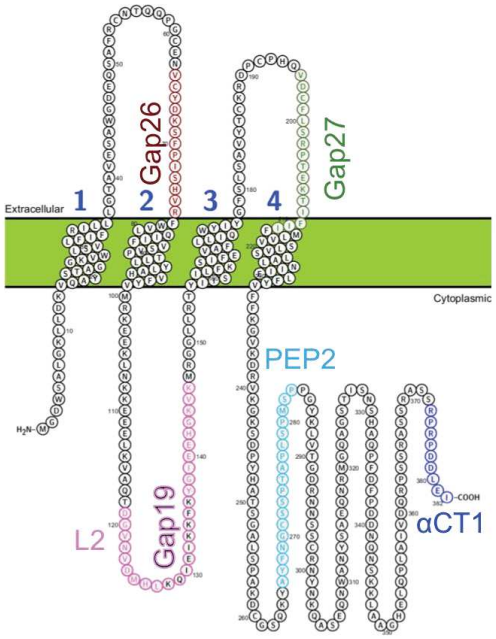

Figure 13 Cx43 amino acid sequence and schematic topology. The sequences used for the generation of the mimetic peptides are highlighted

potent and rapid inhibitor of gap junction activity both in cells[260] and in tissue slices[261]. However, CBX also alters voltage-dependent potassium and calcium channels, P2X7 purinergic receptor and NDMA-evoked currents[262]. In addition, CBX blocks all connexins without any specificity. Some degrees of specificity can be achieved using quinine and derivatives. Indeed, quinine inhibits Cx36, while Cx45 is only moderately affected and Cx26, Cx32, and Cx43 are not blocked[263]. However, since all these products block both gap junctional as well as hemichannel activities of connexins, they cannot be used for discriminating between them[234]. A cation, La^{3+}, was found to block hemichannels without affecting gap junctional activity in astrocytes[264]. However, it also blocks maxi-anion channel and Ca^{2+} channels[234].

BOX 5 Src

Src is a 60-KDa tyrosine kinase. Both Src expression and Src kinase activity are regulated in a variety of cancer types. Src is activated by a multitude of mechanisms including interactions with receptor tyrosine kinases and integrin receptors[265]. As it will be discussed later, Src interacts with and phosphorylates Cx43, disrupting its interaction with ZO-1 and triggering Cx43 internalisation[266].

In order to gain specificity, mimetic peptides against specific connexin sequences have also been generated (**Figure 13**). Since the two extracellular loops of connexin hemichannels dock together for forming a gap junction they were chosen as first target sequences for the generation of Gap26 and 27 peptides. These two peptides were therefore designed for blocking gap junctional activity without blocking the hemichannel one. However, both peptides were found to inhibit both hemichannels and gap junctions[267]. In addition, although they were designed based on Cx43 sequences, they also block Cx37[268]. Later on, less conserved intracellular connexin sequences were chosen as targets. That led to the design of the L2 peptide against the cytoplasmic loop of Cx43. As already mentioned, during connexin closure, the C-terminal tail of Cx43 interacts with the L2 sequence in the particle-receptor model; therefore, the L2 peptide was designed for

keeping Cx43 open. Unexpectedly, L2 was found to block Cx43 hemichannels[269] but not gap junctional activity of Cx43. Likewise, the Gap19 peptide designed against a sequence within the L2 domain was found to block hemichannels but not gap junctions[270]. The PEP-2 peptide designed against the interaction site between Src and Cx43 (**BOX 5**) was found to inhibit hemichannel activity[271,272]. Two peptides against the 10 and 9 C-terminal aminoacids of Cx43 able to block hemichannels activity were also generated[273]. The latter peptides named αCT1, also referred to as aCT1 or ACT1 in publications, have passed phase II clinical trials for wound healing[274]. The biotinylation technique also allows to discriminate between Cx gap junction and hemichannel activities[275–277]. Using a cell-impermeable amine-reactive biotinylation reagent, lysine residues present in the extracellular space are biotinlyated. In the case of Cx, only hemichannel present at the cell surface will be biotinylated[278], whereas engaged in gap junctions will remain non-biotinylated, since the three lysines are involved in the head-to-head docking of the two hemichannels. In addition, Cx in gap junctions and hemichannels can be separated based on their solubility in Triton X-100 [279]. Gap junctions are insoluble whereas hemichannels are soluble.

1.3.4 CONNEXIN 43 (CX43)

As it will be detailed in the “Results” chapter Cx43 was identified as a potential ACKR3 interacting protein. In the brain Cx43 and ACKR3 have overlapping biological functions in physio-pathological conditions and they are also co-expressed in cellular sub-populations. Therefore, the next chapters will focus on the expression and biological functions of Cx43 in the brain.

1.3.4.1 CX43 EXPRESSION

Cx43 is the most ubiquitously expressed member of the connexin family. It is highly expressed in the skin[280], heart[281] and brain. Neurons express several others connexins including Cx26, Cx30.2, Cx36, Cx45, and Cx57; with Cx36 being the principal one. Microglial cells express Cx43, Cx36 and Cx32. Oligodendrocytes express Cx32, Cx47, and Cx29 in vivo. Neuronal precursors express Cx26, Cx30, Cx40 and Cx43. Finally astrocytes express Cx43, Cx26, Cx30, Cx40, Cx45, and Cx46 with Cx43 being the most abundant one[234]. In astrocytes, the expression pattern of Cx43 changes during development. Before spreading throughout all the brain, Cx43 appears around E12 in radial glial cells. In adults, Cx43 is expressed uniformly in all astrocytes with higher abundance in chemical synapses, nodes of

Ranvier and astrocytes end feet surrounding blood vessels[282]. Astrocyte Cx43 can form heteromeric or homomeric gap junctions between astrocytes themselves, astrocytes and other glial cells, astrocytes and neurons as well as astrocytes and cancer cells[283].

1.3.4.2 Cx43 TRAFFICKING AND DEGRADATION

Cx43 has a very short half life (1.5 to 2 hours)[284]. Therefore, its turnover must be tightly controlled (see **Figure 14** for the schematic representation of Cx43 trafficking.). As already stated, Cx43 is synthetized as monomer in the endoplasmic reticulum. Monomers of Cx43 are then transported to the Golgi apparatus. Rab20[285] was identified as a regulator of the trafficking of Cx43 between the endoplasmic reticulum and the Golgi apparatus. In the trans-Golgi network, hexameric hemichannels are formed, and miss-folded or not oligomerized connexins are degraded. CIP75, which belongs to the UbL (ubiquitin- like)-UBA (ubiquitin-associated) domain-containing protein family, was found to interact with the C-terminal domain of Cx43 and to promote its proteosomal degradation[286]. From the Golgi apparatus, Cx43 is packed into vesicles and delivered to the plasma membranes along microtubules[287]. Two models regarding the targeting of Cx43 to the plasma membrane have been proposed. In the classic one, Cx43 channels are transported to the membrane where they freely diffuse laterally[287]. An opposing view hypothesised that assembled Cx43 hemichannels are directly targeted to the area of adherent junctions through the interaction of Cx43 with the EB1 protein and the Dynactin complex[288]. Possibly, the two mechanisms are coexisting. Once in the plasma membrane, from tens to thousands gap junctional channels cluster together forming gap junctional plaques. It has been shown that newly synthetized connexins are added at the border of the plaques[289], whereas the ones at the centre are the first to internalise. Proteins forming adherent junctions, such as cadherins, provide a scaffold necessary for gap junction maintenance and formation[290]. In addition, Zona-Occludens 1 (ZO-1) was found to directly interact with the PDZ-binding motif of Cx43 and to modulate the plaque size[291]. In fact, disruption of the ZO-1/Cx43 interaction leads to a significantly bigger plaque size[292]. In addition to the trafficking to the plasma membrane, internalisation is the second important step the Cx43 lifecycle. Cx43 gap junctions located at the centre of the plaque are constantly internalised as annular junctions in one single cell[293]. Several kinases including the ones involved in the MAPK kinase pathways contribute to the regulation of Cx43 internalisation. In addition to kinases, other Cx43 interacting proteins participate in the internalisation of

Cx43 such as clathrin, myosin, actin and drebrin[290]. After endocytosis, Cx43 can be targeted to either autophagosomal or endolysosomal pathways where it is degraded or recycled back to the plasma membrane. Interestingly, gap junctions have been shown to recycle also as annular junctions[294].

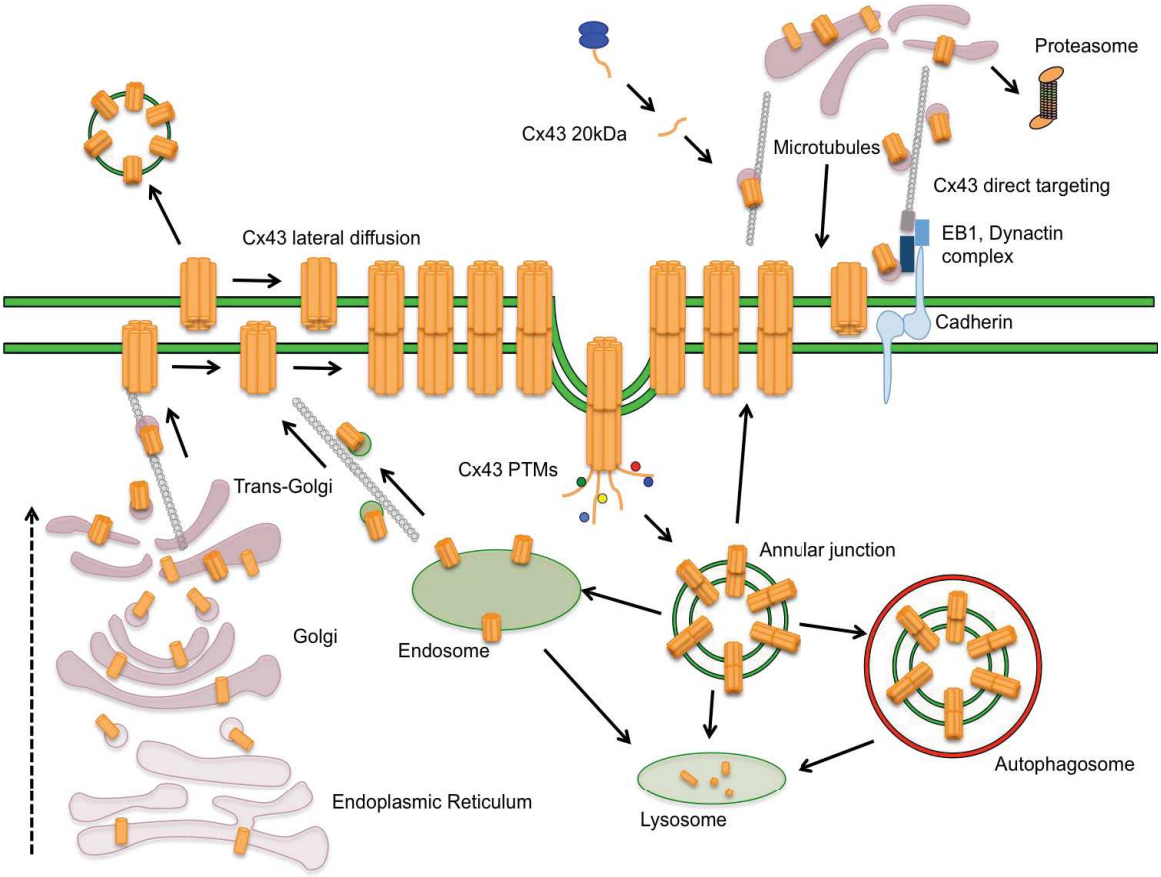

Figure 14 Schematic representation of Cx43 trafficking. Cx43 is synthesized as monomer. Hexameric channels are formed in Trans-Golgi apparatus. After oligomerization, Cx43 hemichannels are transported to the membrane with either a targeted localization (in proximity of tight junctions) or a random one. Cx43 hemichannels are free to diffuse along the cellular membrane. Clusters of Cx43 gap junctions form Cx43 plaques. Cx43 are constantly internalised and synthetized. Internally translated Cx43 also participates in the trafficking of Cx43 hemichannels.

1.3.4.3 POST-TRANSLATIONAL MODIFICATIONS

Several post-translational modifications have been involved in each step of Cx43 trafficking. The most studied one is the phosphorylation. Some phosphorylation processes increase Cx43 gap junctional activity (**Table 5**). In fact, formation of the gap junction requires its phosphorylation mediated by Casein kinase 1 (CK1)[295]. In addition, elevated cAMP levels and activation of protein kinase A leads to phosphorylation of Ser^{364} and increases gap junctional activity of Cx43[296]. AKT-dependent phosphorylayion at Ser^{373} hinders Cx43 interaction with ZO-1 and thereby increases gap junctional activity[297] after wounding or in ischemic conditions. On the other hand, phosphorylation of Cx43 by other kinases leads to a decrease in gap junctional communication (**Table 5**).

Phosphorylation site	Kinases involved	Effect on gap junctional communication
Y247	Src, Tyk2	Decrease
S255	CDK1, ERK1/2	Decrease
S262	CDK, ERK1/2	Decrease
Y265	Src, Tyk2	Decrease
S279	ERK1/2	Decrease
S282	ERK1/2	Decrease
S325	CK1	Increase
S328	CK1	Increase
S330	CK1	Increase
S364	PKA	Increase
S368	PKC	Decrease
S369	AKT	Increase
S373	AKT	Increase

Table 5 Cx43 phosphorylated residues with associated kinases and consequence of their phosphorylation on gap junctional activity of Cx43. Adapted from[438]

PKC activation was found to phosphorylate Ser^{368} and induce closure and internalisation of gap junctions[298]. However, dephosphorylation of the same residue was also found to decrease gap junctional activity [299]. The protein tyrosine kinase v-Src phosphorylates and inhibits Cx43[300] *via* the phosphorylation of Tyr^{247} and Tyr^{265}. Epidermal growth factor (EGF) rapidly inhibits gap junctional activity triggering ERK1/2-mediated phosphorylation of Cx43 at Ser^{255}, Ser^{279} and Ser^{282} [301]. ERK1/2 was also found to phosphorylate Cx43 at Ser^{262}. In addition to phosphorylation, SUMOylation[302], Ubiquitination[303], and Acetylation[304] regulate Cx43 trafficking. Interestingly, Cx43 trafficking can also be regulated by Cx43

"truncated" isoforms originated from AUG starting codons located into the Cx43 gene. Smyth and Shaw showed that at least four of these internally translated Cx43 isoforms, characterized by an N-truncation, arise from translation initiated from internal AUG start codons in a cap-independent fashion[305]. They also showed that one of these isoforms, the 20 kDa fragment corresponding to the C-terminal domain of Cx43 is necessary for the correct translocation of Cx43 into the plasma membrane

1.3.4.4 Cx43 Interactome

As earlier reported, Cx43 trafficking is regulated by its association with interacting proteins. Several studies have shown that trafficking of Cx43 and its channel-dependent and independent functions are controlled by interacting proteins (**Table 6**). In fact, Cx43 regulates important processes such as cell cycle progression, cell motility, cell fusion, autophagy, membrane permeability and mitochondrial redox state through its interaction with other proteins. In turn, interacting proteins might regulate Cx43 activity and turnover.

Interacting protein	Functional role of the interaction	Ref
A-kinase anchoring protein 95 (AKAP8L)	Cell cycle progression	306
Activator of G Protein Signalling 8 (AGS8)	Phosphorylation of Cx43 and internalisation	307
Adherens junction protein p120 (p120ctn)	Neural crest cell motility	308
Ankyrin-3	Maintenance of electrical coupling	309
AP2	Internalisation of annular gap junction	310
Apoptosis regulator BAX	Increased apoptosis in pancreatic cancer cells	311
Apoptosis-inducing factor (AIF)	Regulation of the mitochondrial redox state	312
Atg16L/Atg14/Atg9/Vps34	Autophagy down-regulation	313
Brain-derived integrating factor-1 (BDIF1)	Potential role in molecular trafficking in astrocytes	314
Calmodulin	Inhibits gap junction channels	315
Casein kinase 1	Phosphorylates Cx43 inducing it forward trafficking	295
Caveolin-1,2,3	Regulation of gap junctional communication	316,317
Clathrin	Internalisation of annular gap junction	310
Claudin 5	Thigt junction formation in blood brain barrier	318
Consortin	Trafficking of Cx43 from the Golgi	319
Cyclin E	Increased proliferation	320
Desmocollin-2a	Regulation of Cx43 expression levels	321
Disabled homolog 2-interacting protein (DAB2)	Internalisation of annular gap junction	310
Disks large homolog (Dlg)	Maintenance of a Cx43 cytoplasmic pool	322
Drebrin	Stabilize gap junctions	323
Dynactin	Targeted trafficking of Cx43	288
Dynamin2	Cx43 endocytosis	324
E3 ubiquitin-protein ligase SMURF2	Cx43 endocytosis	325
E3 ubiquitin-protein ligase TRIM21	Down-regulation of gap junctional communication	326
EB1	Cx43 forward trafficking	288
Endoplasmic reticulum protein 29 (ERp29)	Cx43 oligomerization in the endoplasmic reticulum	327

Interacting protein	Functional role of the interaction	Ref
Epidermal growth factor receptor substrate 15 (Eps15)	Cx43 internalisation	328
Ezrin	PKA recruitment to Cx43 and increase GJIC	329
Heat shock 70 kDa (HSP70)	Cell cycle progression	330
Heat shock 90 kDa (HSP90)	Regulate diazoxide-related pathway of preconditioning	331
Hepatocyte growth factor-regulated tyrosine kinase substrate (Hrs)	Trafficking of Cx43 from early endosomes to lysosomes	303
Light chain 3	Targeting Cx43 to autophagic vesicles	332
Mitochondrial import receptor subunit TOM20	Regulate diazoxide-related pathway of preconditioning	331
Myosin-VI	Internalisation of annular gap junction	310
Myotonin-protein kinase (DMPK)	Not known	333
N-cadherin	Direct targeting of Cx43 and neural crest cell motility	288,308
NaV1.5	Not know	334
NEDD4-like E3 ubiquitin-protein ligase WWP1	Down regulation of Cx43 expression	335
Neutral amino acid transporter SLC1A5	Trophoblast cell fusion	336
NOV/CCN3	Possible role in mediating cell growth	337
Occludin	Thigt junction formation in blood brain barrier	318
P2X7	Regulation of gap junctional communication	338
Peripheral plasma membrane protein CASK	Regulation of migration	339
Protein Kinase C (PKC)	Regulate the response of osteoblasts to fibroblast growth factor 2	252
Plakophilin-2	Thigt junction formation	340
Protein kinase A (PKA)	Phosphorylates Cx43 following cAMP accumulation and increase gap junctional communication	329
Small G protein signalling modulator 3 (CIP85)	Cx43 degradation	341
STAM-binding protein (STAMBP)	Cx43 deubiquitination	342
Tight junction protein ZO-1	Modulation of Cx43 plaque size	291
Tight junction protein ZO-2	Possible role in cell cycle progression	343
Tumour susceptibility gene 101 (Tsg101)	Trafficking of Cx43 from early endosomes to lysosomes	303
Ubiquilin-4 (CIP75)	Cx43 degradation in the endoplasmic reticulum	286
Ubiquitin carboxyl-terminal hydrolase 8 (USP8)	Cx43 deubiquination and stabilization	344
β-arrestin	β-arrestin scavenging in osteoblast	345
β-catenin	Increase transcription and modulate gap junction stability	346
β-subunit of the electron-transfer protein	Regulation of the mitochondrial redox state	312

Table 6 Non-exhaustive list of known Cx43 interacting proteins. The biological role of the interaction is also reported.

1.3.4.5 FUNCTIONAL INTERPLAY BETWEEN GPCRS AND CX43

As reported in **Table 6**, β-arrestin, PKA and PKC were found to interact with Cx43. Notably, these proteins are also involved in the signalling cascade evoked by GPCRs. In addition protein kinases that control Cx43 trafficking, such as MAPK and AKT, can also be activated by GPCRs. Consequently, several GPCRs were found to inhibit gap junctional communication such as the α1 and β-adrenergic receptors, the purinergic P2X receptor, cannabinoid, endothelin and lysophospholipid receptors.

- Activation of the α1-adrenergic receptor by noradrenaline inhibits Lucifer Yellow diffusion via activation of PLC in astrocytes [347]. On the other hand, activation of the β-adrenergic receptor with isoproterenol alone did not modify the gap junctional communication but it became effective thanks to the co-treatment with the phosphodiesterase inhibitor IBMX[347].
- ATP inhibits electrical coupling and Lucifer Yellow diffusion through the binding to the P2X receptor in primary cultured astrocytes. This inhibition was increased by pre-treatment with IL-1β[348].
- The cannabinoid agonist anandamide reversibly inhibits gap junctional communication and calcium wave propagation in primary cultured astrocytes. PTX reverses the inhibitory effect of anandamide, suggesting a possible role of $G\alpha_{i/o}$ proteins[349].
- Activation of endothelin receptors by endothelin-1 and 3 also inhibits diffusion of Lucifer Yellow in cultured astrocytes[350]. Endothelin-1 mediated inhibition of Cx43 gap junctional communication is dependent on Gαi/o proteins but independent of PKC, MAPK and Rho/ROCK[299].
- The bioactive lysophospholipids sphingosine-1-phosphate (S1P) and lysophosphatidic acid (LPA) activate GPCRs belonging to the lysophospholipid (LPL) receptor gene family. S1P and LPA transiently inhibit gap junctional communication. Both PTX and inhibition of the Rho/ROCK pathways partially reversed the S1P-induced inhibition of Cx43, suggesting that Gαi/o and Gα12/13 proteins are involved in the observed effect[251].
- Expression of a GTPase-deficient $G\alpha_q$ in Rat-1 fibroblasts inhibits Cx43 gap junctional activity through the activation of PLCβ3 [351].

1.3.4.6 Cx43 in the Physiology of the CNS

Multiple roles have been attributed to Cx43 in the CNS, most often involving glial cells, consistent with its cellular expression pattern. Cx43 expressed on glial cells participates in the buffering of K^+ ions during neuronal activity[352] and provides metabolic sustenance to neurons. In fact, astrocytes end feet surrounding blood vessels are strategically placed for taking up glucose from the blood flow. Glucose is then diffused, from one astrocyte to another, through Cx43 gap junctions and delivered to neurons far away from the energy source[353]. In addition, Cx43 contributes to the propagation of Ca^{2+} waves in the brain (**BOX 6**).

BOX 6 CALCIUM WAVES

Almost 30 years ago, it was shown that astrocytes are not only able to increase intracellular Ca^{2+} in response to extracellular stimuli, but that they also transmit these Ca^{2+} signals to adjacent and non-stimulated astrocytes, as intracellular Ca^{2+} waves[354]. There are two possible routes of Ca^{2+} transmission from cell to cell: one involves the direct transfer of second messengers mobilizing Ca^{2+} through gap junctional-coupled cells, the second relies on the "de novo" generation of second messengers in neighbouring cells *via* membrane receptors[355]. Independent from their way of propagation, Ca^{2+} waves will activate Ca^{2+}-dependent signalling pathways. The most discussed functional consequence is the release of transmitters from astrocytes that regulate neuronal and vascular function (gliotransmission)[356]. Interestingly, Cx43 hemichannels also participate in the diffusion of Ca^{2+} waves through the release of ATP[357] and activation of purinergic receptors.

Cx43 also participates in neuroprotection. Uncoupling of gap junction increases neuronal vulnerability in neurons co-cultured with astrocytes and exposed to oxidative stress or glutamate[282]. In addition Cx43 plays a pivotal role in migration and proliferation processes as well as in the infiltration of leukocytes into the brain[358].

The brain was traditionally considered as an immune-privileged organ isolated via the blood brain barrier (BBB) from normal inflammatory processes. However, it is now recognized that immune cells penetrate the brain in pathological conditions such as neuroinflammation[359]. In addition, the BBB originally thought to be a pure endothelial barrier is now seen as a modulatory interface regulated by integrative signalling between endothelial cells, pericytes, neurons and astrocytes. Cx43 expressed either on endothelial or astrocyte cells have been found to regulate BBB permeability (**Figure 15**). As already reported, Cx43 is associated to tight junctions in endothelial cells. Inhibition of Cx43 via endothelial growth factor (VEGF) or

endothelins induces a rupture of the tight junctions and increases BBB permeability[359]. Astrocyte end feet processes completely wrap around capillaries of the BBB and regulate blood flow and water homeostatis[359]. Cx43 expressed in astrocytes is also necessary for BBB [360]. Invalidation of Cx30 and Cx43 expression specifically in astrocytes leads to a weakening and subsequently higher permeability of the BBB, as measured by sucrose and HRP permeability. This effect was explained by the loss of the dystrophin-associated protein complex (DAPC) necessary for the anchoring of astrocytic end feet around the vessel and the decreased expression of the Aquaporin 4 channel. Single invalidation of Cx30 did not reproduce this phenotype, suggesting that Cx43 is the principal connexin involved in the maintenance of BBB permeability[361].

Cx43 was also shown to play a direct role in leucocyte invasion of the brain. In mice where Cx43 was conditionally KO in GFAP-positive astrocytes, leukocytes were detected in the brain parenchyma. In contrast with previous results, the authors failed to observe a higher BBB permeability or inflammatory processes but they observed a higher production of chemoattractant chemokines, such as CXCL12, that was responsible for the leukocyte infiltration[358]. In addition, Cx43 hemichannels could also be involved in the maintenance of the BBB through the secretion of paracrine signals such as ATP, glutamate, prostaglandins and cytokines[359].

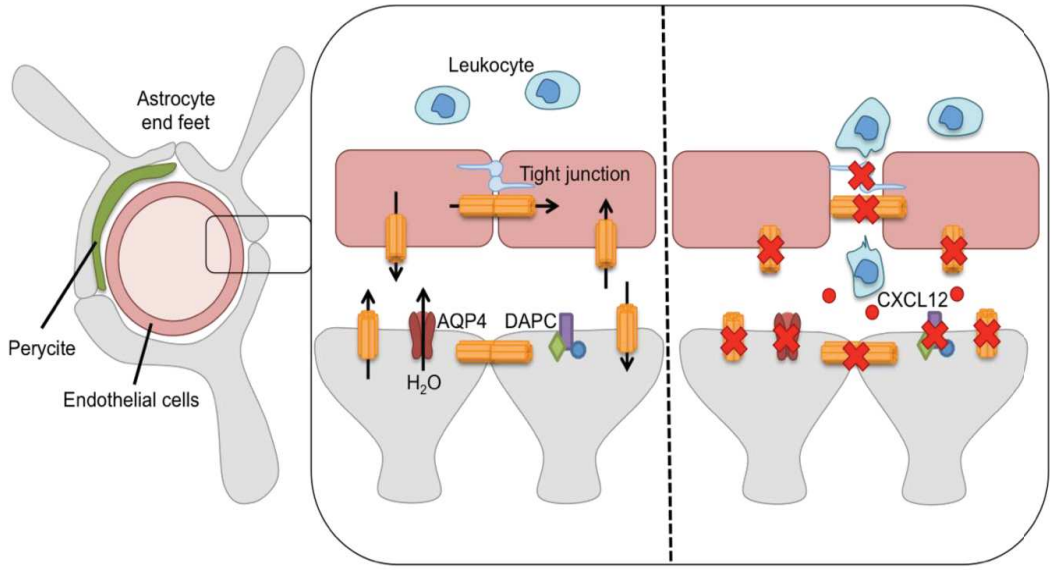

Figure 15 Role of Cx43 in the regulation of BBB permeability and leukocyte entry into the brain parenchyma. The physiological condition is represented on the left hand (correct Aquaporin4 expression, intact DAPC complex and well formed tight junctions). Suppression of Cx43 expression leads to the suppression of Aquaporin4 and the disruption of the DAPC complex (right hand). In addition Cx43 suppression also causes an increase of CXCL12. These effects increase BBB permeability and leukocyte entry into the brain.

Although Cx43 KO mice did not show any macroscopic alterations of the brain[281], a subsequent analysis indicated a slowing down of neuronal progenitor cell (NPC) migration[362]. As reported earlier, Cx43 and Cx26 are both expressed in radial glial cells and Neuronal Progenitor Cells (NPCs). Using shRNA against Cx43 and Cx26, it has been elegantly shown that repression of either Cx impaired NPC migration along radial glia *in vivo*[363]. In addition, NPCs are randomly oriented and they exhibit several, multi-directional protrusions. Interestingly, this effect was mediated by a defect of Cx-mediated adhesion in a channel-independent fashion (**Figure 16**).

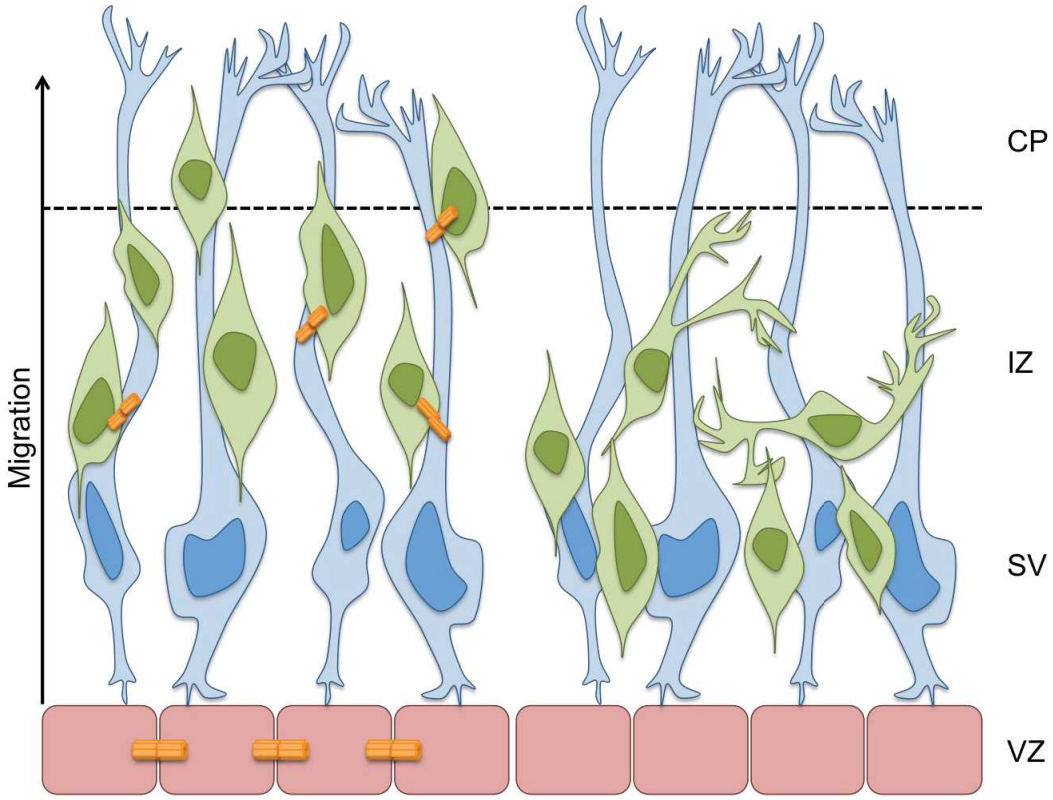

Figure 16 Neuronal progenitor cell (NPC) migration in presence or absence of Cx43. On the left hand the correct migration of NPC (green) along radial glial cells (blue) is represented. Suppression of Cx43 expression, represented on the right hand, impairs migration of NPCs that do not reach the Cortical Plate (CP). In addition NPCs are randomly oriented and exhibit several, multi-directional processes.

Cx43 was also linked to the migration of astrocytes since its invalidation induces an increase in migration in trans-well assays[364]. In addition, Cx43 invalidation using siRNA altered the expression of cytoskeletal proteins involved in cell migration. The release of ATP trough Cx43 hemichannels and calcium wave propagation have also been involved in the migratory process[365].

Contrasting pieces of evidence are linking Cx43 with astrocytes proliferation. On one hand, acute Cx43 inhibition by endothelin-1 or arachidonic acid increases proliferation rate in astrocytes[366]. On the other hand, primary cultures isolated from Cx43 KO mice grow less rapidly than WT ones[367]. Since the role of Cx43 in cell proliferation has been extensively characterized in carcinogenic models, it will be discussed in details below.

1.3.4.7 Cx43 in CNS pathologies

Several diseases affecting the CNS have been linked with a deregulation of Cx43 expression. In Alzheimer's disease, Cx43 expression is up-regulated near amyloid plaques[368], and Cx43 hemichannel activity is increased[369]. In Huntington's disease, Cx43 is up-regulated in the caudate nucleus[370]. Likewise, Cx43 expression is up-regulated in the striatum in Parkinson's disease but its gap junctional activity is not affected[371,372]. In contrast, Cx43 is dramatically down-regulated in mice models of multiple sclerosis[373] and in brain biopsies from patients[374]. Likewise, Cx43 expression is deregulated during epilepsy, but contrasting results (reviewed in [282]) have been reported. Cx43 deregulation at both the expression and functional level in brain tumours have been observed by numerous studies, which clearly demonstrate that this protein plays a pivotal role in brain cancer progression. In fact, as will be discussed below, Cx43 expression and activity influence cell growth, sensitivity to chemotherapeutic agent, invasion and apoptosis.

Regarding cell growth, the first evidence of a possible role of Cx43 in brain cancer progression was collected by transfecting rat C6 glioma cells with cDNA encoding Cx43. These cells proliferate less both *in vitro* and *in vivo*[375] upon Cx43 overexpression. The role of Cx43 as a tumour suppressor in glioma was confirmed when Cx43 was found to be down-regulated in glioma in different studies[376–378]. In a recent study involving the analysis of 474 tumour samples from patients with glioma, Cx43 expression was found to decrease concomitantly with an increase in glioma grade[379]. Based on accumulating evidence, Cx43 is consensually considered as an inhibitor of glioma cell growth that slows down the transition from G1 to S phase[380]. This is achieved *via* two mechanisms. In the first one, Cx43 mediates the exchange of growth suppressor factors in a channel-dependent fashion. In the second one, Cx43 regulates the expression of proteins involved in the cell cycle, such as Cyclins and Cdks, or by scavenging important kinases involved in cell growth such as Src[381], in a channel-independent fashion. In some studies the Cx43 C-terminal tail alone was found to translocate into the nucleus for slowing down cell proliferation[379].

The role of Cx43 in glioma invasion is more heterogeneous. In fact, suppression or inhibition of Cx43 functional activity in U87MG glioma cells decreases their invasiveness indicating that gap junctional communication between glioma cells has a tumour suppressor role. However, gap junctional communication between glioma and astrocytes as well as between astrocytes themselves increase glioma invasiveness[382]. Dissecting the molecular mechanism underlying these effects revealed that inhibition miRNA (miR-5096) transfer between glioma cells and astrocytes decreased invasiveness of glioma cells[382]. Accordingly, suppression of Cx43 expression in mice implanted with GL261 glioma cells decreased the number of cancer cells in the brain parenchyma adjacent to the tumour core and the percentage of infiltrative tumour edge[379]. In contrast with previous observations, these effects were independent of the formation of functional gap junctions[379].

BOX 7 COLLECTIVE MIGRATION

Collective migration is the coordinate movement of cell groups[383]. This process relies on the ability of cells to integrate signals from the neighbouring ones. This cell-cell communication is mediated by several proteins including chemokine and their receptors[384] as well as connexins[385]. Collective migration is crucial for organ development and shaping as well as wound healing. It also plays a pivotal role in tumour progression[386]. This contrasts with single cell migration that occurs independently of the surrounding cells.

As for invasion, the role of Cx43 in migration strongly depends on the type of cells that are coupled. In fact, inhibition of Gap junctional communication between glioma cells increase motility, whereas the inhibition of Gap junctional communication between glioma cells and surrounding astrocytes had opposite effects[387]. In addition, down-regulation of Gap junctional communication between glioma cells change the migratory pattern from collective to single cell migration[385] (**BOX 7**). Although these effects are mediated by channel-dependent functions of Cx43, several studies link Cx43 channel independent functions to migration. In fact, Cx43 was found to mediate the adhesion and migration of glioma cells as it happens for neuronal progenitor cells (NPCs)[388]. In addition, it appears that the C-terminal tail of Cx43 may be sufficient to promote migration[238,389], an effect mediated by the activation of P38 and ERK1/2 signalling [238].

Recent studies have also connected Cx43 with resistance of glioma cells, to the oral alkylating agent used to treat glioblastoma multiforme Temozolomide (TMZ). Intriguingly, suppression or inhibition of Cx43 increase TMZ sensitivity[390]. Gielen *et al.*[391] found that full-length, wild type Cx43 was necessary for the acquired

resistance. In addition, inhibition of Cx43 hemichannels using the αCT1 peptide restored TMZ sensitivity[392]. All these results converge to the idea that Cx43 mediates TMZ resistance by decreasing intracellular concentration of TMZ either by diffusing it to neighbouring cells through gap junctions or by extruding it *via* hemichannels.

The role of Cx43 in apoptosis is quite controversial. Some reports indicate Cx43 as anti-apoptotic whereas others demonstrate a pro-apoptotic action. Both effects are partially mediated by the diffusion of molecules that in the first case are “survival messengers”, such as ATP and reduced glutathione[393], whereas in the latter by the diffusion of “death messengers”, such as calcium[390].

In summary:

- Cx43 down-regulation and inhibition have been linked with higher proliferative states of glioma.
- Cx43 inhibition and suppression of communication between glioma cells has been linked with higher migration and invasiveness. However, increased Cx43-mediated Gap junctional communication between astrocytes and glioma-astrocytes induces higher invasiveness and motility.

This opposing role of Cx43 in glioma could be partially explained by the heterogeneity of Cx43 expression encountered in a recent article[394]. In fact, despite Cx43 expression relatively and inversely correlates with the tumour grade it was heterogeneously expressed within the same grade. Therefore, within the same tumour some cells express Cx43 and they would be expected to migrate and not proliferate whereas others do not express Cx43 and would expect to proliferate but not migrate. Consistent with the fact that heteromeric Cx43 gap junctions between glioma and surrounding astrocytes would promote invasion, Cx43 has been identified in the non-tumoural area surrounding glioma[394,395] and in the tumour cells at the invading front[387]. In addition, cancer cells were found to shunt cGAMP in astrocytes. cGAMP binds to the adaptor protein the Stimulator of interferon genes (STING) triggering a conformational change in STING that translocates from the ER to the Golgi apparatus. This leads to the a release of pro-inflammatory cytokines, such as IFNα and TNF, that provide a growth advantage for brain metastatic cells by protecting against physiological and chemotherapeutic stress[283].

2. AIM & OBJECTIVES

As described in the introduction, CXCR4 activates canonical GPCR signalling pathways involving Gαi protein and β-arrestins. In contrast, the cellular pathways underlying ACKR3-dependent effects remain poorly characterized. Both receptors were shown to interact with several proteins able to modify and mediate either their signalling, trafficking or localization.

Therefore, the aim of the work described in this thesis was to identify novel interacting proteins involved in the signalisation cascade of the two receptors.

The study objectives included:

- Identification of intracellular partners (GIPs) of CXCR4 and ACKR3 using an AP-MS proteomics strategy.
- Validation of the interaction between the receptor and selected GIPs *via* other methods and in authentic tissues.
- Determination of the functional consequences of the association between the receptor and identified GIPs.
- Elucidation of the cellular mechanisms involved in the functional consequences observed.

3. RESULTS

3.1 ACKR3 INTERACTS WITH CX43 AND INHIBITS ITS GAP JUNCTIONAL INTERCELLULAR COMMUNICATION

3.1.1 DECIPHERING THE ACKR3 INTERACTOME IN HEK-293T CELLS BY AP-MS.

ACKR3 interacting proteins were identified in human embryonic kidney HEK-293T cells transiently expressing hemagglutinin (HA)-tagged ACKR3 using an affinity-purification coupled to mass spectrometry (AP-MS) proteomic strategy. ACKR3-interacting proteins were immunoprecipitated using an anti-HA monoclonal antibody immobilized onto agarose beads and identified by nano-flow liquid chromatography coupled to tandem mass spectrometry (nanoLC-MS/MS), as described in the "Materials and Methods" chapter (see page114). Control immuneprecipitations were performed using cells transfected with an empty plasmid (mock). Systematic analysis by tandem MS of the immunoprecipitates identified a total of 4,009 proteins in the three independent experiments performed on different sets of cultured cells. This number was reduced to 1516 after filtering out the proteins either identified only by site, or labelled as contaminant, or not identified in all three biological replicates in at least one group (ACKR3 or mock). Label-free quantification (LFQ) of the relative protein abundances in immunoprecipitates obtained from cells expressing ACKR3 and mock cells showed that 151 proteins were significantly more abundant in immunoprecipitates from ACKR3-expressing cells, using a t-test conducted on both sides and setting a stringent False Discovery Rate (FDR) of 1%, in comparison with mock condition (**Table 7**). These proteins were considered as potential ACKR3 interacting protein partners.

As expected, ACKR3 (bait protein) was the most enriched one (**Figure 17**). Consistent with its constitutive internalisation[143], we identified Clathrin as an ACKR3 interacting protein as well as accessory proteins of the Rab5 and Rab3 complexes that are involved in ACKR3 internalisation[396]. In addition, we identified several enzymes involved in the ubiquitination process, which might be responsible for the basal ubiquitination of the receptor[142]. ACKR3 was also found able to phosphorylate ERK1/2 via activation of MAP2K2[397] that was also retrieved in our interactomic screen. Consistent with a previous study showing a constitutive interaction between ACKR3 and G proteins[150], we identified $G\alpha_{i3}$ as a putative ACKR3 partner.

Among the 151 ACKR3 interacting proteins, we also identified Gap Junction Alpha-1 protein (GJA1, also called Connexin 43 - Cx43), one of the proteins involved in Gap Junctional Intercellular Communication (GJIC) connecting two adjacent cells. Increasing evidence has been showing that numerous proteins that are physically or functionally connected with Cx43 regulate GJIC. Among those proteins, Dynactin (DCTN1)[288] and the Desmosomal cadherin desmoglein 2 (DSG2)[398] were shown to affect the localization of Cx43. Ubiquillin-4 (UBQLN4)[286,399] interacts and promotes the degradation of Cx43. Cytochrome P450 oxidoreductase (CYPOR)[400] down-regulation triggers transcriptional repression and inhibition of Cx43. The solute carrier family 1 member 5 (SLC1A5)[336] interacts with Cx43 to stimulate cytotrophoblast fusion, whereas the beta-subunit of the electron-transfer protein (ETFB)[401] interacts with Cx43 to regulate mitochondrial respiration and reactive oxygen species (ROS) signalling. Consistent with these findings, all these proteins were also identified in ACKR3 interactome (**Figure 17**).

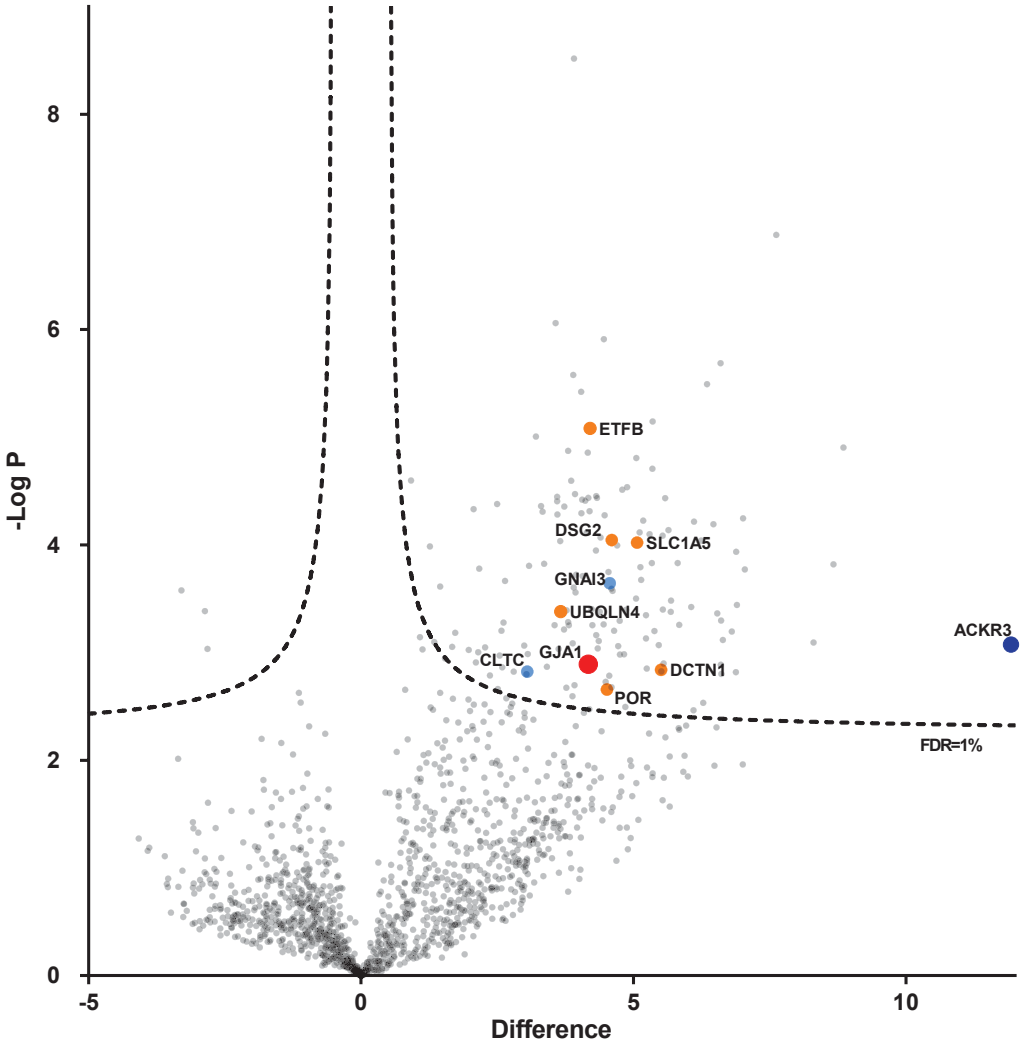

Figure 17 ACKR3 interacting proteins identified in HEK-293T cells and their relative abundance in immunoprecipitates from ACKR3-expressing cells vs. mock cells. HA co-immunoprecipitation followed by nanoLC-MS/MS was performed in three distinct biological replicates in HEK-293T cells transiently expressing HA-tagged ACKR3 and cells transfected with empty plasmid (Mock). Log transformed intensities, obtained by Label Free Quantification (LFQ), of proteins identified in all three biological replicates in at least one set of cultured cells were than used for the comparison. The volcano plot was obtained plotting the differences of LFQ values between ACKR3 and mock cells (X axis) vs. –log of P value (Y axis). The upper part of the graph includes proteins with a high inter-replicate reproducibility whereas the right or left parts include plotted proteins with large differences in abundance between the two conditions. Specifically, on the right there are proteins enriched in the ACKR3 condition. The proteins were considered statistically significant using a T-test conducted on both sides setting the number of randomization at 250 the False Discovery Rate at 0.01 and the S0 at 0.1.Therefore, all proteins “above” the dotted lines are significantly enriched. In dark blue the bait (ACKR3) is represented. In light blue its known interacting partners are depicted. The proteins known to physically or functionally interact with GJA1 (Cx43) are highlighted in orange, whereas Cx43 is in red.

Protein names	UniProtID	Gene names	Difference	P value
Atypical chemokine receptor 3	**P25106**	**ACKR3**	**11.93**	**3.07**
UDP-glucose:glycoprotein glucosyltransferase 1	Q9NYU2	UGGT1	8.85	4.91
26S proteasome non-ATPase regulatory subunit 1	Q99460	PSMD1	8.67	3.82
E3 ubiquitin-protein ligase HUWE1	Q7Z6Z7	HUWE1	8.31	3.09
Protein sel-1 homolog 1	Q9UBV2	SEL1L	7.62	6.88
Proteasome subunit beta type-4	P28070	PSMB4	7.04	3.77
E3 ubiquitin-protein ligase HECTD1	Q9ULT8	HECTD1	7.01	4.25
Proteasome subunit beta type-5	P28074	PSMB5	6.90	3.44
Cleft lip and palate transmembrane protein 1	O96005	CLPTM1	6.88	3.94
Nuclear pore membrane glycoprotein 210	Q8TEM1	NUP210	6.88	2.82
Proteasome subunit beta type-6	P28072	PSMB6	6.80	3.20
Proteasome subunit alpha type-5	P28066	PSMA5	6.64	3.12
Proteasome subunit beta type-1	P20618	PSMB1	6.61	2.80
Proteasome subunit alpha type-1	P25786	PSMA1	6.61	3.30
ATPase WRNIP1	Q96S55	WRNIP1	6.60	2.89
Rab5 GDP/GTP exchange factor	Q9UJ41	RABGEF1	6.60	5.69
26S proteasome non-ATPase regulatory subunit 13	Q9UNM6	PSMD13	6.54	3.37
Calmegin	O14967	CLGN	6.47	4.19
Ankyrin repeat domain-containing protein 13A	Q8IZ07	ANKRD13A	6.35	5.49
Large proline-rich protein BAG6	P46379	BAG6	6.28	2.53
Ubiquilin-1	Q9UMX0	UBQLN1	6.24	4.04
Serine/threonine-protein phosphatase 6 regulatory subunit 1	Q9UPN7	PPP6R1	6.11	4.22
GTPase-activating protein and VPS9 domain-containing protein 1	Q14C86	GAPVD1	6.10	2.46
Importin-9	Q96P70	IPO9	6.06	3.42
E3 ubiquitin-protein ligase AMFR	Q9UKV5	AMFR	5.84	3.26
26S proteasome non-ATPase regulatory subunit 7	P51665	PSMD7	5.81	3.83
Nodal modulator 1	Q5JPE7	NOMO1	5.69	3.48
Carboxypeptidase D	O75976	CPD	5.68	3.38
Nuclear pore complex protein Nup133	Q8WUM0	NUP133	5.64	4.14
V-type proton ATPase subunit S1	Q15904	ATP6AP1	5.58	4.43
Transmembrane and ubiquitin-like domain-containing protein 1	Q9BVT8	TMUB1	5.55	2.90
Transmembrane protein 9	Q9P0T7	TMEM9	5.54	3.40
Pyridoxal-dependent decarboxylase domain-containing protein 1	Q6P996	PDXDC1	5.54	4.09

Protein names	UniProtID	Gene names	Difference	P value
Probable ubiquitin carboxyl-terminal hydrolase FAF-X	Q93008	USP9X	5.51	2.83
Dynactin subunit 1	Q14203	DCTN1	5.51	2.84
Trifunctional purine biosynthetic protein adenosine-3	P22102	GART	5.47	3.07
26S proteasome non-ATPase regulatory subunit 12	O00232	PSMD12	5.38	3.20
Phosphoribosylformylglycinamidine synthase	O15067	PFAS	5.35	5.15
Protein OS-9	Q13438	OS9	5.35	4.71
Nuclear pore complex protein Nup107	P57740	NUP107	5.34	3.83
Condensin complex subunit 1	Q15021	NCAPD2	5.30	4.10
Importin-4	Q8TEX9	IPO4	5.24	2.85
Golgi to ER traffic protein 4 homolog	Q7L5D6	GET4	5.23	3.35
Ubiquitin-40S ribosomal protein S27a	P62979	RPS27A	5.23	3.13
26S proteasome non-ATPase regulatory subunit 10	O75832	PSMD10	5.18	4.23
Rab GTPase-binding effector protein 1	Q15276	RABEP1	5.14	3.68
Protein FAM8A1	Q9UBU6	FAM8A1	5.13	3.79
Exportin-7	Q9UIA9	XPO7	5.11	4.12
Neutral amino acid transporter B(0)	Q15758	SLC1A5	5.06	4.02
Phospholipase D3	Q8IV08	PLD3	5.05	4.81
26S protease regulatory subunit 6B	P43686	PSMC4	5.05	3.50
Proteasomal ubiquitin receptor ADRM1	Q16186	ADRM1	4.88	4.54
Sorting nexin-2	O60749	SNX2	4.86	3.40
Golgi SNAP receptor complex member 1	O95249	GOSR1	4.85	2.49
Rab GTPase-binding effector protein 2	Q9H5N1	RABEP2	4.83	2.98
Rab3 GTPase-activating protein catalytic subunit	Q15042	RAB3GAP1	4.79	4.51
TRAF-type zinc finger domain-containing protein 1	O14545	TRAFD1	4.75	2.98
Armadillo repeat-containing protein 6	Q6NXE6	ARMC6	4.75	3.30
Chloride channel CLIC-like protein 1	Q96S66	CLCC1	4.72	3.06
TATA-binding protein-associated factor 172	O14981	BTAF1	4.70	3.99
Calnexin	P27824	CANX	4.64	3.20
Endoplasmic reticulum lectin 1	Q96DZ1	ERLEC1	4.61	3.57
Desmoglein-2	Q14126	DSG2	4.60	4.05
Rab3 GTPase-activating protein non-catalytic subunit	Q9H2M9	RAB3GAP2	4.60	2.68
Protein ERGIC-53	P49257	LMAN1	4.60	3.59
Guanine nucleotide-binding protein G(k) subunit alpha	P08754	GNAI3	4.56	3.65

Protein names	UniProtID	Gene names	Difference	P value
26S protease regulatory subunit 8	P62195	PSMC5	4.56	2.79
Transmembrane protein 165	Q9HC07	TMEM165	4.54	3.75
NADPH--cytochrome P450 reductase	P16435	POR	4.51	2.66
26S protease regulatory subunit 7	P35998	PSMC2	4.49	2.73
Ancient ubiquitous protein 1	Q9Y679	AUP1	4.47	4.28
Glucosidase 2 subunit beta	P14314	PRKCSH	4.46	5.91
Nuclear pore complex protein Nup155	O75694	NUP155	4.45	3.26
Dual specificity mitogen-activated protein kinase kinase 2	P36507	MAP2K2	4.40	4.07
Peroxisomal biogenesis factor 19	P40855	PEX19	4.38	3.38
A-kinase anchor protein 11	Q9UKA4	AKAP11	4.36	3.11
ER membrane protein complex subunit 7	Q9NPA0	EMC7	4.34	3.04
Wings apart-like protein homolog	Q7Z5K2	WAPAL	4.33	4.44
DNA polymerase delta catalytic subunit	P28340	POLD1	4.32	4.45
Deoxynucleoside triphosphate triphosphohydrolase SAMHD1	Q9Y3Z3	SAMHD1	4.32	3.16
Nuclear protein localization protein 4 homolog	Q8TAT6	NPLOC4	4.31	3.95
Importin-8	O15397	IPO8	4.25	3.25
Signal transducer and activator of transcription 1-alpha/beta	P42224	STAT1	4.23	3.40
Electron transfer flavoprotein subunit beta	P38117	ETFB	4.20	5.08
Mitotic spindle assembly checkpoint protein MAD2A	Q13257	MAD2L1	4.19	4.31
Stromal interaction molecule 1	Q13586	STIM1	4.19	2.47
Isocitrate dehydrogenase [NAD] subunit alpha, mitochondrial	P50213	IDH3A	4.17	4.44
Gap junction alpha-1 protein	**P17302**	**GJA1**	**4.17**	**2.89**
UBX domain-containing protein 4	Q92575	UBXN4	4.16	4.86
NEDD8-activating enzyme E1 regulatory subunit	Q13564	NAE1	4.14	4.11
Integral membrane protein 2B	Q9Y287	ITM2B	4.12	4.41
Plasma membrane calcium-transporting ATPase 1	P20020	ATP2B1	4.07	3.71
Inositol-3-phosphate synthase 1	Q9NPH2	ISYNA1	4.06	4.42
Synembryn-A	Q9NPQ8	RIC8A	4.04	4.29
Calreticulin	P27797	CALR	4.04	5.42
Kinesin-like protein KIF11	P52732	KIF11	3.94	3.72
Exocyst complex component 4	Q96A65	EXOC4	3.93	3.56
Large neutral amino acids transporter small subunit 1	Q01650	SLC7A5	3.93	4.47
E3 ubiquitin-protein ligase synoviolin	Q86TM6	SYVN1	3.92	2.70

Protein names	UniProtID	Gene names	Difference	P value
Atlastin-2	Q8NHH9	ATL2	3.91	8.52
Small glutamine-rich tetratricopeptide repeat-containing protein	O43765	SGTA	3.90	3.60
Epsin-1	Q9Y6I3	EPN1	3.89	5.58
Short/branched chain specific acyl-CoA dehydrogenase	P45954	ACADSB	3.88	3.09
Fibronectin type-III domain-containing protein 3A	Q9Y2H6	FNDC3A	3.88	2.60
E3 ubiquitin-protein ligase HECTD3	Q5T447	HECTD3	3.86	4.60
Sorting nexin-1	Q13596	SNX1	3.82	3.25
26S protease regulatory subunit 4	P62191	PSMC1	3.80	3.28
Catechol O-methyltransferase	P21964	COMT	3.80	4.87
Acetyl-CoA acetyltransferase, mitochondrial	P24752	ACAT1	3.77	3.39
HLA class I histocompatibility antigen, B-73 alpha chain	Q31612	HLA-B	3.77	2.67
Ubiquitin-protein ligase E3A	Q05086	UBE3A	3.73	4.36
Protein SCO2 homolog, mitochondrial	O43819	SCO2	3.73	3.22
Ubiquilin-4	Q9NRR5	UBQLN4	3.66	3.38
Fanconi anemia group D2 protein	Q9BXW9	FANCD2	3.65	4.04
Transitional endoplasmic reticulum ATPase	P55072	VCP	3.63	3.03
Sarcolemmal membrane-associated protein	Q14BN4	SLMAP	3.60	4.28
Tyrosine-protein kinase Lyn	P07948	LYN	3.60	4.41
Prolyl 4-hydroxylase subunit alpha-1	P13674	P4HA1	3.60	4.45
Enhancer of mRNA-decapping protein 3	Q96F86	EDC3	3.57	6.06
Homocysteine-responsive endoplasmic domain member 1 protein	Q15011	HERPUD1	3.55	3.26
Tubulin beta-3 chain	Q13509	TUBB3	3.41	2.87
Spermatogenesis-associated protein 5	Q8NB90	SPATA5	3.36	3.82
Nucleoporin NDC1	Q9BTX1	NDC1	3.33	4.31
FH1/FH2 domain-containing protein 1	Q9Y613	FHOD1	3.30	4.36
V-type proton ATPase subunit H	Q9UI12	ATP6V1H	3.21	5.01
Transmembrane protein 209	Q96SK2	TMEM209	3.08	3.81
Apolipoprotein L2	Q9BQE5	APOL2	3.06	2.99
Clathrin heavy chain 1	Q00610	CLTC	3.05	2.82
Importin-5	O00410	IPO5	3.04	2.80
NSFL1 cofactor p47	Q9UNZ2	NSFL1C	2.99	3.07
Protein YIF1B	Q5BJH7	YIF1B	2.80	2.82
Stress-induced-phosphoprotein 1	P31948	STIP1	2.64	3.67

Protein names	UniProtID	Gene names	Difference	P value
Methylenetetrahydrofolate dehydrogenase	P11586	MTHFD1	2.62	3.28
Selenoprotein O	Q9BVL4	SELO	2.59	2.86
26S proteasome non-ATPase regulatory subunit 3	O43242	PSMD3	2.58	3.20
Zinc finger HIT domain-containing protein 2	Q9UHR6	ZNHIT2	2.54	2.97
Sorting nexin-5	Q9Y5X3	SNX5	2.51	2.66
DnaJ homolog subfamily B member 1	P25685	DNAJB1	2.50	4.38
Ran GTPase-activating protein 1	P46060	RANGAP1	2.36	2.79
Histone acetyltransferase type B catalytic subunit	O14929	HAT1	2.28	3.05
Heat shock protein HSP 90-alpha	P07900	HSP90AA1	2.17	3.78
CCR4-NOT transcription complex subunit 2	Q9NZN8	CNOT2	2.15	3.00
ATP-dependent Clp protease ATP-binding subunit clpX-like	O76031	CLPX	2.11	2.91
Heat shock protein HSP 90-beta	P08238	HSP90AB1	2.07	4.33
Insulin receptor substrate 4	O14654	IRS4	1.98	3.03
Prolactin regulatory element-binding protein	Q9HCU5	PREB	1.73	3.18
Stomatin-like protein 2, mitochondrial	Q9UJZ1	STOML2	1.67	3.05
Cytochrome b-c1 complex subunit 2, mitochondrial	P22695	UQCRC2	1.45	3.61
T-complex protein 1 subunit eta	Q99832	CCT7	1.34	3.10
Ornithine aminotransferase, mitochondrial	P04181	OAT	1.26	3.99
Aladin	Q9NRG9	AAAS	0.92	4.60
Actin-related protein 8	Q9H981	ACTR8	-2.82	3.04
Probable global transcription activator SNF2L1	P28370	SMARCA1	-2.87	3.38
Mediator of RNA polymerase II transcription subunit 23	Q9ULK4	MED23	-3.30	3.58

Table 7 List of proteins that specifically co-immunoprecipitate with ACKR3 in HEK-293T cells. Proteins statistically enriched according to their LFQ level in the ACKR3 complex compared to Mock cells are reported. Protein name, Uniprot ID, gene name, LFQ difference between ACKR3 and mock cell (Difference) and the – log P values (P value) are indicated. The statistical analysis was performed using the Perseus software as detailed in the “Materials and Methods” section. Proteins are ranked based on their difference in abundance in immunoprecipitates from ACK3-expressing cells vs. Mock cells. The bait ACKR3 is shown in blue, its known interacting proteins in light blue and the accessory proteins of Rab and Ubiquitin complexes as well as MAP2K2 are depicted in green. GJA1 (Cx43) is highlighted in red and the proteins already known to interact with Cx43 (at least functionally) in orange.

3.1.2 Cx43 interacts preferentially with ACKR3 compared to CXCR4.

ACKR3 and Cx43 share several important biological functions, including the control of cell migration[362,402]. In addition both proteins are involved in glioma progression during which there is an up-regulation of ACKR3[210] and a concomitant suppression of Cx43 activity and expression[376].

In line with these findings, we decided to focus on ACKR3/CX43 interaction. We first confirmed the interaction between these two proteins by immunoprecipitation followed by Western blotting. We also compared the ability of ACKR3 and CXCR4, another chemokine receptor known to heterodimerize with ACKR3, to recruit Cx43. As shown in **Figure 18** and consistent with LC-MS/MS analyses, endogenously expressed Cx43 co-precipitates with ACKR3 in HEK-239T cells, but not in Mock cells. A much lower Cx43 amount was also detected in CXCR4 immunoprecipitate, but Cx43 abundance in CXCR4 immunoprecipitates was not significantly different from that measured in precipitates obtained from Mock cells ($p = 0.081$, $n = 3$) (**Figure 18B**).

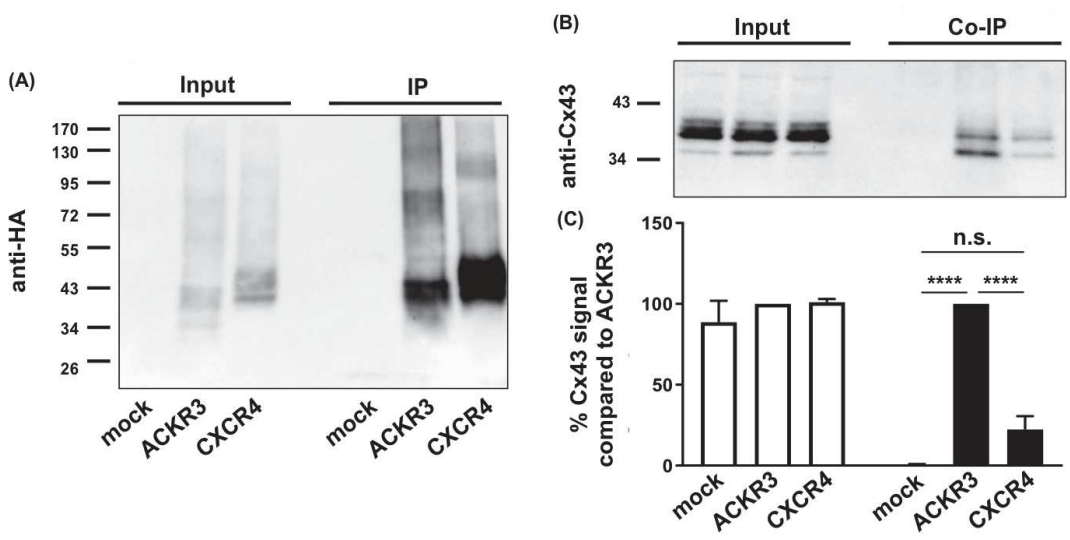

Figure 18 Cx43 co-immunoprecipitates with ACKR3. (A) Immunoprecipitation (IP) of HA-ACKR3 and HA-CXCR4 transiently expressed in HEK-293Tcells compared to Mock cells (transfected with an empty plasmid). (B) Cx-43 co-immunoprecipitation (Co-IP) with HA-ACKR3 vs. HA-CXCR4 and Mock cells. In both (A) and (B) representative blots of the three independent replicates are shown. (C) Average Input and Co-IP Cx43 immunoreactive signal quantified in three independent experiments (± SEM). Values were normalized to those measured in ACKR3 precipitates. Two-way Anova with Turkey's post-hoc test was used (**** P≤0.0001).

We then investigated the interaction between each receptor and Cx43 in living HEK-293T cells using BRET^2. We transiently co-transfected a constant amount of cDNA encoding ACKR3 or CXCR4 C-terminally tagged with Nano Luciferase with an increasing amount of Cx43 C-terminally tagged with YFP. In line with our co-immunoprecipitation experiments, the BRET^2 ratio between ACKR3 and Cx43 increased hyperbolically, indicating a specific and constitutive interaction, whereas the BRET^2 ratio between CXCR4 and Cx43 increased only linearly (**Figure 19A**). ACKR3 activation by CXCL12 (10^{-8} M) did not affect the interaction between ACKR3 and Cx43 (**Figure 19B**) (p = 0.79, n = 4).

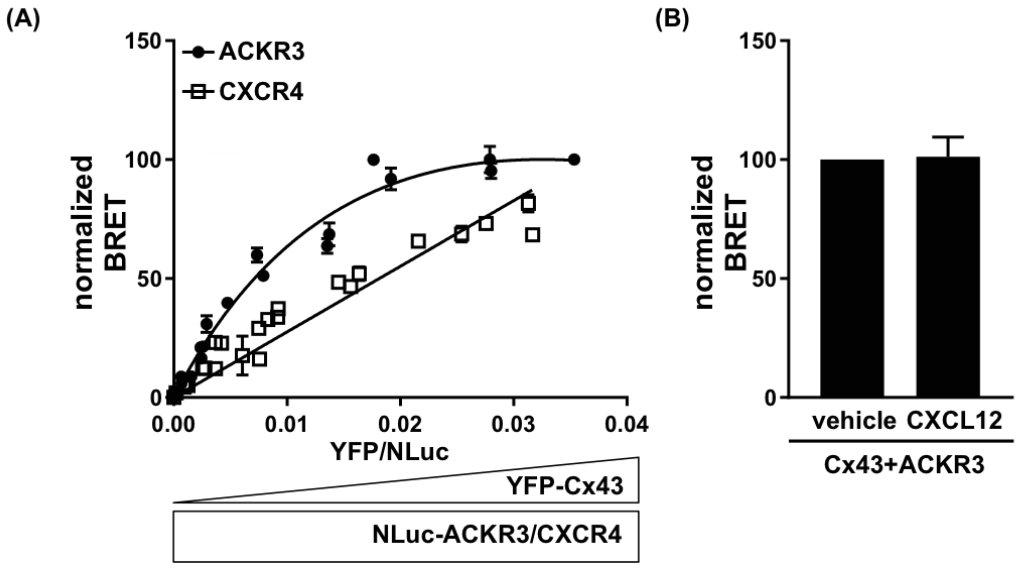

Figure 19 BRET analysis of Cx43 interaction with ACKR3 and CXCR4 in living HEK-293T cells. (A) Titration curves of the Cx43-YFP–ACKR3-NLuc and Cx43-YFP–CXCR4-NLuc interaction in HEK-293T cells. Three biological replicates per conditions are plotted. Points represent the average of the technical triplicates within a biological replicate. BRET values were normalized to the maximum BRET obtained in each replicate. Prism was let decided between fitting a One-site total line with background constraint to 0 and a line through origin. P value of fitting for a One-site total line for ACKR3 is < 0.001. The same curve did not fit for CXCR4. On the other hand, the line trough the origin fits the CXCR4 point with an R^2=0.926. (B) Quantification of the BRET signal between YFP-Cx43 and NLuc ACKR3 expressed in HEK-293T cells with and without ACKR3 activation by CXCL12 (10^{-8} M). The YFP/NLuc ratio used was the one giving the $BRET_{50}$ in saturation curve. The histogram represents averages of three biologically independent replicates (± SEM). Unpaired t-test was used for the difference.

3.1.3 Native ACKR3 and Cx43 show overlapping localizations in mouse brain.

Collectively, these findings indicate that overexpressed ACKR3, but not CXCR4, interacts with Cx43 in HEK-293T cells. ACKR3 and Cx43 are both expressed in the adult brain. In fact, ACKR3 has been shown to be expressed in specific cellular sub-populations in the adult brain such as astroglial, neuronal and vascular cells[134]. On the other hand, Cx43 expression in the adult brain is principally limited to astrocytes[403] even if microglia, neuronal precursors and endothelial cells[234] express low amount of the protein. We next sought to explore their respective regional and cellular distribution in mouse brain to determine whether both proteins exhibit overlapping distributions. As there are no good antibodies against mouse ACKR3 available, we used BAC mice expressing EGFP under the control of the ACKR3 promoter. Therefore, cells expressing ACKR3 also express EGFP, even though EGFP staining cannot establish the precise subcellular localization of ACKR3 nor its putative co-localization with Cx43. We performed a triple labelling staining of EGFP (ACKR3, green), Cx43 (red) and GFAP (astrocytes, magenta) in brain slices of 8 week-old mice, in line with the aforementioned findings indicating that ACKR3 and Cx43 are both expressed in astrocytes. Consistent with previous observations,[404] we observed a strong EGFP (ACKR3) staining in the cortical subventricular zone (SVZ), a region expressing functional Cx43[405]. Furthermore, ACKR3 is highly expressed in GFAP-positive cells co-expressing Cx43 in the subventricular zone (**Figure 20**) and in GFAP positive astrocytes surrounding blood vessels in various brain regions, including cerebral cortex and hippocampus (**Figure 21**). Collectively these findings indicate that in the adult brain ACKR3 is co-expressed by a GFAP-positive sub-population of astroglial cells in the SVZ and in astrocyte end feets surrounding blood vessels in the cortex and hippocampus.

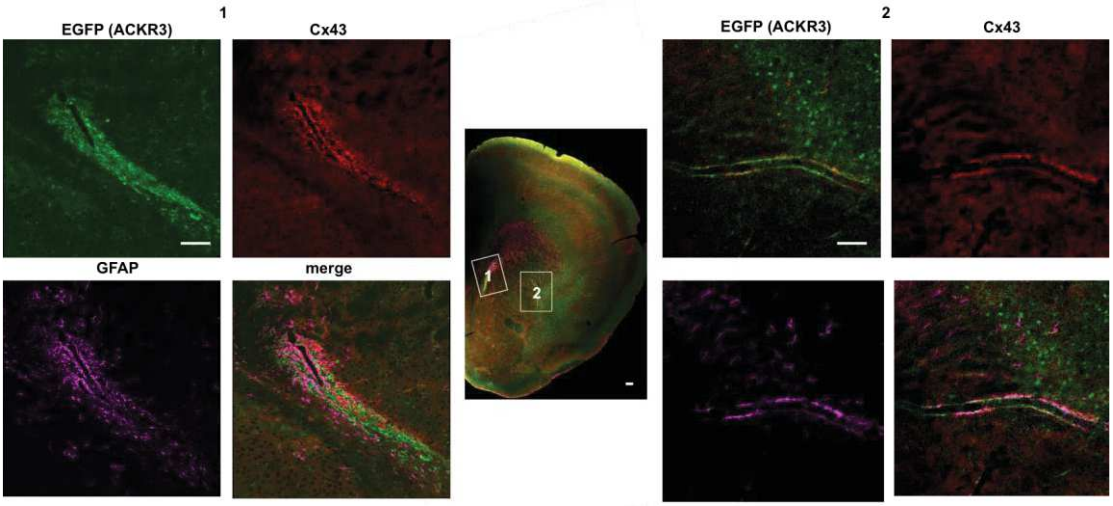

Figure 20 ACKR3 and Cx43 co-expression in astrocytes in the sub-ventricular zone and surrounding blood vessels. Confocal images of 50 µM brain slices obtained from 8 week-old BAC-EGFP-ACKR3 mice. EGFP signal was amplified using an anti-GFP antibody. Scale bar = 100 µm.

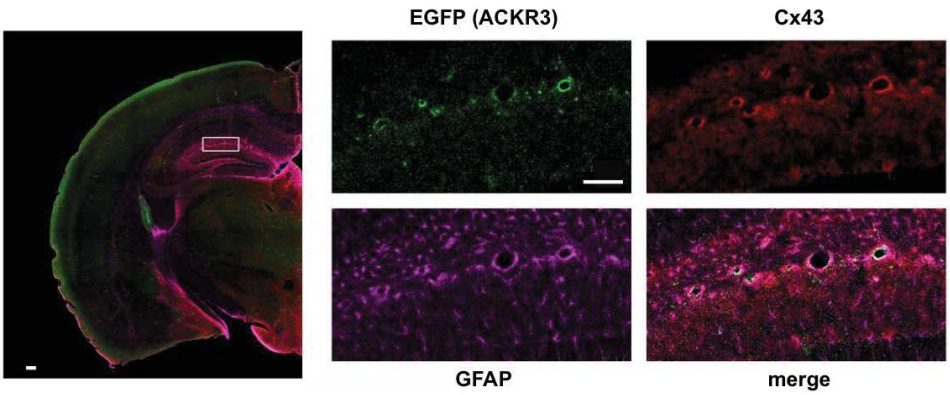

Figure 21 Expression of ACKR3 in astrocyte endfeets surrounding blood vessels. Confocal images of 50 µM brain slices obtained from 8 week-old BAC-EGFP-ACKR3 mice. EGFP signal was amplified using an anti-GFP antibody. Scale bar = 100 µm.

3.1.4 ACKR3 ACTIVATION INHIBITS CX43-MEDIATED GAP JUNCTIONAL INTERCELLULAR COMMUNICATION (GJIC) IN PRIMARY CULTURE OF MOUSE ASTROCYTES.

Since ACKR3 was shown to be expressed in primary culture of astrocytes[153], which are exclusively coupled by Cx43[248,406], we investigated the effect of ACKR3 activation on GJIC in primary cultures of cortical astrocytes from E15.5 mouse embryos. Cells were maintained in culture for five weeks. Under these conditions, cultures showed high enrichment in astrocytes, as assessed by GFAP immunostaining (not shown). Astrocytes were then starved overnight before proceeding to the experiment. GJIC was then investigated by the scrape loading technique[259] and measuring the diffusion of the fluorescent dye Lucifer Yellow (LY) throughout the astrocytic syncytium from the scrape (**Figure 22A**). As previously described[407], LY showed an important diffusion, showing a strong GJIC in primary astrocyte cultures. Further supporting astrocyte coupling through GJs, treating cells with the GJ inhibitor CBX (50 µM, overnight) strongly inhibited LY diffusion (53 ± 8% inhibition *vs.* vehicle-treated cells, n =3, **Figure 22B)**. Exposure of cells to CXCL12 (10^{-8} M) for 30 min significantly inhibited GJIC (31 ± 4% inhibition *vs*. vehicle-treated cells, n=17). A similar level of inhibition (29 ± 5 % inhibition, n = 11) was reached following exposure of astrocytes to CXCL11 (10^{-7} M). Notably, both chemokines can activate several receptors. CXCL12 binds to both ACKR3 and CXCR4, whereas CXCL11 binds to both ACKR3 and CXCR3. Pre-treatment of cells with the CXCR4 antagonist AMD3100 (10^{-6} M, 30 min), which alone did not change GJIC (p = 0.89 *vs.* vehicle-treated cells, n = 4), did not affect CXCL12-induced inhibition of GJIC (p = 0.99 *vs.* AMD+CXCL12 treated cell, n = 4), suggesting that the CXCL12 effect is actually mediated by ACKR3. Likewise, blocking CXCR3 by its antagonist NB-74330 (10^{-6} M, for 30min) (p = 0.78 *vs.* vehicle treated cell, n = 3) did not prevent the ability of CXCL11 to inhibit GJIC (p = 0.97 *vs.* NP-74330+CXCL11, n = 3), indicating that the CXCL11 effect is also mediated by ACKR3. Collectively, these results indicate that activation of endogenously expressed ACKR3 inhibits Cx43-mediated GJIC in primary cultured astrocytes.

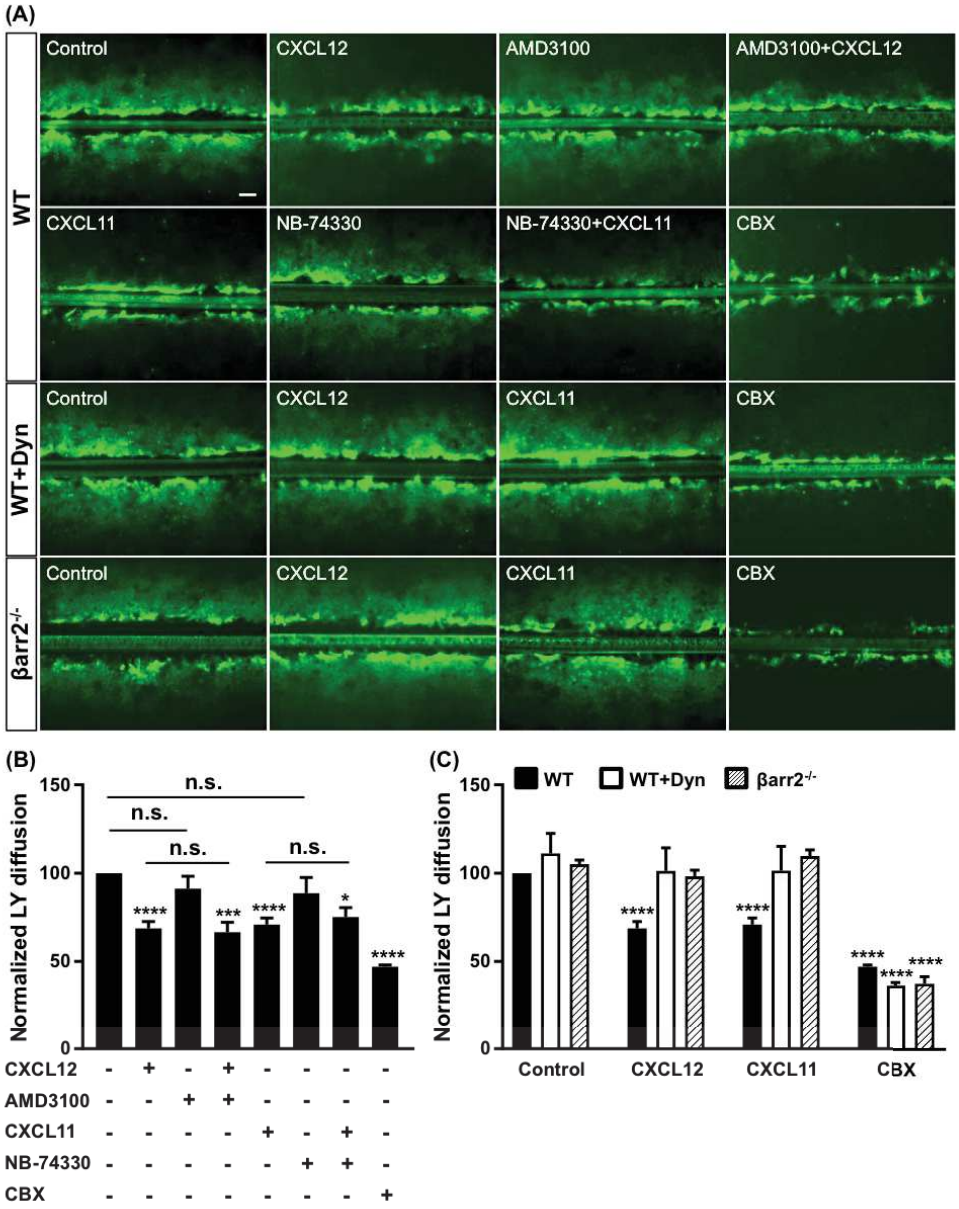

Figure 22 ACKR3 activation inhibits Cx43-mediated GJIC through β-arrestin2-dependent Cx43 internalisation in primary cultures of mouse astrocytes. (A) Representative pictures of the scrape loading assay, performed in confluent primary astrocytes culture obtained from embryonic WT or β-arrestin2$^{-/-}$ mice (E15.5), taken ten minutes after the scrape in the presence of LY. All compounds (CXCL12 (10^{-8} M), AMD3100 (10^{-6} M), CXCL11 (10^{-7} M), NB-74330 (10^{-6} M), Dyn=Dynasore (80 μM)) were applied for 30min but CBX (50μM) was applied overnight. Scale Bar = 100 μm. (B) and (C) Quantification of the LY diffusion by calculation of the distance from the scrape where LY intensity is halved. Values were normalized to LY diffusion in vehicle-treated astrocytes (Control). Average values (± SEM) from at least three independent experiments performed in triplicate are represented. For comparison with control (indicated by *) one-way Anova with Dunnett's post-hoc test was used. For the other comparisons the one-way Anova with Sidak's post-hoc test was used (****P≤0.001, ***P≤0.001, * P≤0.05).

Since Cx43 GJIC mediates an electrical coupling between cells we next investigated the ability of ACKR3 to modulate the electrical coupling between astrocytes using the double whole-cell voltage-clamp technique. In this case, five week-old primary cultures were re-suspended and seeded overnight generating an astrocyte secondary culture[259]. Under these conditions, the purity of the astrocyte cultures increases up to nearly 100%, as assessed by GFAP staining (not shown). Paired astrocytes (*i.e.* cells attached to one another) were then patched. Electrical coupling between paired cells was assessed by double patch-clamp experiments. Though all the recorded cell pairs were not electrically coupled, cells engaged in a gap junctional electrical coupling exhibit lower membrane resistance (94 ± 8.5 MOhms, n = 96) than uncoupled ones (804 ± 80 MOhms, n = 60) indicating that the junctional coupling is a key component of the electrophysiological properties of astrocytes (**Figure 23**).

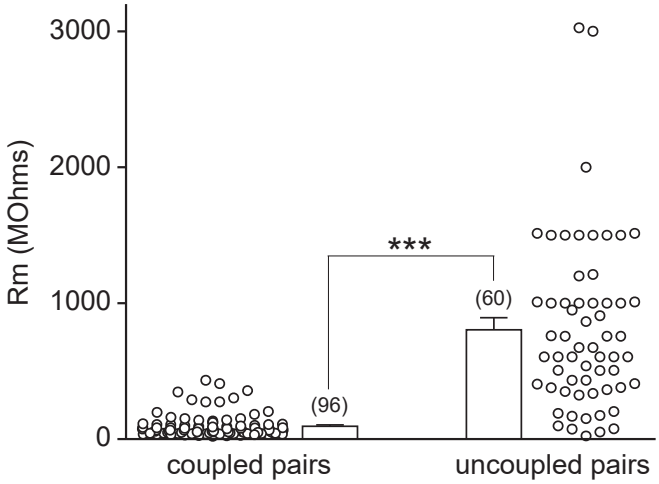

Figure 23 Coupled astrocytes display lower membrane resistances *vs.* uncoupled cells. All cell pairs (cells attached to one an other) were tested for a junctional current. Pairs in which no junctional current was detected were classified as uncoupled, whereas the ones exhibiting a junctional current were classified as coupled. Unpaired t-test was used for the difference. *** P≤0.001.

We thus explored whether activation of ACKR3 does affect the membrane resistance. An increased resistance would suggest an inhibition of coupling, whereas a diminished resistance would suggest an increased coupling. Astrocyte secondary cultures were exposed via bath application to a saline solution (Vehicle), or CXCL12 (10^{-8} M) or CBX (100 µM). Membrane resistance of coupled cells was calculated before and after the treatment. Exposure to the saline solution did not modify the resistance value (48.6 ± 8.8 and 71.4 ± 25.1 MOhms for saline before *vs.* saline after treatment, p = 0.25, n = 5). By contrast, inhibition of Cx43 by CBX significantly

increased cell resistance indicating that the membrane resistance value faithfully reflects a change in gap junction-mediated coupling between two cells. In the same way when cells were challenged with CXCL12, the membrane resistance significantly increased, suggesting that CXCL12 might decrease electrical coupling between astrocytes (**Figure 24**).

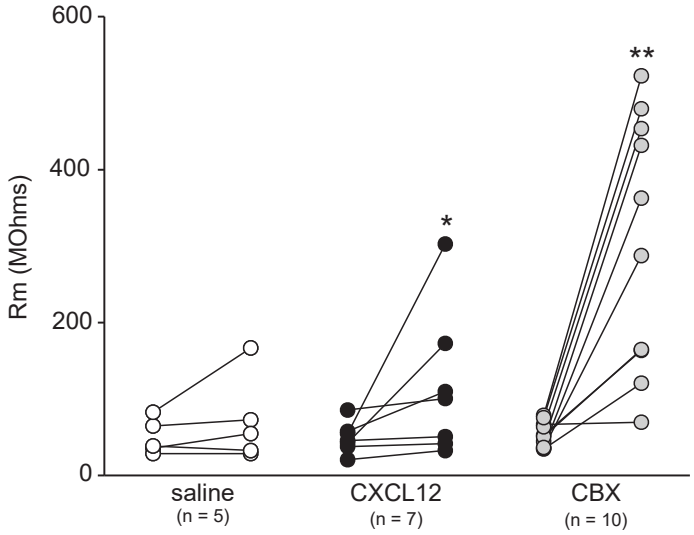

Figure 24 CXCL12 increases membrane resistance. Coupled astrocytes were challenged with either a saline solution, or CXCL12 (10^{-8} M), or CBX (100 µM). Resistance values of each cell measured before and after treatment are plotted. Paired Wilcoxon test was used for the analysis *P≤0.05, **P≤0.01 *vs.* before treatment.

To further confirm the possible role of ACKR3 in the regulation of astrocyte electrical coupling, we calculated the coupling ratio between coupled astrocytes in the presence of either vehicle, CXCL12 (10^{-8} M), CXCL11 (10^{-7}M) or CBX (100µM) (**Figure 25A**). The coupling ratio remained stable during the 15 min recording of vehicle-treated cells. Consistent with a blocking effect of the ACKR3 agonist CXCL12 on gap junction-mediated electrical coupling between astrocytes, the coupling ratio decreased as soon as 5 min after the onset of bath-applied CXCL12 (0.495 ± 0.06 and 0.48 ± 0.07 for saline before *vs.* saline after treatment, p = 0.045, n = 6 *vs.* saline) and remained reduced as far as 11 minutes after application. However, the kinetics of CXCL12 action in this experiment must be interpreted cautiously, because CXCL12 (as the other treatments) was added by bath application and reached the recording chamber after 4 min of perfusion. In the same way, preliminary results indicate that CXCL11 treatment also decreased the coupling ratio between astrocytes (data not shown), but this effect must be confirmed on a larger cell number.

Likewise, and as expected, CBX significantly inhibited the coupling ratio compared to the saline condition. In **Figure 25B** the averaged coupling ratios for the first 4 minutes before treatment (before) and the averaged coupling ratios of the last 5 minutes (after) are plotted for each patched cell pairs. Coupling ratio for the saline treated pairs remained stable for all the six pairs ($p = 0.84$, $n = 6$ before *vs.* after treatment). CXCL12 significantly reduced the coupling ratio. Note that in 2 out of 6 pairs challenged with CXCL12, the coupling ratio remained constant. On the other hand, CBX diminished the coupling ratio in all six-cell pairs recorded. Therefore, ACKR3 activation reduces connexin-mediated electrical coupling in paired astrocytes.

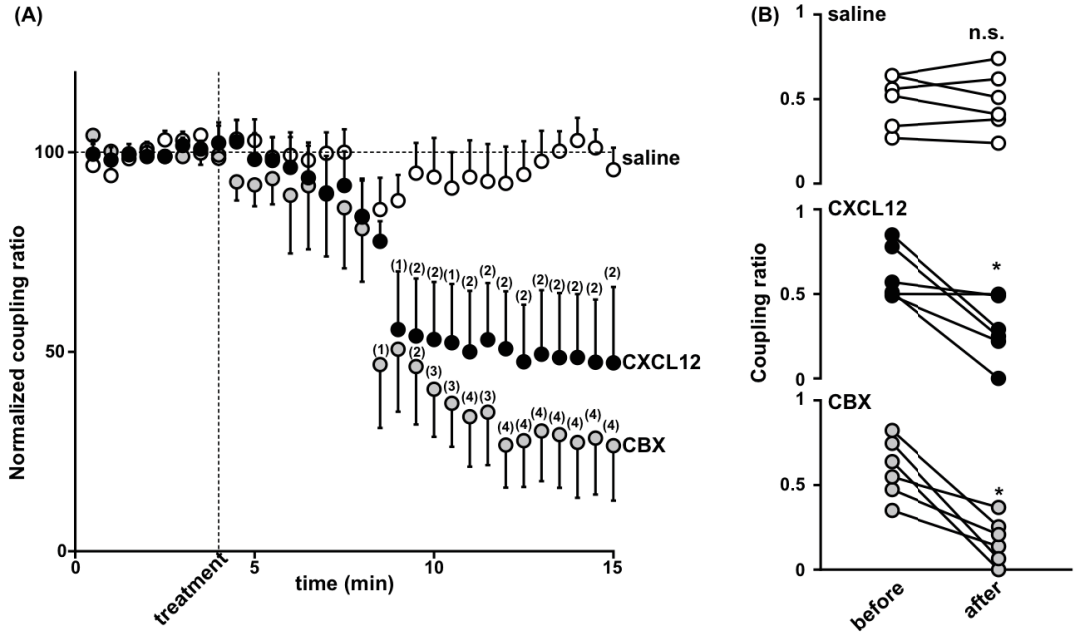

Figure 25 CXCL12 reduces the electrical coupling between secondary mouse astrocytes. (A) Time-course of the effect of CXCL12 (10^{-8} M), CBX (100µM) or saline on the coupling ratio. Depolarizing voltage steps (50 mV) were applied every 30 s to cell 1 and coupling ratio was computed as Ij/I1. Perfusion of the recorded pairs with the drug started at the time indicated by the dotted line. Data are expressed as a percentage of coupling ratio (normalized to the average ratio recorded during the first 4 minutes). Values are the average ± SEM of six pairs. (4)=**** P≤0.0001, (3)=*** P≤0.001, (2)=** P≤0.01, (1)=* P≤0.05 *vs.* saline. Two-way Anova with Tukey's post-hoc test was used for the point-to-point comparison. (B) Coupling ratios before and after treatment for each cell pair recorded in the different conditions are plotted. Paired Wilcoxon test was used for the analysis *P≤0.05 *vs.* before treatment.

3.1.5 ACKR3-MEDIATED INHIBITION OF GJIC IN PRIMARY ASTROCYTES IS DEPENDENT ON BOTH DYNAMIN AND β-ARRESTIN2.

ACKR3 interacts with Cx43 and inhibits its GJIC activity upon activation. Cx43 activity is often regulated by alteration of its trafficking[224]. We therefore decided to investigate if the ACKR3-mediated inhibition of GJIC is mediated by Cx43 internalisation. We first examined whether treating cells with the chemical inhibitor of dynamin Dynasore prevents ACKR3 mediated inhibition of GJIC in primary cultures of astrocytes, using again the scrape loading technique (**Figure 22**). Pre-treatment with astrocytes for 30 min with 80 µM Dynasore abolished the ACKR3-mediated inhibition of GJIC ($p = 0.99$, $n = 3$ for control *vs.* dyn+CXCL12 and control *vs* dyn+CXCL11), but not the effect of CBX that was still able to inhibit GJIC (**Figure 22C**). Thus, inhibition of dynamin reverses inhibition of GJIC induced by agonist stimulation of ACKR3.

ACKR3 is known to signal through β-arrestins, which are also involved in its internalisation[143]. In astrocyte cultures prepared from β-arrestin2 KO mice, neither CXCL12 nor CXCL11 inhibited GJIC ($p = 0.99$, $n = 3$ for control *vs.* $\beta arr2^{-/-}$+CXCL12 and $p = 0.90$, $n = 3$ for control *v.s* $\beta arr2^{-/-}$+CXCL11) (**Figure 22C**). In addition, the magnitude of LY diffusion through vehicle-treated astrocytes was similar to that measured in astrocytes from WT mice ($p = 0.99$, $n = 3$). Collectively, these observations indicate that ACKR3 stimulation by its two natural agonists CXCL12 and CXCL11 inhibits GJIC in primary cultures of astrocytes. Both inhibition of dynamin and suppression of β-arrestin2 expression completely reverse this inhibition suggesting that Cx43 internalisation underlies the ACKR3-mediated GJIC inhibition.

3.1.6 ACKR3 ACTIVATION TRIGGERS CX43 INTERNALISATION IN PRIMARY CULTURES OF MOUSE ASTROCYTES.

To further confirm this hypothesis and demonstrate that ACKR3 activation triggers Cx43 internalisation, we performed Cx43 immunostaining on primary astrocyte cultures. As expected, Cx43 was mainly localized at the interface of cell-cell contacts in cultures treated with vehicle, resulting in a typical “pavement-like” immunostaining (**Figure 26**), though a little proportion of Cx43 was detected inside the cells. Treating cultures with CXCL12 (10^{-8} M) or CXCL11 (10^{-7} M) for 30 min profoundly modified this staining pattern: Cx43 was only marginally detected at the cell interface but mainly in intracellular vesicles (**Figure 26**).

Both inhibition of dynamin by Dynasore and β-arrestin2 suppression prevented the ability of CXCL12 and CXCL11 to promote Cx43 internalisation. In fact, in both conditions Cx43 was mainly detected at the plasma membrane even in CXCL12- and CXCL11-treated cultures (**Figure 26**). Therefore ACKR3 activation by CXCL12 or CXCL11 inhibits GJIC by triggering dynamin and β-arrestin2-dependent Cx43 internalisation in primary culture of mouse astrocytes.

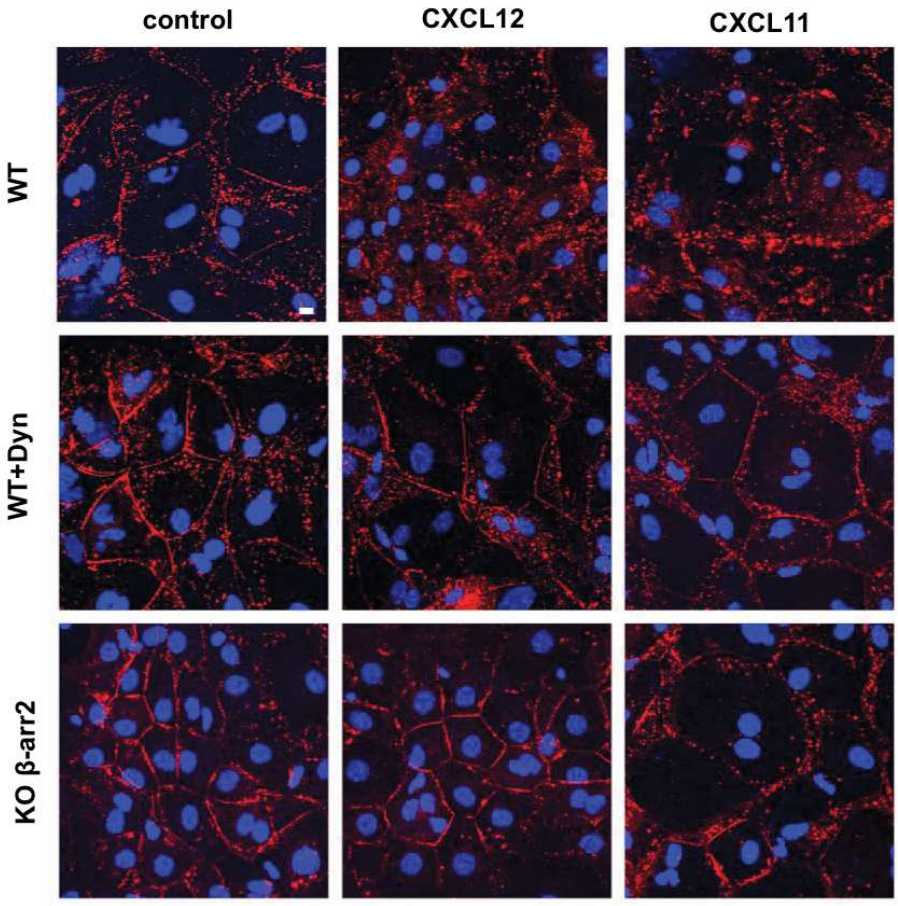

Figure 26 Agonist stimulation of ACKR3 promotes Cx43 internalisation in primary astrocyte cultures. Representative confocal pictures of confluent primary astrocytes cultures obtained from embryonic WT or β-arrestin2-/- mice (E15.5) are illustrated. Cx43 is stained in red. Astrocytes were exposed to either vehicle or CXCL12 (10-8 M) or CXCL11 (10-7 M) in absence or presence of Dynasore (Dyn, 80 µM) for 30 min. Scale bar = 10 µm.

3.1.7 ACKR3 ACTIVATION INCREASES SURFACE LOCALIZATION OF CX43 HEMICHANNELS.

As reported in the introduction, Cx43 also forms hemichannels that mediate the release of ATP, glutathione, glutamate and aspartate in the extracellular space[234]. Hemichannels and gap junctions have previously been shown to be differently regulated by pro-inflammatory cytokines[249]. Specifically, cytokines diminish Cx43 hemichannels activity and concomitantly increase GJIC. Using a biotinylation technique, we investigated the amount of Cx43 hemichannel present at the cellular surface upon ACKR3 activation by CXCL12 or CXCL11. In fact, using the biotinylation technique it is possible to discriminate between Cx43 forming gap junctions and hemichannels[275–277]: only Cx43 in hemichannels, but not Cx43 engaged in gap junctions can be biotinylated by a cell-impermeable amine-reactive biotinylation reagent[278]. Astrocyte cultures were exposed to CXCL12 (10^{-8}M) or CXCL11 (10^{-7}M) for 30 min prior to biotinylation of cell-surface proteins. Afterwards, biotin was quenched, cell lysed and biotinylated proteins purified on streptavidin beads. We have collected preliminary data showing that activation of ACKR3 by CXCL12 increases the amount of biotinylated Cx43, i.e. Cx43 hemichannels at the cell surface of astrocytes (**Figure 27**). Yet, these results must be confirmed on a larger replicate number.

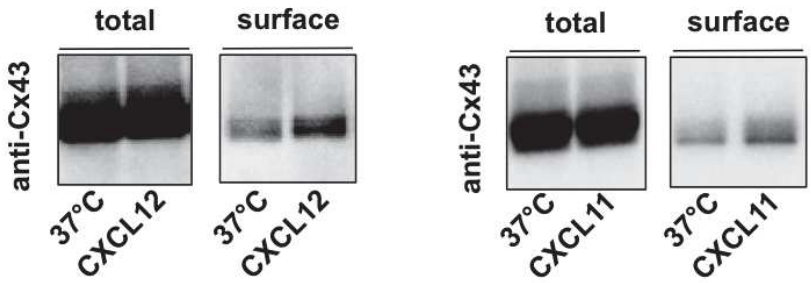

Figure 27 ACKR3 activation increases membrane expression of Cx43 hemichannels. Representative blots of the total and surface Cx43 hemichannel expression in control and either CXCL12 (10-8 M) or CXCL11 (10-7 M) treated (30 min) confluent primary astrocytes culture obtained from embryonic mice (E15.5).

Since more Cx43 hemichannels are present at the cellular surface, we next examined whether this was due to reduced internalisation. Proteins expressed at the cell surface were biotinylated at 4°C. After quenching and removing the biotin in excess, astrocytes were either kept at 4°C or 37°C or exposed to CXCL12 (10^{-8}M) or

CXCL11 (10^{-7}M) for 30 min at 37°C. Thereafter, cells were exposed to a cell-impermeable reducing agent (MESNA) in order to cleave the biotin from cell-surface proteins, so that the remaining biotinylated fraction represents intracellular (internalised) proteins. For each condition, some cells were not exposed to MESNA to measure total biotinylated proteins (internalised + non-internalised). Biotinylated proteins were then purified on streptavidin beads. Neither CXCL12 (p = 0.56, n = 3 *vs.* total 37°C) nor CXCL11 (p = 0.95, n = 3 *vs.* total 37°C) influenced the total expression of Cx43. Consistent with its constitutive internalisation, Cx43 was found to be more internalised at 37°C compared to 4°C. Both CXCL12 and CXCL11 inhibited the internalisation of Cx43 hemichannels when compared to the constitutive internalisation at 37°C (**Figure 28**).

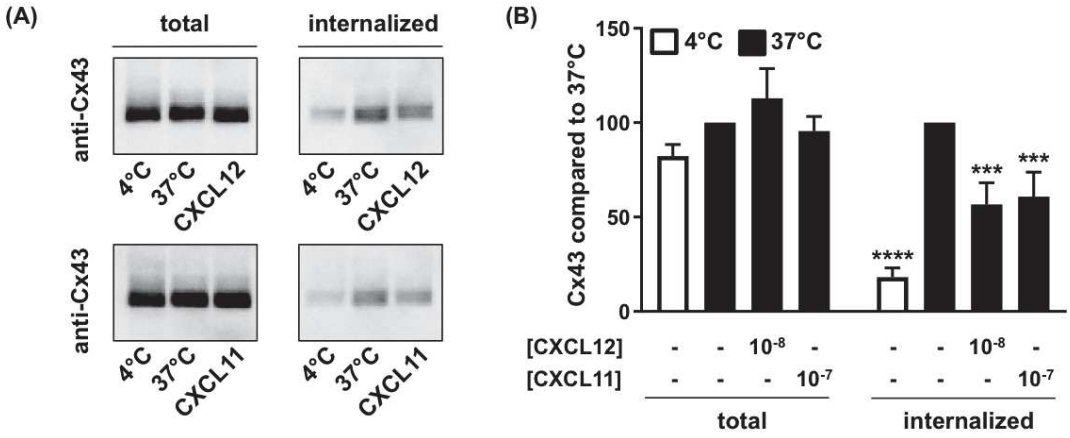

Figure 28 ACKR3 activation by CXCL12 and CXCL11 inhibits Cx43 hemichannel internalisation. (A) Representative blots of the total and internalised Cx43 hemichannel expression in astrocytes kept at 4°C (minimal internalisation) at 37°C (control) or exposed to either CXCL12 (10-8 M) or CXCL11 (10-7 M) for 30 min. (B) Quantification of Cx43 chemiluminescent signal of three biological independent experiments. Average values ± SEM are plotted. Values were normalized to the signal obtained at 37°C. Two-way Anova with Sidak's post-hoc test was used for the analysis comparing values to the 37°C condition. **** P≤0.0001, *** P≤0.01.

Therefore, ACKR3 activation inhibits Cx43 hemichannels internalisation in astrocytes and, thus, increases the cell surface localization of the Cx43 hemichannel in primary culture astrocytes. Interestingly, dynamin is involved in this process since its inhibition abolished CXCL12-mediated inhibition of Cx43 hemichannel internalisation (p=0.96, n=3 *vs.* internalised 37°C) (**Figure 29**).

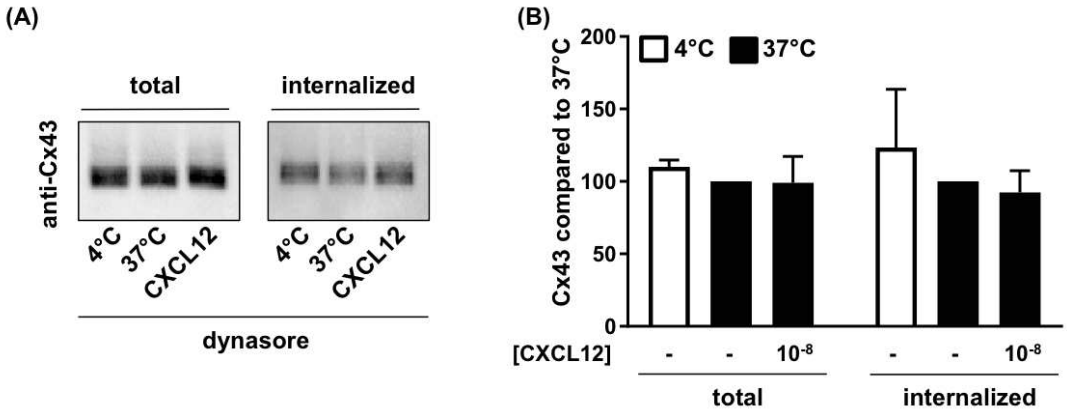

Figure 29 Dynasore impairs CXCL12-mediated inhibition of Cx43 hemichannel internalisation. (A) Representative blots of the total and internalised Cx43 hemichannel expression in astrocytes treated with Dynasore (80µM) and kept at 4°C at 37°C (control) or exposed to CXCL12 (10^{-8} M) for 30 min. (B) Quantification of Cx43 chemiluminescent signal of three biological independent experiments. Average and SEM are plotted. Values were normalized comparing the signal to the one obtained at 37°C. Two way Anova with Sidak's post-hoc test was used for the analysis comparing values to the 37°C condition.

3.1.7 ACKR3 IS CO-LOCALIZED WITH CX43 IN GLIOBLASTOMA.

As reported in the introduction, both Cx43 and ACKR3 play pivotal role in glioma progression. Co-localization analysis after double labelling of ACKR3 or CXCR4 and Cx43 indicates that ACKR3, but not CXCR4, is co-localized with Cx43 in two different glioma-initiating cell lines (R633 and TG1) isolated from human glioblastoma endogenously expressing ACKR3, CXCR4 and Cx43. Specifically, using the overlap approach[408] and setting an automatic threshold[409] we defined the overlapping volume where Cx43 co-localizes with ACKR3 or CXCR4 (**Figure 30**). To quantify co-localization we firstly calculated the percentage of the signal intensity of Cx43 in the overlapping volume when compared to the total Cx43 signal. We found that 68 ± 8.2 (n = 5) and 55 ± 3.8 (n = 4) % of Cx43 co-localizes with ACKR3 in R633 and TG1 cells, respectively. On the other hand, a much smaller fraction of Cx43 co-localizes with CXCR4 in the same cell lines (21 ± 4.5, n = 5 and 13 ± 3.2 %, n = 7 co-localization in R633 and TG1 cells, respectively) (**Figure 30B**). In order to confirm these results, we also quantified the percentage of either receptor present in the overlapping volume. 54±12.3 and 42 ± 7.5% of ACKR3 signal was co-localized with Cx43 in the R633 and TG1 cells, respectively; whereas only 25 ± 7.0 and 7 ± 2.7 % of CXCR4 signal was co-localized with Cx43 (**Figure 30C**).

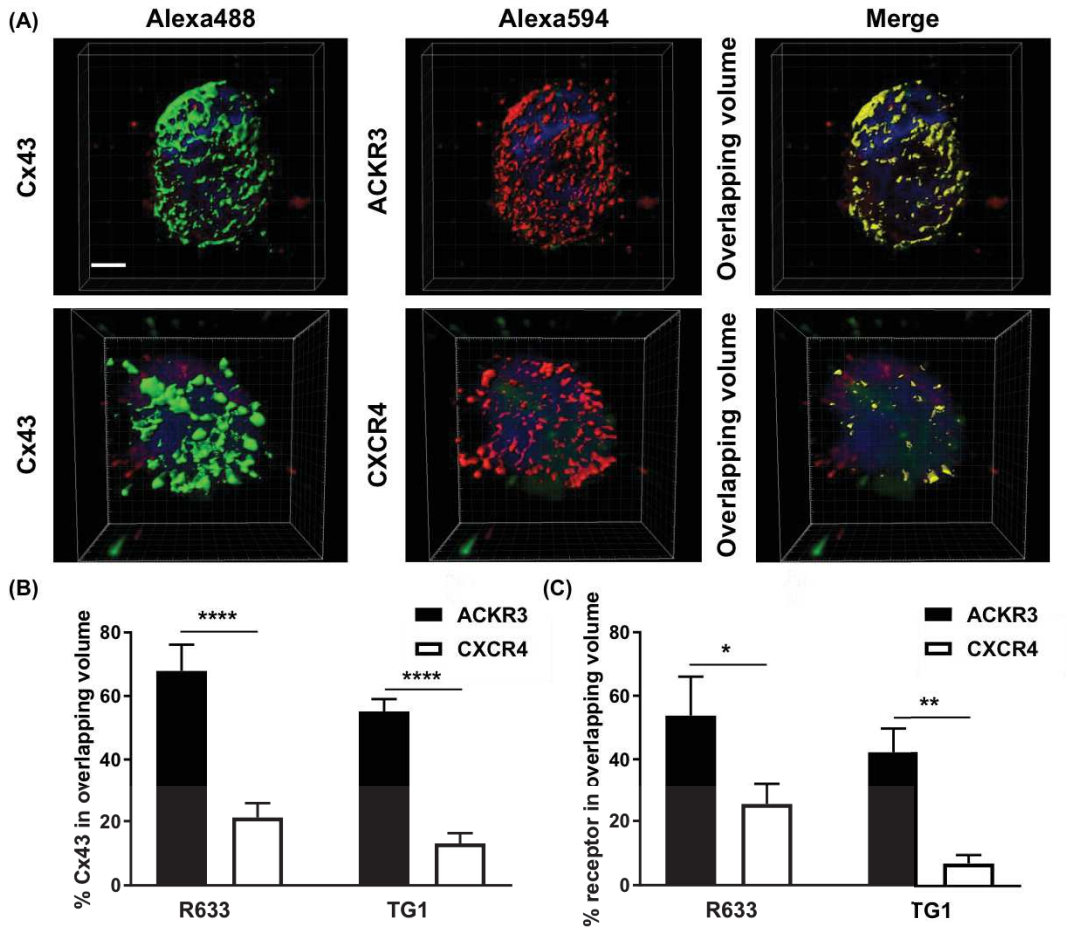

Figure 30 ACKR3 but not CXCR4 co-localizes with Cx43 in a glioma initiating cell line isolated from human glioblastoma. (A) Representative 3D reconstruction of the signal obtained from confocal images of R633 cells using the Imaris software. The overlapping volume has been calculated as described in the material and methods section. (B) Quantification of the % of Cx43 intensities present in the co-localizing volume in each cell type. Average values collected from at least four cells (50 z-stacks for cell) are plotted. (C) Quantification of the % of receptor (ACKR3 or CXCR4) intensities present in the co-localizing volume in each cell type. Average values collected from at least four cells (50 z-stacks for cell) are plotted ±SEM. Two-way Anova with the Sidak's post-hoc test were used for statistics (**** P≤0.0001, ** P≤0.001, * P≤0.05). Scale bar = 3μm.

3.1.8 ACKR3 LIGAND INDEPENDENTLY INHIBITS CX-MEDIATED GJIC IN HEK293T CELLS.

ACKR3 is overexpressed in various cancer types, including glioblastoma[69]. After showing that ACKR3 *activation* inhibits GJIC in astrocytes primary cultures triggering Cx43 internalisation, we examined whether ACKR3 *overexpression* alone would also be able to modulate Cx43 activity. Therefore, we transiently transfected HEK-293T cells with cDNAs encoding either ACKR3 or CXCR4. Using a glass patch pipette we microinjected single transiently transfected HEK-293T cell with a 1mg/ml LY solution. Cells were perfused with LY for 5 min. LY diffused for an additional 5-min period. GJIC was then quantified counting the number of neighbouring cells stained with LY after the 10 min period (**Figure 31A**). LY injected into cells transfected with empty vector diffused into more than 14 ± 1.05 neighbouring cells (n = 17) (**Figure 31B**). This value slightly but not significantly decreased to 11 ± 1.7 cells when CXCR4-transfected cells were microinjected (n = 10), indicating that CXCR4 expression does not affect GJIC (p=0.24 *vs.* mock). On the other hand, LY diffused into 2 ± 0.43 cells from ACKR3 transfected cells (n = 19). Likewise, Carbenexolone (80 µM) strongly reduced LY diffusion from microinjected, empty vector-transfected cells (0.2 ± 0.2 LY-stained cells, n = 5). Collectively, these results indicate that ACKR3 expression constitutively inhibits GJIC to a comparable extend as Carbenexolone (CBX), a GJIC chemical inhibitor in HEK-293T cells.

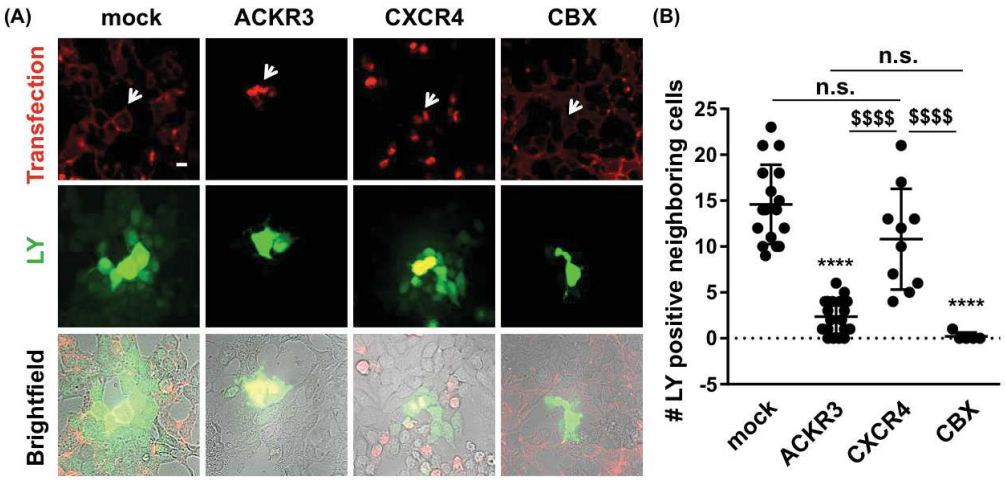

Figure 31 ACKR3 expression inhibits GJIC in HEK-293T cells. (A) Representative pictures obtained after LY microinjection in single HEK-293T cells transiently expressing mCherry targeted to cell membrane (mock and CBX) as described in [439], mCherry-tagged ACKR3 and mCherry CXCR4. Scale bar = 10 µm (B) Quantification of neighbouring cells receiving LY. Individual values and SD are represented. One-way Anova with Tukey's post-hoc test was used for the analysis. **** P≤0.0001 *vs.* mock, $$$$ P≤0.0001.

3.1.9 LIGAND-INDEPENDENT INHIBITION OF GJIC IN HEK-293 CELLS DOES NOT DEPEND ON DYNAMIN.

ACKR3 is known for its high degree of constitutive and ligand-induced internalization[142]. We confirmed the constitutive internalization using a DERET internalization assay[410]. In brief, HEK-293T cells were transfected with cDNA encoding N-terminally SNAP-tagged ACKR3 or CXCR4. Cell surface expressed receptors were labelled with SNAP-Lumi4®-Terbium (energy donor) at 16°C, which upon excitation with a laser at 347 nm emits at 620 nm. Cells were then exposed to a solution of cell impermeable fluorescein. Fluorescein quenches the signal coming from membrane-expressed receptors, by absorbing the energy transferred from terbium and then emit at 520 nm because of an energy transfer between the Terbium and fluorescein. Internalized receptors will be free to emit at 620 nm when excited. Therefore, recording the change over time in the ratio of the signal at 620 nm (internalized receptor) divided by the signal at 520 nm (receptor at the membrane) will allow quantifying the receptor internalization. In this assay ACKR3 constitutively internalized at higher rate, compared to CXCR4 (**Figure 32A**). Corroborating the higher constitutive internalisation rate of ACKR3 internalisation, compared with CXCR4 demonstrated by DERET, immunocytochemistry experiments showed a diffuse cytoplasmic staining of ACKR3 **(**Figure 32B), whereas CXCR4 staining was mainly confined into the plasma membrane. DERET experiments also confirmed that ACKR3 internalisation is induced by CXCL12 (**Figure 32C**).

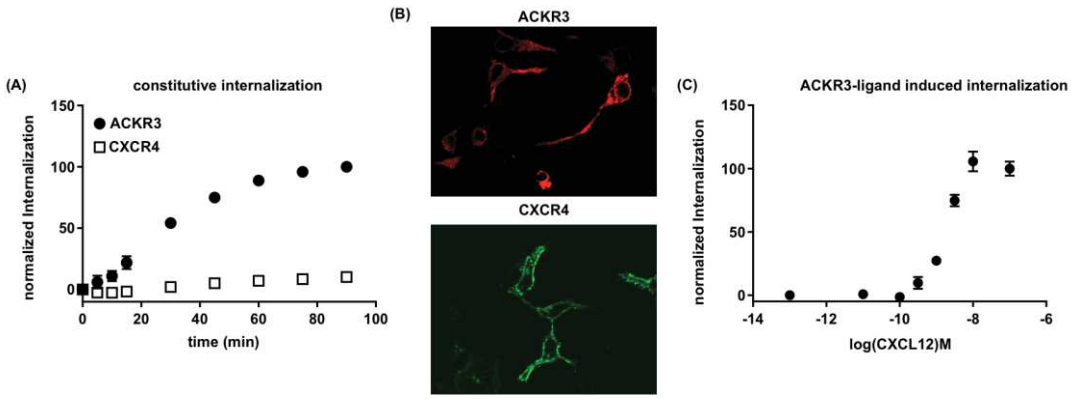

Figure 32 ACKR3 constitutively and ligand dependently internalises in HEK-293T cells. (A) Constitutive internalisation of SNAP-tagged ACKR3 and CXCR4 transiently expressed in HEK293T over time measured using a DERET assay. Average of three independent replicates ± SEM are plotted. Values were normalized to the maximal internalisation. (B) Representative pictures taken from HEK-293T cells transiently expressing HA-tagged ACKR3 and CXCR4 stained with anti-HA antibodies. (C) SNAP-ACKR3 internalisation upon CXCL12 stimulation in transfected HEK-293T cells. Average of three independent replicates ± SEM are plotted. Values were normalized to the ACKR3 internalisation at the highest CXCL12 concentration.

As in astrocytes, we next investigated the role of dynamin in the ligand-independent inhibition of GJIC elicited by ACKR3 expression by microinjection of LY in HEK-293 cells (**Figure 33A**). Dynasore treatment, which alone slightly but not significantly LY diffusion from microinjected cells (14 ± 1.05, n=17 in absence of Dynasore *vs.* 12 ± 1.35, n = 12, in presence of Dynasore p= 0.33), did not prevent the reduction of LY diffusion from ACKR3-expressing cells (2 ± 0.68, n = 12 in presence of Dynasore *vs.* 2 ± 0.43 in absence of Dynasore, n = 19, p > 0.99) (**Figure 33B**), suggesting that dynamin does not mediate the agonist-independent ACKR3-mediated GJIC inhibition in HEK-293T cells.

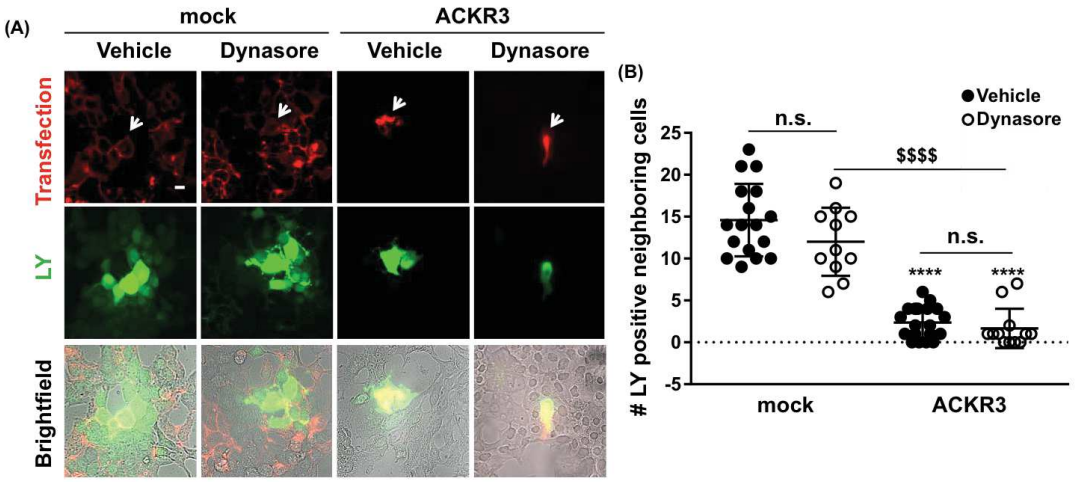

Figure 33 Dynasore does not reverse ligand-independent inhibition of GJIC mediated by ACKR3 in HEK-293T cells. (A) Representative pictures obtained after LY microinjection in single HEK-293T cells transiently expressing mCherry targeted to cell membrane (mock) as described in [439] and mCherry tagged ACKR3 treated or not with dynasore (80 µM) for 30min. (B) Quantification of neighbouring cells receiving LY. Individual values and SD are represented. One-way Anova with Tukey's post-hoc test was used for the analysis. **** P≤0.0001 vs. mock, $$$$ P≤0.0001.

3.1.10 ACKR3 C-TERMINAL DOMAIN IS NOT ESSENTIAL FOR INTERACTION WITH Cx43 BUT IS REQUIRED FOR ACKR3-MEDIATED GJIC INHIBITION.

To further explore the molecular mechanisms underlying Cx43-mediated GJIC inhibition induced by ACKR3 expression, we tried to characterize the site of interaction between Cx43 and ACKR3. Given that the C-terminal domain of GPCRs is a major site mediating protein-protein interactions, we generated ACKR3 mutants partially or totally truncated of the C-terminal domains (ACKR3Δ16 and ACKR3ΔCt) and examined the ability of the truncated receptors to interact with Cx43 in HEK-293T cells by co-immunoprecipitation (**Figure 34A & B**). Both mutants retained unaltered ability to interact with Cx43 ($p = 0.84$, $n = 3$ and $p = 0.34$, $n = 3$ for ACKR3 *vs.* ACKR3Δ16 and ACKR3ΔCt, respectively) (**Figure 34C**), suggesting that the C-terminal domain of ACKR3 is not involved in the interaction.

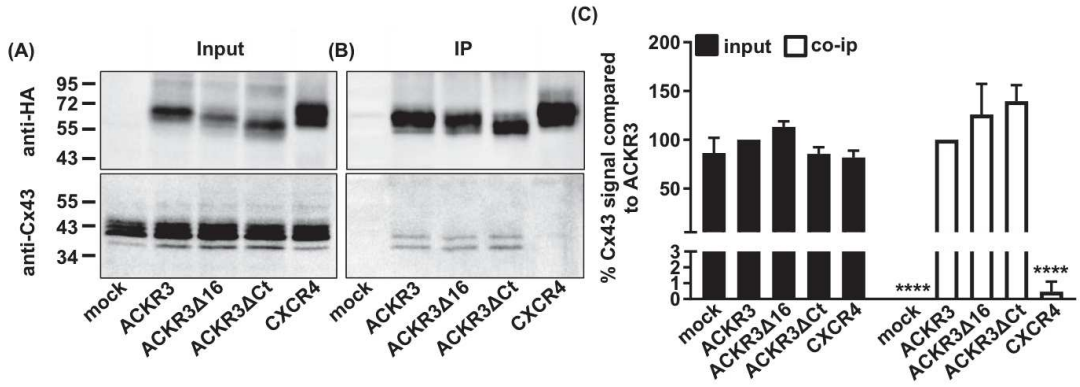

Figure 34 The C-terminal domain of ACKR3 does not mediate its interaction with Cx43. (A) Immunoprecipitation (IP) of HA-ACKR3, HA-ACKR3Δ16, HA-ACKR3ΔCt and HA-CXCR4 transiently expressed in HEK-293Tcells compared to mock cells. (B) Cx43 co-immunoprecipitation in the same conditions as (A). In both (A) and (B) representative blots of the three independent replicates are shown. (C) Average Input and Co-IP Cx43 chemiluminescence quantified in three independent experiments (± SEM). Values were normalized comparing them to ACKR3. Two-way Anova with Tukey's post-hoc test was used for the comparisons. **** P≤0.0001 vs. ACKR3.

This domain also plays a pivotal role in signal transduction, especially β-arrestin-dependent signalling, as well as receptor internalisation. Therefore we next explored whether expression of the truncated ACKR3 mutants inhibits GJIC (**Figure 35A**). Expression of the two mutants did not inhibit LY diffusion in HEK-293 cells ($p = 0.99$, $n = 10$ for ACKR3Δ16 and $p = 0.83$, $n = 9$ for ACKR3Δ16 both *vs.* mock) (**Figure 35B**), indicating that the C-terminal domain of ACKR3 is essential for inhibiting but not for interacting with Cx43.

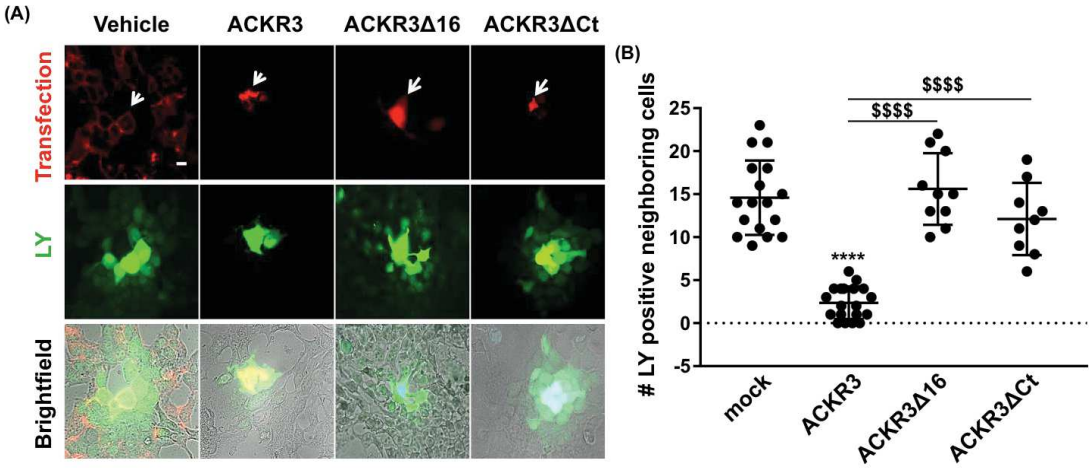

Figure 35 Expression of ACKR3 C-terminally truncated mutants does not inhibit Cx43 activity in HEK-293T cells. (A) Representative pictures obtained after LY microinjection in single HEK-293T cells transiently expressing mCherry targeted to cell membrane (mock) as described in [439], mCherry-tagged ACKR3, CFP-tagged ACKR3Δ16 and ACKR3ΔCt. (B) Quantification of neighbouring cells receiving LY. Individual values and SD are represented. One-way Anova with Tukey post-hoc test was used for the analysis. **** P≤0.0001 vs. mock, $$$$ P≤0.0001.

3.2 ACKR3 ACTIVATES G PROTEINS IN MOUSE PRIMARY ASTROCYTES BUT NOT IN HEK-293T CELLS

3.2.1 ACKR3 INHIBITION OF GJIC IN PRIMARY ASTROCYTES DEPENDS ON Gαi/o PROTEINS.

Although ACKR3 signals canonically trough β-arrestins, a few studies have shown that it can also recruit and activate G proteins in specific cell types, including astrocytes[150,153]. In addition, Cx43 is regulated by several GPCRs by pathways involving the activation of G proteins[299]. We thus examined if GJIC inhibition elicited by agonist stimulation of ACKR3 could be mediated by G proteins in cultured astrocytes, using the scrape loading technique (**Figure 36A**). Pre-treatment of astrocytes with *Pertussis Toxin* (PTX) 100 ng/ml, which irreversibly blocks $G_{i/o}$ protein activation abolished CXCL12 (10^{-8} M)- or CXCL11 (10^{-7} M)-induced inhibition of GJIC ($p = 0.79$, n= 5 for PTX + CXCL12 and $p = 0.91$, n = 5 for PTX + CXCL11 both *vs.* Control + PTX, n=8), whereas it did not reverse the CBX GJIC inhibition (**Figure 36B**). Interestingly, PTX significantly increased (122 ± 8.8%, n = 8) the basal GJIC communication in astrocytes. Together, these results show that Cx43-mediated GJIC inhibition induced by ACKR3 activation is dependent on $G_{i/o}$ proteins.

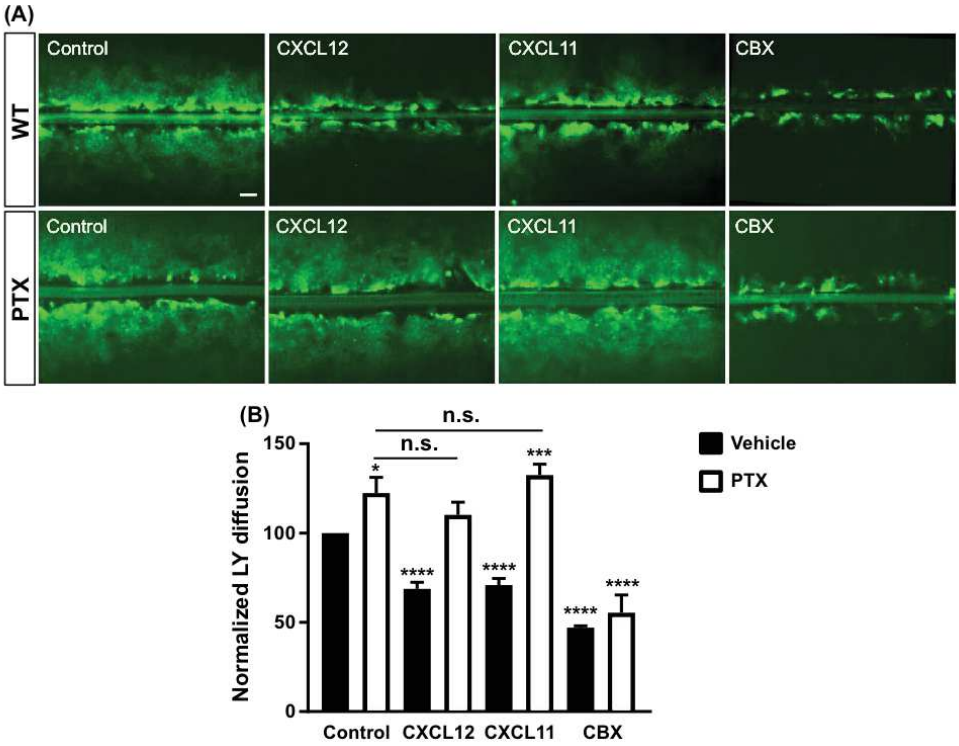

Figure 36 PTX inhibits ligand-induced inhibition of GJIC mediated by ACKR3 in primary cultures of mouse astrocytes. (A) Representative pictures of the scrape loading assay, performed in confluent primary astrocyte cultures obtained from embryonic WT mice (E15.5), taken ten minutes after scraping in the presence of LY. PTX (100 ng/ml) and CBX (50 µM) treatments were applied overnight. CXCL12 (10-8 M) and CXCL11 (10-7 M) were applied for 30 min. Scale bar = 100 µm. (B) Quantification of the LY diffusion by calculation of the distance from the scrape where LY intensity is halved. Values were normalized by comparison to the LY diffusion in Control. Average values (± SEM) from of at least three independent experiments performed in triplicate are represented. One-way Anova with Tukey's post-hoc test was used for the comparison. **** P≤0.0001, *** P≤0.001, * P≤0.05 vs. control

3.2.2 ACKR3 ACTIVATES $G\alpha_{i/o}$ PROTEINS IN ASTROCYTES

Intrigued by the possible involvement of $G_{i/o}$ proteins in the ACKR3-mediated inhibition of GJIC, we investigated the ability of the receptor to engage $G\alpha_i$-dependent signalling proteins by measuring the inhibition of cAMP production in astrocytes challenged with the adenylyl cyclase activator forskolin. Treating cells with CXCL12 (10^{-8} M) or CXCL11 (10^{-7} M) for 5 min inhibited cAMP production (-36.51 ± 6.44%, n = 4 and -19.25 ± 5.83%, n = 3) (**Figure 37**). As expected and reminiscent of the scrape loading studies, PTX (100 ng/ml, 18 h) reversed this inhibition. Pre-treatment of cells with the CXCR4 antagonist AMD3100 (10^{-6} M) for 30 min was unable to prevent the CXCL12-induced inhibition of cAMP production (-39.4 ± 3.62%, n = 5), suggesting that ACKR3 (and not CXCR4) is involved in the CXCL12 effect. Taken together, these results show that ACKR3 stimulation by CXCL12 and CXCL11 triggers activation of $G\alpha_{i/o}$ proteins in primary cultures of murine astrocytes.

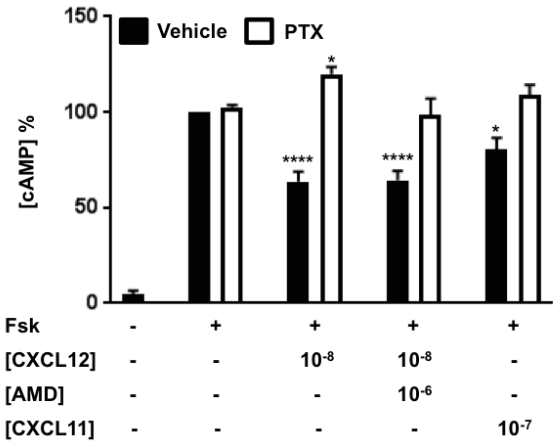

Figure 37 ACKR3 activation by CXCL12 and 11 inhibits cAMP production in primary cultured astrocytes. Quantification of endogenous cAMP was performed after stimulation of cAMP production with the adenylyl cyclase activator forskolin (FSK, 10^{-6} M) for 5 min and treatment of cells with CXCL12 or CXCL12 or saline solution for 5 min. In the case of AMD3100-treated cells, the antagonist (10^{-6} M) was added for 30 min before the CXCL12 challenge. Values represented are the average of three independent replicates ± SEM. Two-way Anova with Dunnett's post-hoc test was used for the analysis. **** P≤0.0001, * P≤0.05 vs. Fsk

3.2.3 ACKR3 CAN CONSTITUTIVELY RECRUIT G PROTEINS BUT IT IS UNABLE TO ACTIVATE THEM IN HEK-293T CELLS.

We found that ACKR3 activates G proteins in astrocytes and that G proteins are necessary for the inhibition of GJIC. We then tested if this is also valid in another context such as HEK-293T cells in line with the results of our interactomic screen that demonstrated agonist-independent interaction of ACKR3 with $G\alpha_{i3}$. We first confirmed this interaction by saturation BRET (**Figure 38A**). HEK-293T cells were co-transfected with increasing amounts of cDNA encoding ACKR3 C-terminally-tagged with YFP and a constant amount of RLuc-tagged $G\alpha_{i3}$. The data show a constitutive interaction between ACKR3 and $G\alpha_{i3}$ proteins (**Figure 38A**). Neither PTX nor CXCL12 (10^{-8} M) treatments modified the interaction (p = 0.79, n=3 for vehicle *vs.* CXCL12 and p = 0.86, n = 3 for vehicle *vs.* PTX) (**Figure 38B**).

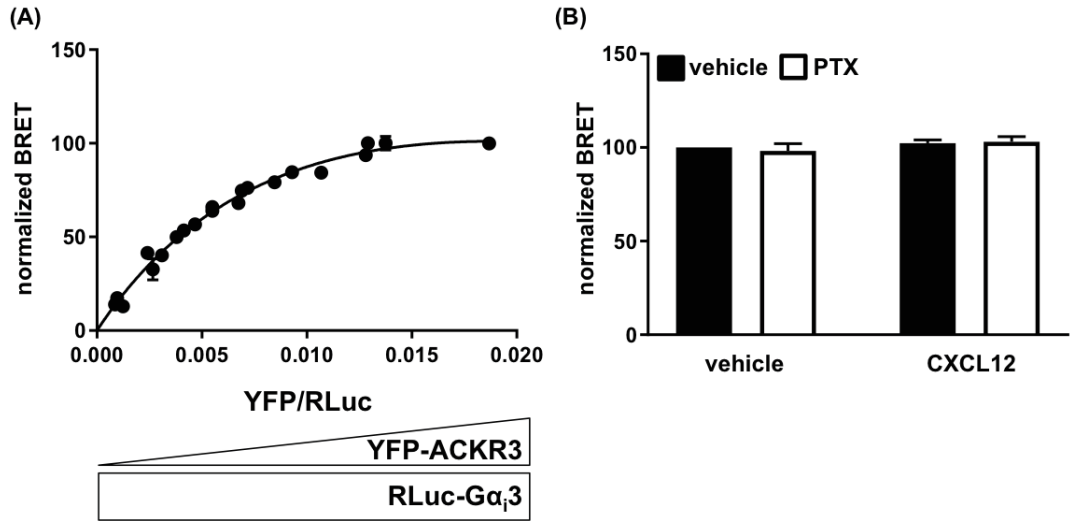

Figure 38 ACKR3 constitutively interacts with Gαi3 in living HEK-293Tcells. (A) Titration curves of the ACKR3-YFP–Gαi3-RLuc interaction in HEK-293T cells. Values represented are the average of three independent replicates ± SEM. BRET values were normalized to the maximum BRET obtained in each replicate. Again, the one site total curve was fitted as described in Figure 3. (B) Quantification of the BRET signal between YFP-ACKR3 and RLuc-Gαi3 expressed in HEK-293T cells with and without ACKR3 activation by CXCL12 (10^{-8} M) for 5 min and PTX (100 ng/ml, 18 h). YFP/RLuc ratio used was the one giving the BRET50 in saturation curve. Graph represents average of three biologically independent replicates (±SEM). Two-way Anova with Sidak's post-hoc test was used for the statistical analysis.

Since ACKR3 can recruit G proteins in HEK-293T, we tested if the receptor can also activate them by measuring cAMP inhibition. Intriguingly, agonist stimulation of CXCR4, but not ACKR3 ($p = 0.91$, $n = 16$ *vs.* ACKR3 Fsk), inhibited cAMP production in forskolin-treated HEK-293T down to 68 ± 3.5 % (n=15) (**Figure 39A**), suggesting that ACKR3 does not engage G_i signalling in HEK-293T cells, consistent with previously published results[139,150]. Corroborating this hypothesis, PTX did not reverse the inhibition of GJIC induced by ACKR3 expression ($p = 0.67$, $n = 6$ ACKR3 + PTX *vs.* ACKR3) in HEK-293T cells when tested by microinjection of LY (**Figure 39B**).

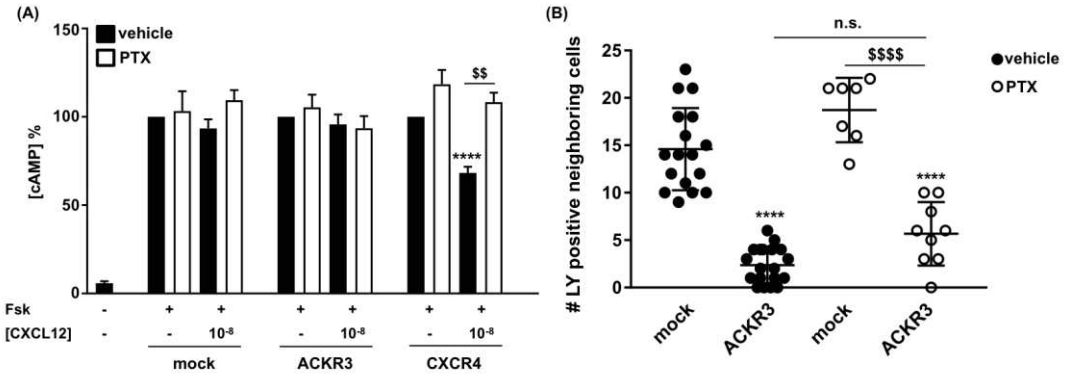

Figure 39 ACKR3 does not activate Gαi/o proteins in HEK-293T. (A) cAMP production in HEK-293T cells transiently transfected with empty plasmid (mock) or cDNAs encoding ACKR3 or CXCR4. cAMP production was stimulated by addition of forskolin (Fsk, 10-6 M) in cells pre-treated or not with PTX (100 ng/ml, 18 h). Values represented are the average of three independent replicates ± SEM. Two-way Anova with Tukey's post-hoc test was used for the analysis. **** P≤0.0001 vs. Fsk mock, $$ P≤0.01. (B) Quantification of neighbouring cells receiving LY in three independent biological replicates after microinjection of LY in HEK-293T cells, pre-treated or not overnight with PTX (100 ng/ml), expressing mCherry-tagged ACKR3 or mCherry targeted to cell membrane (Mock). Individual values and SD are represented. One-way Anova with Turkey's post-hoc test was used for the analysis. **** P≤0.0001 vs. mock, $$$$ P≤0.0001.

Therefore, ACKR3 activates G_i proteins in primary cultures astrocytes but not in HEK-293T cells. A possibility can be that only the murine receptor is coupled to G protein. Therefore we transfected HEK-293T cells with plasmids encoding RLuc tagged $G\alpha_{i1}$ protein, venus-tagged $G\gamma_2$ and non-tagged $G\beta_2$ with either mouse ACKR3 or mouse CXCR4. Again, only CXCR4 activation, but not ACKR3, was able to decrease the BRET between Gγ-venus and Rluc-Gα indicating that only CXCR4 is able to active G proteins in HEK-293T cells (**Figure 40**).

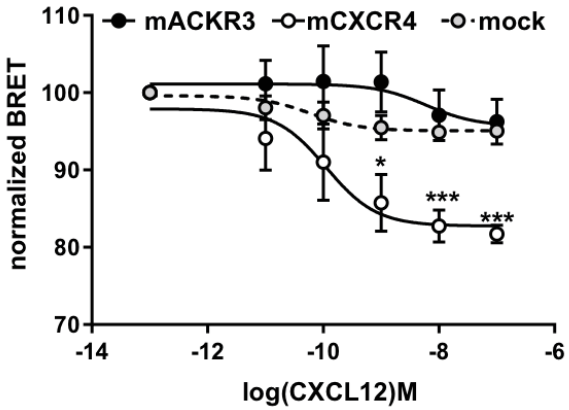

Figure 40 Only mouse CXCR4 but not ACKR3 activates G proteins in HEK-293T cells. HEK-293T transiently expressing RLluc-Gαi1 protein, Venus-γ2 and β2 alone (mock) or with mouse ACKR3 (mACKR) or mouse CXCR4 (mCXCR4) were used. G protein activation was quantified by measuring BRET decrease upon CXCL12 stimulation. Values represented the average of three independent biological replicates ± SEM. Two-way Anova with Dunnett's post-hoc test was used for the analysis *** P≤0.001, * P≤0.05 vs. staring BRET value in each condition.

3.3 MAPPING CXCR4 INTERACTOME

3.3.1 DECIPHERING THE CXCR4 INTERACTOME IN HEK-293T CELLS BY AP-MS.

As for ACKR3, CXCR4 interacting proteins were identified in human embryonic kidney HEK-293T cells transiently expressing hemagglutinin (HA)-tagged CXCR4 using an affinity-purification coupled to mass spectrometry (AP-MS) proteomic strategy. CXCR4-interacting proteins were immunoprecipitated using an anti-HA monoclonal antibody immobilized onto agarose beads and identified by nano-flow liquid chromatography coupled to tandem mass spectrometry (nanoLC-MS/MS). Control immunoprecipitations were performed using cells transfected with empty plasmid (mock). Systematic analysis by tandem MS of the immunoprecipitates identified a total of 3,802 proteins in the three independent experiments performed on different sets of cultured cells. This number reduced down to 1,203 after filtering out the proteins either identified only by site, or labelled as contaminant, or not identified in all three biological replicates in at least one group (CXCR4 or mock). Label-free quantification (LFQ) of the relative protein abundances in immunoprecipitates obtained from cells expressing CXCR4 and mock cells showed that 19 proteins were significantly more abundant in immunoprecipitates from CXCR4-expressing cells, using a t-test conducted on both sides and setting a False Discovery Rate (FDR) of 1%, in comparison with mock condition (**Table 8**).

Analysis of the relative abundance of proteins in immunoprecipitates showed, as expected, that CXCR4 is the most abundant protein (**Figure 41**). Identified CXCR4 partners included Glutaredoxin-3 (GLRX3), an enzyme belonging to the protein disulphide isomerase (PDI) family. Another PDI, GLRX1, is known to reduce intramolecular disulphide bonds of HIV envelope glycoprotein gp120 during virus entry[411]. Since gp120 interacts with CXCR4, GLRX enzymes could in turn indirectly interact with CXCR4[412,413]. CXCR4 also recruits COUP-TF 2 (NRF2F2), an orphan nuclear receptor that plays a critical role in organogenesis. Overexpression of COUP-TF1, characterized by 84.13% identity with COUP-TF 2 when aligned[414], inhibits expression of both CXCR4 and its endogenous ligand CXCL12 in breast cancer cells through EGFR activation [415]. The Minor histocompatibility antigen HM13, a peptidase required for the genesis of monomeric peptides, was also detected as a CXCR4 interacting protein. HM 13 that is a member of the HIV-1 envelope interactome as CXCR4[416].

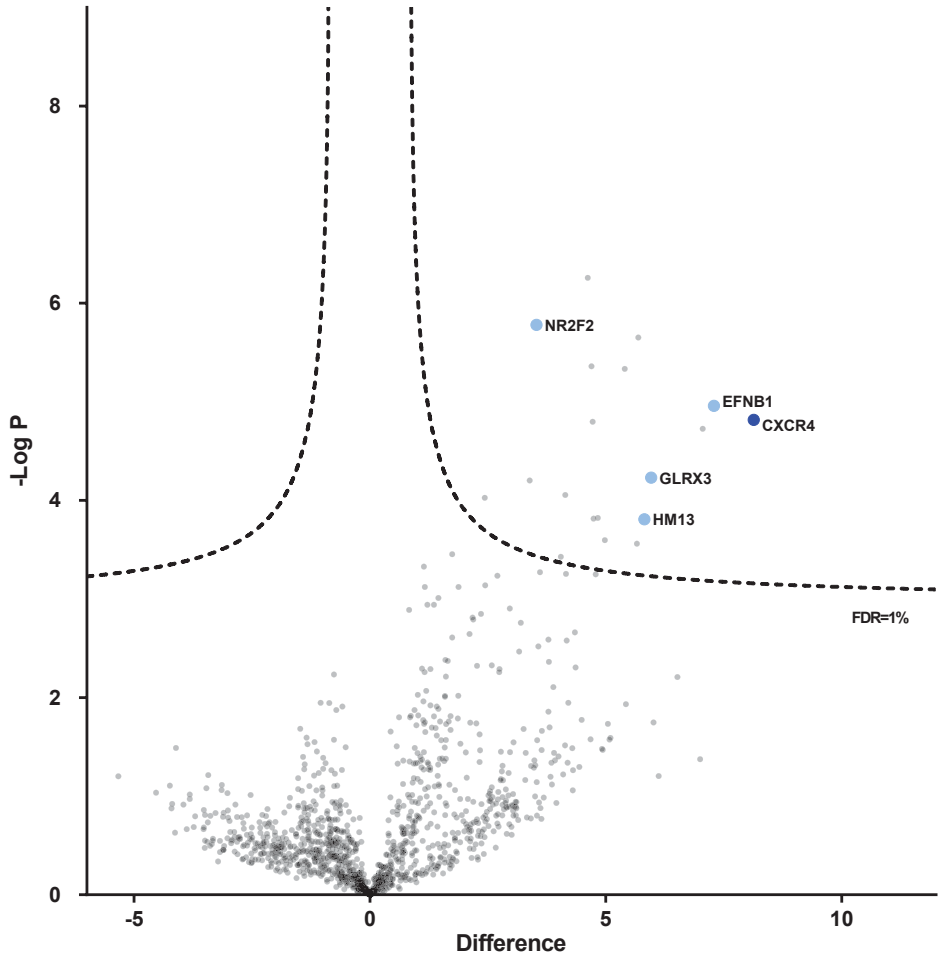

Figure 41 CXCR4 interacting proteins identified in HEK-293Tcells and their relative abundance in immunoprecipitates from CXCR4-expressing cells vs. mock cells. HA co-immunoprecipitation followed by nanoLC-MS/MS was performed in three distinct biological replicates in HEK-293T cells transiently expressing HA-tagged CXCR4 and cells transfected with empty plasmid (Mock). Log transformed intensities, obtained by Label Free Quantification (LFQ), of proteins identified in all three biological replicates in at least one set of cultured cells were than used for the comparison. The volcano plot was obtained plotting the differences of LFQ values between CXCR4 and mock cells (X axis) vs. –log of P value (Y axis). The upper part of the graph includes proteins with a high inter-replicate reproducibility whereas the right or left parts include plotted proteins with large differences in abundance between the two conditions. Specifically, on the right there are proteins enriched in the CXCR4 condition. The proteins were considered statistically significant using a T-test conducted on both sides setting the number of randomization at 250 the False Discovery Rate at 0.01 and the S0 at 0.1. Therefore, all proteins “above” the dotted lines are significantly enriched. The bait protein (CXCR4) is illustrated in blue; proteins already known to interact with CXCR4 (at least functionally) are in light blue.

Protein names	UniProtID	Gene names	Difference	P value
C-X-C chemokine receptor type 4	**P61073**	**CXCR4**	**8.13412**	**4.81752**
Ephrin-B1	P98172	EFNB1	7.29111	4.95875
Speckle targeted PIP5K1A-regulated poly(A) polymerase	Q9H6E5	TUT1	7.05343	4.7274
Glutaredoxin-3	O76003	GLRX3	5.96408	4.23064
Minor histocompatibility antigen H13	Q8TCT9	HM13	5.81814	3.8084
26S proteasome non-ATPase regulatory subunit 14	O00487	PSMD14	5.69013	5.6534
Short/branched chain specific acyl-CoA dehydrogenase, mitochondrial	P45954	ACADSB	5.65867	3.56233
Nuclear pore membrane glycoprotein 210	Q8TEM1	NUP210	5.40417	5.33476
Electron transfer flavoprotein subunit beta	P38117	ETFB	4.97812	3.59581
Beta-1,4-glucuronyltransferase 1	O43505	B4GAT1	4.82992	3.82343
Baculoviral IAP repeat-containing protein 6	Q9NR09	BIRC6	4.74226	3.81439
NEDD8-activating enzyme E1 regulatory subunit	Q13564	NAE1	4.72246	4.79763
Nucleoporin NDC1	Q9BTX1	NDC1	4.69831	5.36129
FH1/FH2 domain-containing protein 1	Q9Y613	FHOD1	4.6166	6.25869
Inositol-3-phosphate synthase 1	Q9NPH2	ISYNA1	4.14048	4.05474
ER membrane protein complex subunit 4	Q5J8M3	EMC4	4.04863	3.42766
COUP transcription factor 2	P24468	NR2F2	3.53283	5.77999
Origin recognition complex subunit 4	O43929	ORC4	3.38933	4.20258
26S protease regulatory subunit 6B	P43686	PSMC4	2.43658	4.02678

Table 8 List of proteins that specifically co-immunoprecipitate with CXCR4 in HEK-293T cells. Proteins statistically enriched according to their LFQ level in the CXCR4 complex compared to Mock cells are reported. Protein name, Uniprot ID, gene name, LFQ difference between CXCR4 and mock cell (Difference) and the – log P values (P value) are indicated. The statistical analysis was performed using the Perseus software as detailed in the “Materials and Methods” section. Proteins are ranked based on their difference in abundance in immunoprecipitates from CXCR4-expressing cells vs. Mock cells.

3.3.2 EPHRIN B1 INTERACTS WITH CXCR4.

Ephrin B1 (EFNB1), a cell surface anchored ligand for Ephrin B receptors, likewise co-immunoprecipitated with CXCR4 in our interactomic screen. Binding of Ephrin B1 to its receptor by direct cell-cell contact triggers both a forward and a backward signalling cascade in two adjacent cells. EFNB1 inhibits, in its backward signalling, G protein activation elicited by CXCR4 upon activation by CXCL12[417] and influences chemotaxis of HUVEC cells[418]. We next collect preliminary results, which must be repeated on a larger replicate number, confirming by western blotting the interaction between CXCR4 and Ephrin B1 using ACKR3 as negative control (**Figure 42**).

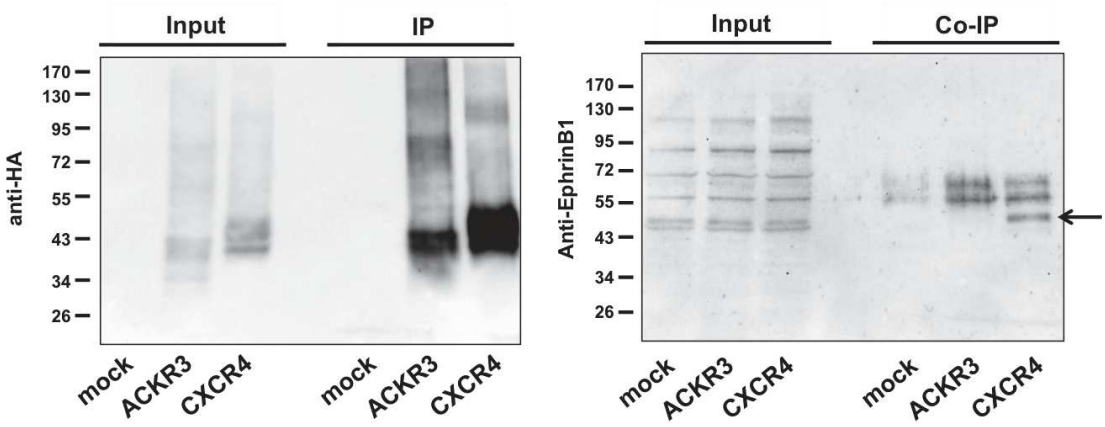

Figure 42 EphrinB1 co-immunoprecipitates with CXCR4 but not ACKR3 in HEK-293T cells. On the left immunoprecipitation (IP) of HA-ACKR3 and HA-CXCR4 transiently expressed in HEK-293T cells compared to mock cells (transfected with empty plasmid). On the right Ephrin-B1 co-immunoprecipitation (Co-IP) with HA-ACKR3 and HA-CXCR4 transiently expressed in HEK-293T cells compared to mock cells.

4. DISCUSSION

4.1 PROTEOMIC SCREENING OF CXCR4 AND ACKR3

Although ACKR3 has been found playing a pivotal role in fundamental biological processes such as migration[49], proliferation[148] and differentiation[167,168] of different cellular populations, the cellular pathways transducing these effects remain poorly characterized. The receptor was initially described as a silent receptor able only to shape the CXCL12 and CXCL11 chemo-attractant gradients and to lower the extracellular chemokine concentrations by binding and internalising them[124]. Several studies [139–142] showing that ACKR3 activates β-arrestin dependent signalling have now overcome this simplistic conception of the role of ACKR3. In addition, the notion that ACKR3 physically and functionally interacts with non-canonical G Protein Interacting Proteins (GIPs) such as the other chemokine receptor CXCR4[119] and the Epidermal Growth Factor Receptor (EGFR) [155] has expanded the possible signalling pathways activated by the receptor. CXCR4 shares with ACKR3 the capacity to bind to CXCL12. Upon activation CXCR4 triggers canonically associated GPCR signalling pathways[79], including Gαi and β-arrestin pathways. As ACKR3, CXCR4 has also been found to interact with several proteins able to modify its signalling, trafficking and localization.

Collectively, these findings provided the impetus for ACKR3 and CXCR4 interactome characterization using an AP-MS proteomics strategy. Thus, we immunoprecipitated (HA)-tagged ACKR3 or CXCR4 expressed in human embryonic kidney (HEK)-293T cells and we systematically identified co-immunoprecipitating proteins by mass spectrometry.

Analysis of the CXCR4 interacting network based on Label Free Quantification (LFQ) and setting a stringent False Discovery Rate (FDR) of 1% revealed that 19 proteins specifically co-immunoprecipitated with the receptor (they were not detected in control immunoprecipitations performed from cells transfected with empty plasmid). In accordance with its constitutive internalisation[142] and presence in intracellular compartments, the same analysis performed on the ACKR3 interacting network resulted in 151 proteins that were significantly more abundant in immunoprecipitates from ACKR3-expressing cells compared to mock cells. Therefore, by AP-MS, we identified 19 and 151 *potential* interacting proteins for CXCR4 and ACKR3, respectively. Indeed, it is important to keep in mind that interacting proteins identified

following AP-MS protocols, especially when performed in cells overexpressing the protein of interest, must be considered as *potential* partners whose interaction must be further validated *via* other assays including functional ones. In fact, overexpressed proteins might interact with more proteins (false positive) only because of their mislocalization in different subcellular compartments compared to the endogenously expressed ones. Despite this limitation, our group has already applied the same strategy with other GPCRs whose *potential* interacting proteins firstly identified with a similar AP-MS screen have been further validated[26,27]. In addition, the Functional Proteomic Platform (FPP) of Montpellier has generated a database including the proteins considered as "contaminants", due to their frequent appearance as co-immunoprecipitating proteins, in overexpressed system, that helps in the discrimination between "false" and "real" interacting proteins.

As expected, and validating the relevance of the co-immunoprecipitation strategy used for affinity-purification of partners, the two bait receptors (CXCR4 and ACKR3) were the most abundant proteins in each Co-IP. In addition, consistent with the constitutive internalisation and ubiquitination[142] of ACKR3, clathrin, Rab3 and Rab 5 complexes were retrieved in the ACKR3 complexes together with ubquitinin enzymes.

Amongst the 19 potential CXCR4-interacting proteins identified, we decided to validate by Western Blotting (WB) its interaction with Ephrin B1 in line with its high relative abundance in the co-immunoprecipitating complex and previous results[417] showing that Ephrin B1 inhibits G protein signalling triggered by CXCR4 upon activation by CXCL12[417]. Despite these promising preliminary results, further studies validating the interaction in endogenous settings are needed before considering EphrinB1 as a CXCR4-interacting protein

4.2 ACKR3 INTERACTS WITH Cx43 AND INHIBITS ITS GAP JUNCTIONAL INTERCELLULAR COMMUNICATION

Connexin 43 (Cx43) was among the 151 proteins identified as *potential* ACKR3-interacting proteins in our proteomic screen. Cx43 is a 43kDa protein that after synthesis oligomerizes in hexameric channels (hemichannels). Hemichannels present on adjacent cells dock head-to-head together forming gap junctions permeable to ions and small molecules, which ensure Gap Junctional Intercellular Communication (GJIC)[224].

Only a few studies suggested a possible functional link between gap junctions and the CXCL12/CXCR4/ACKR3 axis. Two of them focused on the CXCL12/CXCR4 axis. In fact, in a large phosphoproteomic screen aimed at identifying proteins phosphorylated upon CXCL12 stimulation, CXCR4 triggered phosphorylation of Cx43 at Ser^{279} and Ser^{282} in breast cancer cells [419]. In line with these findings, an other study conducted on breast cancer showed that low CXCL12 concentrations influence Cx43 phosphorylation states and GJIC[420]. Specifically, CXCL12 through activation of CXCR4 induces PKC activation and increases GJIC. However, the data reported in this study are fragmentary and sometimes contradictory. In fact, the data illustrated on Fig 2C showed that high CXCL12 concentrations reduce Cx43 expression in confluent cells. However, this result was not reproduced in Fig 4A. This contradiction could originate from the fact that the experiments might have been conducted only once (number of replicates is not indicated). In addition, the authors attributed the effect solely to CXCR4 and not ACKR3 based on the evidence that pre-treatment with AMD3100 reduced CXCL12 dependent Cx43 phosphorylation. However, the effect of AMD3100 on GJIC was not investigated.

Schajnovitz and colleagues elegantly showed a dual regulatory control of connexin 43 in CXCL12 production and release in bone marrow-derived mesenchymal stem cells (schematically represented in **Figure 43**). Specifically, Cx43 involved in gap junctions controls CXCL12 release whereas Cx43 that is not involved in gap junctions regulates Cxcl12 transcription by regulating the nuclear localization of the transcription factor Sp1[421] (**Figure 43**). In line with previous results indicating that Cx43 suppression leads to the inhibition of CXCL12 expression in adult brains[422], they showed that Cx43 and Cx45 expression levels correlated with the CXCL12 one. Yet, inhibition of Cx43 activity by CBX and the mimetic peptide Gap27 inhibited CXCL12 secretion. The authors also observed that the propagation of Ca^{2+} waves

between coupled cells was necessary for the release of the chemokine into the extracellular space. A possible Cx43-mediated release of CXCL12 is also suggested in an other paper where CXCL12 was found co-localizing with Cx43 plaques in radial glial cells[423].

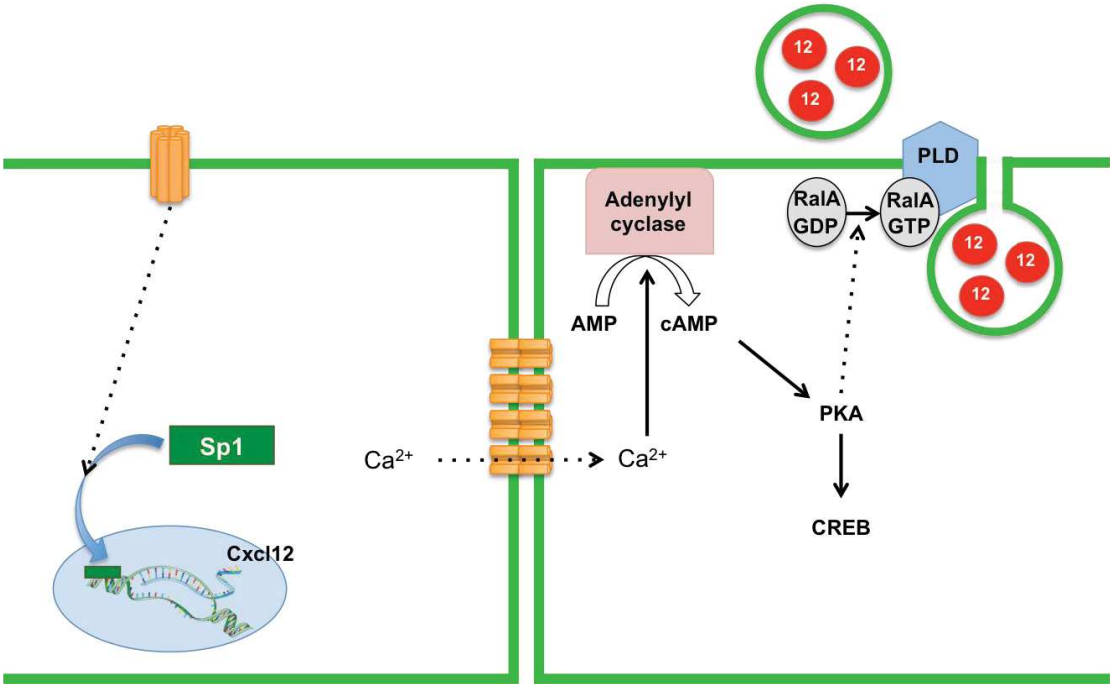

Figure 43 Schematic representation of Cx43 influence on CXCL12 secretion and production. Cx43 not involved in gap junctions stimulates the translocation of the Sp1 transcription factor into the nucleus. Sp1 then promotes the transcription of the Cxcl12 gene. Gap junctional-dependent Ca2+ mobilization stimulates adenylyl cyclase activity, which leads to increase in cAMP levels. cAMP activates the small GTPase RalA proteins (catalyzing the GDP-GTP exchange) via a PKA-dependent mechanism, which in turns mediate CXCL12 secretion via exocytosis.

Only two studies based on large screening showed a correlation between ACKR3 and gap junctions. In fact, Cx43 mRNA levels were up-regulated in ACKR3 expressing papillary thyroid carcinoma cells[424] and the receptor was previously found to interact with the gap junction beta-2 protein GJB2[95] in a large interactomic screen.

Therefore, these studies clearly show that Cx43 mediates the release of CXCL12 and suggest that CXCR4 might influence the Cx43 phosphorylation state. However, a functional link between ACKR3 and Cx43 has never been demonstrated. In line with these considerations and the aforementioned overlapping biological functions of these two proteins in interneuron migration, leukocyte entry into the brain and glioma progression, we decided to further explore and validate the interaction between ACKR3 and Cx43.

4.2.1 Cx43-ACKR3 INTERACTION VALIDATION

As a first step, we confirmed the interaction by WB and BRET. Overexpressed CXCR4 was chosen as negative control, as Cx43 was not identified in the CXCR4 interactome. Both experiments showed that Cx43 preferentially interacts with ACKR3 compared to CXCR4. Yet, a weak though statistically non-significant interaction was observed between CXCR4 and ACKR3 in WB. Cx43 was probably not identified by MS-MS in the CXCR4 immune complex due to the lower sensitivity of MS detection compared to immune detection. Since ACKR3 and CXCR4 are known to heterodimerize[119] it is possible that Cx43 is indirectly recruited to CXCR4 *via* its interaction with ACKR3. This point must be addressed using two sequential immunoprecipitations where ACKR3 and CXCR4, tagged with two different tags, are co-expressed in the same cell population. Starting from the same lysate, the two receptors can then be immunoprecipitated one after the other in two steps. The resulting co-immunoprecipitating proteins would be the one exclusively associated with the CXCR4/ACKR3 heterodimer.

Since the experiments conducted so far were all performed in HEK-293T cells transiently expressing the receptor, we decided to validate the interaction in an authentic biological context endogenously expressing both Cx43 and ACKR3. In line with previous studies showing that ACKR3 (see Table 3) and Cx43[234] are both expressed in the brain we performed immunohistochemistry (IHC) on mouse brain slices. Since there is no commercially available antibody against the mouse ACKR3 isoform we performed the IHC on brains obtained from BAC mice expressing EGFP under the ACKR3 promoter[402]. Immunostaining revealed that ACKR3 and Cx43 are co-expressed in GFAP-positive astrocytes of the Sub Ventricular Zone (SVZ). Both proteins[363,402] have been shown to play a pivotal role in the migration of neuronal progenitor cells and interneuron migration along the radial glia cells of the SVZ. Interestingly the phenotypes obtained from the suppression of either Cx43 or ACKR3 show opposite effects upon interneuron migration: in ACKR3$^{-/-}$ mice, interneurons leave the migratory streams and enter the cortical plate prematurely, which disrupts their regional distribution within the neocortex[160,402], whereas suppression of Cx43[363] leads to the accumulation of the interneurons in the ventricular zone with very few interneurons reaching the cortical plate. Furthermore, Cx43 and ACKR3 were found in our study to co-localize in end-feet surrounding blood vessels from GFAP-positive astrocytes. Previous studies showed that Cx43 suppression increases the Blood Brain Barrier (BBB) permeability and leukocyte entry into the brain *via* disrupting the

DAPC complex, deregulating Aquaporin channel 4[360] and increasing CXCL12 production[358]. In contrast, CCX771-mediated ACKR3 activation was found to reduce leukocyte entry[169]. Given our results on the site of ACKR3/Cx43 interaction, it is tempting to speculate that an ACKR3-Cx43 cross talk might control interneuron migration and the BBB permeability. Regarding its potential role in interneuron migration, it is of utmost importance to repeat the IHC in the embryonic brain. Considering their role in the BBB permeability more studies are needed to better dissect the BBB cellular populations co-expressing the two proteins. Specifically, CD31 and CD13 should be used for assessing a potential interaction of both proteins in endothelial cells and pericytes, respectively.

4.2.2 ACKR3 ACTIVATION AND EXPRESSION INHIBIT GJIC

To investigate a possible functional relationship between Cx43 and ACKR3, we firstly found that ACKR3 activation by its two endogenous ligands CXCL12 and CXCL11 inhibits Cx43 gap junctional-mediated dye diffusion in primary cultured astrocytes. Since CXCL12 affinity for ACKR3 is 10-fold higher than that of CXCL11[65,108], CXCL12 was used at 10^{-8} M, whereas CXCL11 was used at 10^{-7} M. CXCL12 binds to both CXCR4 and ACKR3, whereas CXCL11 also binds to CXCR3. Therefore, the CXCR4 antagonist AMD3100 and the CXCR3 antagonist NB-74330[425] were used for blocking CXCR4 and CXCR3, respectively. Since AMD3100 was found to have allosteric agonistic properties on ACKR3 at 10^{-5} M[426], we used it at 10^{-6} M. Both antagonists did not have any effect on GJIC when applied alone and did not reverse the CXCL12- and CXCL11-induced GJIC inhibition, suggesting that only ACKR3 and not CXCR4 or CXCR3 is involved in GJIC inhibition. Since one of our collaborators completed the selection and characterization of ACKR3 nanobodies with antagonistic properties against the mouse ACKR3 receptor, we are planning to investigate if these nanobodies are able to reverse the CXCL12 and CXCL11-mediated GJIC inhibition. Several studies showed that Cx43 is rapidly and transiently inhibited by GPCR agonists. For example GJIC inhibition by SP-1 and ET1 was evident as soon as 3 min after their addition and was completely reversed 30 min after agonist washout[299]. Both agonists were found to promote dephosphorylation of Cx43 Ser[368]. On the other hand, in our experimental conditions, CXCL12 and CXCL11 inhibited GJIC 30 min after the onset of chemokine application and GJIC was still inhibited 20 min after their withdrawing (data not shown). As it will be discussed in the next sections, we have collected data supporting the hypothesis that ACKR3 inhibits GJIC by promoting Cx43 internalization. Therefore, this persistent effect might be due to

the fact that Cx43 is targeted to lysosomes for degradation after internalization. This hypothesis must be tested by investigating if firstly Cx43 co-localizes with lysosome markers and secondly if even longer chemokine exposures would lead to Cx43 degradation. It would be also interesting to investigate if the different kinetics between chemokines and SP-1 or ET1 is due to a different mechanism of action and if CXCL11 and CXCL12 are able to induce dephosphorylation of Cx43 Ser^{368} using a specific antibody.

After establishing that ACKR3 activation inhibits GJIC in primary astrocytes, as assessed indirectly by the diffusion of Lucifer Yellow, we then investigated the possibility that ACKR3 inhibits gap junctional mediated electrical coupling that is a more direct measure of GJIC[259]. Confirming what was already observed by measuring LY diffusion, activation of ACKR3 by CXCL12 significantly inhibited electrical coupling of astrocytes. Interestingly, CXCL12 significantly inhibited electrical coupling in four out of the six coupled cell pairs that were patched, whereas CBX was effective in all six pairs. This might either reflect a heterogeneous distribution of the receptor in primary cultured astrocytes or a lower efficacy of CXCL12. The first hypothesis can be investigated generating primary cultures from BAC EGFP mice. In addition, as already mentioned in the “Results” section, these findings must be confirmed by the demonstration that CXCL11 also inhibits electrical coupling of astrocytes. Furthermore, the chemokines were delivered by bath application, making the interpretation of the kinetics of their effect challenging. Therefore, further experiments must be performed using faster drug delivery systems for better interpreting the kinetics of the ACKR3-mediated inhibition of electrical coupling.

4.2.3 ACKR3-MEDIATED GJIC INHIBTION: MECHANISM OF ACTION

Cx43 activity is often regulated by alteration of its trafficking[224]. Thus, we investigated if ACKR3 could inhibit Cx43 by increasing its internalisation. Previous studies showed that inflammatory cytokines, including interleukin-1β and tumour necrosis factor-α, reduce gap junctional communication and concomitantly increase Cx43 hemichannel-mediated membrane permeability[249]. In line with these results, we found that ACKR3 activation oppositely regulates Cx43 gap junctions and hemichannel trafficking. Specifically, we observed that ACKR3 activation triggered internalisation of Cx43 involved in gap junctions, while it inhibited Cx43 hemichannel internalisation, increasing their expression at the cell surface. Further studies investigating the activity of Cx43 hemichannels, by ethidium bromide uptake, are

planned. Inhibition of Cx43 internalisation by the dynamin inhibitor Dynasore completely reversed the ability of ACKR3 stimulation to inhibit GJIC and to promote Cx43 internalisation, suggesting that internalisation is needed for blocking GJIC. Consistent with the ability of the receptor to interact with and to activate β-arrestins[139], the GJIC inhibition and concomitant Cx43 internalisation elicited by ACKR3 stimulation was dependent on β-arrestin2. In fact, activation of ACKR3 in primary cultured astrocytes obtained from β-arrestin2$^{-/-}$ mice neither inhibited GJIC nor induced Cx43 internalisation.

Therefore, ACKR3 activation by its two endogenous agonists CXCL12 and CXCL11 inhibits GJIC through a mechanism involving Cx43 internalisation. In addition, these data show that both β-arrestin2 and dynamin are necessary for the ACKR3-dependent inhibition of GJIC. However, an important question remains unanswered: is ACKR3 co-internalising with Cx43 or is ACKR3 *indirectly* inducing Cx43 internalisation?

Regarding an *indirect* inhibition, upon stimulation ACKR3 might activate β-arrestin2 that in turn will engage an intracellular signalling cascade resulting in an ACKR3-*indirect* Cx43 internalisation and GJIC inhibition. However, this hypothesis is in contrast with previous results showing that inhibition of dynamin increases β-arrestin-dependent ERK1/2 phosphorylation[141].

In the second hypothesis, consistent with the aforementioned interaction between ACKR3 and Cx43, Cx43 might *directly* co-internalise with activated ACKR3 as an ACKR3/Cx43 complex. Indeed, as shown by the DERET assay and by previous results, ACKR3 internalises upon activation. In addition, both inhibition of dynamin[141] and β-arrestin suppression[142] were shown to reduce ACKR3 internalisation. Consolidating the importance of ACKR3 internalisation in Cx43 inhibition, transient expression in HEK-293T cells of C-terminally truncated ACKR3 mutant that are not capable of internalising[143], does not inhibit GJIC even though they retain ability to interact with Cx43.

Collectively, these results suggest that the direct internalisation of the ACKR3/Cx43 might be more plausible than the indirect one. However, very recent and unpublished results from two independent laboratories (Prof Martine Smit, University of Amsterdam and Prof Ralf Stumm, University of Jena, personal communications) suggest that β-arrestin is not essential for ACKR3 internalisation. Therefore we are currently initiating experiments in collaboration with Prof Ralf Stumm to investigate whether ACKR3 and Cx43 are co-localized in intracellular vesicles using HA-tagged

ACKR3 knock-in mice. In addition, since β-arrestin2 can directly interact with Cx43[345] it would be interesting to investigate if ACKR3 and Cx43 form a multi-protein complex with β-arrestin2.

4.2.4 ACKR3-DEPENDENT GJIC INHIBTION IN TUMOUR PROGRESSION

Both Cx43[380] and ACKR3[211] play an important role in the progression of several cancer types, including glioma. ACKR3 is overexpressed in glioma[211] and its expression correlates with higher proliferative state of cancer cells[210,212–214]. On the other hand, Cx43 expression and activity is inversely correlated with the proliferative state of cancer cells[379]. Our interactomic screen, Co-IP followed by WB and BRET studies revealed that Cx43 preferentially interacts with ACKR3, compared to CXCR4. Further supporting these biochemical studies, Cx43 is strongly co-localized with ACKR3 but not CXCR4 in glioma-initiating cell lines isolated from human glioblastoma. In next steps, we are planning to check if Cx43 and ACKR3 are also co-localized in biopsies obtained from human glioma.

ACKR3 is characterized by a high level of constitutive activity and internalisation in various cancer cell types[143]. Thus, we investigated if expression of ACKR3 would by itself inhibit GJIC. Single cell microinjection of Lucifer Yellow in HEK-293T cells transiently expressing ACKR3 or CXCR4 showed that only ACKR3 expression inhibits dye diffusion. As already reported, transient expression of two C-terminally truncated ACKR3 mutants did not inhibit GJIC even though they retain ability to interact with Cx43, suggesting that ACKR3 trafficking and internalisation are key components for the GJIC inhibition. However, in HEK-293T cells, Dynasore did not reverse the ACKR3 effect though it does inhibit its internalisation[143], suggesting that newly synthesized ACKR3 might interact with Cx43 in the synthetic pathway. This interaction might affect Cx43 forward trafficking to the plasma membrane and thereby retain it in intracellular compartments, explaining the inhibition of GJIC observed in cells expressing ACKR3. Immunofluorescence microscopy and BRET experiments will be performed to characterize the intracellular compartments where ACKR3 interacts with Cx43. In addition, before completely ruling out the involvement of ACKR3 internalisation in GJIC inhibition, other conditions known to inhibit ACKR3 internalisation (sucrose, dynamin K44A mutant) will be tested.

Several lines of evidence suggest that engagement of a β-arrestin2-dependent signalling cascade might be responsible for the agonist-independent ACKR3-mediated inhibition of GJIC in HEK293T cells: i) ACKR3 is known to constitutively

activate β-arrestin-dependent signalling, ii) the two C-terminally truncated ACKR3 mutants are characterized by lower β-arrestin recruitment[143] and iii) Dynasore does not reverse the ACKR3 mediated inhibition of GJIC, consistent with the aforementioned higher ACKR3-dependent β-arrestin activation upon dynamin inhibition[143]. Therefore, the impact of β-arrestin2 knockdown using RNA interference on the ACKR3-mediated ligand independent GJIC inhibition will be investigated to further explore this hypothesis.

The fact that the two ACKR3 C-terminally truncated mutants interact with Cx43 but do not inhibit its activity raise questions about the role of the physical interaction between the two proteins. Clearly, the interaction is not sufficient for mediating the ACKR3-dependent GJIC inhibition but is it necessary? The identification of peptide sequences mediating the interaction is essential to address that issue. In this regard, considering that the C-terminal domain of ACKR3 is not involved in the interaction and that CXCR4 only marginally interacts with Cx43, the best strategy would be to swap ACKR3 domains with CXCR4 ones until the peptide sequence(s) mediating the interaction would be found. Once this (these) sequences are identified, interfering peptides could be designed to disrupt the interaction and to investigate its functional impact.

4.3 ACKR3 ACTIVATES $G\alpha_{I/O}$ PROTEINS IN MOUSE PRIMARY ASTROCYTES BUT NOT IN HEK-293T CELLS

Since a few studies have shown that ACKR3 recruits and activates G proteins in specific cell types, including astrocytes[150,153], and that Cx43 is regulated by several GPCRs through pathways involving the activation of G proteins[299], we decided to investigate if $G\alpha_{i/o}$ protein activation is involved in the observed ACKR3-dependent GJIC inhibition.

Inhibition of $G\alpha_{i/o}$ protein activation by PTX treatment completely reversed the inhibition of GJIC induced by agonist stimulation of ACKR3 in primary cultured astrocytes. Interestingly, we observed that PTX increases basal GJIC. In line with previous works showing that activation of G proteins inhibits GJIC[299] and that GPCR are able to constitutively activate G proteins[427], PTX treatment might impair constitutive activation of $G\alpha_{i/o}$ proteins by endogenously expressed GPCRs, thereby increasing GJIC.

In line with these results showing that $G\alpha_{i/o}$ protein activation is needed for GJIC inhibition, we investigated if ACKR3 is indeed able to activate them. We thus examined the ability of ACKR3 to activate $G\alpha_i$ proteins and consequently to inhibit cAMP production in astrocytes. Consistent with a previous study[153] showing that CXCL12, induces $G\alpha_i$ protein activation in primary cultured astrocytes, we found that ACKR3 activation by CXCL12 inhibited cAMP production induced by the adenylyl cyclase activator Forskolin. However, in contrast with the same study, we found that CXCL11 also inhibited cAMP production in astrocytes. This discrepancy might result from the 10 time higher concentration of CXCL11 used in our experiment. In order to check this point, the same experiments will be repeated using increasing concentrations of both chemokines. Future experiments employing other readouts for measuring G protein activation, such as monitoring Ca^{2+} mobilization, are also planned.

Although these data suggest that ACKR3 might directly activate $G\alpha_i$ proteins a possible indirect activation of another $G\alpha_i$ coupled GPCR cannot be completely excluded. In fact, chemokine challenge might induce the release of GPCR agonists, such as glutamate or adenosine, which would in turn activate their endogenously expressed receptors, thereby inhibiting cAMP production. Although this process seems unlikely due to the short duration of the chemokine challenge (5 min), this certainly warrants further exploration. Specifically, astrocytes will be treated for 5 min

with the chemokine before collecting the cell supernatant. A novel astrocyte culture will then be challenged with the conditioned supernatant in presence of CXCR4 and ACKR3 antagonists (AMD3100 and the aforementioned nanobodies). If one rules out an indirect effect, cAMP levels should remain unchanged.

Though this control experiment remains to be carried out, our results suggest that ACKR3 activates $G\alpha_i$ protein in primary cultured astrocytes obtained from embryonic mouse brains. In our interactomic screen, we identified $G\alpha_{i3}$ as a *potential* ACKR3 interacting protein. In line with previous results showing that ACKR3 interacts with $G\alpha_i$ proteins[19], we validated by BRET that ACKR3 constitutively recruits $G\alpha_{i3}$ in HEK-293T cells. Neither CXCL12 nor PTX could modulate the interaction, already suggesting that ACKR3 might be unable to activate them in HEK-293T cells. Accordingly, only CXCR4 but not ACKR3 (transiently expressed in HEK-293T cells) was able to inhibit cAMP production upon CXCL12 stimulation. In line with these results, PTX was unable to reverse the ligand-independent, ACKR3-mediated inhibition of GJIC in HEK-293T cells, confirming that $G\alpha i_{/o}$ proteins are not involved. Intrigued by this discrepancy between mouse astrocytes and human HEK-293T cells we investigated if only the mouse isoform of ACKR3 and not the human one was able to activate $G\alpha_{i/o}$ proteins. Therefore, we transiently expressed mouse ACKR3 and CXCR4 in HEK-293T cells. However, only the mouse isoform of CXCR4 and not the ACKR3 one was able to trigger G protein, as previously demonstrated for human receptors.

Therefore, these results suggest that ACKR3 might be coupled to $G\alpha_{i/o}$ proteins only in astrocytes. The peculiarity of this cellular environment could be granted by the astrocyte expression of scaffolding proteins necessary for the activation of G proteins. It would be interesting therefore to study the interactome of ACKR3 expressed in astrocytes using, once again, the HA-ACKR3 knock-in mouse model just generated in the Ralf Stumm's laboratory.

5. CONCLUSIONS

Starting from a large-scale interatomic study, we identified Ephrin B1 and Connexin 43 (Cx43) as novel *potential* interacting proteins of CXCR4 and ACKR3, respectively. Validation of the ACKR3-Cx43 interaction showed that the two proteins can constitutively interact in living cells and they are co-expressed in specific astrocyte populations of authentic in physiological conditions. In addition, Cx43 and ACKR3 were found to co-localize in glioma-initiating cell lines isolated from human glioblastoma.

Functional validation of the ACKR3-Cx43 interaction revealed that ACKR3 influences Cx43 trafficking and functionality at multiple levels. Mimicking ACKR3 overexpression detected in several cancer types, we found that transient expression of ACKR3 in HEK-293T was sufficient for GJIC inhibition. Further investigations revealed that *activation* of endogenously expressed ACKR3, in primary cultured astrocytes, affects GJIC through a mechanism requiring activation of $G\alpha_{i/o}$ proteins and involving β-arrestin2- and dynamin-dependent internalisation of Cx43 engaged in gap junction. The proposed mechanism for the ACKR3-mediated regulation of Cx43 trafficking and activity is represented in **Figure 44**.

Collectively, these results define Cx43 as a new player in the ACKR3 signalisation cascade. This new paradigm might play an important role in physiological as well as pathological processes in the brain. In the former, ACKR3 expressed in astrocytes might regulate Cx43 activity influencing both interneuron migration and blood brain barrier permeability. In the latter, ACKR3 overexpression and activation might regulate glioma progression through the inhibition of Cx43 GJIC. Therefore, this thesis work provides one of the first functional links between the CXCL11/CXCL12/ACKR3 axes and gap junctions that might underlie their critical role in glioma progression.

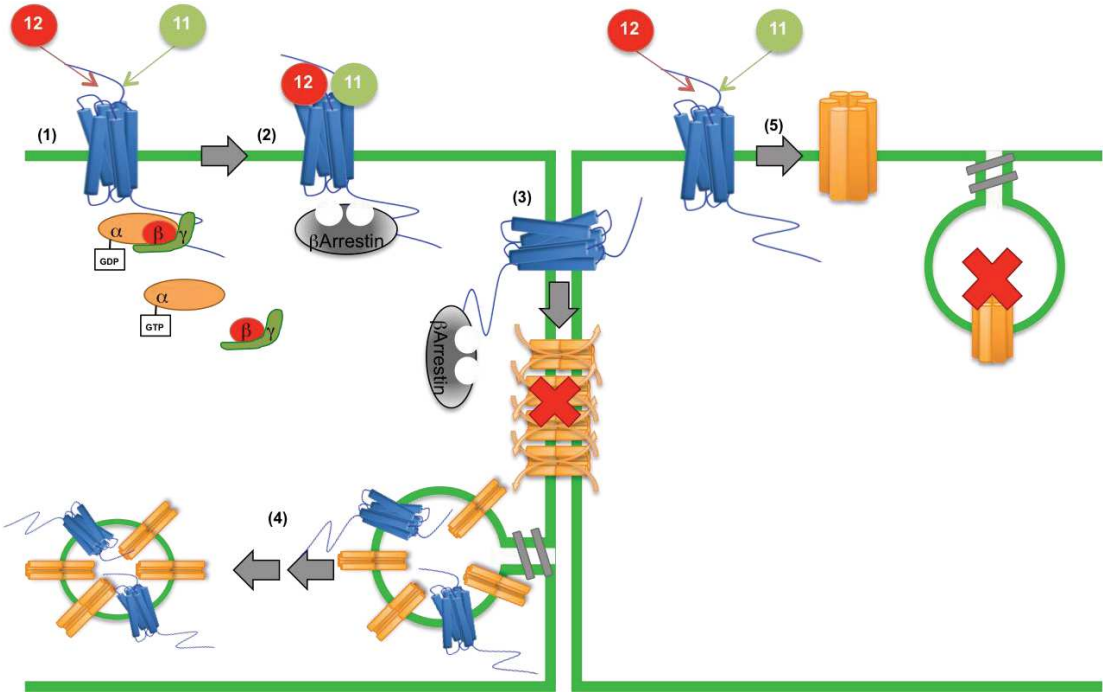

Figure 44 Proposed mechanism for the ACKR3-mediated Cx43 regulation. (1-5) Integrating our results with the canonical time course of GPCR activation the following series of molecular events starting with the activation of ACKR3 and concluding with Cx43 internalisation and GJIC inhibition can be proposed. (1) ACKR3 stimulation triggers G protein activation and dissociation of the Gα subunit from the βγ complex. (2) Dissociation of the G proteins allows the recruitment and activation of β-arrestin2. (3) ACKR3 activation leads to the β-arrestin2- and dynamin-dependent inhibition of GJIC and concomitant Cx43 internalisation. (4) We suggest that ACKR3 and Cx43 are co-internalising as ACKR3/Cx43 complex. (5) ACKR3 activation inhibits dynamin-dependent Cx43 hemichannels internalisation, increasing their plasma membrane expression.

6. MATERIAL AND METHODS

6.1 PLASMIDS

ID	Protein	Tag	Plasmid	Provenience	Experiments used
1	ACKR3	HA-N terminal	pcDNA 3.1	Sub-cloned from HA ACKR3 pcDEF3 (provided by prof. dr.M.J. Smit (Faculty of Science, Medicinal chemistry, AIMMS, Amsterdam, Netherlands) to pCDNA3.1	Immunoprecipitation cAMP
2	CXCR4	3XHA-N terminal	pcDNA 3.1	Sub-cloned from 3xHA CXCR4 pcDEF3 (provided by prof. dr.M.J. Smit (Faculty of Science, Medicinal chemistry, AIMMS, Amsterdam, Netherlands) to pCDNA3.1	Immunoprecipitation cAMP
3	ACKR3	NLuc-C terminal	pcDNA 3.1	Provided by A. Isbilir (Max-Delbrück-Zentrum für Molekulare Medizin (MDC), Berlin, Germany)	BRET
4	CXCR4	NLuc-C terminal	pcDNA 3.1	Provided by A. Isbilir (Max-Delbrück-Zentrum für Molekulare Medizin (MDC), Berlin, Germany)	BRET
5	Cx43	YFP-C terminal	pcDNA 3.1	Obtained from the human ORFeome collection (Montpellier, France)	BRET
6	ACKR3	Red Cherry-N terminal	pcDNA 3.1	Obtained from the human ORFeome collection (Montpellier, France)	Microinjection
7	CXCR4	Red Cherry-N terminal	pcDNA 3.1	Obtained subcloning plasmid 2 in 6	Microinjection
8	ACKR3	Flag and SNAP N-terminal	pcDNA 3.1	Provided by Cisbio (Parc Marcel Boiteux, 30200 Codolet, France)	Internalisation assay
9	CXCR4	Flag and SNAP N-terminal	pcDNA 3.1	Provided by Cisbio (Parc Marcel Boiteux, 30200 Codolet, France)	Internalisation assay
10	ACKR3	HA N-terminal	pcDNA 3.1	Provided by C.P. Viciano (Bio-Imaging-Center/Rudolf-Virchow-Center,	Immunoprecipitation

ID	Protein	Tag	Plasmid	Provenience	Experiments used
		CFP C-terminal		Institute of Pharmacology, University of Wuerzburg, Wuerzburg, Germany)	Microinjection
11	ACKR3Δ16	HA N-terminal	pcDNA 3.1	Provided by C.P. Viciano (Bio-Imaging-Center/Rudolf-Virchow-Center,	Immunoprecipitation
		CFP C-terminal		Institute of Pharmacology, University of Wuerzburg, Wuerzburg, Germany)	Microinjection
12	ACKR3ΔCt	HA N-terminal	pcDNA 3.1	Provided by C.P. Viciano (Bio-Imaging-Center/Rudolf-Virchow-Center,	Immunoprecipitation
		CFP C-terminal		Institute of Pharmacology, University of Wuerzburg, Wuerzburg, Germany)	Microinjection
13	CXCR4ΔCt	HA N-terminal	pcDNA 3.1	Provided by C.P. Viciano (Bio-Imaging-Center/Rudolf-Virchow-Center,	Immunoprecipitation
		CFP C-terminal		Institute of Pharmacology, University of Wuerzburg, Wuerzburg, Germany)	Microinjection
14	ACKR3	YFP C-terminal	pcDNA 3.1	Provided by dr. Françoise Bachelerie Université Paris-Sud 11 (Paris, France)	BRET
15	CXCR4	YFP C-terminal	pcDNA 3.1	Provided by dr. Françoise Bachelerie Université Paris-Sud 11 (Paris, France)	BRET
16	B-arrestin 2	RLuc8 N-terminal	pcDNA 3.1	Provided by the ARPEGE platform of the (Institut de Génomique Fonctionnelle (IGF), Montpellier, France)	BRET
17	mouse ACKR3	None	pcDNA 3.1	Provided by prof. dr.M.J. Smit (Faculty of Science, Medicinal chemistry, AIMMS, Amsterdam, Netherlands)	G protein activation
18	mouse CXCR4	None	pcDNA 3.1	provided by prof. dr.M.J. Smit (Faculty of Science, Medicinal chemistry, AIMMS, Amsterdam, Netherlands)	G protein Activation
19	Cx43	GFP C-terminal	pEGFP N1	Obtained from the human ORFeome collection (Montpellier, France)	BRET
22	$G\alpha_i3$	RLuc8 C-terminal	pcDNA 3.1	ARPEGE	BRET

6.2 ANTIBODY

ID	Protein	Host species	Clone	Code	Dilution	Brand	Species	Others
1	**HA**	Rat	3F10	11867423001	1/1000 WB/IF	Sigma-Aldrich	/	
2	**Cx43**	Rabbit	Polyclonal	C6219	1/500 IHC 1/1000 IF 1/10000 WB	Sigma-Aldrich	Human Mouse	
3	**Cx43**	Mouse	2/Connexin-43	610062	1/100 IF	BD transduction laboratories	Human	
4	**ACKR3**	Mouse	11G8	MAB42273	1/50 IF	R&D	Human	Antigen retrieval is needed
5	**CXCR4**	Rabbit	UMB2	ab124824	1/500 IF	Abcam	Human	Antigen retrieval is needed
6	**GFAP**	Rabbit	Polyclonal	Z 0334	1/500 IF	Dako	Mouse	
7	**GFAP**	Mouse	Polyclonal	Z 0334	1/500 IHC	Dako	Mouse	
8	**GFP**	Chicken	Polyclonal	A10262	1/1000 IHC	Invitrogen	/	
9	**Ephrin B1**	Goat	Polyclonal	AF473	1/1000 WB	R&D	Human	

6.3 CELLS & MICE

HEK293T cells were provided by prof. Dr M.J. Smit (Faculty of Science, Medicinal chemistry, AIMMS, Amsterdam, Netherlands). They were grown in Dulbecco's modified Eagle's medium (DMEM) purchased from Gibco (419960) supplemented with 10% heat-inactivated foetal bovine serum purchased from Gibco (10099-133) and maintained in humidified atmosphere containing 5% CO_2 at 37°C. Cells were used between passage 10 and 20 and passed twice a week.

Primary cultures of cortical astrocytes were prepared from Swiss mice (purchased from Janvier labs) embryos at embryonic day 15.5 and grown in a 1:1 mixture of DMEM and F-12 nutrient supplemented with glucose (30 mM), glutamine (2 mM), $NaHCO_3$ (13 mM), HEPES buffer (5 mM, pH 7.4) and penicillin-streptomycin (100 unit/ml–0.1 mg/ml) and 10% heat inactivated Nu-Serum (Corning 355500). Cells were maintained in atmosphere containing 5% CO_2 at 37°C. Medium was not changed for one week after seeding and then changed twice a week. Cultures were used after 5 weeks from seeding. The enrichment in astrocytes was routinely checked via GFAP staining. Only cultures where GFAP positive cells represented at least the 75% of the cellular population were used for experiments. Cultures were starved in DMEM medium supplemented with penicillin-streptomycin (100 unit/ml–0.1 mg/ml) overnight before experiment.

Secondary cultures of cortical astrocytes were prepared starting from five-week old primary cultures. After PBS washing primary cultures were incubated for 15 min with trypsin-EDTA 0.05% (GIBCO 25300-054) in humidified atmosphere containing 5% CO_2 at 37°C. After resuspension in DMEM/F-12 medium cells were plated on coated glass coverslips.

β-arrestin2$^{-/-}$ astrocytes cortical primary cultures were obtained from C57BL/6J β-arrestin2$^{-/-}$ mice (provided by Dr Gyslaine Bertrand (Institut de Génomique Fonctionnelle) embryos at embryonic day 15.5 and grown as the WT cultures.

R633 and TG1 glioblastoma cancer stem cells were provided already fixed in PFA by Dr M.P Junier (Institut de Biologie Paris Seine, Paris, France). Their isolation and characterization are described elsewhere[428–430].

Mice. EGFP-ACKR3 mice are BAC mice from GENSAT already characterized in[118,161]. They express EGFP under the promoter of ACKR3, which has been inserted

into a random location of the genome ensuring germline transmission. They are maintained heterozygous on a Hsd:ICR (CD-1®) background.

6.4 PRINCIPAL REAGENTS USED

Chemokines. Recombinant mouse CXCL11 and Human/Feline/Rhesus Macaque CXCL12 were purchased from R&D System (572-MC and 350-NS). Both were dissolved in PBS with 0.1% BSA to a concentration of 10^{-5} M, aliquoted and stored at -80°C.

Antagonist. AMD3100 (purchased from Tocris, ref 3299) was dissolved in PBS to a final concentration of 20 mM, aliquoted and stored at -20°C. NBI-74330 was purchased from R&D (4528/10) dissolved to a final concentration of 0.01 M in DMSO, aliquoted and stored at -20°C.

Principal chemicals used. Lucifer Yellow CH dilithium salt (LY) was purchased from Sigma (L0259) as Dynasore hydrate (D7693) and Carbenoxolone disodium salt (CBX) (C4790). Pertussis Toxin from *Bordetella pertussis* was purchased from Calbiochem (516560).

6.5 METHODS

Coating was performed incubating plates and coverslips with a solution of Poly-L-ornithine hydrobromide 10mg/ml (Sigma P3655) for 2hrs in humidified 5% CO_2 incubator at 37 °C. Coverslips and plates were washed twice with PBS before usage. All plates and coverslips were coated in all experiments.

Transfection of cDNA was performed using Polyethylenimine (PEI) from Polyscience (24765). Cells were seeded one-day prior transfection and used two days after for all experiments but BRET. For BRET cells were transfected in suspension 24hrs before experiment. In both cases, a solution of optiMEM purchased from Gibco (11058-021) containing the cDNA was mixed with a solution of PEI. The ratio maintained for all experiment was 4ng PEI for each ng of cDNA. In all conditions of every experiment the total amount of cDNA was equilibrated using empty plasmid. For mock cells only empty plasmid was transfected. The solution was gently mixed. After 20min the solution was added to the cells.

Co-immunoprecipitation. HEK293T cells expressing either HA-ACKR3 or HA-CXCR4 or ACKR3-mutants or mock cells were lysed in ice cold Lysis Buffer (LB)

containing 1% n-Dodecyl-β-D-Maltopyranosid (DDM) purchased from Antrace (D310), 20mM TRIS (pH=7.5), 100mM NaCl, 2.5mM $CaCl_2$, 10mM, phosphatase inhibitors (NaF, 10 mM; Na^+-vanadate, 2 mM; Na^+-pyrophosphate, 1 mM; and β-glycerophosphate, 50 mM) protease inhibitor cocktail (Roche) for 1 h at 4 °C. Lysate was mixed for 1hr at 4°C. afterwards, samples were centrifuged at 15,000*g* for 15 min at 4 °C. Soluble proteins were quantified by bicinchoninic acid (BCA) assay from Sigma (B29643 and C2284)) and equal protein amount per each condition was incubated with the agarose-conjugated anti-HA antibody (Sigma A2095) overnight at 4 °C. Beads were then washed two times with an ice cold PBS solution containing 0.5M of NaCl and phosphatase inhibitors and two times with an ice cold PBS solution containing 0.150M of NaCl and phosphatase inhibitors. Immunoprecipitated proteins were then eluted in Laemmli sample buffer by shaking them at 37°C for 2hrs.

Mass spectrometry. Proteins were separated on SDS-PAGE gels (12 % polyacrylamide, Mini-PROTEAN® TGX™ Precast Gels, Bio-Rad, Hercules USA) and stained with Protein Staining Solution (Euromedex, Souffelweyersheim France). Gel lanes were cut into7 gel pieces and destained with 50 mM TriEthylAmmonium BiCarbonate (TEABC) and three washes in 100% acetonitrile. After protein reduction (with 10 mM dithiothreitol in 50mM TEABC at 60 °C for 30 min) and alkylation (55 mM iodoacetamide TEABC at room temperature for 60 min) proteins were digested in-gel using trypsin (500 ng/band, Gold, Promega, Madison USA) as previously described[431]. Digest products were dehydrated in a vacuum centrifuge and reduced to 3 µL. The generated peptides were analysed online by nano-flowHPLC–nanoelectrospray ionization using an Orbitrap Elite mass spectrometer (Thermo Fisher Scientific, Waltham USA) coupled to an Ultimate 3000 HPLC (Thermo Fisher Scientific). Desalting and pre-concentration of samples were performed on-line on a Pepmap® pre-column (0.3 mm × 10 mm, Dionex). A gradient consisting of 0-40% B for 60 min and 80% B for 15 min (A = 0.1% formic acid, 2% acetonitrile in water; B = 0.1 % formic acid in acetonitrile) at 300 nL/min was used to elute peptides from the capillary reverse-phase column (0.075 mm × 150 mm, Acclaim Pepmap 100® C18, Thermo Fisher Scientific). Eluted peptides were electrosprayed online at a voltage of 1.8 kV into an Oribtrap Elite mass spectrometer. A cycle of one full-scan mass spectrum (400– 2,000 m/z) at a resolution of 120,000 (at 400 m/z), followed by 20 data-dependent MS/MS spectra was repeated continuously throughout the nanoLC separation. All MS/MS spectra were recorded using normalised collision energy (33%, activation Q 0.25 and activation time 10 ms) with an isolation window of 2 m/z. Data were acquired using the Xcalibur software (v 2.2). For all full scan

measurements with the Orbitrap detector a lock-mass ion from ambient air (m/z 445.120024) was used as an internal calibrant as described[432]. Analysis of MS data was performed using MaxQuant software package (v 1.5.5.1) as described by J Cox and M Mann[433]. Tandem mass spectra (MS/MS) were searched by the Andromeda search engine[434] against the UniProtKB Reference proteome UP000005640 database for Homo sapiens (release 2017_10) using the following parameters: enzyme specificity was set as Trypsin/P, and a maximum of two missed cleavages and a mass tolerance of 0.5 Da for fragment ion were applied. A second database of known contaminants provided with the MaxQuant suite was also employed. The "match between runs", "iBAQ" and "LFQ" options were checked. Oxidation (M) and Phosphorylation (STY) were specified as variable modification and carbamidomethyl (C) as fixed modification. Database searches were performed with a mass tolerance of 20 ppm for precursor ion for mass calibration, and with a 4.5 ppm tolerance after calibration. The maximum false peptide and protein discovery rate was specified as 0.01. Seven amino acids were required as minimum peptide length. The MaxQuant software generates several output files that contain information about identified peptides and proteins. The "proteinGroups.txt" file is dedicated to identified proteins: each single row collapses into protein groups all proteins that cannot be distinguished based on identified proteins. An in-house bioinformatics tool have been developed to automatically select a representative protein ID in each protein group. First, proteins with the most identified peptides are isolated in a so called "match group" (proteins from the "Protein IDs" column with the maximum number of "peptides counts (all)"). For 1% of the remaining match groups where more than one protein ID existed, the "leading" protein has been chosen as the best annotated protein according to the number of Gene Ontology annotations (retrieved performed from UniProtKB 03/10/2017). The Perseus software (v 1.5.6.0[435]) enabled protein quantification (label free quantification) *via* the intensity values and performed subsequent statistical analysis of these data. Quantification were performed using LFQ values for further analysis, after elimination of reverse and contaminant entries. Experiments were repeated three times to assess biological reproducibility.

Analysis MS data. Co-IP data were analysed and compared to mock cells using Perseus v1.5.6.0. Proteins identified only by site and labelled as contaminant were eliminated. Log_2(LFQ intensities) were used for the analysis and only proteins identified in all three biological replicates in at least one group (ACKR3/CXCR4 or mock) were maintained. For the statistical analysis missing values were substitute with the minimum LFQ value quantified in the remaining list. The proteins were

considered statistically significant using a T-test conducted on both sides setting the number of randomization at 250 the False Discovery Rate at 0.01 and the $S0^{436}$ at 0.1.

Western blotting. Proteins were electrophoretically transferred to nitrocellulose membranes (Bio-Rad) after resolution onto 10% polyacrylamide gels. After blockage with a 5% milk solution, membranes were immunoblotted with primary antibodies dissolved in a 5% Bovine Serum Albumin (from Sigma A2153) solution overnight at 4°C. Then membranes were immunoblotted with either anti-mouse (Sigma-Aldrich GENA931V) or anti-rat (Jackson ImmunoResearch 112-035-003) or anti-rabbit (Sigma-Aldrich GENA934V) horseradish peroxidase (HRP)-conjugated secondary antibodies diluted 1 in 5000 in a 5% milk solution for 2hrs at room temperature. Immunoreactivity was detected with an enhanced chemiluminescence method (Western lightning® Plus-ECL,Perkin Elmer) on a ChemiDoc™ Touch Imaging System (Bio-Rad). Quantification was performed using the dedicated Bio-rad software Image Lab.

BRET. 50,000 transfected HEK293T were seeded per well in white and black 96 well plates (Greiner). For saturation BRET an increasing amount of acceptor (YFP-tagged) was transfected with a constant amount of donor (RLuc or NanoLuc). For ligand induced BRET the amount of plasmids (donor and acceptor) needed for generating the $BRET_{50}$ signal in the saturation curve were used. After 24hrs cells were gently washed two times with PBS. Coelenterazine was added at a final concentration of 5 µM in the white plate. Readings were then immediately performed after the addition of different ligands or PBS at 37°C using the Mithras LB 940 plate reader (Berthold Biotechnologies, Bad Wildbad, Germany) that allows the sequential integration of light signals detected with two filter settings (Rluc/NLuc filter, 485 ± 20 nm; and YFP filter, 530 ± 25 nm). Data were collected using the MicroWin2000 software (Berthold Biotechnologies). BRET for saturation curve was expressed as % of net BRET compared to the maximal BRET. For the ligand induced BRET the BRET was expressed as % of BRET compared to the non stimulated. YFP used for calculating the NLuc or RLuc/YFP ratio was measured from the black plate using the INFINITE500 plate reader (TECAN) setting the excitation filter at 485±20nm and the emission one at 520±10nm. When needed PTX (100 ng/mL) was added overnight before the experiment.

Immunofluorescence was performed on paraformaldehyde fixed cells. Specifically, cells were fixed with a 4% solution of PFA in PBS for 10min. Excess of PFA was

quenched washing three times with a 0.1M solution of glycine in PBS. Cells were permeabilized and blocked with a PBS solution of 5% heat inactivated goat serum (Vector Laboratories S-100) and 0.1 % Triton X-100 for 20min. Primary antibodies were then incubated overnight at 4°C in a 2.5 and 0.05% PBS solution of goat serum and Triton X-100, respectively. After extensive PBS washings cells were incubated for 2hrs, at room temperature and protected from light, with a PBS solution with 2.5% goat serum and 0.05% Triton X-100 PBS solution containing the appropriate secondary antibody and Hoechst 33342 (2 μM, Thermo Scientific Pierce). Antigen retrieval was performed heating up cells to 80°C for 20min in a citrate buffer solution (pH=6) containing Tween 0.05%. After cooling down to a room temperature, cells were washed three times and IF performed.

Co-localization. TG1 and R633 cells were stained using the general protocol described earlier. Antibody 2, 3, 4 and 5 were used for staining Cx43, ACKR3 and CXCR4. Alexa Fluor 594-conjugated anti-mouse and Alexa Fluor 488-conjugated anti-rabbit were used. Pictures were taken with a Leica SP8-UV confocal microscope imaging between 20 and 50 different confocal plans for each cells. 3D pictures were then reconstructed using the Imaris software (Bitplane). Overlapping volume was defined firstly identifying the center of mass of each object belonging to group A (Cx43) or B (ACKR3/CXCR4). Then, two objects were considered co-localized if the center of one falls within the area of the other[408]. Following a non-biased approach the different objects were defined setting an automatic threshold[409]. The intensity of Cx43 or ACKR3/CXCR4 signal coming from the overlapping volume was quantified. For comparison this intensity was divided by the total intensity of each group before plotting.

IHC. Mice were anesthetized with pentobarbital (100 mg/kg i.p., Ceva SA) and perfused transcardiacally with fixative solution containing 4% w/v paraformaldehyde, 0.1 M sodium phosphate buffer (pH 7.5), sodium fluoride (10 mM), and sodium orthovanadate (2 mM). Brains were post fixed for 48 h in the same solution. Brains were then dehydrated by immersion in ice-cold solutions containing first 10 then 20 and 30% sucrose. Solutions were changed when brains were sinking. Brains were then embedded in OCT and rapidly frozen with SnapFrost® (Excilone). Brains were then stored at - 80°C. 50μM brain slices were cut using a Cryostat Leica CM3050 and IHC was performed on floating slices. Specifically, slices were permeabilized and blocked with a PBS solution of 10% heat inactivated goat serum and 0.3 % Triton X-100 for 20min. Primary antibodies were then incubated overnight at 4°C in a 3 and 0.1% PBS solution of goat serum and Triton X-100, respectively. After

extensive PBS washings cells were incubated for 2hrs, at room temperature and protected from light, with a PBS solution with 3% goat serum and 1% Triton X-100 PBS solution containing the appropriate secondary antibody and Hoechst 33342.

Scrape loading. Five week old astrocytes were starved overnight in presence, if necessary, of PTX (100 ng/mL) or CBX (50μM). Culture when then pre-treated with the appropriate antagonist or Dynasore (80μM) for 30min at 37°C. Removed from the incubator cells were exposed to the appropriate concentration of chemokine dissolved in a solution containing 130mM $CaCl_2$, 2.8mM KCl, 1mM $CaCl_2$, 2mM $MgCl_2$ and 10mM HEPES (pH=7.2), for 30min at room temperature. For the dynasore and CBX treated conditions the two chemicals were added also in this step. Cells were then exposed to the same solution without $CaCl_2$ for 1min. After that, monolayer is scraped using a razor blade in the presence of Lucifer Yellow (1mg/ml) dissolved in the same calcium-free solution. LY is let diffusing for 1min. Cells are then washed 5 times with the calcium-containing solution. After ten minutes picture were taken using the inverted microscope Zeiss Axiovert 40CFL equipped with Axiocam ICCL1 (Zeiss) with the green filter using the Zeiss Axiovision 4.8 software. For the quantification picture were analyzed with the Fiji software. Specifically, fluorescence was plotted against the distance from the cut. The average fluorescence of the 50 most distant pixels from the cut was considered as background and subtracted from all values. Fluorescence was then normalized setting the highest value as 100%. One exponential decay was then interpolated using Prism (v. 7.0,GraphPad Software Inc.) constraining the Y0 at 100 and the plateau at 0. Half-life (distance from the cut where the fluorescence is 50% of the maximum) of the interpolate curves where used for comparison. For each experiment the half-life was normalized setting the half-life of the control as 100%. At least three technical replicates for each condition were repeated in every biological replicate.

Double patch clamp. To assess the effect of CXLC12 on gap-junction-mediated electrical coupling between astrocytes, junctional currents (Ij) were recorded in astrocyte pairs using the dual voltage-clamp technique[246]. Overnight cultured secondary cultures of cortical astrocytes were used for this experiments. For testing, coverslips were transferred to a recording chamber attached to the stage of an upright microscope (Axioskop FS; Zeiss, Le Pecq, France) and continuously superfused with Ringer's saline (in mM): 125 NaCl, 2.5 KCl, 2 $CaCl_2$, 1 $MgCl_2$, 1.25 NaH_2PO_4, 26 $NaHCO_3$, 12 glucose and buffered to pH 7.4. The saline was maintained at 32°C and continuously bubbled with carbogen (95% O_2 / 5% $C0_2$). Patch pipettes were pulled to a resistance of 4-5 M□ from borosilicate glass (1.5 mm

outer diameter; 1.17 mm inner diameter) and filled with the following internal solution (in mM): 140 potassium-gluconate, 2 $MgCl_2$, 1.1 EGTA, 5 Hepes, that was titrated to pH 7.2 with KOH. Electrical signals were acquired with an EPC-9 dual patch-clamp amplifier (HEKA Electronik, Lambrecht/Pfalz, Germany) in cell pairs voltage-clamped at -50 mV and were filtered at 3 kHz, as previously reported[437]. Membrane resistance of the recorded cells was calculated from an hyperpolarizing voltage step (-10 mV, 50 ms duration). Cells were challenged with depolarizing voltage steps (40 mV amplitude, 300 ms duration, a step every 30 s) and the amplitude of resulting Ij in the non-stimulated cell was continuously monitored for 15-20 min. Results are expressed as the coupling ratio, which corresponds to the amplitude of Ij over the total current amplitude recorded in the stimulated cell. Consistent with the presence of weakly and robustly coupled astrocyte pairs, the coupling ratio exhibited disparate values between pairs, ranging from 0.07 to 0.91 (n = 42 cell pairs). Pairs with a coupling ratio <0.25 were discarded. CXCL12- or carbenoxolone (CBX)-containing solutions were bath-applied through the perfusion system at a rate of 2 ml/min. Control cell pairs were challenged with saline, using the same protocol.

Cx43 internalisation via IF. Primary astrocyte cultures isolates from WT or β-arrestin2$^{-/-}$ mice were seeded on glass coverslips for 5 weeks. After overnight starvation, when necessary, cells were pre-treated for 30min with 80µM Dynasore. Cells were then exposed to either CXCL12 or CXCL11 for other 30min. Cells were then fixed and IF performed. Antibody 2 and Alexa Fluor 594-conjugated anti-rabbit were used. Pictures were taken with a Leica SP8-UV confocal microscope.

Quantification of cAMP production. Astrocytes or HEK293T cells were cultured in 24 well plates. HEK293T were transfected 48hrs prior experiment. Both cell types were starved overnight in presence or absence of PTX (100 ng/mL). When necessary cells were pre-exposed for 30min to the CXCR4 antagonist. Cells were then stimulated for 5min with CXCL11 or CXCL12 dissolved in a DMEM solution with 1% BSA before stimulation of cAMP production using Forskolin (10^{-6}M) in the presence of 1 mM of the phosphodiesterase inhibitor 3-isobutyl-1methylxanthine (IBMX). After 5 minutes cells were then lysed in 1% Triton X-100 and cAMP production was quantified using the cAMP dynamic kit (Cisbio Bioassays) according to the manufacturer's instructions. All conditions were performed in triplicate within each biological replicate.

Biotinylation. Biotinylation experiments were performed using the Pierce™ Cell Surface Protein Isolation Kit (Thermo Fisher) according to the according to the

manufacturer's instructions. In brief, for the internalisation assay, overnight starved astrocyte primary cultures were washed twice with ice cold PBS and incubate for 45min with biotine at 4°C on a plate shaker. Biotin was then quenched and cells washed twice again with ice cold PBS. Cells were then incubate either with ice cold DMEM, 37°C DMEM or the appropriate agonist for 30min. In the case of dynasore treated cells, cells were pre-trated for 30min with dynasore prior to agonist stimulation. After the 30min surface biotin was cleaved by two incubations with MESNA (50mM) of 20 at 4°C. Cells were then washed twice with ice cold PBS and lysed in LB. Lysates were then mixed for 2hrs at 4°C and centrifuged for 10min at 15,000g. Before overnight incubation at 4°C with NeutrAvidin Agarose beads a portion of lysate was saved for using as total control. The next day, beads were washed twice with the lysis buffer and one with PBS. Protein were eluted in Laemmli sample buffer with DTT (50mM) by shaking them at 37°C for 2hrs.

For quantifying the amount of Cx43 at the cell surface, overnight starved astrocyte primary cultures were washed twice with PBS and incubated at 37°C with DMEM or the appropriate agonist for 30min. Cells were then washed twice with ice cold PBS and incubate for 45min with biotine at 4°C on a plate shaker. Cells were then washed twice with ice cold PBS and lysed in LB. Lysates were then mixed for 2hrs at 4°C and centrifuged for 10min at 15,000g. Before overnight incubation at 4°C with NeutrAvidin Agarose beads a portion of lysate was saved for using as total control. The next day, beads were washed twice with the lysis buffer and one with PBS. Protein were eluted in Laemmli sample buffer with DTT (50mM) by shaking them at 37°C for 2hrs.

Microinjection. 75,000 HEK293T/well were seeded in a 24 well plate containing glass coverslips. The day after seeding cells were transfected with PEI. Two days after transfection coverslips were transferred to the recording chamber of a patch clamp setup equipped with the Zeiss Axiovert 5100TV fluorescence inverse microscope having the required filters. Cells were then maintained in a solution of NaCl 140mM, $CaCl_2$ 2mM, KCl 3mM, Hepes 10mM, D-glucose 10mM pH 7,4, 320mosm. LY was dissolved, to a concentration of 5mg/ml, in a recording solution composed of CsCl 140mM, $CaCl_2$ 0,5mM, EGTA 20mM, Hepes 10mM, D-glucose 10mM, ATP-Na2 2mM, pH 7,2, 300mosm. LY was then microinjected in a single cell using a glass patch pipette. With the perfusion activated cells were microinjected for 5min. After 5min perfusion was stopped and patch pipette removed. Neighboring cells receiving the LY were manually counted after other 5min. For representative pictures coverslips were fixed in PFA and picture were taken using an AxioImagerZ1 microscope equipped with epifluorescence (Zeiss). Dynasore treated cell were

pretreated for 30min with the chemical before microinjection. Dynasore was kept in the recording chamber during the whole recording. PTX(100 ng/mL) and CBX(50μM) treated cells were treated overnight. CBX was kept in the recording chamber during the whole recording.

DERET. DERET internalisation assay was performed as described in[410]. Briefly, 48 after transfection of cDNA encoding SNAP tagged receptor culture medium was substituted with 50 μl of 100 nM SNAP-Lumi4-Tb diluted in Tag-lite labeling medium. Cells were then incubated for 1 h at 4°C. After wasing the excess SNAP-Lumi4-Tb internalisation experiments were carried on by incubating cells at 37°C with Tag-lite labeling medium, either alone or containing CXCL12, in the presence of fluorescein (48μM). Singal emitted at at 620 and 520nm were collected using a PHERAstar FS. Ratio 620/520 was obtained dividing the donor signal by the acceptor signal and multyopling this value for 10,000. Data are expressed as % of Maximal internalisation after subtraction of the Internalisation at time 0.

7. BIBLIOGRAPHY

1. Lefkowitz, R. J. A brief history of G-protein coupled receptors (Nobel Lecture). *Angewandte Chemie - International Edition* **52,** 6366–6378 (2013).

2. Hu, G.-M., Mai, T.-L. & Chen, C.-M. Visualizing the GPCR Network: Classification and Evolution. *Sci. Rep.* **7,** 15495 (2017).

3. Neubig, R. R., Gantzos, R. D. & Thomsen, W. J. Mechanism of Agonist and Antagonist Binding to a2Adrenergic Receptors: Evidence for a Precoupled Receptor-Guanine Nucleotide Protein Complex. *Biochemistry* **27,** 2374–2384 (1988).

4. Nobles, M., Benians, A. & Tinker, A. Heterotrimeric G proteins precouple with G protein-coupled receptors in living cells. *Proc. Natl. Acad. Sci.* **102,** 18706–18711 (2005).

5. Qin, K., Dong, C., Wu, G. & Lambert, N. A. Inactive-state preassembly of G(q)-coupled receptors and G(q)heterotrimers. *Nat. Chem. Biol.* **7,** 740–747 (2011).

6. Bai, B., Jiang, Y., Cai, X. & Chen, J. Dynamics of apelin receptor/G protein coupling in living cells. *Exp. Cell Res.* **328,** 401–409 (2014).

7. Goricanec, D. *et al.* Conformational dynamics of a G-protein α subunit is tightly regulated by nucleotide binding. *Proc. Natl. Acad. Sci.* **113,** E3629–E3638 (2016).

8. Syrovatkina, V., Alegre, K. O., Dey, R. & Huang, X. Y. Regulation, Signaling, and Physiological Functions of G-Proteins. *Journal of Molecular Biology* **428,** 3850–3868 (2016).

9. Wettschureck, N. Mammalian G Proteins and Their Cell Type Specific Functions. *Physiol. Rev.* **85,** 1159–1204 (2005).

10. Logothetis, D. E., Kurachi, Y., Galper, J., Neer, E. J. & Clapham, D. E. The βγ subunits of GTP-Binding proteins activate the muscarinic K+channel in heart. *Nature* **325,** 321–326 (1987).

11. Khan, S. M. *et al.* The Expanding Roles of G Subunits in G Protein-Coupled Receptor Signaling and Drug Action. *Pharmacol. Rev.* **65,** 545–577 (2013).

12. Benovic, J. L., Strasser, R. H., Caron, M. G. & Lefkowitz, R. J. Beta-adrenergic receptor kinase: identification of a novel protein kinase that phosphorylates the agonist-occupied form of the receptor. *Proc Natl Acad Sci U S A* **83,** 2797–2801 (1986).

13. Kühn, H. & Wilden, U. Deactivation of photoactivated rhodopsin by rhodopsin-kinase and arrestin. *J. Recept. Signal Transduct.* **7,** 283–298 (1987).

14. Attramadal, H. *et al.* Beta-arrestin2, a novel member of the arrestin/beta-arrestin gene family. *J Biol Chem* **267,** 17882–17890 (1992).

15. Smith, J. S. & Rajagopal, S. The β-Arrestins: Multifunctional regulators of G protein-coupled receptors. *J. Biol. Chem.* **291,** 8969–8977 (2016).

16. Cassier, E. *et al.* Phosphorylation of β-arrestin2 at Thr383 by MEK underlies β-arrestin-dependent activation of Erk1/2 by GPCRs. *Elife* **6,** (2017).

17. Evron, T., Daigle, T. L. & Caron, M. G. GRK2: multiple roles beyond G protein-coupled receptor desensitization. *Trends Pharmacol. Sci.* **33,** 154–164 (2012).

18. Ferré, S. *et al.* G protein-coupled receptor oligomerization revisited: functional and pharmacological perspectives. *Pharmacol. Rev.* **66,** 413–34 (2014).

19. Levoye, A., Balabanian, K., Baleux, F., Bachelerie, F. & Lagane, B. CXCR7 heterodimerizes with CXCR4 and regulates CXCL12-mediated G protein signaling. *Blood* **113,** 6085–93 (2009).

20. Murat, S. *et al.* 5-HT2A receptor-dependent phosphorylation of mGlu2 receptor at Serine 843 promotes mGlu2 receptor-operated Gi/o signaling. *Mol. Psychiatry* (2018). doi:10.1038/s41380-018-0069-6

21. Ritter, S. L. & Hall, R. A. Fine-tuning of GPCR activity by receptor-interacting proteins. *Nat. Rev. Mol. Cell Biol.* **10,** 819–30 (2009).

22. Sauvageau, E. *et al.* CNIH4 Interacts with Newly Synthesized GPCR and Controls Their Export from the Endoplasmic Reticulum. *Traffic* **15,** 383–400 (2014).

23. Deraredj Nadim, W. *et al.* Physical interaction between neurofibromin and serotonin 5-HT6 receptor promotes receptor constitutive activity. *Proc. Natl. Acad. Sci. U. S. A.* **113,** 12310–12315 (2016).

24. Godeny, M. D. *et al.* The N-terminal SH2 domain of the tyrosine phosphatase, SHP-2, is essential for Jak2-dependent signaling via the angiotensin II type AT1 receptor. *Cell. Signal.* **19,** 600–9 (2007).

25. Hall, R. A. *et al.* The beta2-adrenergic receptor interacts with the Na+/H+-exchanger regulatory factor to control Na+/H+ exchange. *Nature* **392,** 626–30 (1998).

26. Duhr, F. *et al.* Cdk5 induces constitutive activation of 5-HT6 receptors to promote neurite growth. *Nat. Chem. Biol.* **10,** 590–597 (2014).

27. Meffre, J. *et al.* 5-HT $_6$ receptor recruitment of mTOR as a mechanism for perturbed cognition in schizophrenia. *EMBO Mol. Med.* **4,** 1043–1056 (2012).

28. Kach, J., Sethakorn, N. & Dulin, N. O. A finer tuning of G-protein signaling through regulated control of RGS proteins. *Am. J. Physiol. Circ. Physiol.* **303,** H19–H35 (2012).

29. Labasque, M., Reiter, E., Becamel, C., Bockaert, J. & Marin, P. Physical Interaction of Calmodulin with the 5-Hydroxytryptamine $_{2C}$ Receptor C-Terminus Is Essential for G Protein-independent, Arrestin-dependent Receptor Signaling. *Mol. Biol. Cell* **19,** 4640–4650 (2008).

30. Tu, J. C. *et al.* Coupling of mGluR/Homer and PSD-95 complexes by the Shank family of postsynaptic density proteins. *Neuron* **23,** 583–92 (1999).

31. Smith, J. S., Lefkowitz, R. J. & Rajagopal, S. Biased signalling: From simple switches to allosteric microprocessors. *Nature Reviews Drug Discovery* **17,** 243–260 (2018).

32. Magalhaes, A. C., Dunn, H. & Ferguson, S. S. G. Regulation of GPCR activity, trafficking and localization by GPCR-interacting proteins. *Br. J. Pharmacol.* **165,** 1717–1736 (2012).

33. Fields, S. & Song, O. A novel genetic system to detect protein-protein interactions. [Yeast two hybrid]. *Nature* **340,** 245–246 (1989).

34. Stagljar, I., Korostensky, C., Johnsson, N. & te Heesen, S. A genetic system based on split-ubiquitin for the analysis of interactions between membrane proteins in vivo. *Proc. Natl. Acad. Sci. U. S. A.* **95,** 5187–92 (1998).

35. Petschnigg, J. *et al.* The mammalian-membrane two-hybrid assay (MaMTH) for probing membrane-protein interactions in human cells. *Nat. Methods* **11,** 585–592 (2014).

36. Lievens, S. *et al.* Kinase Substrate Sensor (KISS), a mammalian in situ protein interaction sensor. *Mol. Cell. Proteomics* **13,** 3332–42 (2014).

37. Xu, Y., Piston, D. W. & Johnson, C. H. A bioluminescence resonance energy transfer (BRET) system: application to interacting circadian clock proteins. *Proc. Natl. Acad. Sci. U. S. A.* **96,** 151–6 (1999).

38. Clegg, R. M. Fluorescence resonance energy transfer. *Curr. Opin. Biotechnol.* **6,** 103–10 (1995).

39. Fredriksson, S. *et al.* Protein detection using proximity-dependent DNA ligation assays. *Nat. Biotechnol.* **20,** 473–477 (2002).

40. Hu, C.-D., Chinenov, Y. & Kerppola, T. K. Visualization of interactions among bZIP and Rel family proteins in living cells using bimolecular fluorescence complementation. *Mol. Cell* **9,** 789–98 (2002).

41. Puig, O. *et al.* The Tandem Affinity Purification (TAP) Method: A General Procedure of Protein Complex Purification. *Methods* **24,** 218–229 (2001).

42. Daulat, A. M. *et al.* Purification and Identification of G Protein-coupled Receptor Protein Complexes under Native Conditions. *Mol. Cell. Proteomics* **6,** 835–844 (2007).

43. Roux, K. J., Kim, D. I. & Burke, B. in *Current Protocols in Protein Science* **74,** 19.23.1-19.23.14 (John Wiley & Sons, Inc., 2013).

44. Zlotnik, A., Yoshie, O. & Nomiyama, H. The chemokine and chemokine receptor superfamilies and their molecular evolution. *Genome Biol.* **7,** 243 (2006).

45. Zlotnik, A. Chemokines: A New Classification Review System and Their Role in Immunity. *Immunity* **12,** 121–127 (2000).

46. Wilkinson, P. C. in *Encyclopedia of Immunology* 533–537 (Elsevier, 1998). doi:10.1006/rwei.1999.0140

47. Wang, L., Fuster, M., Sriramarao, P. & Esko, J. D. Endothelial heparan sulfate deficiency impairs L-selectin- and chemokine-mediated neutrophil trafficking during inflammatory responses. *Nat. Immunol.* **6,** 902–910 (2005).

48. Middleton, J., Patterson, A. M., Gardner, L., Schmutz, C. & Ashton, B. A. Leukocyte extravasation: Chemokine transport and presentation by the endothelium. *Blood* **100,** 3853–3860 (2002).

49. Boldajipour, B. *et al.* Control of Chemokine-Guided Cell Migration by Ligand Sequestration. *Cell* **132,** 463–473 (2008).

50. Iglesias, P. A. & Devreotes, P. N. Navigating through models of chemotaxis. *Current Opinion in Cell Biology* **20,** 35–40 (2008).

51. Stone, M. J., Hayward, J. A., Huang, C., Huma, Z. E. & Sanchez, J. *Mechanisms of regulation of the chemokine-receptor network*. *International Journal of Molecular Sciences* **18,** (2017).

52. Winkler, C. *et al.* Genetic restriction of AIDS pathogenesis by an SDF-1 chemokine gene variant. *Science* **279,** 389–393 (1998).

53. Salanga, C. L. & Handel, T. M. Chemokine oligomerization and interactions with receptors and glycosaminoglycans: the role of structural dynamics in function. *Exp. Cell Res.* **317,** 590–601 (2011).

54. Proudfoot, A. E. I. *et al.* Glycosaminoglycan binding and oligomerization are essential for the in vivo activity of certain chemokines. *Proc. Natl. Acad. Sci.* **100,** 1885–1890 (2003).

55. Loos, T. *et al.* Citrullination of CXCL10 and CXCL11 by peptidylarginine deiminase: a naturally occurring posttranslational modification of chemokines and new dimension of immunoregulation. *Blood* **112,** 2648–56 (2008).

56. Janssens, R. *et al.* Natural nitration of CXCL12 reduces its signaling capacity and chemotactic activity in vitro and abrogates intra-articular lymphocyte recruitment in vivo. *Oncotarget* **7,** 62439–62459 (2016).

57. Richter, R., Schulz-Knappe, P., John, H. & Forssmann, W.-G. Posttranslationally Processed Forms of the Human Chemokine HCC-1. *Biochemistry* **39,** 10799–10805 (2000).

58. Vanheule, V., Metzemaekers, M., Janssens, R., Struyf, S. & Proost, P. How post-translational modifications influence the biological activity of chemokines. *Cytokine* **109,** 29–51 (2018).

59. Brandt, E., Van Damme, J. & Flad, H.-D. Neurphils can generate their activator neutrophil-activating peptide 2 by proteolytic cleavage of platelet-derived connective tissue-activating peptide III. *Cytokine* **3,** 311–321 (1991).

60. Detheux, M. *et al.* Natural proteolytic processing of hemofiltrate CC chemokine 1 generates a potent CC chemokine receptor (CCR)1 and CCR5 agonist with anti-HIV properties. *J. Exp. Med.* **192,** 1501–8 (2000).

61. Joseph, P. R. B. *et al.* Dynamic conformational switching in the chemokine ligand is essential for G-protein-coupled receptor activation. *Biochem. J.* **456,** 241–251 (2013).

62. Pease, J. E., Wang, J., Ponath, P. D. & Murphy, P. M. The N-terminal extracellular segments of the chemokine receptors CCR1 and CCR3 are determinants for MIP-1alpha and eotaxin binding, respectively, but a second domain is essential for efficient receptor activation. *J. Biol. Chem.* **273,** 19972–6 (1998).

63. Crump, M. P. Solution structure and basis for functional activity of stromal cell-derived factor-1; dissociation of CXCR4 activation from binding and inhibition of HIV-1. *EMBO J.* **16,** 6996–7007 (1997).

64. Oberlin, E. *et al.* The CXC chemokine SDF-1 is the ligand for LESTR/fusin and prevents infection by T-cell-line-adapted HIV-1. *Nature* **382,** 833–5 (1996).

65. Balabanian, K. *et al.* The chemokine SDF-1/CXCL12 binds to and signals through the orphan receptor RDC1 in T lymphocytes. *J. Biol. Chem.* **280,** 35760–35766 (2005).

66. Nagasawa, T. CXC chemokine ligand 12 (CXCL12) and its receptor CXCR4. *J. Mol. Med.* **92,** 433–439 (2014).

67. DeVries, M. E. *et al.* Defining the origins and evolution of the chemokine/chemokine receptor system. *J. Immunol.* **176,** 401–415 (2006).

68. Nagasawa, T. *et al.* Defects of B-cell lymphopoiesis and bone-marrow myelopoiesis in mice lacking the CXC chemokine PBSF/SDF-1. *Nature* **382,** 635–638 (1996).

69. Sánchez-Martín, L., Sánchez-Mateos, P. & Cabañas, C. CXCR7 impact on CXCL12 biology and disease. *Trends Mol. Med.* **19,** 12–22 (2013).

70. Cole, K. E. *et al.* Interferon-inducible T Cell Alpha Chemoattractant (I-TAC): A Novel Non-ELR CXC Chemokine with Potent Activity on Activated T Cells through Selective High Affinity Binding to CXCR3. *J. Exp. Med.* **187,** 2009–2021 (1998).

71. Burns, J. M. *et al.* A novel chemokine receptor for SDF-1 and I-TAC involved in cell survival, cell adhesion, and tumor development. *J. Exp. Med.* **203,** 2201–2213 (2006).

72. Zohar, Y. *et al.* CXCL11-dependent induction of FOXP3-negative regulatory T cells suppresses autoimmune encephalomyelitis. *J. Clin. Invest.* **124,** 2009–22 (2014).

73. Torraca, V. *et al.* The CXCR3-CXCL11 signaling axis mediates macrophage recruitment and dissemination of mycobacterial infection. *Dis. Model. Mech.* **8,** 253–269 (2015).

74. Murphy, P. M. *et al.* International union of pharmacology. XXII. Nomenclature for chemokine receptors. *Pharmacol. Rev.* **52,** 145–176 (2000).

75. Bachelerie, F. *et al.* International Union of Basic and Clinical Pharmacology. [corrected]. LXXXIX. Update on the extended family of chemokine receptors and introducing a new nomenclature for atypical chemokine receptors. *Pharmacol. Rev.* **66,** 1–79 (2014).

76. Rossi, D. & Zlotnik, A. The Biology of Chemokines and their Receptors. *Annu. Rev. Immunol.* **18,** 217–242 (2000).

77. Tachibana, K. *et al.* The chemokine receptor CXCR4 is essential for vascularization of the gastrointestinal tract. *Nature* **393,** 591–594 (1998).

78. Wu, B. *et al.* Structures of the CXCR4 chemokine GPCR with small-molecule and cyclic peptide antagonists. *Science* **330,** 1066–71 (2010).

79. Pozzobon, T., Goldoni, G., Viola, A. & Molon, B. CXCR4 signaling in health and disease. *Immunol. Lett.* **177,** 6–15 (2016).

80. Busillo, J. M. *et al.* Site-specific phosphorylation of CXCR4 is dynamically regulated by multiple kinases and results in differential modulation of CXCR4 signaling. *J. Biol. Chem.* **285,** 7805–7817 (2010).

81. Gómez-Moutón, C. *et al.* Filamin A interaction with the CXCR4 third intracellular loop regulates endocytosis and signaling of WT and WHIM-like receptors. *Blood* **125,** 1116–25 (2015).

82. Bhandari, D., Robia, S. L. & Marchese, A. The E3 ubiquitin ligase atrophin interacting protein 4 binds directly to the chemokine receptor CXCR4 via a novel WW domain-mediated interaction. *Mol. Biol. Cell* **20,** 1324–39 (2009).

83. Li, H., Liang, R., Lu, Y., Wang, M. & Li, Z. RTN3 Regulates the Expression Level of Chemokine Receptor CXCR4 and is Required for Migration of Primordial Germ Cells. *Int. J. Mol. Sci.* **17,** 382 (2016).

84. Schwartz, V. *et al.* A functional heteromeric MIF receptor formed by CD74 and CXCR4. *FEBS Lett.* **583,** 2749–2757 (2009).

85. Hajishengallis, G., Wang, M., Liang, S., Triantafilou, M. & Triantafilou, K. Pathogen induction of CXCR4/TLR2 cross-talk impairs host defense function. *Proc. Natl. Acad. Sci.* **105,** 13532–13537 (2008).

86. Triantafilou, M. *et al.* Chemokine receptor 4 (CXCR4) is part of the lipopolysaccharide "sensing apparatus". *Eur. J. Immunol.* **38,** 192–203 (2008).

87. Forde, S. *et al.* Endolyn (CD164) modulates the CXCL12-mediated migration of umbilical cord blood CD133+ cells. *Blood* **109,** 1825–33 (2007).

88. Huang, A.-F. *et al.* CD164 regulates the tumorigenesis of ovarian surface epithelial cells through the SDF-1α/CXCR4 axis. *Mol. Cancer* **12,** 115 (2013).

89. Pérez-Martínez, M. *et al.* F-actin-binding protein drebrin regulates CXCR4 recruitment to the immune synapse. *J. Cell Sci.* **123,** 1160–70 (2010).

90. Gordón-Alonso, M. *et al.* Actin-binding protein drebrin regulates HIV-1-triggered actin polymerization and viral infection. *J. Biol. Chem.* **288,** 28382–28397 (2013).

91. Wyse, M. M., Goicoechea, S., Garcia-Mata, R., Nestor-Kalinoski, A. L. & Eisenmann, K. M. mDia2 and CXCL12/CXCR4 chemokine signaling intersect to drive tumor cell amoeboid morphological transitions. *Biochem. Biophys. Res. Commun.* **484,** 255–261 (2017).

92. Rey, M. *et al.* Cutting edge: association of the motor protein nonmuscle myosin heavy chain-IIA with the C terminus of the chemokine receptor CXCR4 in T lymphocytes. *J. Immunol.* **169,** 5410–4 (2002).

93. Schmid, M. C. *et al.* Receptor tyrosine kinases and TLR/IL1Rs unexpectedly activate myeloid cell PI3kγ, a single convergent point promoting tumor inflammation and progression. *Cancer Cell* **19,** 715–27 (2011).

94. dela Paz, N. G., Melchior, B., Shayo, F. Y. & Frangos, J. A. Heparan sulfates mediate the interaction between platelet endothelial cell adhesion molecule-1 (PECAM-1) and the Gαq/11 subunits of heterotrimeric G proteins. *J. Biol. Chem.* **289,** 7413–24 (2014).

95. Usenovic, M. *et al.* Identification of novel ATP13A2 interactors and their role in α-synuclein misfolding and toxicity. *Hum. Mol. Genet.* **21,** 3785–94 (2012).

96. Wang, J. *et al.* Toward an understanding of the protein interaction network of

the human liver. *Mol. Syst. Biol.* **7,** 536–536 (2014).

97. Hein, M. Y. *et al.* A human interactome in three quantitative dimensions organized by stoichiometries and abundances. *Cell* **163,** 712–23 (2015).

98. Sugiyama, T., Kohara, H., Noda, M. & Nagasawa, T. Maintenance of the Hematopoietic Stem Cell Pool by CXCL12-CXCR4 Chemokine Signaling in Bone Marrow Stromal Cell Niches. *Immunity* **25,** 977–988 (2006).

99. Stein, J. V. & Nombela-Arrieta, C. Chemokine control of lymphocyte trafficking: a general overview. *Immunology* **116,** 1–12 (2005).

100. Ma, Q. *et al.* Impaired B-lymphopoiesis, myelopoiesis, and derailed cerebellar neuron migration in CXCR4- and SDF-1-deficient mice. *Proc. Natl. Acad. Sci. U. S. A.* **95,** 9448–9453 (1998).

101. Eash, K. J., Means, J. M., White, D. W. & Link, D. C. CXCR4 is a key regulator of neutrophil release from the bone marrow under basal and stress granulopoiesis conditions. *Blood* **113,** 4711–9 (2009).

102. Molon, B. *et al.* T cell costimulation by chemokine receptors. *Nat. Immunol.* **6,** 465–471 (2005).

103. Feng, Y., Broder, C. C., Kennedy, P. E. & Berger, E. A. HIV-1 entry cofactor: functional cDNA cloning of a seven-transmembrane, G protein-coupled receptor. *Science* **272,** 872–7 (1996).

104. Hernandez, P. A. *et al.* Mutations in the chemokine receptor gene CXCR4 are associated with WHIM syndrome, a combined immunodeficiency disease. *Nat. Genet.* **34,** 70–4 (2003).

105. Chatterjee, S., Behnam Azad, B. & Nimmagadda, S. *The intricate role of CXCR4 in cancer*. *Advances in Cancer Research* **124,** (Elsevier Inc., 2014).

106. Pérez-martínez, M. *et al.* F-actin-binding protein drebrin regulates CXCR4 recruitment to the immune synapse. 1160–1170 (2010). doi:10.1242/jcs.064238

107. Libert, F., Parmentier, M., Lefort, A., Dumont, J. E. & Vassart, G. Complete nucleotide sequence of a putative G protein coupled receptor: RDC1. *Nucleic Acids Res.* **18,** 1917 (1990).

108. Burns, J. M. A novel chemokine receptor for SDF-1 and I-TAC involved in cell survival, cell adhesion, and tumor development. *J. Exp. Med.* **203,** 2201–2213 (2006).

109. Gustavsson, M. *et al.* Structural basis of ligand interaction with atypical chemokine receptor 3. *Nat. Commun.* **8,** (2017).

110. Kapas, S. & Clark, A. J. L. Identification of an orphan receptor gene as a type 1 calcitonin gene-related peptide receptor. *Biochem. Biophys. Res. Commun.* **217,** 832–838 (1995).

111. Klein, K. R. *et al.* Decoy receptor CXCR7 modulates adrenomedullin-mediated cardiac and lymphatic vascular development. *Dev. Cell* **30,** 528–540 (2014).

112. Alampour-Rajabi, S. *et al.* MIF interacts with CXCR7 to promote receptor internalisation, ERK1/2 and ZAP-70 signaling, and lymphocyte chemotaxis.

FASEB J. **29,** 4497–4511 (2015).

113. Rao, S. *et al.* CXCL12 mediates trophic interactions between endothelial and tumor cells in glioblastoma. *PLoS One* **7,** (2012).

114. Wang, H. *et al.* The CXCR7 chemokine receptor promotes B-cell retention in the splenic marginal zone and serves as a sink for CXCL12. *Immunobiology* **119,** 465–468 (2012).

115. Zabel, B. A. *et al.* Elucidation of CXCR7-Mediated Signaling Events and Inhibition of CXCR4-Mediated Tumor Cell Transendothelial Migration by CXCR7 Ligands. *J. Immunol.* **183,** 3204–3211 (2009).

116. Neubig, R. R., Spedding, M., Kenakin, T. & Christopoulos, A. International Union of Pharmacology Commitee on Receptorn Nomenclature and Drug Classification. *Pharmacol. Rev.* **55,** 597–606 (2003).

117. Heesen, M. *et al.* Cloning and chromosomal mapping of an orphan chemokine receptor: mouse RDC1. *Immunogenetics* **47,** 364–70 (1998).

118. Haege, S. *et al.* CXC chemokine receptor 7 (CXCR7) regulates CXCR4 protein expression and capillary tuft development in mouse kidney. *PLoS One* **7,** 1–10 (2012).

119. Sierro, F. *et al.* Disrupted cardiac development but normal hematopoiesis in mice deficient in the second CXCL12/SDF-1 receptor, CXCR7. *Proc. Natl. Acad. Sci. U. S. A.* **104,** 14759–64 (2007).

120. Berahovich, R. D. *et al.* Differences in CXCR7 protein expression on rat versus mouse and human splenic marginal zone B cells. *Immunol. Lett.* **154,** 77–79 (2013).

121. Kin, N. W., Crawford, D. M., Liu, J., Behrens, T. W. & Kearney, J. F. DNA Microarray Gene Expression Profile of Marginal Zone versus Follicular B Cells and Idiotype Positive Marginal Zone B Cells before and after Immunization with Streptococcus pneumoniae. *J. Immunol.* **180,** 6663–6674 (2008).

122. Stolp, J. *et al.* Intrinsic Molecular Factors Cause Aberrant Expansion of the Splenic Marginal Zone B Cell Population in Nonobese Diabetic Mice. *J. Immunol.* **191,** 97–109 (2013).

123. Hartmann, T. N. *et al.* A crosstalk between intracellular CXCR7 and CXCR4 involved in rapid CXCL12-triggered integrin activation but not in chemokine-triggered motility of human T lymphocytes and CD34+ cells. *J. Leukoc. Biol.* **84,** 1130–1140 (2008).

124. Humpert, M.-L. *et al.* Complementary methods provide evidence for the expression of CXCR7 on human B cells. *Proteomics* **12,** 1938–48 (2012).

125. Choy, J. C. *et al.* CXCL12 Induction of Inducible Nitric Oxide Synthase in Human CD8 T Cells. *J. Hear. Lung Transplant.* **27,** 1333–1339 (2008).

126. Berahovich, R. D. *et al.* CXCR7 Protein Is Not Expressed on Human or Mouse Leukocytes. *J. Immunol.* **185,** 5130–5139 (2010).

127. Rath, D. *et al.* Expression of stromal cell-derived factor-1 receptors CXCR4 and CXCR7 on circulating platelets of patients with acute coronary syndrome and association with left ventricular functional recovery. *Eur. Heart J.* **35,** 386–

394 (2014).

128. Rath, D. *et al.* Platelet surface expression of stromal cell-derived factor-1 receptors CXCR4 and CXCR7 is associated with clinical outcomes in patients with coronary artery disease. *J. Thromb. Haemost.* **13,** 719–728 (2015).

129. Tripathi, V. *et al.* Differential expression of RDC1/CXCR7 in the human placenta. *J. Clin. Immunol.* **29,** 379–386 (2009).

130. Zhou, W.-H., Wu, X., Hu, W.-D. & Du, M.-R. Co-expression of CXCR4 and CXCR7 in human endometrial stromal cells is modulated by steroid hormones. *Int. J. Clin. Exp. Pathol.* **8,** 2449–60 (2015).

131. Westernströer, B. *et al.* Developmental expression patterns of chemokines CXCL11, CXCL12 and their receptor CXCR7 in testes of common marmoset and human. *Cell Tissue Res.* **361,** 885–898 (2015).

132. Berahovich, R. D. *et al.* Endothelial expression of CXCR7 and the regulation of systemic CXCL12 levels. *Immunology* **141,** 111–122 (2014).

133. Hunger, C., Ödemis, V. & Engele, J. Expression and function of the SDF-1 chemokine receptors CXCR4 and CXCR7 during mouse limb muscle development and regeneration. *Exp. Cell Res.* **318,** 2178–2190 (2012).

134. Schönemeier, B. *et al.* Regional and cellular localization of the CXCl12/SDF-1 chemokine receptor CXCR7 in the developing and adult rat brain. *J. Comp. Neurol.* **510,** 207–220 (2008).

135. Schönemeier, B., Schulz, S., Hoellt, V. & Stumm, R. Enhanced expression of the CXCl12/SDF-1 chemokine receptor CXCR7 after cerebral ischemia in the rat brain. *J. Neuroimmunol.* **198,** 39–45 (2008).

136. Tiveron, M. C., Boutin, C., Daou, P., Moepps, B. & Cremer, H. Expression and function of CXCR7 in the mouse forebrain. *J. Neuroimmunol.* **224,** 72–79 (2010).

137. Banisadr, G., Podojil, J. R., Miller, S. D. & Miller, R. J. Pattern of CXCR7 Gene Expression in Mouse Brain Under Normal and Inflammatory Conditions. *J. Neuroimmune Pharmacol.* **11,** 26–35 (2016).

138. Shimizu, S., Brown, M., Sengupta, R., Penfold, M. E. & Meucci, O. CXCR7 protein expression in human adult brain and differentiated neurons. *PLoS One* **6,** (2011).

139. Rajagopal, S. *et al.* Beta-arrestin- but not G protein-mediated signaling by the 'decoy' receptor CXCR7. *Proc. Natl. Acad. Sci. U. S. A.* **107,** 628–32 (2010).

140. Hoffmann, F. *et al.* Rapid uptake and degradation of CXCL12 depend on CXCR7 carboxyl-terminal serine/threonine residues. *J. Biol. Chem.* **287,** 28362–28377 (2012).

141. Ray, P. *et al.* Carboxy-terminus of CXCR7 regulates receptor localization and function. *Int. J. Biochem. Cell Biol.* **44,** 669–678 (2012).

142. Canals, M. *et al.* Ubiquitination of CXCR7 controls receptor trafficking. *PLoS One* **7,** e34192 (2012).

143. Luker, K. E., Steele, J. M., Mihalko, L. A., Ray, P. & Luker, G. D. Constitutive

and chemokine-dependent internalisation and recycling of CXCR7 in breast cancer cells to degrade chemokine ligands. *Oncogene* **29,** 4599–610 (2010).

144. Lee, E. *et al.* CXCR7 mediates SDF1-induced melanocyte migration. *Pigment Cell Melanoma Res.* **26,** 58–66 (2013).

145. Bao, J., Zhu, J., Luo, S., Cheng, Y. & Zhou, S. CXCR7 suppression modulates microglial chemotaxis to ameliorate experimentally-induced autoimmune encephalomyelitis. *Biochem. Biophys. Res. Commun.* **469,** 1–7 (2016).

146. Odemis, V., Boosmann, K., Heinen, A., Kury, P. & Engele, J. CXCR7 is an active component of SDF-1 signalling in astrocytes and Schwann cells. *J. Cell Sci.* **123,** 1081–1088 (2010).

147. Lipfert, J., Ödemis, V. & Engele, J. Grk2 is an essential regulator of CXCR7 signalling in astrocytes. *Cell. Mol. Neurobiol.* **33,** 111–118 (2013).

148. Torossian, F. *et al.* -arrestin − dependent Akt activation CXCR7 participates in CXCL12-induced CD34 1 cell cycling through b -arrestin – dependent Akt activation. **123,** 191–202 (2014).

149. Cao, Z. *et al.* CXCR7/p-ERK-Signaling is a novel target for therapeutic vasculogenesis in patients with coronary artery disease. *PLoS One* **11,** 1–11 (2016).

150. Levoye, A., Balabanian, K., Baleux, F., Bachelerie, F. & Lagane, B. CXCR7 heterodimerizes with CXCR4 and regulates CXCL12-mediated G protein signaling. *Blood* **113,** 6085–6093 (2009).

151. Decaillot, F. M. *et al.* CXCR7/CXCR4 Heterodimer Constitutively Recruits -Arrestin to Enhance Cell Migration. *J. Biol. Chem.* **286,** 32188–32197 (2011).

152. Mangmool, S. & Kurose, H. Gi/o protein-dependent and -independent actions of pertussis toxin (ptx). *Toxins (Basel).* **3,** 884–899 (2011).

153. Ödemis, V. *et al.* The presumed atypical chemokine receptor CXCR7 signals through Gi/o proteins in primary rodent astrocytes and human glioma cells. *Glia* **60,** 372–381 (2012).

154. Décaillot, F. M. *et al.* CXCR7/CXCR4 heterodimer constitutively recruits β-arrestin to enhance cell migration. *J. Biol. Chem.* **286,** 32188–32197 (2011).

155. Salazar, N. *et al.* The chemokine receptor CXCR7 interacts with EGFR to promote breast cancer cell proliferation. *Mol. Cancer* **13,** 198 (2014).

156. Kallifatidis, G. *et al.* -Arrestin-2 Counters CXCR7-Mediated EGFR Transactivation and Proliferation. *Mol. Cancer Res.* **14,** 493–503 (2016).

157. Dela Paz, N. G., Melchior, B., Shayo, F. Y. & Frangos, J. A. Heparan sulfates mediate the interaction between platelet endothelial cell adhesion molecule-1 (PECAM-1) and the Galpha q/11 subunits of heterotrimeric G proteins. *J. Biol. Chem.* **289,** 7413–7424 (2014).

158. Quinn, K. E., Mackie, D. I. & Caron, K. M. Emerging roles of atypical chemokine receptor 3 (ACKR3) in normal development and physiology. *Cytokine* **109,** 17–23 (2018).

159. Humpert, M. L., Pinto, D., Jarrossay, D. & Thelen, M. CXCR7 influences the

migration of B cells during maturation. *Eur. J. Immunol.* **44,** 694–705 (2014).

160. Wang, Y. *et al.* CXCR4 and CXCR7 Have Distinct Functions in Regulating Interneuron Migration. *Neuron* **69,** 61–76 (2011).

161. Sánchez-Alcañiz, J. A. *et al.* Cxcr7 Controls Neuronal Migration by Regulating Chemokine Responsiveness. *Neuron* **69,** 77–90 (2011).

162. Abe, P. *et al.* CXCR7 prevents excessive CXCL12-mediated downregulation of CXCR4 in migrating cortical interneurons. *Development* **141,** 1857–1863 (2014).

163. Trousse, F. *et al.* CXCR7 receptor controls the maintenance of subpial positioning of cajal-retzius cells. *Cereb. Cortex* **25,** 3446–3457 (2015).

164. Abe, P., Wüst, H. M., Arnold, S. J., van de Pavert, S. A. & Stumm, R. CXCL12-mediated feedback from granule neurons regulates generation and positioning of new neurons in the dentate gyrus. *Glia* (2018). doi:10.1002/glia.23324

165. Mazzinghi, B. *et al.* Essential but differential role for CXCR4 and CXCR7 in the therapeutic homing of human renal progenitor cells. *J. Exp. Med.* **205,** 479–490 (2008).

166. Liu, Y., Carson-Walter, E. & Walter, K. A. Chemokine receptor CXCR7 is a functional receptor for CXCL12 in brain endothelial cells. *PLoS One* **9,** 4–12 (2014).

167. Göttle, P. *et al.* Activation of CXCR7 receptor promotes oligodendroglial cell maturation. *Ann. Neurol.* **68,** 915–924 (2010).

168. Kremer, D. *et al.* CXCR7 is involved in human oligodendroglial precursor cell maturation. *PLoS One* **11,** 1–12 (2016).

169. Cruz-Orengo, L. *et al.* CXCR7 influences leukocyte entry into the CNS parenchyma by controlling abluminal CXCL12 abundance during autoimmunity. *J. Exp. Med.* **208,** 327–339 (2011).

170. Shimizu, N. *et al.* A putative G protein-coupled receptor, RDC1, is a novel coreceptor for human and simian immunodeficiency viruses. *J. Virol.* **74,** 619–26 (2000).

171. Zheng, K. *et al.* Chemokine receptor CXCR7 regulates the invasion,angiogenesis and tumor growth of human hepatocellular carcinoma cells. *J. Exp. Clin. Cancer Res.* **29,** 31 (2010).

172. Monnier, J. *et al.* CXCR7 is up-regulated in human and murine hepatocellular carcinoma and is specifically expressed by endothelial cells. *Eur. J. Cancer* **48,** 138–148 (2012).

173. Ieranò, C. *et al.* CXCR4 and CXCR7 transduce through mTOR in human renal cancer cells. *Cell Death Dis.* **5,** e1310 (2014).

174. Yu, Y. *et al.* SDF-1/CXCR7 Axis Enhances Ovarian Cancer Cell Invasion by MMP-9 Expression Through p38 MAPK Pathway. *DNA Cell Biol.* **33,** 543–549 (2014).

175. Liu, Z., Yang, L., Teng, X., Zhang, H. & Guan, H. The involvement of CXCR7

in modulating the progression of papillary thyroid carcinoma. *J. Surg. Res.* **191,** 379–388 (2014).

176. Liu, Z. *et al.* Expression of stromal cell-derived factor 1 and CXCR7 in papillary thyroid carcinoma. *Endocr. Pathol.* **23,** 247–53 (2012).

177. ZHU, X. *et al.* Expression and function of CXCL12/CXCR4/CXCR7 in thyroid cancer. *Int. J. Oncol.* **48,** 2321–2329 (2016).

178. Zhang, Y. *et al.* Knockdown of CXCR7 inhibits proliferation and invasion of osteosarcoma cells through inhibition of the PI3K/Akt and β-arrestin pathways. *Oncol. Rep.* **32,** 965–972 (2014).

179. Salmaggi, A. *et al.* CXCL12, CXCR4 and CXCR7 expression in brain metastases. *Cancer Biol. Ther.* **8,** 1608–14 (2009).

180. Iwakiri, S. *et al.* Higher expression of chemokine receptor CXCR7 is linked to early and metastatic recurrence in pathological stage I nonsmall cell lung cancer. *Cancer* **115,** 2580–2593 (2009).

181. Wu, Y. C., Tang, S. J., Sun, G. H. & Sun, K. H. CXCR7 mediates TGFβ1-promoted EMT and tumor-initiating features in lung cancer. *Oncogene* **35,** 2123–2132 (2016).

182. Wang, J. *et al.* The Role of CXCR7/RDC1 as a Chemokine Receptor for CXCL12/SDF-1 in Prostate Cancer. *J. Biol. Chem.* **283,** 4283–4294 (2008).

183. Singh, R. K. & Lokeshwar, B. L. The IL-8-regulated chemokine receptor CXCR7 stimulates EGFR signaling to promote prostate cancer growth. *Cancer Res.* **71,** 3268–3277 (2011).

184. Puddinu, V. *et al.* ACKR3 expression on diffuse large B cell lymphoma is required for tumor spreading and tissue infiltration. *Oncotarget* **8,** 85068–85084 (2017).

185. Zabel, B. A., Lewén, S., Berahovich, R. D., Jaén, J. C. & Schall, T. J. The novel chemokine receptor CXCR7 regulates trans-endothelial migration of cancer cells. *Mol. Cancer* **10,** 1–8 (2011).

186. Cao, Y. *et al.* MicroRNA-100 suppresses human gastric cancer cell proliferation by targeting CXCR7. *Oncol. Lett.* **15,** 453–458 (2017).

187. Qian, T. *et al.* CXCR7 regulates breast tumor metastasis and angiogenesis in vivo and in vitro. *Mol. Med. Rep.* 3633–3639 (2017). doi:10.3892/mmr.2017.8286

188. Wu, W., Qian, L., Chen, X. & Ding, B. Prognostic significance of CXCL12, CXCR4, and CXCR7 in patients with breast cancer. *Int. J. Clin. Exp. Pathol.* **8,** 13217–24 (2015).

189. Stacer, A. C. *et al.* Endothelial CXCR7 regulates breast cancer metastasis. *Oncogene* **35,** 1716–1724 (2016).

190. Hernandez, L., Magalhaes, M. A. O., Coniglio, S. J., Condeelis, J. S. & Segall, J. E. Opposing roles of CXCR4 and CXCR7 in breast cancer metastasis. *Breast Cancer Res.* **13,** 19–21 (2011).

191. Li, X.-J. *et al.* Mechanisms of CXCR7 induction in malignant melanoma

development. *Oncol. Lett.* **14,** 4106–4114 (2017).

192. Qiao, Y. *et al.* IL6 derived from cancer-associated fibroblasts promotes chemoresistance via CXCR7 in esophageal squamous cell carcinoma. *Oncogene* **37,** 873–883 (2018).

193. Hu, S. C.-S., Yu, H.-S., Yen, F.-L., Chen, G.-S. & Lan, C.-C. E. CXCR7 expression correlates with tumor depth in cutaneous squamous cell carcinoma skin lesions and promotes tumor cell survival through ERK activation. *Exp. Dermatol.* 902–908 (2014). doi:10.1111/exd.12557

194. Guo, J.-C. *et al.* CXCL12-CXCR7 axis contributes to the invasive phenotype of pancreatic cancer. *Oncotarget* **5,** (2016).

195. Heckmann, D. *et al.* The disparate twins: A comparative study of CXCR4 and CXCR7 in SDF-1α-induced gene expression, invasion and chemosensitivity of colon cancer. *Clin. Cancer Res.* **20,** 604–616 (2014).

196. Schrevel, M. *et al.* CXCR7 expression is associated with disease-free and disease-specific survival in cervical cancer patients. *Br. J. Cancer* **106,** 1520–1525 (2012).

197. Hao, M. *et al.* Role of chemokine receptor CXCR7 in bladder cancer progression. *Biochem. Pharmacol.* **84,** 204–214 (2012).

198. Inaguma, S. *et al.* GLI1 orchestrates CXCR4/CXCR7 signaling to enhance migration and metastasis of breast cancer cells. *Oncotarget* **6,** 33648–57 (2015).

199. Kerdivel, G., Boudot, A. & Pakdel, F. Estrogen represses CXCR7 gene expression by inhibiting the recruitment of NFκB transcription factor at the CXCR7 promoter in breast cancer cells. *Biochem. Biophys. Res. Commun.* **431,** 729–733 (2013).

200. Romain, B. *et al.* Hypoxia differentially regulated CXCR4 and CXCR7 signaling in colon cancer. *Mol. Cancer* **13,** 58 (2014).

201. Liu, Z., Teng, X.-Y., Meng, X.-P. & Wang, B.-S. Expression of stromal cell-derived factor 1 and CXCR7 ligand receptor system in pancreatic adenocarcinoma. *World J. Surg. Oncol.* **12,** 348 (2014).

202. Huang, Y. *et al.* Silencing of CXCR4 and CXCR7 expression by RNA interference suppresses human endometrial carcinoma growth in vivo. *Am. J. Transl. Res.* **9,** 1896–1904 (2017).

203. Gao, W., Mei, X., Wang, J., Zhang, X. & Yuan, Y. ShRNA-mediated knock-down of CXCR7 increases TRAIL-sensitivity in MCF-7 breast cancer cells. *Tumor Biol.* **36,** 7243–7250 (2015).

204. Ieranò, C. *et al.* CXCR4 and CXCR7 transduce through mTOR in human renal cancer cells. *Cell Death Dis.* **5,** e1310–e1310 (2014).

205. Chen, Q. *et al.* CXCR7 Mediates Neural Progenitor Cells Migration to CXCL12 Independent of CXCR4. *Stem Cells* **33,** 2574–2585 (2015).

206. Liu, Y., Carson-Walter, E. & Walter, K. A. Targeting chemokine receptor CXCR7 inhibits glioma cell proliferation and mobility. *Anticancer Res.* **35,** 53–64 (2015).

207. Lin, L. *et al.* CXCR7 stimulates MAPK signaling to regulate hepatocellular carcinoma progression. *Cell Death Dis.* **5,** e1488 (2014).

208. Veenstra, M. *et al.* Frontline Science: CXCR7 mediates CD14 $^{+}$ CD16 $^{+}$ monocyte transmigration across the blood brain barrier: a potential therapeutic target for NeuroAIDS. *J. Leukoc. Biol.* **102,** jlb.3HI0517-167R (2017).

209. Parsons, D. W. *et al.* An Integrated Genomic Analysis of Human Glioblastoma Multiforme. *Science (80-.).* **321,** 1807–1812 (2008).

210. Birner, P., Tchorbanov, A., Natchev, S., Tuettenberg, J. & Guentchev, M. The chemokine receptor CXCR7 influences prognosis in human glioma in an IDH1-dependent manner. *J. Clin. Pathol.* **68,** 830–4 (2015).

211. Calatozzolo, C. *et al.* Expression of the new CXCL12 receptor, CXCR7, in gliomas. *Cancer Biol. Ther.* **11,** 242–253 (2011).

212. Hattermann, K. *et al.* The chemokine receptor CXCR7 is highly expressed in human glioma cells and mediates antiapoptotic effects. *Cancer Res.* **70,** 3299–3308 (2010).

213. Walters, M. J. *et al.* Inhibition of CXCR7 extends survival following irradiation of brain tumours in mice and rats. *Br. J. Cancer* **110,** 1179–1188 (2014).

214. Bianco, A. M. *et al.* CXCR7 and CXCR4 Expressions in Infiltrative Astrocytomas and Their Interactions with HIF1α Expression and IDH1 Mutation. *Pathol. Oncol. Res.* **21,** 229–240 (2014).

215. Touat, M., Idbaih, A., Sanson, M. & Ligon, K. L. Glioblastoma targeted therapy: updated approaches from recent biological insights. *Ann. Oncol. Off. J. Eur. Soc. Med. Oncol.* **28,** 1457–1472 (2017).

216. Han, X., Xue, X., Zhou, H. & Zhang, G. A molecular view of the radioresistance of gliomas. *Oncotarget* **8,** 100931–100941 (2017).

217. Stavrovskaya, A. A., Shushanov, S. S. & Rybalkina, E. Y. Problems of Glioblastoma Multiforme Drug Resistance. *Biochem. Biokhimiiâ`* **81,** 91–100 (2016).

218. Gilbert, M. R. *et al.* A Randomized Trial of Bevacizumab for Newly Diagnosed Glioblastoma. *N. Engl. J. Med.* **370,** 699–708 (2014).

219. Hattermann, K., Mentlein, R. & Held-Feindt, J. CXCL12 mediates apoptosis resistance in rat C6 glioma cells. *Oncol. Rep.* **27,** 1348–1352 (2012).

220. Ricci-Vitiani, L. *et al.* Tumour vascularization via endothelial differentiation of glioblastoma stem-like cells. *Nature* **468,** 824–830 (2010).

221. Yu, H. *et al.* Knockdown of long non-coding RNA XIST increases blood–tumor barrier permeability and inhibits glioma angiogenesis by targeting miR-137. *Oncogenesis* **6,** e303 (2017).

222. Beyer, E. C. & Berthoud, V. M. Gap junction gene and protein families: Connexins, innexins, and pannexins. *Biochim. Biophys. Acta - Biomembr.* **1860,** 5–8 (2018).

223. Oshima, A. Structure and closure of connexin gap junction channels. *FEBS Lett.* **588,** 1230–1237 (2014).

224. Aasen, T., Johnstone, S., Vidal-Brime, L., Lynn, K. S. & Koval, M. Connexins: Synthesis, post-translational modifications, and trafficking in health and disease. *Int. J. Mol. Sci.* **19,** (2018).

225. Koval, M., Molina, S. A. & Burt, J. M. Mix and match: Investigating heteromeric and heterotypic gap junction channels in model systems and native tissues. *FEBS Lett.* **588,** 1193–1204 (2014).

226. Unwin, P. N. T. & Ennis, P. D. Two configurations of a channel-forming membrane protein. *Nature* **307,** 609–613 (1984).

227. Bargiello, T. A. *et al.* Gating of Connexin Channels by transjunctional-voltage: Conformations and models of open and closed states. *Biochim. Biophys. Acta - Biomembr.* **1860,** 22–39 (2018).

228. Verselis, V. K., Trelles, M. P., Rubinos, C., Bargiello, T. A. & Srinivas, M. Loop gating of connexin hemichannels involves movement of pore-lining residues in the first extracellular loop domain. *J. Biol. Chem.* **284,** 4484–4493 (2009).

229. Morley, G. E., Taffet, S. M. & Delmar, M. Intramolecular interactions mediate pH regulation of connexin43 channels. *Biophys. J.* **70,** 1294–1302 (1996).

230. Wang, H. Z. & Veenstra, R. D. Monovalent ion selectivity sequences of the rat connexin43 gap junction channel. *J. Gen. Physiol.* **109,** 491–507 (1997).

231. Harris, A. L. Connexin channel permeability to cytoplasmic molecules. *Prog. Biophys. Mol. Biol.* **94,** 120–143 (2007).

232. DeVries, S. H. & Schwartz, E. A. Hemi-gap-junction channels in solitary horizontal cells of the catfish retina. *J. Physiol.* **445,** 201–30 (1992).

233. Paul, D. L., Ebihara, L., Takemoto, L. J., Swenson, K. I. & Goodenough, D. A. Connexin46, a novel lens gap junction protein, induces voltage-gated currents in nonjunctional plasma membrane of Xenopus oocytes. *J. Cell Biol.* **115,** 1077–89 (1991).

234. Giaume, C., Leybaert, L., Naus, C. C. & Sáez, J. C. Connexin and pannexin hemichannels in brain glial cells: Properties, pharmacology, and roles. *Front. Pharmacol.* **4 JUL,** 1–17 (2013).

235. Contreras, J. E., Saez, J. C., Bukauskas, F. F. & Bennett, M. V. Gating and regulation of connexin 43 (Cx43) hemichannels. *Proc Natl Acad Sci U S A* **100,** 11388–11393 (2003).

236. Huang, R. P. *et al.* Reversion of the neoplastic phenotype of human glioblastoma cells by connexin 43 (cx43). *Cancer Res.* **58,** 5089–96 (1998).

237. Moorby, C. & Patel, M. Dual Functions for Connexins: Cx43 Regulates Growth Independently of Gap Junction Formation. *Exp. Cell Res.* **271,** 238–248 (2001).

238. Behrens, J., Kameritsch, P., Wallner, S., Pohl, U. & Pogoda, K. The carboxyl tail of Cx43 augments p38 mediated cell migration in a gap junction-independent manner. *Eur. J. Cell Biol.* **89,** 828–838 (2010).

239. Machtaler, S. *et al.* The gap junction protein Cx43 regulates B-lymphocyte spreading and adhesion. *J. Cell Sci.* **124,** 2611–2621 (2011).

240. Aasen, T., Mesnil, M., Naus, C. C., Lampe, P. D. & Laird, D. W. Gap junctions and cancer: communicating for 50 years. *Nat. Rev. Cancer* **16,** 775–788 (2016).

241. Srinivas, M., Verselis, V. K. & White, T. W. Human diseases associated with connexin mutations. *Biochim. Biophys. Acta - Biomembr.* **1860,** 192–201 (2018).

242. Laird, D. W. Syndromic and non-syndromic disease-linked Cx43 mutations. *FEBS Lett.* **588,** 1339–1348 (2014).

243. Richardson, R. J. *et al.* A nonsense mutation in the first transmembrane domain of connexin 43 underlies autosomal recessive oculodentodigital syndrome. *J. Med. Genet.* **43,** e37 (2006).

244. Hu, Y. *et al.* A novel autosomal recessive GJA1 missense mutation linked to Craniometaphyseal dysplasia. *PLoS One* **8,** e73576 (2013).

245. Van Norstrand, D. W. *et al.* Connexin43 Mutation Causes Heterogeneous Gap Junction Loss and Sudden Infant Death. *Circulation* **125,** 474–481 (2012).

246. Neyton, J. & Trautmann, A. Single-channel currents of an intercellular junction. *Nature* **317,** 331–335 (1985).

247. Abbaci, M., Barberi-Heyob, M., Blondel, W., Guillemin, F. & Didelon, J. Advantages and limitations of commonly used methods to assay the molecular permeability of gap junctional intercellular communication. *Biotechniques* **45,** 33–62 (2008).

248. Giaume, C. *et al.* Gap junctions in cultured astrocytes: Single-channel currents and characterization of channel-forming protein. *Neuron* **6,** 133–143 (1991).

249. Retamal, M. A. *et al.* Cx43 hemichannels and gap junction channels in astrocytes are regulated oppositely by proinflammatory cytokines released from activated microglia. *J. Neurosci.* **27,** 13781–13792 (2007).

250. Stewart, W. W. Lucifer dyes--highly fluorescent dyes for biological tracing. *Nature* **292,** 17–21 (1981).

251. Rouach, N. *et al.* S1P inhibits gap junctions in astrocytes: Involvement of Gi and Rho GTPase/ROCK. *Eur. J. Neurosci.* **23,** 1453–1464 (2006).

252. Lima, F., Niger, C., Hebert, C. & Stains, J. P. Connexin43 Potentiates Osteoblast Responsiveness to Fibroblast Growth Factor 2 via a Protein Kinase C-Delta/ Runx2–dependent Mechanism. *Mol. Biol. Cell* **82,** 327–331 (2009).

253. Hou, B. *et al.* Homeostatic Plasticity Mediated by Rod-Cone Gap Junction Coupling in Retinal Degenerative Dystrophic RCS Rats. *Front. Cell. Neurosci.* **11,** 98 (2017).

254. Pastor, A., Kremer, M., Möller, T., Kettenmann, H. & Dermietzel, R. Dye coupling between spinal cord oligodendrocytes: differences in coupling efficiency between gray and white matter. *Glia* **24,** 108–20 (1998).

255. Duval, N. *et al.* Cell coupling and Cx43 expression in embryonic mouse neural progenitor cells. *J. Cell Sci.* **115,** 3241–51 (2002).

256. Raptis, L. H., Brownell, H. L., Firth, K. L. & Mackenzie, L. W. A novel

technique for the study of intercellular, junctional communication: electroporation of adherent cells on a partly conductive slide. *DNA Cell Biol.* **13,** 963–75 (1994).

257. Goldberg, G. S., Bechberger, J. F. & Naus, C. C. A pre-loading method of evaluating gap junctional communication by fluorescent dye transfer. *Biotechniques* **18,** 490–7 (1995).

258. Dakin, K., Zhao, Y. & Li, W.-H. LAMP, a new imaging assay of gap junctional communication unveils that Ca2+ influx inhibits cell coupling. *Nat. Methods* **2,** 55–62 (2005).

259. Giaume, C., Orellana, J. A., Abudara, V. & Sáez, J. C. Connexin-Based Channels in Astrocytes: How to Study Their Properties. *Methods Mol Biol.* **814,** 283–303 (2012).

260. Même, W. *et al.* Proinflammatory cytokines released from microglia inhibit gap junctions in astrocytes: potentiation by β-amyloid. *FASEB J.* **20,** 494–496 (2006).

261. Blomstrand, F. *et al.* Endothelins regulate astrocyte gap junctions in rat hippocampal slices. *Eur. J. Neurosci.* **19,** 1005–1015 (2004).

262. Giaume, C. & Theis, M. Pharmacological and genetic approaches to study connexin-mediated channels in glial cells of the central nervous system. *Brain Res. Rev.* **63,** 160–176 (2010).

263. Srinivas, M., Hopperstad, M. G. & Spray, D. C. Quinine blocks specific gap junction channel subtypes. *Proc. Natl. Acad. Sci.* **98,** 10942–10947 (2001).

264. Contreras, J. E. *et al.* Metabolic inhibition induces opening of unapposed connexin 43 gap junction hemichannels and reduces gap junctional communication in cortical astrocytes in culture. *Proc. Natl. Acad. Sci.* **99,** 495–500 (2002).

265. Irby, R. B. & Yeatman, T. J. *Role of Src expression and activation in human cancer*. at <www.nature.com/onc>

266. Gilleron, J. *et al.* Molecular reorganization of Cx43, Zo-1 and Src complexes during the endocytosis of gap junction plaques in response to a non-genomic carcinogen. *J. Cell Sci.* **121,** 4069–4078 (2008).

267. Matchkov, V. V *et al.* Analysis of effects of connexin-mimetic peptides in rat mesenteric small arteries. *Am. J. Physiol. Heart Circ. Physiol.* **291,** H357-67 (2006).

268. Martin, P. E. M., Wall, C. & Griffith, T. M. Effects of connexin-mimetic peptides on gap junction functionality and connexin expression in cultured vascular cells. *Br. J. Pharmacol.* **144,** 617–27 (2005).

269. Ponsaerts, R. *et al.* Intramolecular loop/tail interactions are essential for connexin 43-hemichannel activity. *FASEB J.* **24,** 4378–95 (2010).

270. Wang, N. *et al.* Selective inhibition of Cx43 hemichannels by Gap19 and its impact on myocardial ischemia/reperfusion injury. *Basic Res. Cardiol.* **108,** 309 (2013).

271. Gangoso, E. *et al.* A c-Src Inhibitor Peptide Based on Connexin43 Exerts

Neuroprotective Effects through the Inhibition of Glial Hemichannel Activity. *Front. Mol. Neurosci.* **10,** (2017).

272. Gangoso, E., Thirant, C., Chneiweiss, H., Medina, J. M. & Tabernero, A. A cell-penetrating peptide based on the interaction between c-Src and connexin43 reverses glioma stem cell phenotype. *Cell Death Dis.* **5,** e1023 (2014).

273. De Bock, M. *et al.* Connexin 43 hemichannels contribute to cytoplasmic Ca2+ oscillations by providing a bimodal Ca2+-dependent Ca2+ entry pathway. *J. Biol. Chem.* **287,** 12250–66 (2012).

274. Montgomery, J., Ghatnekar, G., Grek, C., Moyer, K. & Gourdie, R. Connexin 43-Based Therapeutics for Dermal Wound Healing. *Int. J. Mol. Sci.* **19,** 1778 (2018).

275. Schalper, K. A. *et al.* Connexin hemichannel composition determines the FGF-1-induced membrane permeability and free [Ca2+]i responses. *Mol. Biol. Cell* **19,** 3501–13 (2008).

276. Sánchez, H. A., Orellana, J. A., Verselis, V. K. & Sáez, J. C. Metabolic inhibition increases activity of connexin-32 hemichannels permeable to Ca2+ in transfected HeLa cells. *Am. J. Physiol. Cell Physiol.* **297,** C665-78 (2009).

277. Retamal, M. A., Cortés, C. J., Reuss, L., Bennett, M. V. L. & Sáez, J. C. S-nitrosylation and permeation through connexin 43 hemichannels in astrocytes: induction by oxidant stress and reversal by reducing agents. *Proc. Natl. Acad. Sci. U. S. A.* **103,** 4475–80 (2006).

278. Musil, L. S. & Goodenough, D. A. Biochemical-Analysis of Connexin43 Intracellular-Transport, Phosphorylation, and Assembly Into Gap Junctional Plaques. *J. Cell Biol.* **115,** 1357–1374 (1991).

279. VanSlyke, J. K. & Musil, L. S. Analysis of connexin intracellular transport and assembly. *Methods* **20,** 156–164 (2000).

280. Zhang, X.-F. & Cui, X. Connexin 43: Key roles in the skin. *Biomed. reports* **6,** 605–611 (2017).

281. Reaume, A. *et al.* Cardiac malformation in neonatal mice lacking connexin43. *Science (80-.).* **267,** 1831–1834 (1995).

282. Rouach, N. *et al.* Gap junctions and connexin expression in the normal and pathological central nervous system. *Biol. Cell.* **94,** 457–475 (2002).

283. Chen, Q. *et al.* Carcinoma–astrocyte gap junctions promote brain metastasis by cGAMP transfer. *Nature* **533,** 493–498 (2016).

284. Beardslee, M. A., Laing, J. G., Beyer, E. C. & Saffitz, J. E. Rapid turnover of connexin43 in the adult rat heart. *Circ. Res.* **83,** 629–35 (1998).

285. Sarma, J. Das, Kaplan, B., Willemsen, D. & Koval, M. Identification of rab20 as a potential regulator of connexin43 trafficking. *Cell Commun. Adhes.* **15,** 65–74 (2008).

286. Li, X., Su, V., Kurata, W. E., Jin, C. & Lau, A. F. A novel connexin43-interacting protein, CIP75, which belongs to the UbL-UBA protein family, regulates the turnover of connexin43. *J. Biol. Chem.* **283,** 5748–5759 (2008).

287. Lauf, U. *et al.* Dynamic trafficking and delivery of connexons to the plasma membrane and accretion to gap junctions in living cells. *Proc. Natl. Acad. Sci. U. S. A.* **99,** 10446–10451 (2002).

288. Shaw, R. M. *et al.* Microtubule Plus-End-Tracking Proteins Target Gap Junctions Directly from the Cell Interior to Adherens Junctions. *Cell* **128,** 547–560 (2007).

289. Gaietta, G. *et al.* Multicolor and Electron Microscopic Imaging of Connexin Trafficking. *Science (80-.).* **296,** 503–507 (2002).

290. Hesketh, G. G., Van Eyk, J. E. & Tomaselli, G. F. Mechanisms of gap junction traffic in health and disease. *J. Cardiovasc. Pharmacol.* **54,** 263–272 (2009).

291. Toyofuku, T. *et al.* Direct association of the gap junction protein connexin-43 with ZO-1 in cardiac myocytes. *J. Biol. Chem.* **273,** 12725–31 (1998).

292. Hunter, A. W., Barker, R. J., Zhu, C. & Gourdie, R. G. Zonula occludens-1 alters connexin43 gap junction size and organization by influencing channel accretion. *Mol. Biol. Cell* **16,** 5686–98 (2005).

293. Jordan, K., Chodock, R., Hand, a R. & Laird, D. W. The origin of annular junctions: a mechanism of gap junction internalisation. *J. Cell Sci.* **114,** 763–73 (2001).

294. Carette, D. *et al.* New cellular mechanisms of gap junction degradation and recycling. *Biol. Cell* **107,** 218–231 (2015).

295. Cooper, C. D. & Lampe, P. D. Casein Kinase 1 Regulates Connexin-43 Gap Junction Assembly. *J. Biol. Chem.* **277,** 44962–44968 (2002).

296. Tenbroek, E. M., Lampe, P. D., Solan, J. L., Reynhout, J. K. & Johnson, R. G. Ser364 of connexin43 and the upregulation of gap junction assembly by cAMP. *J. Cell Biol.* **155,** 1307–1318 (2001).

297. Dunn, C. A. & Lampe, P. D. Injury-triggered Akt phosphorylation of Cx43: a ZO-1-driven molecular switch that regulates gap junction size. *J. Cell Sci.* **127,** 455–64 (2014).

298. Solan, J. L., Fry, M. D., TenBroek, E. M. & Lampe, P. D. Connexin43 phosphorylation at S368 is acute during S and G2/M and in response to protein kinase C activation. *J. Cell Sci.* **116,** 2203–2211 (2003).

299. Tencé, M., Ezan, P., Amigou, E. & Giaume, C. Increased interaction of connexin43 with zonula occludens-1 during inhibition of gap junctions by G protein-coupled receptor agonists. *Cell. Signal.* **24,** 86–98 (2012).

300. Filson, A. J., Azarnia, R., Beyer, E. C., Loewenstein, W. R. & Brugge, J. S. Tyrosine phosphorylation of a gap junction protein correlates with inhibition of cell-to-cell communication. *Cell Growth Differ.* **1,** 661–8 (1990).

301. Fong, J. T., Nimlamool, W. & Falk, M. M. EGF induces efficient Cx43 gap junction endocytosis in mouse embryonic stem cell colonies via phosphorylation of Ser262, Ser279/282, and Ser368. *FEBS Lett.* **588,** 836–44 (2014).

302. Kjenseth, A. *et al.* The Gap Junction Channel Protein Connexin 43 Is Covalently Modified and Regulated by SUMOylation. *J. Biol. Chem.* **287,**

15851–15861 (2012).

303. Leithe, E. *et al.* Ubiquitylation of the gap junction protein connexin-43 signals its trafficking from early endosomes to lysosomes in a process mediated by Hrs and Tsg101. *J. Cell Sci.* **122,** 3883–3893 (2009).

304. Colussi, C. *et al.* Nε-lysine acetylation determines dissociation from GAP junctions and lateralization of connexin 43 in normal and dystrophic heart. *Proc. Natl. Acad. Sci. U. S. A.* **108,** 2795–800 (2011).

305. Smyth, J. W. & Shaw, R. M. Autoregulation of connexin43 gap junction formation by internally translated isoforms. *Cell Rep.* **5,** 611–618 (2013).

306. Chen, X. *et al.* Dynamic changes in protein interaction between AKAP95 and Cx43 during cell cycle progression of A549 cells. *Sci. Rep.* **6,** 21224 (2016).

307. Sato, M. *et al.* Activator of G Protein Signaling 8 (AGS8) Is Required for Hypoxia-induced Apoptosis of Cardiomyocytes. *J. Biol. Chem.* **284,** 31431–31440 (2009).

308. Xu, X. *et al.* Modulation of mouse neural crest cell motility by N-cadherin and connexin 43 gap junctions. *J. Cell Biol.* **154,** 217–30 (2001).

309. Sato, P. Y. *et al.* Interactions Between Ankyrin-G, Plakophilin-2, and Connexin43 at the Cardiac Intercalated Disc. *Circ. Res.* **109,** 193–201 (2011).

310. Piehl, M. *et al.* Internalisation of Large Double-Membrane Intercellular Vesicles by a Clathrin-dependent Endocytic Process. *Mol. Biol. Cell* **18,** 337–347 (2007).

311. SUN, Y. *et al.* Connexin 43 interacts with Bax to regulate apoptosis of pancreatic cancer through a gap junction-independent pathway. *Int. J. Oncol.* **41,** 941–948 (2012).

312. Denuc, A. *et al.* New protein-protein interactions of mitochondrial connexin 43 in mouse heart. *J. Cell. Mol. Med.* **20,** 794–803 (2016).

313. Bejarano, E. *et al.* Connexins modulate autophagosome biogenesis. **16,** 401–414 (2014).

314. Ito, T., Ueki, T., Furukawa, H. & Sato, K. The identification of novel protein, brain-derived integrating factor-1 (BDIF1), which interacts with astrocytic gap junctional protein. *Neurosci. Res.* **70,** 330–333 (2011).

315. Zou, J. *et al.* Gap junction regulation by calmodulin. *FEBS Lett.* **588,** 1430–8 (2014).

316. Liu, L. *et al.* Connexin43 interacts with Caveolin-3 in the heart. *Mol. Biol. Rep.* **37,** 1685–1691 (2010).

317. Langlois, S., Cowan, K. N., Shao, Q., Cowan, B. J. & Laird, D. W. Caveolin-1 and -2 Interact with Connexin43 and Regulate Gap Junctional Intercellular Communication in Keratinocytes. *Mol. Biol. Cell* **19,** 912–928 (2008).

318. Nagasawa, K. *et al.* Possible involvement of gap junctions in the barrier function of tight junctions of brain and lung endothelial cells. *J. Cell. Physiol.* **208,** 123–132 (2006).

319. del Castillo, F. J. *et al.* Consortin, a trans-Golgi network cargo receptor for the plasma membrane targeting and recycling of connexins. *Hum. Mol. Genet.* **19,** 262–275 (2010).

320. Johnstone, S. R. *et al.* MAPK Phosphorylation of Connexin 43 Promotes Binding of Cyclin E and Smooth Muscle Cell Proliferation. *Circ. Res.* **111,** 201–211 (2012).

321. Gehmlich, K. *et al.* A novel desmocollin-2 mutation reveals insights into the molecular link between desmosomes and gap junctions. *Hear. Rhythm* **8,** 711–718 (2011).

322. MacDonald, A. I. *et al.* A functional interaction between the MAGUK protein hDlg and the gap junction protein connexin 43 in cervical tumour cells. *Biochem. J.* **446,** 9–21 (2012).

323. Butkevich, E. *et al.* Drebrin Is a Novel Connexin-43 Binding Partner that Links Gap Junctions to the Submembrane Cytoskeleton. *Curr. Biol.* **14,** 650–658 (2004).

324. Gilleron, J. *et al.* The large GTPase dynamin2: A new player in connexin 43 gap junction endocytosis, recycling and degradation. *Int. J. Biochem. Cell Biol.* **43,** 1208–1217 (2011).

325. Fykerud, T. A. *et al.* Smad ubiquitination regulatory factor-2 controls gap junction intercellular communication by modulating endocytosis and degradation of connexin43. *J. Cell Sci.* **125,** 3966–3976 (2012).

326. Chen, V. C., Kristensen, A. R., Foster, L. J. & Naus, C. C. Association of Connexin43 with E3 Ubiquitin Ligase TRIM21 Reveals a Mechanism for Gap Junction Phosphodegron Control. *J. Proteome Res.* **11,** 6134–6146 (2012).

327. Das, S. *et al.* ERp29 Restricts Connexin43 Oligomerization in the Endoplasmic Reticulum. *Mol. Biol. Cell* **20,** 2593–2604 (2009).

328. Girão, H., Catarino, S. & Pereira, P. Eps15 interacts with ubiquitinated Cx43 and mediates its internalisation. *Exp. Cell Res.* **315,** 3587–3597 (2009).

329. Pidoux, G. *et al.* A PKA-ezrin-Cx43 signaling complex controls gap junction communication and thereby trophoblast cell fusion. *J. Cell Sci.* **127,** 4172–4185 (2014).

330. Hatakeyama, T. *et al.* Connexin43 Functions as a Novel Interacting Partner of Heat Shock Cognate Protein 70. *Sci. Rep.* **3,** 2719 (2013).

331. Rodriguez-Sinovas, A. *et al.* Translocation of Connexin 43 to the Inner Mitochondrial Membrane of Cardiomyocytes Through the Heat Shock Protein 90-Dependent TOM Pathway and Its Importance for Cardioprotection. *Circ. Res.* **99,** 93–101 (2006).

332. Martins-Marques, T. *et al.* Ischaemia-induced autophagy leads to degradation of gap junction protein connexin43 in cardiomyocytes. *Biochem. J.* **467,** 231–245 (2015).

333. Schiavon, G., Furlan, S., Marin, O. & Salvatori, S. Myotonic dystrophy protein kinase of the cardiac muscle: Evaluation using an immunochemical approach. *Microsc. Res. Tech.* **58,** 404–411 (2002).

334. Malhotra, J. D., Thyagarajan, V., Chen, C. & Isom, L. L. Tyrosine-phosphorylated and Nonphosphorylated Sodium Channel β1 Subunits Are Differentially Localized in Cardiac Myocytes. *J. Biol. Chem.* **279,** 40748–40754 (2004).

335. Basheer, W. A. *et al.* Cardiomyocyte-specific overexpression of the ubiquitin ligase Wwp1 contributes to reduction in Connexin 43 and arrhythmogenesis. *J. Mol. Cell. Cardiol.* **88,** 1–13 (2015).

336. Dunk, C. E. *et al.* The molecular role of connexin 43 in human trophoblast cell fusion. *Biol. Reprod.* **86,** 115 (2012).

337. Fu, C. T., Bechberger, J. F., Ozog, M. A., Perbal, B. & Naus, C. C. CCN3 (NOV) Interacts with Connexin43 in C6 Glioma Cells. *J. Biol. Chem.* **279,** 36943–36950 (2004).

338. Fortes, F. S. A. *et al.* Modulation of intercellular communication in macrophages: possible interactions between GAP junctions and P2 receptors. *J. Cell Sci.* **117,** 4717–4726 (2004).

339. Marquez-Rosado, L., Singh, D., Rincon-Arano, H., Solan, J. L. & Lampe, P. D. CASK (LIN2) interacts with Cx43 in wounded skin and their coexpression affects cell migration. *J. Cell Sci.* **125,** 695–702 (2012).

340. Li, M. W. M., Mruk, D. D., Lee, W. M. & Cheng, C. Y. Connexin 43 and plakophilin-2 as a protein complex that regulates blood-testis barrier dynamics. *Proc. Natl. Acad. Sci.* **106,** 10213–10218 (2009).

341. Lan, Z., Kurata, W. E., Martyn, K. D., Jin, C. & Lau, A. F. Novel Rab GAP-like protein, CIP85, interacts with connexin43 and induces its degradation. *Biochemistry* **44,** 2385–2396 (2005).

342. Ribeiro-Rodrigues, T. M. *et al.* AMSH-mediated deubiquitination of Cx43 regulates internalisation and degradation of gap junctions. *FASEB J.* **28,** 4629–4641 (2014).

343. Singh, D., Solan, J. L., Taffet, S. M., Javier, R. & Lampe, P. D. Connexin 43 Interacts with Zona Occludens-1 and -2 Proteins in a Cell Cycle Stage-specific Manner. *J. Biol. Chem.* **280,** 30416–30421 (2005).

344. Sun, J. *et al.* The ubiquitin-specific protease USP8 deubiquitinates and stabilizes Cx43. *J. Biol. Chem.* **293,** 8275–8284 (2018).

345. Bivi, N., Lezcano, V., Romanello, M., Bellido, T. & Plotkin, L. I. Connexin43 interacts with βarrestin: A pre-requisite for osteoblast survival induced by parathyroid hormone. *J. Cell. Biochem.* **112,** 2920–2930 (2011).

346. Ai, Z., Fischer, A., Spray, D. C., Brown, A. M. & Fishman, G. I. Wnt-1 regulation of connexin43 in cardiac myocytes. *J. Clin. Invest.* **105,** 161–71 (2000).

347. Giaume, C., Marin, P., Cordier, J., Glowinski, J. & Premont, J. Adrenergic regulation of intercellular communications between cultured striatal astrocytes from the mouse. *Proc. Natl. Acad. Sci.* **88,** 5577–5581 (1991).

348. Même, W., Ezan, P., Venance, L., Glowinski, J. & Giaume, C. ATP-induced inhibition of gap junctional communication is enhanced by interleukin-1 β treatment in cultured astrocytes. *Neuroscience* **126,** 95–104 (2004).

349. Venance, L., Piomelli, D., Glowinski, J. & Glaume, C. Inhibition by anandamide of gap junctions and intercellular calcium signalling in striatal astrocytes. *Nature* **376,** 590–594 (1995).

350. Giaume, C., Cordier, J. & Glowinski, J. Endothelins Inhibit Junctional Permeability in Cultured Mouse Astrocytes. *Eur. J. Neurosci.* **4,** 877–881 (1992).

351. Van Zeijl, L. *et al.* Regulation of connexin43 gap junctional communication by phosphatidylinositol 4,5-bisphosphate. *J. Cell Biol.* **177,** 881–891 (2007).

352. Newman, E. A. Membrane physiology of retinal glial (Müller) cells. *J. Neurosci.* **5,** 2225–39 (1985).

353. Medina, J. M., Giaume, C. & Tabernero, A. Metabolic coupling and the role played by astrocytes in energy distribution and homeostasis. *Adv. Exp. Med. Biol.* **468,** 361–71 (1999).

354. Cornell-Bell, A. H., Finkbeiner, S. M., Cooper, M. S. & Smith, S. J. Glutamate induces calcium waves in cultured astrocytes: long-range glial signaling. *Science* **247,** 470–3 (1990).

355. Scemes, E. & Giaume, C. Astrocyte CalciumWaves: What They Are and What They Do. *Glia* **54,** 716–725 (2006).

356. Bazargani, N. & Attwell, D. Astrocyte calcium signaling: the third wave. *Nat. Neurosci.* **19,** 182–189 (2016).

357. Arcuino, G. *et al.* Intercellular calcium signaling mediated by point-source burst release of ATP. *Proc. Natl. Acad. Sci. U. S. A.* **99,** 9840–5 (2002).

358. Boulay, A.-C. *et al.* Immune Quiescence of the Brain Is Set by Astroglial Connexin 43. *J. Neurosci.* **35,** 4427–4439 (2015).

359. De Bock, M., Leybaert, L. & Giaume, C. Connexin Channels at the Glio-Vascular Interface: Gatekeepers of the Brain. *Neurochem. Res.* **42,** 2519–2536 (2017).

360. Ezan, P. *et al.* Deletion of astroglial connexins weakens the blood-brain barrier. *J. Cereb. Blood Flow Metab.* **32,** 1457–1467 (2012).

361. Boulay, A.-C. *et al.* The Sarcoglycan complex is expressed in the cerebrovascular system and is specifically regulated by astroglial Cx30 channels. *Front. Cell. Neurosci.* **9,** 1–9 (2015).

362. Fushiki, S. *et al.* Changes in neuronal migration in neocortex of connexin43 null mutant mice. *J. Neuropathol. Exp. Neurol.* **62,** 304–14 (2003).

363. Elias, L. A. B., Wang, D. D. & Kriegstein, A. R. Gap junction adhesion is necessary for radial migration in the neocortex. *Nature* **448,** 901–907 (2007).

364. Matsuuchi, L. & Naus, C. C. Gap junction proteins on the move: Connexins, the cytoskeleton and migration. *Biochim. Biophys. Acta - Biomembr.* **1828,** 94–108 (2013).

365. Kameritsch, P., Pogoda, K. & Pohl, U. Channel-independent influence of connexin 43 on cell migration. *Biochim. Biophys. Acta - Biomembr.* **1818,** 1993–2001 (2012).

366. Tabernero, A., Jiménez, C., Velasco, A., Giaume, C. & Medina, J. M. The enhancement of glucose uptake caused by the collapse of gap junction communication is due to an increase in astrocyte proliferation. *J. Neurochem.* **78,** 890–898 (2001).

367. Naus, C. C. *et al.* Altered gap junctional communication, intercellular signaling, and growth in cultured astrocytes deficient in connexin 43. *J. Neurosci. Res.* **49,** 528–540 (1997).

368. Nagy, J. I., Li, W., Hertzberg, E. L. & Marotta, C. A. Elevated connexin43 immunoreactivity at sites of amyloid plaques in Alzheimer's disease. *Brain Res.* **717,** 173–8 (1996).

369. Yi, C. *et al.* Astroglial connexin43 contributes to neuronal suffering in a mouse model of Alzheimer's disease. *Cell Death Differ.* **23,** 1691–701 (2016).

370. Vis, J. C. *et al.* Connexin expression in Huntington's diseased human brain. *Cell Biol. Int.* **22,** 837–47 (1998).

371. Rufer, M. *et al.* Regulation of connexin-43, GFAP, and FGF-2 is not accompanied by changes in astroglial coupling in MPTP-lesioned, FGF-2-treated parkinsonian mice. *J. Neurosci. Res.* **46,** 606–17 (1996).

372. Kawasaki, A. *et al.* Modulation of connexin 43 in rotenone-induced model of Parkinson's disease. *Neuroscience* **160,** 61–8 (2009).

373. Brand-Schieber, E. *et al.* Connexin43, the major gap junction protein of astrocytes, is down-regulated in inflamed white matter in an animal model of multiple sclerosis. *J. Neurosci. Res.* **80,** 798–808 (2005).

374. Masaki, K. *et al.* Connexin 43 Astrocytopathy Linked to Rapidly Progressive Multiple Sclerosis and Neuromyelitis Optica. *PLoS One* **8,** e72919 (2013).

375. Naus, C. C., Elisevich, K., Zhu, D., Belliveau, D. J. & Del Maestro, R. F. In vivo growth of C6 glioma cells transfected with connexin43 cDNA. *Cancer Res.* **52,** 4208–4213 (1992).

376. Soroceanu, L., Manning, T. J. & Sontheimer, H. Reduced expression of connexin-43 and functional gap junction coupling in human gliomas. *Glia* **33,** 107–117 (2001).

377. Caltabiano, R., Torrisi, A., Condorelli, D., Albanese, V. & Lanzafame, S. High levels of connexin 43 mRNA in high grade astrocytomas. Study of 32 cases with in situ hybridization. *Acta Histochem.* **112,** 529–535 (2010).

378. Pu, P., Xia, Z., Yu, S. & Huang, Q. Altered expression of Cx43 in astrocytic tumors. *Clin. Neurol. Neurosurg.* **107,** 49–54 (2004).

379. Sin, W. C. *et al.* Astrocytes promote glioma invasion via the gap junction protein connexin43. *Oncogene* **35,** 1–13 (2015).

380. Sin, W. C., Crespin, S. & Mesnil, M. Opposing roles of connexin43 in glioma progression. *Biochim. Biophys. Acta - Biomembr.* **1818,** 2058–2067 (2012).

381. Herrero-González, S. *et al.* Connexin43 inhibits the oncogenic activity of c-Src in C6 glioma cells. *Oncogene* **29,** 5712–5723 (2010).

382. Hong, X., Chey Sin, W., Harris, A. L. & Naus, C. C. Gap junctions modulate

glioma invasion by direct transfer of microRNA. *Oncotarget* **6,** 15566–15577 (2015).

383. Friedl, P. & Mayor, R. Tuning Collective Cell Migration by Cell – Cell Junction Regulation. *Cold Spring Harb. Perspect. Biol.* 1–18 (2017). doi:10.1101/cshperspect.a029199

384. Aman, A. & Piotrowski, T. Wnt/β-Catenin and Fgf Signaling Control Collective Cell Migration by Restricting Chemokine Receptor Expression. *Dev. Cell* **15,** 749–761 (2008).

385. Aftab, Q., Sin, W.-C. & Naus, C. C. Reduction in gap junction intercellular communication promotes glioma migration. *Oncotarget* **6,** 11447–11464 (2015).

386. De Pascalis, C. & Etienne-Manneville, S. Single and collective cell migration: the mechanics of adhesions. *Mol. Biol. Cell* **28,** 1833–1846 (2017).

387. Oliveira, R. *et al.* Contribution of gap junctional communication between tumor cells and astroglia to the invasion of the brain parenchyma by human glioblastomas. *BMC Cell Biol.* **6,** 1–17 (2005).

388. Lin, J. H. C. *et al.* Connexin 43 enhances the adhesivity and mediates the invasion of malignant glioma cells. *J. Neurosci.* **22,** 4302–4311 (2002).

389. Crespin, S., Bechberger, J., Mesnil, M., Naus, C. C. & Sin, W. C. The carboxy-terminal tail of connexin43 gap junction protein is sufficient to mediate cytoskeleton changes in human glioma cells. *J. Cell. Biochem.* **110,** 589–597 (2010).

390. Contreras, J. E. *et al.* Role of connexin-based gap junction channels and hemichannels in ischemia-induced cell death in nervous tissue. *Brain Res. Rev.* **47,** 290–303 (2004).

391. Gielen, P. R. *et al.* Connexin43 confers Temozolomide resistance in human glioma cells by modulating the mitochondrial apoptosis pathway. *Neuropharmacology* **75,** 539–548 (2013).

392. Murphy, S. F. *et al.* Connexin 43 inhibition sensitizes chemoresistant glioblastoma cells to temozolomide. *Cancer Res.* **76,** 139–149 (2016).

393. Goldberg, G. S., Valiunas, V. & Brink, P. R. Selective permeability of gap junction channels. *Biochim. Biophys. Acta - Biomembr.* **1662,** 96–101 (2004).

394. Crespin, S. *et al.* Expression of a gap junction protein, connexin43, in a large panel of human gliomas: new insights. *Cancer Med.* **5,** 1742–1752 (2016).

395. Baklaushev, V. P. *et al.* Visualization of Connexin 43-positive cells of glioma and the periglioma zone by means of intravenously injected monoclonal antibodies. *Drug Deliv.* **18,** 331–337 (2011).

396. Mahabaleshwar, H., Tarbashevich, K., Nowak, M., Brand, M. & Raz, E. B-Arrestin Control of Late Endosomal Sorting Facilitates Decoy Receptor Function and Chemokine Gradient Formation. *Development* **139,** 2897–2902 (2012).

397. Hattermann, K. *et al.* The chemokine receptor CXCR7 is highly expressed in human glioma cells and mediates antiapoptotic effects. *Cancer Res.* **70,**

3299–3308 (2010).

398. Kant, S., Holthöfer, B., Magin, T. M., Krusche, C. A. & Leube, R. E. Desmoglein 2-Dependent Arrhythmogenic Cardiomyopathy Is Caused by a Loss of Adhesive Function. *Circ. Cardiovasc. Genet.* **8,** 553–563 (2015).

399. Su, V., Nakagawa, R., Koval, M. & Lau, A. F. Ubiquitin-independent proteasomal degradation of endoplasmic reticulum-localized connexin43 mediated by CIP75. *J. Biol. Chem.* **285,** 40979–40990 (2010).

400. Polusani, S. R., Kar, R., Riquelme, M. A., Masters, B. S. & Panda, S. P. Regulation of gap junction function and Connexin 43 expression by cytochrome P450 oxidoreductase (CYPOR). *Biochem. Biophys. Res. Commun.* **411,** 490–495 (2011).

401. Denuc, A. *et al.* New protein-protein interactions of mitochondrial connexin 43 in mouse heart. *J. Cell. Mol. Med.* **20,** 794–803 (2016).

402. Sánchez-Alcañiz, J. A. *et al.* Cxcr7 Controls Neuronal Migration by Regulating Chemokine Responsiveness. *Neuron* **69,** 77–90 (2011).

403. Theis, M., Söhl, G., Speidel, D., Kühn, R. & Willecke, K. Connexin43 is not expressed in principal cells of mouse cortex and hippocampus. *Eur. J. Neurosci.* **18,** 267–74 (2003).

404. Banisadr, G., Podojil, J. R., Miller, S. D. & Miller, R. J. Pattern of CXCR7 Gene Expression in Mouse Brain Under Normal and Inflammatory Conditions. *J. Neuroimmune Pharmacol.* **11,** 26–35 (2016).

405. Freitas, A. S. *et al.* Dye coupling and connexin expression by cortical radial glia in the early postnatal subventricular zone. *Dev. Neurobiol.* **72,** 1482–1497 (2012).

406. Dermietzel, R., Hertberg, E. L., Kessler, J. A. & Spray, D. C. Gap junctions between cultured astrocytes: immunocytochemical, molecular, and electrophysiological analysis. *J. Neurosci.* **11,** 1421–1432 (1991).

407. Jeanson, T. *et al.* Antidepressants Impact Connexin 43 Channel Functions in Astrocytes. *Front. Cell. Neurosci.* **9,** 1–9 (2016).

408. Lachmanovich, E. *et al.* Co-localization analysis of complex formation among membrane proteins by computerized fluorescence microscopy: application to immunofluorescence co-patching studies. *J. Microsc.* **212,** 122–31 (2003).

409. Costes, S. V *et al.* Automatic and quantitative measurement of protein-protein colocalization in live cells. *Biophys. J.* **86,** 3993–4003 (2004).

410. Levoye, A. *et al.* A broad G protein-coupled receptor internalisation assay that combines SNAP-tag labeling, diffusion-enhanced resonance energy transfer, and a highly emissive terbium cryptate. *Front. Endocrinol. (Lausanne).* **6,** 167 (2015).

411. Reiser, K. *et al.* Thioredoxin-1 and protein disulfide isomerase catalyze the reduction of similar disulfides in HIV gp120. *Int. J. Biochem. Cell Biol.* **44,** 556–62 (2012).

412. Auwerx, J. *et al.* Human glutaredoxin-1 catalyzes the reduction of HIV-1 gp120 and CD4 disulfides and its inhibition reduces HIV-1 replication. *Int. J. Biochem.*

Cell Biol. **41,** 1269–75 (2009).

413. Yuan, Y., Kan, H., Fang, Q., Chen, F. & Finkel, M. S. CXCR4 receptor antagonist blocks cardiac myocyte p38 MAP kinase phosphorylation by HIV gp120. *Cardiovasc. Toxicol.* **8,** 173–80 (2008).

414. Soding, J. Protein homology detection by HMM-HMM comparison. *Bioinformatics* **21,** 951–960 (2005).

415. Boudot, A. *et al.* COUP-TFI modifies CXCL12 and CXCR4 expression by activating EGF signaling and stimulates breast cancer cell migration. *BMC Cancer* **14,** 407 (2014).

416. Luo, Y. *et al.* HIV-host interactome revealed directly from infected cells. *Nat. Microbiol.* **1,** 16068 (2016).

417. Lu, Q., Sun, E. E., Klein, R. S. & Flanagan, J. G. Ephrin-B reverse signaling is mediated by a novel PDZ-RGS protein and selectively inhibits G protein-coupled chemoattraction. *Cell* **105,** 69–79 (2001).

418. Salvucci, O., Basik, M., Bouchard, A., Bianchi, R. & Tosato, G. *Crosstalk between the CXCR4/SDF1 axis and Ephrin B2/ephrin B1 receptors in human endothelial cells*. *Cancer Research* **65,** (Waverly Press, 2005).

419. Kiyotsugu, Y. *et al.* Correction for Yi et al., Quantitative phosphoproteomic analysis reveals system-wide signaling pathways downstream of SDF-1/CXCR4 in breast cancer stem cells. *Proc. Natl. Acad. Sci.* **111,** 11223–11223 (2014).

420. Park, J. M. *et al.* Exogenous CXCL12 activates protein kinase C to phosphorylate connexin 43 for gap junctional intercellular communication among confluent breast cancer cells. *Cancer Lett.* **331,** 84–91 (2013).

421. Schajnovitz, A. *et al.* CXCL12 secretion by bone marrow stromal cells is dependent on cell contact and mediated by connexin-43 and connexin-45 gap junctions. *Nat. Immunol.* **12,** 391–398 (2011).

422. Chalovich, J. M. & Eisenberg, E. The connexin43-dependent transcriptome during brain development: Importance of genetic background. *Biophys. Chem.* **257,** 2432–2437 (2005).

423. Errede, M. *et al.* The contribution of CXCL12-expressing radial glia cells to neuro-vascular patterning during human cerebral cortex development. *Front. Neurosci.* **8,** 324 (2014).

424. Zhang, H., Teng, X., Liu, Z., Zhang, L. & Liu, Z. Gene expression profile analyze the molecular mechanism of CXCR7 regulating papillary thyroid carcinoma growth and metastasis. *J Exp Clin Cancer Res* **34,** 16 (2015).

425. Heise, C. E. *et al.* Pharmacological characterization of CXC chemokine receptor 3 ligands and a small molecule antagonist. *J. Pharmacol. Exp. Ther.* **313,** 1263–71 (2005).

426. Kalatskaya, I. *et al.* AMD3100 is a CXCR7 ligand with allosteric agonist properties. *Mol. Pharmacol.* **75,** 1240–1247 (2009).

427. Seifert, R. & Wenzel-Seifert, K. Constitutive activity of G-protein-coupled receptors: cause of disease and common property of wild-type receptors.

Naunyn. Schmiedebergs. Arch. Pharmacol. **366,** 381–416 (2002).

428. Lesueur, P. *et al.* Radiosensitization Effect of Talazoparib, a Parp Inhibitor, on Glioblastoma Stem Cells Exposed to Low and High Linear Energy Transfer Radiation. *Sci. Rep.* **8,** 3664 (2018).

429. El-Habr, E. A. *et al.* A driver role for GABA metabolism in controlling stem and proliferative cell state through GHB production in glioma. *Acta Neuropathol.* **133,** 645–660 (2017).

430. Assad Kahn, S. *et al.* The anti-hypertensive drug prazosin inhibits glioblastoma growth via the PKCδ-dependent inhibition of the AKT pathway. *EMBO Mol. Med.* **8,** 511–26 (2016).

431. Thouvenot, E. *et al.* Enhanced Detection of CNS Cell Secretome in Plasma Protein-Depleted Cerebrospinal Fluid. *J. Proteome Res.* **7,** 4409–4421 (2008).

432. Olsen, J. V. *et al.* Parts per Million Mass Accuracy on an Orbitrap Mass Spectrometer via Lock Mass Injection into a C-trap. *Mol. Cell. Proteomics* **4,** 2010–2021 (2005).

433. Cox, J. & Mann, M. MaxQuant enables high peptide identification rates, individualized p.p.b.-range mass accuracies and proteome-wide protein quantification. *Nat. Biotechnol.* **26,** 1367–72 (2008).

434. Cox, J. *et al.* Andromeda: A peptide search engine integrated into the MaxQuant environment. *J. Proteome Res.* **10,** 1794–1805 (2011).

435. Tyanova, S. *et al.* The Perseus computational platform for comprehensive analysis of (prote)omics data. *Nat. Methods* **13,** 731–40 (2016).

436. Tusher, V. G., Tibshirani, R. & Chu, G. Significance analysis of microarrays applied to the ionizing radiation response. *Proc. Natl. Acad. Sci.* **98,** 5116–5121 (2001).

437. Martin, A. O., Mathieu, M.-N. & Guérineau, N. C. Evidence for long-lasting cholinergic control of gap junctional communication between adrenal chromaffin cells. *J. Neurosci.* **23,** 3669–78 (2003).

438. Leithe, E., Mesnil, M. & Aasen, T. The connexin 43 C-terminus: A tail of many tales. *Biochim. Biophys. Acta - Biomembr.* **1860,** 48–64 (2018).

439. Balla, A. *et al.* Demonstration of angiotensin II-induced Ras activation in the trans-Golgi network and endoplasmic reticulum using bioluminescence resonance energy transfer-based biosensors. *J. Biol. Chem.* **286,** 5319–27 (2011).

ANNEX

CXCR4/ACKR3 phosphorylation and recruitment of interacting proteins: key mechanisms regulating their functional status

Amos FUMAGALLI[1], Aurélien ZARCA[2*], Maria NEVES[3*], Birgit CASPAR[4], Stephen Hill[4], Federico Mayor[3], Martine Smit[2], Philippe Marin[1]

[1] IGF, Université de Montpellier, CNRS, INSERM, Montpellier, France.

[2] Amsterdam Institute for Molecules, Medicines and Systems (AIMMS), Division of Medicinal Chemistry, Faculty of Science, Vrije Universiteit Amsterdam, De Boelelaan 1108, 1081 HZ Amsterdam, The Netherlands

[3] Departamento de Biología Molecular and Centro de Biología Molecular “Severo Ochoa” (UAM-CSIC), 28049 Madrid, Spain.

[4] Division of Physiology, Pharmacology and Neuroscience, School of Life Sciences, University of Nottingham, Nottingham NG7 2UH, UK; Centre of Membrane Proteins and Receptors, University of Birmingham and University of Nottingham, The Midlands, UK

* Both authors contributed equally to this work.

a) Running title:
Phosphorylation/interactome regulate CXCR4/ACKR3 functions
b) Corresponding author:

Amos FUMAGALLI

141, rue de la Cardonille

34094 Montpellier Cedex 5

France

Tel: +33 434 35 92 06

Fax: +33 467 54 24 32

amos.fumagalli@igf.cnrs.fr

c) **Number of text pages:** 18
Number of figures: 4
Number of tables: 2
Number of references: 118
Number of words abstract: 187
Number of words introduction: 273
Number of words discussion: 5407

d) List of nonstandard abbreviations:
ACACA, acetyl-CoA carboxylase 1

ACKR3, atypical chemokine receptor 3

AIP4, E3 ubiquitin ligase atrophin Interacting protein 4;

AMFR, E3 ubiquitin-protein ligase AMFR

AP-MS, affinity purification coupled with mass spectrometry

ARIH1, E3 ubiquitin-protein ligase ARIH1

AUP1, ancient ubiquitous protein 1

BiFC, bimolecular fluorescent complementation assay

BioID, proximity-dependent biotin identification

BIRC6, baculoviral IAP repeat-containing protein 6

BRET, bioluminescence resonance energy transfer

CD164, endolyn

CH2K, checkpoint kinase 2

CHEK2, Serine/threonine-protein kinase Chk2

Co-IP, co-immunoprecipitation

CXCL12, C-X-C motif chemokine 12

CXCR4, C-X-C motif chemokine receptor 4

EFNB1, ephrin-B1

EGF, epidermal growth factor

EGFR, epidermal growth factor receptor

ERK, extracellular signal–regulated kinases

ETFA, electron transfer flavoprotein subunit alpha

ETFB, electron transfer flavoprotein subunit beta

FRET, fluorescence resonance energy transfer

GET4, Golgi to ER traffic protein 4 homolog

GIP, G protein-coupled receptor interacting protein

GLRX3, glutaredoxin-3

GNAI, guanine nucleotide-binding protein G(i) subunit alpha-1

GOLT1B, vesicle transport protein GOT1B

GPCR, G protein-coupled receptor

GRK, G protein-coupled receptor kinase

HA, hemagglutinin

HEK293, human embryonic kidney 293 cells

Herg, heregulin

HM13, minor histocompatibility antigen H13

HUWE1, E3 ubiquitin-protein ligase HUWE1

iBAQ, intensity-based absolute quantification

IP, immunoprecipitation

KCNK1, potassium channel subfamily K member 1

KISS, kinase substrate sensor

LC-MS/MS, liquid chromatography coupled to tandem mass spectrometry

LYN, tyrosine-protein kinase Lyn

MaMTH, mammalian membrane two-hybrid assay

MAP2K2, dual specificity mitogen-activated protein kinase kinase 2

mDIA2, diaphanous-related formin-2

MIF, macrophage migration inhibitory factor

MYBL2, myb-related protein B

MYTH, membrane yeast two-hybrid assay

NMMHC, motor protein non-muscle myosin H chain

NR2F2, COUP transcription factor 2

PECAM-1, platelet endothelial cell adhesion molecule

PI3Kγ, PI3-kinase isoform p110γ

PKC, protein kinase C

PLA, proximity ligation assay

POLD1, DNA polymerase delta catalytic subunit

PPP6R1, protein phosphatase 6 regulatory subunit 1

RIC-8A, guanine nucleotide exchange factor synembryn-A

RNF5, E3 ubiquitin-protein ligase RNF5

RTN3, reticulon-3

STAT, signal transducer and activator of transcription

TLR2, toll-like receptor 2

TMEM63B, CSC1-like protein 2

UBE2K, ubiquitin-conjugating enzyme E2 K

WHIM, warts, hypogammaglobulinemia, infections, and myelokathexis

Y2H, yeast two-hybrid assay

Abstract.

The C-X-C chemokine receptor type 4 CXCR4 and the atypical chemokine receptor 3 (ACKR3/CXCR7) are class A G protein-coupled receptors (GPCRs). Accumulating evidence indicates that GPCR sub-cellular localization, trafficking, transduction properties and, ultimately, their pathophysiological functions are regulated by both interacting proteins and post translational modifications. This has encouraged the development of novel techniques to characterize the GPCR interactome and to identify residues subjected to post-transitional modifications, with a special focus on phosphorylation. This review first describes state-of-art methods for the identification of GPCR-interacting proteins and GPCR phosphorylated sites. In addition, we provide an overview of the current knowledge of CXCR4 and ACKR3 post-translational modifications and their consequences upon receptor functional status and an exhaustive list of previously identified CXCR4 or ACKR3 interacting proteins. Finally, we present an original dataset comprising a CXCR4 interactome deciphered using an affinity purification coupled to mass spectrometry strategy, which revealed novel CXCR4 interacting proteins potentially involved in oncogenic signalling. A deeper knowledge of the CXCR4/ACKR3 interactomes along with their phosphorylation and ubiquitination status would shed new lights on their regulation and pathophysiological functions.

Visual abstract:

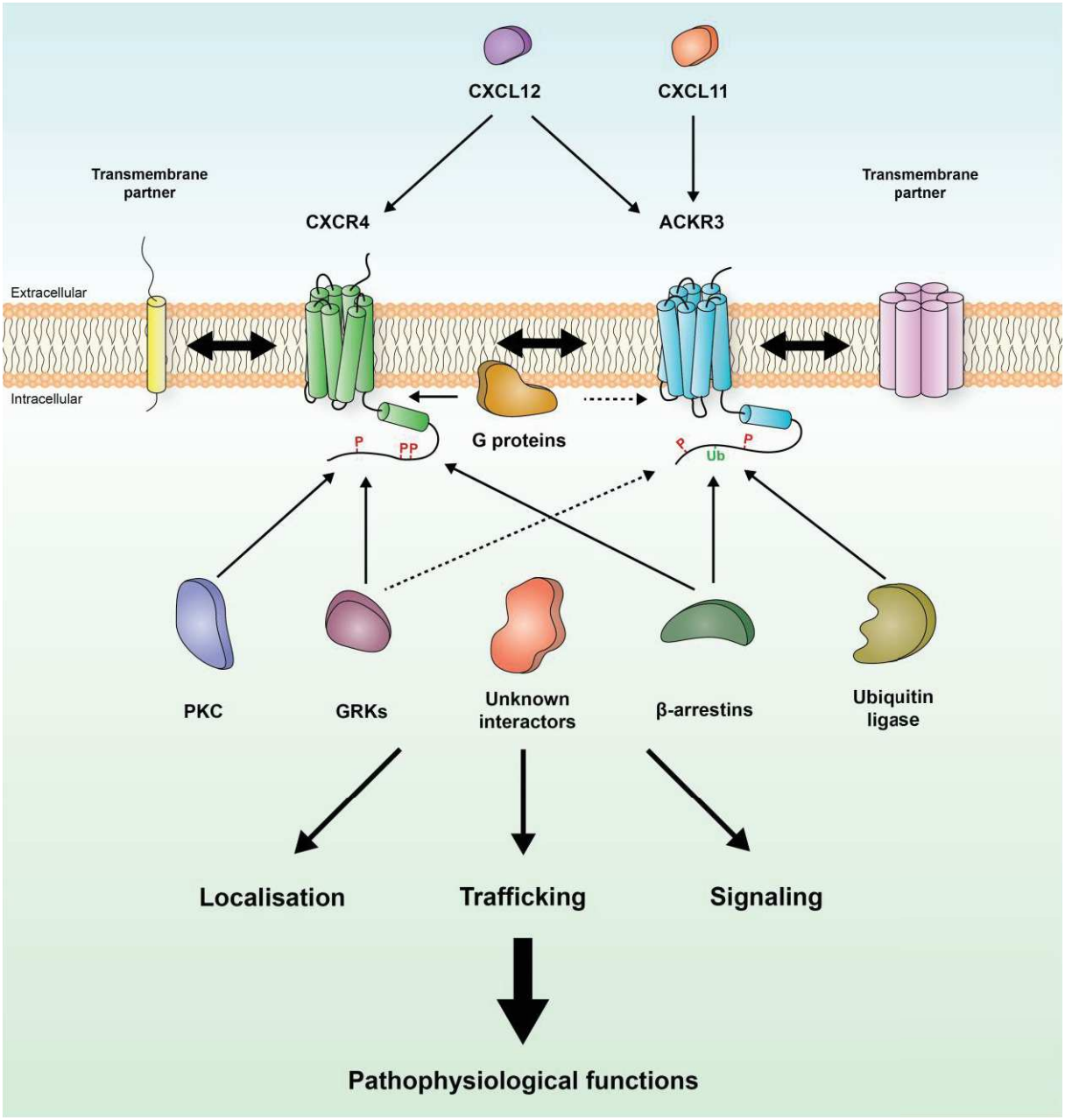

Introduction

The C-X-C chemokine receptor type 4 (CXCR4) and the atypical chemokine receptor 3 (ACKR3), earlier referred to as CXCR7, are class A G protein-coupled receptors (GPCRs). Stromal cell-derived factor-1/ C-X-C motif chemokine 12 (CXCL12) binds to both CXCR4 and ACKR3 receptors, whereas CXCL11 binds only to the latter and the C-X-C chemokine receptor type 3. CXCR4 and ACKR3 are co-expressed in various cell types (e.g. endothelial cells (Volin., 1998; Berahovich, 2014), neurons (Banisadr, 2002; Sánchez-Alcañiz, 2011) and glial cells (Banisadr, 2002, 2016; Odemis, 2010)) where they play a pivotal role in migration, proliferation and differentiation. They are also over-expressed in various tumours and control invasion and metastasis (Sun, 2010; Zhao, 2015; Nazari, 2017). There is now considerable evidence indicating that GPCRs do not operate as isolated proteins within the plasma membrane. Instead, they physically interact with numerous proteins that influence their activity, trafficking, and signal transduction properties (Bockaert, 2004; Ritter and Hall, 2009; Magalhaes, 2012). These include proteins canonically associated with most GPCRs such as G proteins, G protein-coupled receptor kinases (GRKs) and β-arrestins, specific partner proteins and even GPCRs themselves. In fact, in comparison to monomers, GPCRs can form homo and heteromers with specific pharmacological and signal transduction properties (Ferré, 2014). Phosphorylation is another key mechanism contributing to the regulation of GPCR functional activity (Tobin, 2008). Again, GPCR phosphorylation can be elicited by canonical GRKs but also by other specific protein kinases (Luo, 2017). This review will describe recent data highlighting the influence of the CXCR4 and ACKR3 interactome on their functional activity and signal transduction properties. A special focus will be paid to the influence of the interactome on CXCR4/ACKR3 phosphorylation and ubiquitination and their impact on the functional status of each receptor.

Methods for the identification of GPCR-interacting proteins

Considerable evidence suggests that GPCRs recruit GPCR-interacting proteins (GIPs) (Maurice, 2011). This prompted investigations aimed at identifying GIPs and at characterising GPCR-GIP interactions, using either unbiased or targeted approaches. In unbiased methods, no knowledge of the GIPs is required beforehand and the GPCR of interest is used as bait to purify unknown GIPs. Meanwhile, targeted methods are devoted to the validation and characterisation of previously identified GPCR-GIP interactions. Methods for identifying GIPs or characterising GPCR-GIP interactions include genetic, biophysical or proteomic approaches and are summarised in **Table 1**.

a) Genetic methods

The first method belonging to this class is the yeast two-hybrid assay (Fields and Song, 1989). In this method, the protein of interest (the bait protein) is expressed in yeast as a fusion to the DNA-binding domain of a transcription factor lacking the transcription activation domain. To identify partners of this bait, a plasmid library that expresses cDNA-encoded proteins fused to a transcription activation domain is introduced into the yeast strain. Interaction of a cDNA-encoded protein with the bait protein results in the activation of the transcription factor and expression of a reporter gene, enabling growth on specific media or a colour reaction and the identification of the cDNA encoding the target proteins. A first disadvantage is the loss of spatial-temporal localisation of the interaction; in fact, the yeast two-hybrid assay only captures a snapshot of potential interactions in an artificial biological system. A second disadvantage is that it is not possible to investigate membrane-anchored proteins since the two proteins must cross the nuclear membrane to carry the reconstituted transcription factor to the DNA. To overcome this issue, the membrane yeast two-hybrid assay (Stagljar, 1998) was developed. In this assay, the ubiquitin protein is split into two fragments, which are fused to the two proteins of interest. The ubiquitin C-terminal fragment is then conjugated to a transcription factor that is released when the interaction occurs, and ubiquitin protein is reformed. However, as in the yeast two-hybrid assay, the spatial-temporal localisation of the interaction is lost. A second limitation is that the ubiquitin C-terminus carrying the transcription factor cannot be fused to soluble proteins because they could diffuse into the nucleus. Thereafter, a mammalian version of the assay called mammalian membrane two-hybrid (Petschnigg, 2014) has been developed. The kinase substrate sensor assay (Lievens, 2014), using the signal transducer and activator of transcription (STAT)3 as transcription factor, can also be used for investigating protein-protein interactions including those involving cytosolic and membrane proteins in mammalian cells. However, the kinase substrate sensor assay cannot be used for studying GPCR interaction with proteins involved in the STAT3 cascade.

b) Biophysical methods

Energy transfer-based methods, such as bioluminescence and fluorescent resonance energy transfer (BRET (Xu, 1999) and FRET (Clegg, 1995)) assays, are targeted methods that are generally used to investigate previously reported interactions. Both are based on the transfer of energy from a donor to a nearby acceptor (<100 Å). Their high sensitivity allows the study of weak and transient interactions. The high spatial-temporal resolution permits accurate kinetic studies for investigating interaction dynamics.

The proximity ligation assay (Fredriksson, 2002) is another powerful targeted fluorescence-based method. In the direct version of the technique, two DNA oligonucleotide-conjugated antibodies are used against the proteins of interest. In the indirect version, secondary DNA-conjugated antibodies are used after targeting the proteins of interest with an appropriate primary antibody. If the two conjugated antibodies are close enough (30-40nm), they can bind together. The DNA connecting the two probes is then amplified and hybridised with fluorophores. This allows the visualisation of the interaction in the place where it occurs, at a single molecule resolution. The main disadvantages of the approach are the high costs and the necessity for specific antibodies that are not always available.

In the bimolecular fluorescent complementation assay (Hu, 2002), a fluorescent protein is divided into two non-fluorescent fragments that are fused to the proteins of interest. Interaction reconstitutes the entire fluorescent protein. This method allows the direct visualisation of the interaction and can be used for soluble or membrane-bound proteins. In addition, several interactions can be investigated in parallel using different fluorescent proteins. Since there is a delay in fluorescence formation upon reconstitution of the fluorescent proteins, and the fluorophore formation is irreversible, these methods are not well suited for kinetic studies.

c) Proteomics methods

Proteomic methods aim at identifying GIPs of a receptor of interest *via* the use of affinity purification combined with mass spectrometry (AP-MS). This approach is usually employed as a unbiased method for screening virtually all the GIPs of a GPCR of interest. Targeted versions of the method also exist and rely on GIP identification by Western blotting. However, the requirement for specific antibodies seriously limits its application. Several strategies can be used for the affinity purification step. In co-immunoprecipitation (Co-IP), specific antibodies against the protein of interest are used for precipitating the bait from a protein lysate. As specific GPCR antibodies providing high immunoprecipitation (IP) yields are rarely available, epitope-tagged versions of the receptor of interest are often expressed in the cell type or the organism of interest and precipitated using antibodies against the tag. The main advantages of Co-IP are the purification of proteins interacting with the entire receptor (whenever possible the native receptor) in living cells or tissues and its ability to purify the entire associated protein complex. The main limitations are the necessity for specific antibodies to precipitate GPCRs, the loss of spatial-temporal information and the use of detergents for cell lysis that might disrupt weak interactions. Alternatively, pull-down assays can be performed to purify GPCR partners from a cell or tissue lysate. This approach uses the receptor (or one of its domains) fused with an affinity tag (e.g. glutathione S-

transferase) and immobilized on beads as bait. Such *in vitro* binding assays can also be used to prove direct physical interaction between two protein partners. In this case, the bait is incubated with a purified protein instead of a cell or tissue lysate. In all methods, affinity purified proteins are systematically identified by liquid chromatography coupled to tandem mass spectrometry (LC-MS/MS). A two-step version, named tandem affinity purification (Puig, 2001), has also been reported (Daulat, 2007) and applies to both Co-IPs or pull-downs. Although tandem affinity purification methods drastically reduce the number of false-positive identifications, they require larger amounts of starting material.

In the proximity-dependent biotin identification method (Roux, 2013), the bait protein is fused to a prokaryotic biotin ligase molecule that biotinylates proteins in close proximity once expressed in cells. The method can detect weak and transient interactions occurring in living cells and detergents do not affect the results. However, the fusion of biotin ligase to the bait might alter its targeting or functions.

Methods for the identification of GPCR phosphorylated sites

GPCR phosphorylation is a key regulatory mechanism of receptor function (Lefkowitz, 2004). Over the past years, numerous techniques have appeared with increasing resolution to pinpoint phosphorylated residues (summarized in Table 1), which consist of serines, threonines or tyrosines.

a) Radioactive labelling method

The first method that was introduced for deciphering the phosphorylation status of GPCRs is a radioactivity-based technique, consisting of culturing cells in a medium in which phosphate is replaced with its radioactive counterpart ^{32}P, resulting in radioactive phosphorylated residues (Meisenhelder, 2001). After culturing, cells are lysed and receptors are immunoprecipitated using specific antibodies and then resolved by SDS-polyacrylamide gel electrophoresis. Receptors are then digested using an enzyme, such as trypsin, and the resulting peptides are separated by 2D migration using electrophoresis and chromatography. The radioactivity of the digested peptides in the gel is finally measured using a phosphorimager yielding a phosphorylation map for a given receptor in a given cell line (Chen, 2013). This method is very sensitive but cannot give information on the number of phosphorylated sites nor their position.

b) Liquid chromatography coupled to tandem mass spectrometry method

More recently, radioactive labelling-based methods have been progressively supplanted by the identification of phosphorylated residues by LC-MS/MS. In this method, the GPCR of interested is digested enzymatically, using one or several proteases, to generate peptides that cover a large part of the receptor sequence. The resulting peptides are then analysed by LC-MS/MS (Dephoure, 2013). Although this approach can pinpoint any phosphorylated residue with high confidence, few limitations complicate phosphorylated residue identification. Firstly, phosphorylation can be lost during fragmentation. Secondly, since phosphorylation sites have a limited level of phosphorylation, only a small percentage of peptide is actually phosphorylated (Wu, 2011). Thirdly, the identification of the phosphorylated residues in peptides with multiple adjacent phosphorylated residues can be challenging. For each modified site, a phosphorylation index can be estimated by dividing the ion signal intensity corresponding to the phosphorylated peptide by the sum of the ion signals of the phosphorylated peptide and its non-phosphorylated counterpart. Absolute quantification, and thus the stoichiometry of phosphorylation, can also be determined for each modified residue by spiking the sample with a known concentration of high purity heavy isotope-labelled peptides (AQUA peptides) corresponding to the phosphorylated peptide and not phosphorylated one and comparing the respective ion signals of un-labelled and labelled peptides (Gerber, 2003).

c) Mutagenesis method

Another approach that can be used as a stand-alone technique or in complement with the previously described methods is to mutate potential or predicted phosphorylated residues to assess functional differences compared to the wild-type receptor. Mutating residues to alanine prevents phosphorylation (Canals, 2012) while mutating residues to aspartic acid mimics phosphorylation (Okamoto and Shikano, 2017). Nevertheless, introducing those mutations can potentially alter expression of the receptor, its conformation or its cellular localisation.

d) Phospho-specific antibody method

To be able to detect and assess phosphorylation of residues in cells or tissues, antibodies that specifically target previously identified phosphorylated residues of GPCRs can be generated by immunising animals with purified synthetic phosphorylated peptides encompassing the phosphorylated residues (Chen, 2013). After selection and functional validation, those antibodies can be used in Western blot or immunohistochemistry experiments. Phosphorylation can also be indirectly detected using antibodies specific to the unphosphorylated GPCR, showing decreased binding to the target when residues are

phosphorylated (Busillo, 2010), and recovery of the binding by using a protein phosphatase to dephosphorylate the receptor (Hoffmann, 2012).

Association of CXCR4 and ACKR3 with canonical GPCR interacting proteins

G proteins, GRKs and β□arrestins are the protein families considered as canonical GPCR interacting proteins controlling receptor activity or being involved in signal transduction. GPCR activity is a result of a tightly regulated balance between activation, desensitisation and re-sensitisation events. After receptor activation and interaction with G proteins, several mechanisms integrate to trigger GPCR desensitisation and/or modulate additional signalling cascades including phosphorylation by GRKs and recruitment of β-arrestins (Penela, 2010; Nogués, 2018).

a) G proteins

CXCR4 is known to couple to the *pertussis toxin* sensitive $G\alpha_i$ protein family that mediate most of its signalling pathways (Busillo and Benovic, 2007). The coupling of CXCR4 to other G proteins such as $G\alpha_{13}$ (Kumar, 2011) and $G\alpha_q$ (Soede, 2001) has been described but studied to a lesser extent.

As an atypical chemokine receptor, ACKR3 is missing the DRYLAIV (Asp-Arg-Tyr-Leu-Ala-Ile-Val) motif necessary for interaction with G proteins. Nevertheless, some reports have shown the interaction of the receptor with G proteins (Levoye, 2009; Ulvmar, 2011). ACKR3 was shown to form a heterodimer with CXCR4 in transfected cell lines (Levoye, 2009). Furthermore, the organisation of CXCR4 and ACKR3 in heterodimers appears to induce a down regulating effect on the CXCR4 interaction with G proteins, shifting the signalling to β-arrestin mediated pathways.

b) GRKs

Agonist-occupied GPCRs are specifically phosphorylated by different GRKs, a family of 7 serine/threonine kinases (Ribas., 2007; Petronila Penela, 2010). GRK 2, 3, 5 and 6 phosphorylate CXCR4 in the C-terminus, which contains 15 serine and 3 threonine residues that are potential phosphorylation sites (**Figure 1**). At least six of these residues were shown to be phosphorylated following receptor activation by CXCL12 (Busillo, 2010; Barker and Benovic, 2011; Mueller, 2013). In human embryonic kidney 293 cells (HEK293) cells, Ser^{321}, Ser^{324}, Ser^{325}, Ser^{330}, Ser^{339}, and two sites between Ser^{346} and Ser^{352} were shown to be phosphorylated in response to CXCL12 in the CXCR4 C-terminus using LC-MS/MS and

phosphosite-specific antibodies (Busillo, 2010). GRK6 is able to phosphorylate $Ser^{324/5}$, Ser^{339} and Ser^{330}, the latter with slower kinetics, whereas GRK2 and GRK3 phosphorylate residues between Ser^{346} and Ser^{352} (**Figure 2**) (Busillo, 2010), and specifically $Ser^{346/347}$ (Mueller, 2013). Interestingly, the latter study suggested a hierarchy in such phosphorylation events, since $Ser^{346/347}$ phosphorylation is achieved faster and is needed for the subsequent phosphorylation of $Ser^{338/339}$ and $Ser^{324/325}$. Notably, ligand washout resulted in rapid $Ser^{324/325}$ and $Ser^{338/339}$ de-phosphorylation, whereas $Ser^{346/347}$ residues did not exhibit major dephosphorylation during the 60-minute period studied (Mueller, 2013). Phosphorylation of CXCR4 by different GRKs can elicit several molecular responses, such as fluctuations in intracellular calcium concentration and extracellular signal–regulated kinases (ERK) 1 and 2 phosphorylation, leading to integrated cellular responses. In HEK293 cells, calcium mobilisation is negatively regulated by GRK2, GRK6, and β-arrestin2. On the other hand, GRK3 and 6 together with β-arrestins act as positive regulators of ERK1/2 (Busillo, 2010). Overall, these studies show non-overlapping roles of the different GRKs in the regulation of CXCR4 signalling. These differential roles may explain distinct cell type-dependent responses to CXCL12. However, what dictates the specific GRK subtype recruitment still needs to be investigated. Changes in the normal CXCR4 phosphorylation pattern as a result of receptor mutations or altered GRK activity can lead to abnormal receptor expression and/or responsiveness, promoting aberrant cell signalling and thus can contribute to several pathologies. Deletion of $Ser^{346/347}$ leads to a gain-of-CXCR4-function and decreases receptor internalisation and subsequent desensitisation, indicating that mutations in the far C-terminus affect CXCR4-mediated signalling (Mueller, 2013). In this regard, a subpopulation of patients affected by WHIM (warts, hypogammaglobulinemia, infections, and myelokathexis) syndrome, a rare primary immunodeficiency disease, display C-terminally truncated CXCR4, leading to refractoriness to desensitisation and enhanced signalling (Balabanian, 2005). On the contrary, increased CXCR4 phosphorylation at Ser^{339} is associated with poor survival in adults with B-acute lymphoblastic leukaemia and correlates with poor prognosis in acute myeloid leukaemia patients (Konoplev, 2011; Brault, 2014). Altered GRK expression/activity can also impair CXCR4 phosphorylation patterns. GRK3 suppression may contribute to abnormally sustained CXCR4 signalling in classical types of glioblastomas (Woerner, 2012), some WHIM patients (Balabanian, 2008) and in triple negative breast cancer, thus potentiating CXCR4-dependent migration, invasion and metastasis (Billard, 2016; Nogués, 2018). It is interesting to note that, although GRK2 and 3 share a high homology and are able to phosphorylate the same residues in CXCR4 in model cells, their function is not redundant. Whereas both CXCR4 and GRK2 levels are increased in breast cancer patients, GRK3 is decreased, suggesting a differential role for both GRKs in a cancer context (Billard, 2016; Nogués, 2018). In fact, deregulation of GRK2 potentiates several malignant features of

breast cancer cells, and its level positively correlates with tumour growth and increased metastasis occurrence (Nogués, 2016), but whether these roles involve changes in CXCR4 modulation is still under investigation. On the other hand, impaired chemotaxis of T and B cells towards CXCL12 is noted in the absence of GRK6, whilst GRK6 deficiency potentiates neutrophil chemotactic response to CXCL12 (Fong, 2002; Vroon, 2004), suggesting that the occurrence of highly cell-type specific mechanisms in the control of the CXCL12-CXCR4-GRK6 axis. Overall, these data indicate the complexity of CXCR4 modulation by GRKs and support the need for a better characterization of cell type or disease-specific CXCR4-GRKs interactions.

ACKR3 has lately been the focus of many studies, in particular because of its role in cancer progression and metastasis. However, the mechanisms underlying its regulation are still not well understood, although this receptor has been shown to interact with GRKs and arrestins and to associate with other partners. The C-terminus of ACKR3 contains five serine and four threonine residues that can potentially be phosphorylated (**Figure 2**). Contrary to CXCR4, little is known about their actual phosphorylation status during the activation of the receptor, as no mass spectrometry data is available to date and only few mutational studies have been conducted (Canals, 2012; Hoffmann, 2012). In fact, only one study conducted in astrocytes showed that ACKR3 is phosphorylated by GRK2, but not other GRKs, and that this phosphorylation is essential for subsequent ACKR3-operated activation of ERK1/2 and AKT pathways (Lipfert, 2013). This study suggests that ACKR3 is indeed phosphorylated by GRKs, but the isoform(s) involved and subsequent responses are likely cell type-dependent and remain to be investigated in detail.

c) Arrestins

GRK-modified GPCRs in turn recruit β-arrestins, an event that attenuates G protein-mediated signalling and promotes receptor internalisation (Smith and Rajagopal, 2016). Moreover, β-arrestins are scaffold proteins for several signalling mediators, thus eliciting additional GPCR signalling pathways (Shenoy and Lefkowitz, 2011; Peterson and Luttrell, 2017).

Since in HEK293 cells β-arrestin recruitment and association with CXCR4 seems to be driven by phosphorylation of the C-terminal residues, this long-term phosphorylation may be a key event in promoting the formation and maintenance of stable CXCR4/β-arrestin complexes (Oakley, 2000; Busillo, 2010; Mueller, 2013).

Upon activation by its cognate ligands CXCL11 and CXCL12, ACKR3 recruits β-arrestin-2 both *in vitro* (Rajagopal, 2010; Benredjem, 2016) and *in vivo* (Luker, 2009), a process leading to receptor internalisation (Canals *et al.*, 2012) and degradation of both ACKR3 and

receptor-bound chemokine (Hoffmann, 2012). Systematic mutation of C-terminal serine/threonine residues to alanine abolishes ligand-induced β-arrestin2 recruitment to ACKR3, as monitored by BRET (Canals, 2012), and decreases ACKR3 internalisation and subsequent degradation of radiolabelled CXCL12 in HEK293 cells (Hoffmann, 2012). Selective mutations of the two C-terminal serine/threonine clusters to alanine revealed differences in their functional properties. Mutating Ser^{335}, Thr^{338} and Thr^{341} (first cluster) or Ser^{350}, Thr^{352} and Ser^{355} (second cluster) to alanine decreased CXCL12 internalization only after a 5-min challenge but not following longer agonist receptor stimulation, but only mutation of the second cluster prevented CXCL12 degradation. In addition, ACKR3 appears to undergo ligand-independent internalisation to a much greater extent than CXCR4 (Ray, 2012), and residues 339–362 (the two serine/threonine clusters) are essential for this peculiar cell fate in HEK293 cells.

Association of CXCR4 with non-canonical GPCR interacting proteins

Functional interaction of CXCR4 with second messenger-dependent kinases and receptor tyrosine kinases

Accumulating evidence indicates that phosphorylation of CXCR4 by second messenger-dependent kinases such as protein kinase A and protein kinase C (PKC) (Lefkowitz, 1993; Ferguson, Barak,, 1996; Ferguson, Downey,, 1996; Krupnick and Benovic, 1998) as well as modulation by members of the receptor tyrosine kinase family (Woerner, 2005) participate in the regulation of CXCL12 signalling via CXCR4. CXCR4 is phosphorylated by PKC at $Ser^{324/5}$ upon CXCL12 stimulation (Busillo, 2010), and this kinase has also been involved in $Ser^{346/7}$ phosphorylation (Luo, 2017), although these results are not entirely consistent with a previous study using different PKC inhibitors (Mueller et al, 2013). In some glioblastoma cell types, CXCR4 is phosphorylated at Ser^{339} in response to the PKC activator Phorbol myristate acetate. This suggests that Ser^{339} is also a PKC phosphorylation site (Woerner, 2005; Busillo and Benovic, 2007), but the functional impact of such modifications remains to be fully established. Epidermal growth factor (EGF) through activation of its receptor can also promote CXCR4 phosphorylation at Ser^{339} in glioblastoma cells (Woerner, 2005), and both EGF and heregulin trigger $Ser^{324/325}$ and Ser^{330} phosphorylation in the breast cancer T47D cell line. Interestingly, in MCF7 breast cancer cells, heregulin also promotes CXCR4 phosphorylation on tyrosine residues via Epidermal Growth Factor Receptor (EGFR), leading to β□arrestin2 association with CXCR4 and downstream activation of the PRex1/Rac1 axis. However, it is still unclear whether the EGFR-CXCR4 functional interaction is direct or depends on other kinases (Sosa, 2010). In another breast cancer line, BT-474, CXCR4 is

phosphorylated on tyrosine residues in response to CXCL12, but specific residues or kinases responsible were not described (Sosa, 2010). The crosstalk between CXCR4 and EGFR remains an interesting avenue for future research, given the involvement of both receptors in cancer.

Physical interaction with non-canonical GPCR interacting proteins

Beside canonical GIPs, CXCR4 has been shown to interact with additional proteins that modulate CXCR4 trafficking, subcellular localisation and signalling and proteins whose functions are still unknown. CXCR4 interacting proteins, the methods used for the identification of these proteins, the site of their interaction in the receptor sequence and their functional impact are summarised in **Table 2**.

a) Proteins controlling CXCR4 localization or trafficking

Filamin A directly interacts with CXCR4 and stabilises the receptor at the plasma membrane by blocking its endocytosis (Gómez-Moutón, 2015). CXCR4 association with the E3 ubiquitin ligase atrophin interacting protein 4 (AIP4) has opposite consequences: ubiquitination of CXCR4 by AIP4 targets the receptor to multi-vesicular bodies, which is followed by receptor degradation. In addition, agonist treatment increases CXCR4/AIP4 interaction, as assessed by Co-IP and FRET experiments (Bhandari, 2009), indicating that this interaction is dynamically regulated by a receptor conformational state. Reticulon-3 is another CXCR4 interacting protein that promotes its translocation to the cytoplasm (Li, 2016).

b) Proteins modulating CXCR4 signalling and functions

CD74, a single-pass type II membrane protein that shares with CXCR4 the ability to bind to the macrophage migration inhibitory factor (MIF), was also shown to interact with CXCR4. The CXCR4/CD74 complex is involved in AKT activation (Schwartz, 2009). In fact, blocking either CXCR4 or CD74 inhibits MIF-induced AKT activation. Using FRET, an interaction between CXCR4 and the toll like receptor 2 was observed in human monocytes upon activation by Pg-fimbria (fimbriae produced by the major pathogen associated with periodontitis named *Porphyromonas gingivalis*). Analysis of a possible crosstalk between the two receptors showed that Pg-fimbria, directly binds to CXCR4 and inhibits toll like receptor 2-induced NF-κB activation by *P. gingivali* (Hajishengallis, 2008; Triantafilou, 2008). In Jurkat cells, CD164 co-precipitates with CXCR4 in the presence of CXCL12 presented on fibronectin (Forde, 2007). CXCR4-CD164 interaction participates in CXCL12-induced activation of AKT and protein kinase C zeta ***(***PKCζ***).*** In fact, the down-regulation of CD164 reduces the activation of both kinases measured upon exposure of Jurkat cells to CXCL12. CXCR4/CD164 interaction has been detected in additional cell

lines, such as primary human ovarian surface epithelial cells stably expressing CD164 (Huang, 2013).

The ability of CXCR4 to promote cell migration requires deep cytoskeletal rearrangements that can be modulated by CXCR4 interacting proteins. In Jurkat J77 cells, CXCR4 constitutively associates with drebrin (Pérez-Martínez, 2010), a protein known to bind to F-actin and stabilise actin filaments. Drebrin is also involved in CXCR4- and CD4-dependent HIV cellular penetration (Gordón-Alonso, 2013). CXCR4 interacts with diaphanous-related formin-2 (mDIA2). This interaction induces cytoskeletal rearrangements that lead to non-apoptotic blebbing. mDIA2-CXCR4 interaction is only detected during non-apoptotic amoeboid blebbing and is confined to non-apoptotic blebs upon CXCL12 stimulation (Wyse, 2017), suggesting a fine spatio-temporal regulation of the interaction. CXCR4 also constitutively associates with the motor protein non-muscle myosin H chain (NMMHC) *via* its C-terminus (Rey, 2002). The authors showed that NMMHC and CXCR4 are co-localised in the leading edge of migrating lymphocytes, suggesting that this association might have a role in lymphocyte migration. The PI3-kinase isoform p110γ co-precipitates with CXCR4 in CXCL12-stimulated human myeloid cells. This interaction contributes to receptor-operated integrin activation and chemotaxis of myeloid cells (Schmid, 2011). Finally, CXCR4 was found to be part of a junctional mechano-sensitive complex through its interaction with the platelet endothelial cell adhesion molecule (PECAM-1) (Dela Paz, 2014).

c) Proteins with unknown functions

Other potential CXCR4-interacting proteins have been identified using unbiased methods. These include the lysosomal protein ATP13A2 (Usenovic, 2012) and the nuclear protein Myb-related protein B that is involved in cell cycle progression (Wang, 2014). In a study aimed at characterising the human interactome by Co-IP of 1,125 GFP-tagged proteins and LC-MS/MS analysis, CXCR4 was found to co-precipitate with the potassium channel subfamily K member 1, the CSC1-like protein 2 and the vesicle transport protein GOT1B (Hein, 2015).

CXCR4-interacting proteins identified in HEK293 cells by AP-MS

To get a global overview of CXCR4 interacting proteins, we transiently expressed hemagglutinin (HA)-tagged CXCR4 in HEK293 cells, immunoprecipitated the receptor-associated complex with an agarose bead-conjugated anti-HA antibody and systematically identified co-immunoprecipitated proteins by LC-MS/MS. These studies identified 79 proteins that co-immunoprecipitate with the receptor and are not detected in control

immunoprecipitations performed from cells that do not express the epitope-tagged receptor (**Table 3**). Analysis of the relative abundance of proteins in immunoprecipitates using spectral count normalised to protein length and intensity-based absolute quantification (iBAQ) showed, as expected, that CXCR4 is the most abundant protein (**Figure 2**). Moreover, the classical transducer of CXCR4 signalling guanine nucleotide-binding protein G(i) subunit alpha-1 (GNAI1) (Roland, 2003) and its guanine nucleotide exchange factor synembryn-A (RIC-8A) (Thomas, 2008) are among the most abundant proteins identified in the CXCR4-associated complex. Consistent with these findings, "adenylate cyclase-modulating G-protein coupled receptor signalling pathway" and "c-AMP mediated signalling" are two biological processes statistically overrepresented in the CXCR4-associated complex (**Figure 3**). In line with the activation of MAP kinase (MAPK) by CXCR4 (Sun, 2002) and its role in oligodendrocyte progenitor differentiation (Patel, 2010), we also identified "activation MAPK activity", "regulation of MAPK activity" and "regulation of glial cell differentiation" as overrepresented biological processes. Identified CXCR4 partners also included glutaredoxin-3, an enzyme belonging to the protein disulphide isomerase family. Another disulphide isomerase, glutaredoxin-1, is known to reduce intramolecular disulphide bonds of HIV envelope glycoprotein gp120 during virus entry (Reiser, 2012). Since gp120 interacts with CXCR4, glutaredoxin enzymes could in turn indirectly interact with CXCR4 (Yuan, 2008; Auwerx, 2009). CXCR4 also recruited COUP-transcription factor 1 and 2, two orphan nuclear receptors that play a critical role in organogenesis. Overexpression of COUP-transcription factor 1 in breast cancer cells inhibits expression of both CXCR4 and its endogenous ligand CXCL12 through EGFR activation (Boudot, 2014). Ephrin B1, a cell surface anchored ligand for ephrin B receptors likewise co-immunoprecipitated with CXCR4. Binding of ephrin B1 to its receptor triggers both a forward (in the cell expressing the ephrin receptor) and a reverse (in the cell expressing ephrin) signalling cascade in two adjacent cells. Ephrin B1 inhibits, in its reverse signalling, G protein activation elicited by CXCR4 upon activation by CXCL12 (Lu, 2001) and influences chemotaxis of Human umbilical vein endothelial cell (Salvucci, 2005).

The CXCR4 interactome also includes several protein kinases. These include 1) Lyn, a Src family tyrosine kinase involved in activation of immune cells (Xu, 2005). Lyn autophosphorylation is increased by CXCR4, and the kinase also reduces CXCL12-driven migration in various cell lines (Ptasznik, 2002; Nakata, 2006) as well as β2 integrin-dependent cell adhesion (Nakata, 2006). 2) Mitogen-activated protein kinase kinase 2 (MAP2K2, also known as MEK2). CXCL12, *via* CXCR4, activates a signalling cascade including protein kinase A, MAP2K2 and ERK1/2. 3) Checkpoint kinase 2 (CHK2), a tumour suppressor gene that regulates cell division and hence plays a crucial role in cancer (Cai, 2009). CHK2 is also known to interact with tumour suppressor p53 (Cai, 2009) and has been

shown to be down-regulated by $CXCR4^{1013}$ (Meuris, 2016), a CXCR4 WHIM variant. The CXCR4-associated proteins identified also include COPS5, a protein of the COP9 signalosome complex that interact with casein kinase 2 and protein kinase D both involved in p53 phosphorylation (Uhle, 2003). COPS5 is also part of the MIF-CXCR4 axis, that is responsible for the regulation of gene transcription involved in adhesion in multiple myeloma (Zheng, 2016). In addition to protein kinases, the CXCR4 interactome included protein phosphatase 6 (PP6) that is necessary for DNA repair (Zhong, 2011) and is known to negatively regulate NF-κB (Ziembik, 2017). Active NF-κB directly binds to CXCR4 promoter and regulates CXCR4 expression affecting CXCL12-mediated migration of cells (Helbig, 2003).

Association of ACKR3 with non-canonical GPCR interacting proteins

Contrary to CXCR4, only few proteins are described as ACKR3 interacting proteins. Given the described role of ACKR3 in cancer, several studies have addressed ACKR3 crosstalk with well-known pro-oncogenic growth factor receptors. ACKR3 co-localises with and phosphorylates EGFR in breast and prostate cancer cells (Singh and Lokeshwar, 2011; Salazar, 2014; Kallifatidis, 2016), *via* cell-type specific mechanisms. However, a potential role of EGFR in ACKR3 cross-activation was not assessed in these studies. Some reports also suggest a possible functional interaction between ACKR3 and Transforming growth factor beta (TGF-β) (Rath, 2015) or Vascular endothelial growth factor (VEGF) (Singh and Lokeshwar, 2011) receptors, but whether they involve physical interaction with ACKR3 and/or ACKR3 phosphorylation and activation was not assessed. ACKR3 weakly interacts with the MIF receptor CD74 (Alampour-Rajabi, 2015). Moreover, ACKR3 co-localizes with PECAM-1, the cell adhesion molecule required for leukocyte transendothelial migration in human coronary artery endothelial cells (Dela Paz, 2014). Using a Membrane Yeast two Hybrid assay screen, ATP13A2 was identified as a putative ACKR3 interacting protein (Usenovic, 2012). In the study aimed at characterizing the human interactome of 1,125 GFP-tagged proteins, ACKR3 was found to interact with the gap junction beta-2 protein (GJB2), the 54S ribosomal protein L4, mitochondrial MRPL4, different ATP synthases (ATP5H, ATP5B, ATP5A1, ATP50), ACKR3 itself, the caspase Separin ESPL1, the probable E3 ubiquitin-protein ligase HECTD2 and the Putative E3 ubiquitin-protein ligase UBR7 (Hein, 2015). Ubiquitination is an essential mechanism of receptor regulation (Marchese and Benovic, 2001; Shenoy, 2007). ACKR3 can undergo ubiquitination in an agonist-dependent and independent manner, regulating receptor trafficking. Ubiquitination is promoted by three enzymes, E1 E2 and E3 that ubiquitinate proteins on lysine residues (Dores and Trejo, 2012;

Alonso and Friedman, 2013). Unexpectedly, ACKR3 is ubiquitinated by E3-ubiquitin ligase (E3) in the absence of an agonist and undergoes deubiquitination upon CXCL12 activation (Canals, 2012). Mutation of the five lysines in the receptor C-terminus to alanine, to prevent ubiquitination, impaired ACKR3 cell trafficking and decreased ACKR3-mediated CXCL12 degradation (Hoffmann, 2012).

Conclusions

The identification of GPCR-interacting proteins and residues subjected to post-translational modification is of utmost importance. Several techniques are nowadays available to decipher GPCR interactome and phosphorylation profile. These techniques have been successfully applied to CXCR4 revealing important interacting proteins as well as key residues involved in the regulation of receptor-mediated signal transduction. Using an AP-MS strategy we identified novel potential CXCR4 interacting proteins that might reveal new mechanisms of CXCR4-dependent signalling. Systematic studies of the ACKR3 interactome and its key phosphorylated residues might likewise open new avenues in the understanding of ACKR3 pathophysiological functions and the underlying molecular mechanisms.

Acknowledgments:

We thank all our colleagues from the ONCORNET consortium for the continuous scientific discussions and insights.

Author contributions: **AF** Conducted experiments, Performed data analysis, Wrote or contributed to the writing of the manuscript. **AZ** Wrote or contributed to the writing of the manuscript. **MN** Wrote or contributed to the writing of the manuscript. **BC** Wrote or contributed to the writing of the manuscript. **SH** contributed to the writing of the manuscript. **FM** contributed to the writing of the manuscript. **MS** contributed to the writing of the manuscript. **PM** Wrote or contributed to the writing of the manuscript, Participated in research design.

Methods for the identification of GPCR-interacting proteins (1 to 3) and phosphorylated residues (4)				
Classification	**Method**	**Screening**	**Advantages**	**Disadvantages**
1.Genetic	**Y2H**	Highly suitable	Easy to perform. Inexpensive.	Loss of spatial-temporal information. Membrane anchored proteins cannot be investigated. Performed in yeast.
	MYTH	Highly suitable	Easy to perform. Membrane anchored proteins can be investigated.	Loss of spatial-temporal information. Soluble proteins cannot be investigated. Performed in yeast.
	MaMTH	Highly suitable	Easy to perform. Membrane anchored proteins can be investigated. Performed in mammalian cells	Loss of spatial-temporal information. Soluble proteins cannot be investigated.
	KISS	Possible	Sensitive enough for studying interaction dynamic. Both membrane and cytosolic proteins can be investigated.	Loss of spatial-temporal information Proteins involved in the STAT3 cascade cannot be investigated.
2.Biophysical	**BRET/FRET**	Not suitable.	Precise spatial-temporal information. High sensitivity. Possibility to study interactions in living cells.	Generation of fusion proteins. Relies on the proximity and relative orientation between donor and acceptor.
	PLA	Not suitable.	Precise spatial information (single molecule resolution). Possibility to perform in *ex-vivo* models.	Relies on antibodies. High cost. Not easy to scale up in large studies
	BioID	Suitable	Precise spatial information. Several interactions in parallel. Possibility to perform in living cells.	Not well suited for studying interaction dynamic (fluorescent signal is delayed).

Methods for the identification of GPCR-interacting proteins (1 to 3) and phosphorylated residues (4)				
Classification	**Method**	**Screening**	**Advantages**	**Disadvantages**
3.Proteomic	**Co-IP**	Highly suitable	Purification of protein complexes in living cells and tissues.	Rely on antibodies. Loss of spatial-temporal information. Lysis conditions might influence results.
	Pull-down	Highly suitable	Can prove direct interaction.	Loss of spatial-temporal information. *In vitro* binding assays. Fusion of the receptor on the beads might alter receptor conformation.
	BioID	Highly suitable	Can detect weak and transient interactions in living cells.	Fusion of the biotin to the receptor might alter its targeting or functions.
4.Phosphorylation	**[^{32}P]**	Suitable	Very sensitive.	Radioactive method. Cannot give information on the number of phosphorylated residues nor their position.
	LC-MS	Highly suitable	Can pinpoint phosphorylated residues.	Can yield false negatives. Not quantitative unless combined with very expensive isotope tags.
	Mutagenesis	Suitable	Cheap and easy. Based on functional data in living cells. Can pinpoint phosphorylated residues.	Indirect method. Mutagenesis of the C-terminus can impair expression and/or localization of the receptor. Labor intensive in case of multiple phosphosites. Not quantitative.

Methods for the identification of GPCR-interacting proteins (1 to 3) and phosphorylated residues (4)				
Classification	**Method**	**Screening**	**Advantages**	**Disadvantages**
4.Phosphorylation	**Phospho-antibodies**	Suitable	Direct and indirect. Can be used in any cell line. Semi-quantitative and qualitative.	Time consuming and expensive for the generation of the antibodies. Useless with low affinity antibodies. Cannot give information on contiguous phosphorylated residues.

Table 1. Principal methods used to identify GPCR-interacting proteins and phosphorylated residues.

Y2H, yeast two-hybrid assay; MYTH, membrane yeast two-hybrid assay; MaMTH, mammalian membrane two-hybrid assay; KISS, kinase substrate sensor; PLA, proximity ligation assay; BiFC, bimolecular fluorescent complementation assay; BioID, proximity-dependent biotin identification.

Protein	Method of identification	Cellular context	Direct	Constitutive / induced	Site of interaction	Role	Ref
Filamin A	Pull-Down Co-IP	HEK293 cells Recombinant protein	Yes	Constitutive and CXCL12-induced. The ROCK inhibitor Y27632, reverses CXCL12-induced increased interaction	C-terminal tail and third loop of CXCR4	Stabilise CXCR4 at the surface	(Gómez-Moutón, 2015)
AIP4	Pull Down Co-IP FRET	HEK293 cells	Yes	Constitutive and CXCL12-induced.	CXCR4 C-tail serines and WW domains of AIP4. Serine 324 and 325 when phosphorylated increase interaction	Increase CXCR4 degradation	(Bhandari, 2009)
RTN3	Y2H Co-IP	HEK293 cells	NA	Constitutive, induction not tested	Carboxyl terminal of RTN3	Increase cytoplasmic localisation of CXCR4	(Li, 2016)
CD74	Co-IP Co-localisation	HEK293 and MonoMac6 cells	NA	Constitutive, induction not tested	NA	Phosphorylation of AKT	(Schwartz, 2009)

Protein	Method of identification	Cellular context	Direct	Constitutive / induced	Site of interaction	Role	Ref
TLR2	FRET Co-IP	Human monocyte and HEK293 cells	NA	Induced by Pg-fimbria	NA	CXCR4 inhibits TLR2-induced NF-κB activation. In addition, CXCR4 found to be receptor of the pattern-recognition receptor complex	(Hajishengallis, 2008; Triantafilou, 2008)
NMMHC	Pull-Down Co-IP Co-localisation	Jurkat T and Peer T cells lymphocytes	NA	Constitutive and not induced by CXCL12	CXCR4 C-terminus	Lymphocytes migration	(Rey, 2002)
Drebrin	Pull Down Co-IP FRET	J77 T, HEK293T and HIV-infected T cells	YES	Constitutive and induced by superantigen E which also re-localise the interaction to the leading edge of migrating lymphocytes.	Drebrin N-terminus positively regulates interaction whereas the C-terminus seems to negatively regulate it.	Drebrin affects key physiological processes during antigen presentation in HIV entry.	(Pérez-Martínez, 2010; Gordón-Alonso, 2013)
CD164	Co-IP Co-localisation	Jurkat and Ovarian surface epithelial cells	NA	Only induced when CXCL12 is presented on fibronectin.	NA	CD164 participates to the CXCL12 mediated AKT and PKC-ζ phosphorylation.	(Forde, 2007; Huang, 2013)

Protein	Method of identification	Cellular context	Direct	Constitutive / induced	Site of interaction	Role	Ref
mDIA2	Co-IP Co-localisation	MDA-MB-231 cells	NA	Constitutive (very weak) and CXCL12 induced.	NA	Cytoskeletal rearrangement necessary for non-apoptotic blebbing	(Wyse, 2017)
ATP13A2	MYTH	Yeast	YES	Constitutive	NA	NA	(Usenovic, 2012)
PI3Kγ	Co-IP	Human myeloid cells	NA	Only CXCL12 induced	NA	Integrin activation and chemotaxis.	(Schmid, 2011)
PECAM-1	PLA	Human Coronary Artery Endothelial Cells	NO	Constitutive. Induction not studied	NA	CXCR4 part of a junctional meccano-sensitive complex	(Dela Paz, 2014)
MYBL2	2HY	Yeast	Yes	NA	NA	NA	(Hein, 2015)
KCNK1	Co-IP	HeLa cells	NA	NA	NA	NA	(Hein, 2015)
TMEM63B	Co-IP	HeLa cells	NA	NA	NA	NA	(Hein, 2015)
GOLT1B	Co-IP	HeLa cells	NA	NA	NA	NA	(Hein, 2015)

Table 2. CXCR4 interacting proteins described in the literature.

TLR2, toll-like receptor 2; AIP4, E3 ubiquitin ligase atrophin Interacting protein 4; RTN3, reticulon3, NMMHC, motor protein non-muscle myosin H chain; CD164, endolyn; mDIA2, diaphanous-related formin-2; PI3Kγ, PI3-kinase isoform p110γ; PECAM-1, platelet endothelial cell adhesion molecule; MYBL2, Myb-related protein B; KCNK1, potassium channel subfamily K member 1; TMEM63B, CSC1-like protein 2; GOLT1B, vesicle transport protein GOT1B.

Protein name	Gene name	UniProt ID	Normalized MS/MS count	Average iBAQ CXCR4
C-X-C chemokine receptor type 4	CXCR4	P61073	0.06491	20,274,390
Electron transfer flavoprotein subunit alpha, mitochondrial	ETFA	P13804	0.02703	10,292,830
Minor histocompatibility antigen H13	HM13	Q8TCT9	0.02299	737,054
Electron transfer flavoprotein subunit beta	ETFB	P38117	0.02092	849,859
Ephrin-B1	EFNB1	P98172	0.01927	1,070,764
Short/branched chain specific acyl-CoA dehydrogenase, mitochondrial	ACADSB	P45954	0.01775	1,081,997
Proteasome subunit alpha type-5	PSMA5	P28066	0.01521	524,028
Glutaredoxin-3	GLRX3	O76003	0.01493	521,983
General transcription factor II-I	GTF2I	P78347	0.01470	780,642
Nucleoporin NDC1	NDC1	Q9BTX1	0.01434	682,147
26S proteasome non-ATPase regulatory subunit 14	PSMD14	O00487	0.01398	631,800
Importin-9	IPO9	Q96P70	0.01377	1,029,703
Cysteine-rich and transmembrane domain-containing protein 11	CYSTM1	Q9H1C7	0.01375	658,329
Proteasome subunit alpha type-3	PSMA3	P25788	0.01307	324,119
Golgi to ER traffic protein 4 homolog	GET4	Q7L5D6	0.01223	345,230
Speckle targeted PIP5K1A-regulated poly(A) polymerase	TUT1	Q9H6E5	0.01220	597,661

Protein name	Gene name	UniProt ID	Normalized MS/MS count	Average iBAQ CXCR4
Evolutionarily conserved signalling intermediate in Toll pathway	ECSIT	Q9BQ95	0.01160	586,114
E3 ubiquitin-protein ligase RNF5	RNF5	Q99942	0.01111	178630
Dynactin subunit 5	DCTN5	Q9BTE1	0.01099	120954
Calpain small subunit 1	CAPNS1	P04632	0.00995	193850
Guanine nucleotide-binding protein G(i) subunit alpha-1	GNAI1	P63096	0.00942	237333
Integral membrane protein 2B	ITM2B	Q9Y287	0.00877	130,189
Inositol-3-phosphate synthase 1	ISYNA1	Q9NPH2	0.00836	137,886
Dihydrolipoyl dehydrogenase, mitochondrial	DLD	P09622	0.00786	258,572
Ancient ubiquitous protein 1	AUP1	Q9Y679	0.00770	278,788
Synembryn-A	RIC8A	Q9NPQ8	0.00753	203,420
Proteasome activator complex subunit 2	PSME2	Q9UL46	0.00697	217,121
Ubiquitin-conjugating enzyme E2 K	UBE2K	P61086	0.00667	197,517
Nucleoporin p54	NUP54	Q7Z3B4	0.00657	149,909
Proteasome subunit alpha type-1	PSMA1	P25786	0.00634	114,455
Dual specificity mitogen-activated protein kinase kinase 2	MAP2K2	P36507	0.00583	139,521
Zinc finger CCCH-type antiviral protein 1-like	ZC3HAV1L	Q96H79	0.00556	106,885

Protein name	Gene name	UniProt ID	Normalized MS/MS count	Average iBAQ CXCR4
N-terminal kinase-like protein	SCYL1	Q96KG9	0.00536	186,696
E3 ubiquitin-protein ligase KCMF1	KCMF1	Q9P0J7	0.00525	197,300
E3 ubiquitin-protein ligase HUWE1	HUWE1	Q7Z6Z7	0.00518	181,922
Protein FAM134C	FAM134C	Q86VR2	0.00501	203,073
Integrator complex subunit 11	CPSF3L	Q5TA45	0.00500	102,079
Rap1 GTPase-GDP dissociation stimulator 1	RAP1GDS1	P52306	0.00494	105,848
COUP transcription factor 2	NR2F2	P24468	0.00483	111,176
E3 ubiquitin-protein ligase ARIH1	ARIH1	Q9Y4X5	0.00479	124,675
Basic leucine zipper and W2 domain-containing protein 1	BZW1	Q7L1Q6	0.00477	119,855
NEDD4 family-interacting protein 1	NDFIP1	Q9BT67	0.00452	136,055
Ribonuclease H2 subunit A	RNASEH2A	O75792	0.00446	325,037
Monofunctional C1-tetrahydrofolate synthase, mitochondrial	MTHFD1L	Q6UB35	0.00443	374,534
Exportin-7	XPO7	Q9UIA9	0.00429	212,689
Dimethyladenosine transferase 2, mitochondrial	TFB2M	Q9H5Q4	0.00421	122,863
Transmembrane protein 209	TMEM209	Q96SK2	0.00416	73,409
Protein FAM8A1	FAM8A1	Q9UBU6	0.00404	839,75

Protein name	Gene name	UniProt ID	Normalized MS/MS count	Average iBAQ CXCR4
Nuclear pore complex protein Nup107	NUP107	P57740	0.00396	96,797
Peptidase M20 domain-containing protein 2	PM20D2	Q8IYS1	0.00382	101,885
Acyl-CoA dehydrogenase family member 9, mitochondrial	ACAD9	Q9H845	0.00376	251,019
Equilibrative nucleoside transporter 1	SLC29A1	Q99808	0.00365	206,126
Proteasome subunit beta type-7	PSMB7	Q99436	0.00361	116,231
TraB domain-containing protein	TRABD	Q9H4I3	0.00355	130,584
Transmembrane 9 superfamily member 2	TM9SF2	Q99805	0.00352	73,594
Serine/threonine-protein phosphatase 6 regulatory subunit 1	PPP6R1	Q9UPN7	0.00341	93,490
GTPase-activating protein and VPS9 domain-containing protein 1	GAPVD1	Q14C86	0.00338	205,182
Fascin	FSCN1	Q16658	0.00338	187,190
Spermatogenesis-associated protein 5	SPATA5	Q8NB90	0.00336	68,425
Condensin complex subunit 1	NCAPD2	Q15021	0.00333	82,016
Probable methyltransferase-like protein 15	METTL15	A6NJ78	0.00328	42,614
Tyrosine-protein kinase Lyn	LYN	P07948	0.00326	67,845
Sideroflexin-3	SFXN3	Q9BWM7	0.00312	127,637
Serine/threonine-protein kinase Chk2	CHEK2	O96017	0.00307	87,680

Protein name	Gene name	UniProt ID	Normalized MS/MS count	Average iBAQ CXCR4
C-terminal-binding protein 1	CTBP1	Q13363	0.00303	108,421
COP9 signalosome complex subunit 5	COPS5	Q92905	0.00299	108,293
Transmembrane 9 superfamily member 3	TM9SF3	Q9HD45	0.00283	50,251
Putative HLA class I histocompatibility antigen, alpha chain H	HLA-H	P01893	0.00276	148,707
Nuclear pore membrane glycoprotein 210	NUP210	Q8TEM1	0.00247	203,550
MAGUK p55 subfamily member 6	MPP6	Q9NZW5	0.00247	109,651
Nuclear envelope pore membrane protein POM 121C	POM121C	A8CG34	0.00217	104,673
E3 ubiquitin-protein ligase AMFR	AMFR	Q9UKV5	0.00207	124,862
Nuclear pore complex protein Nup133	NUP133	Q8WUM0	0.00202	92,921
Clustered mitochondria protein homolog	CLUH	O75153	0.00153	74,561
DNA polymerase delta catalytic subunit	POLD1	P28340	0.00151	49,692
Baculoviral IAP repeat-containing protein 6	BIRC6	Q9NR09	0.00103	44,825
Acetyl-CoA carboxylase 1	ACACA	Q13085	0.00085	38,883
Deubiquitinating protein VCIP135	VCPIP1	Q96JH7	0.00082	30,284

Table 3. List of proteins that specifically co-immunoprecipitate with CXCR4 in HEK293T cells.

Hemagglutinin (HA)-tagged CXCR4 was transiently expressed in HEK293T cells. We then immunoprecipitated the receptor-associated complex with an agarose bead-conjugated anti-HA antibody and co-immunoprecipitated proteins were systematically identified by nano-flow liquid chromatography coupled to tandem mass spectrometry (nano-LC-MS/MS). Proteins identified at MS level in the CXCR4 co-precipitating complex in all three triplicated and absent in the three controls (Co-IP performed in HEK293T cells transfected with empty plasmid) are here reported. Protein name, gene name, Uniprot ID, normalized MS/MS count and average iBAQ are indicated. The normalized MS/MS was calculated dividing the average MS/MS count of the triplicate for the protein length

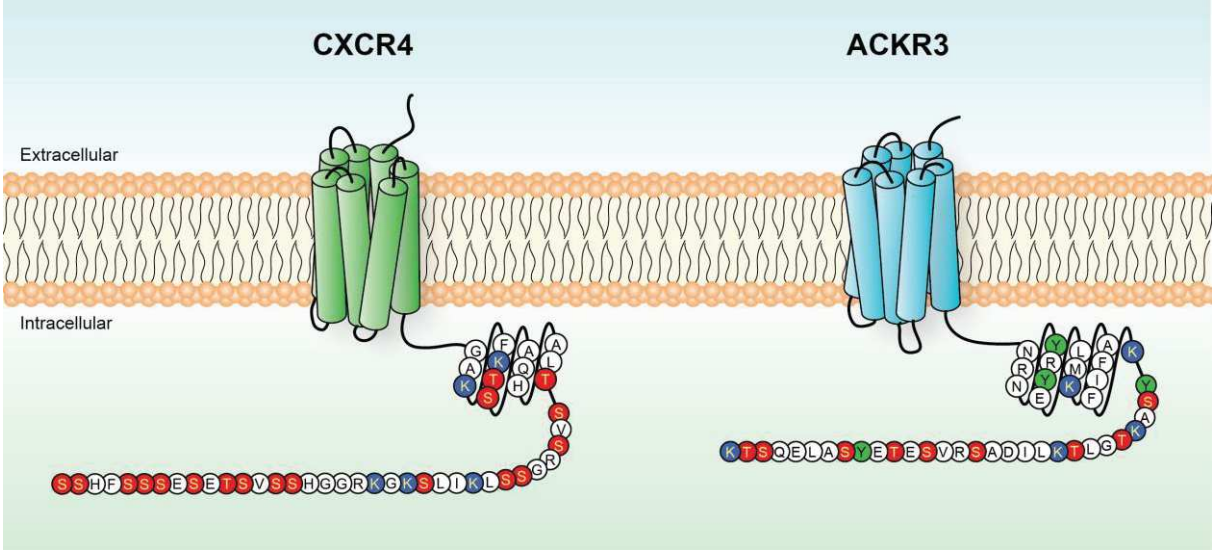

Figure 1. CXCR4 and ACKR3 residues potentially subjected to post-transitional modification.

Schematic representation of the C-terminal tail of CXCR4 and ACKR3 where serine/threonine (red), tyrosine (red) and lysine (blue) residues potentially subjected to post-transitional modification are highlighted.

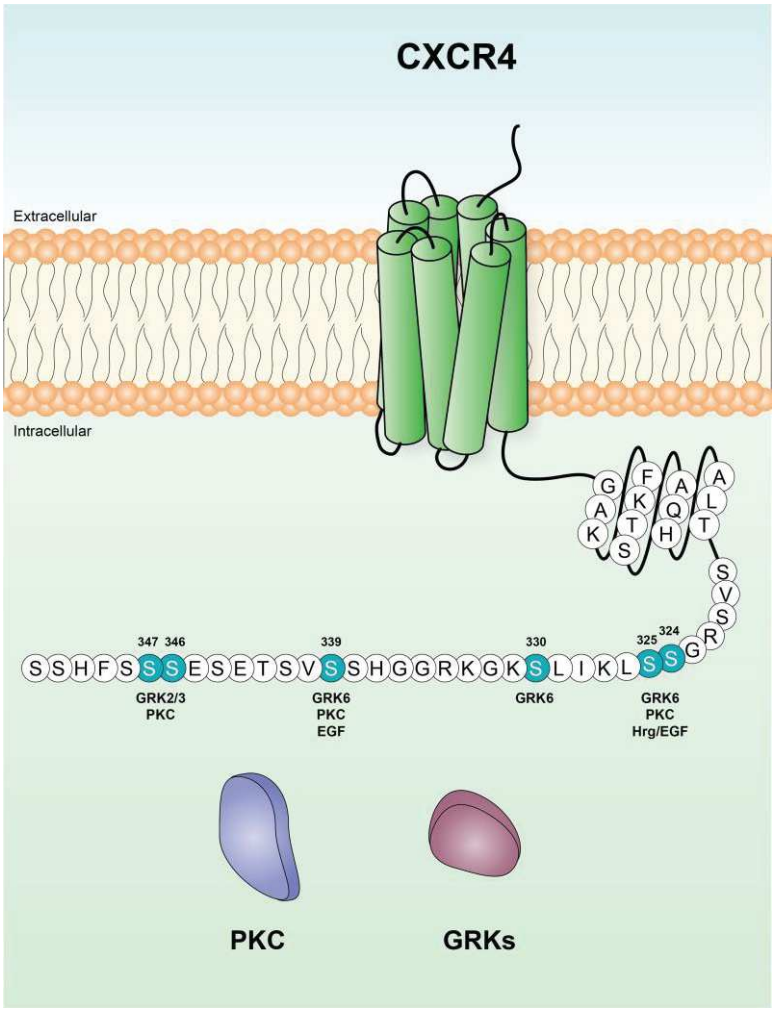

Figure 2. CXCR4 C-terminus phosphosites.

Schematic representation of the C-terminal tail of CXCR4 where serine residues known to be phosphorylated are highlighted in light blue. The kinases or the extracellular stimulus responsible for the phosphorylation are also specified. GRK, G protein-coupled receptor kinase; PKC, protein kinase C; EGF, epidermal growth factor receptor; Hrg, heregulin.

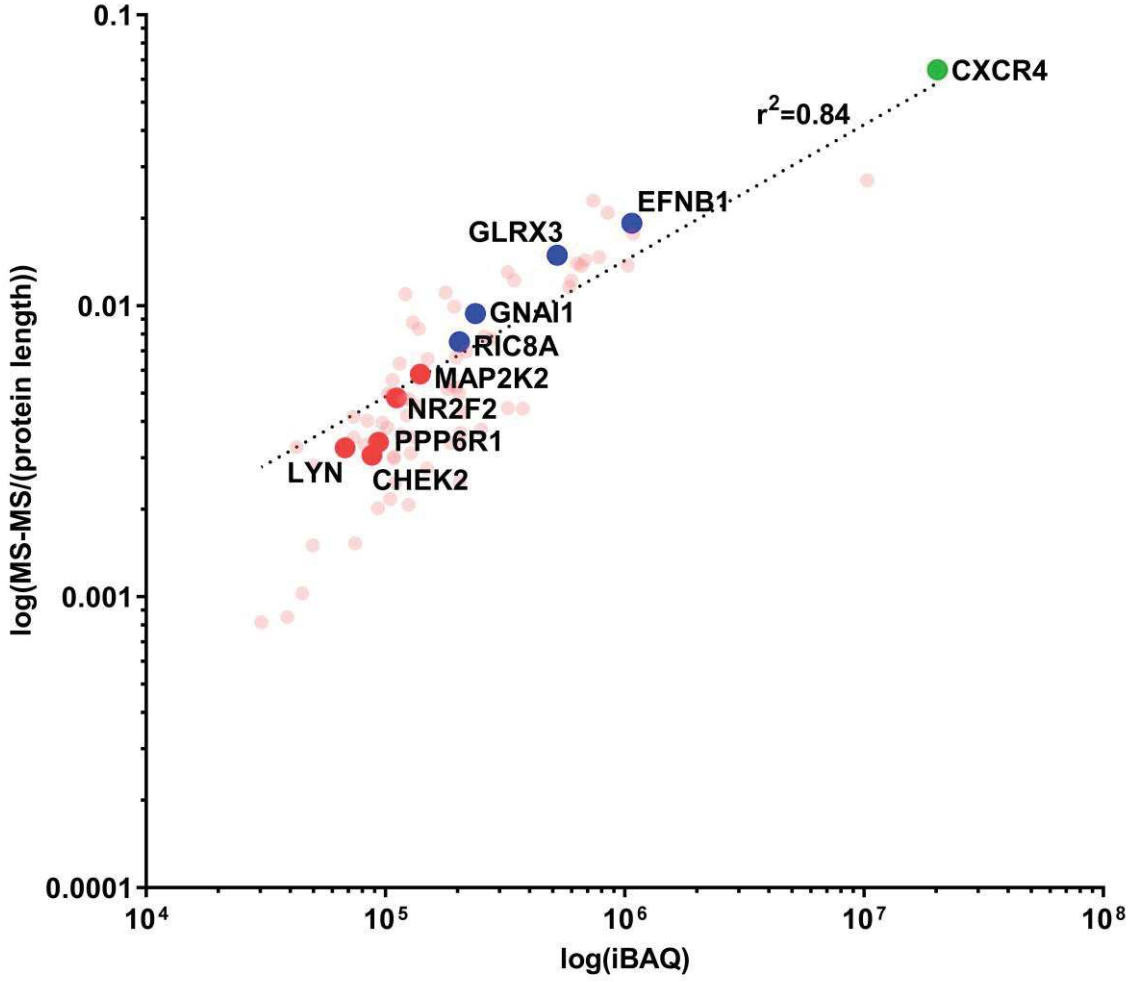

Figure 3. CXCR4 interacting proteins

The linear correlation between MS-MS count normalised to the protein length and iBAQ is reported as dotted line. The bait protein (CXCR4) is illustrated in green, kinases and phosphatases in red, proteins already known to interact with CXCR4 (at least functionally) in blue. EFNB1, ephrin-B1; GLRX3, glutaredoxin-3; GNAI1, guanine nucleotide-binding protein G(i) subunit alpha-1; RIC8A, synembryn-A; MAP2K2, mitogen-activated protein kinase kinase 2; NR2F2, COUP transcription factor 2; PPP6R1, protein phosphatase 6 regulatory subunit 1; CHEK2, serine/threonine-protein kinase Chk2; LYN, tyrosine-protein kinase Lyn.

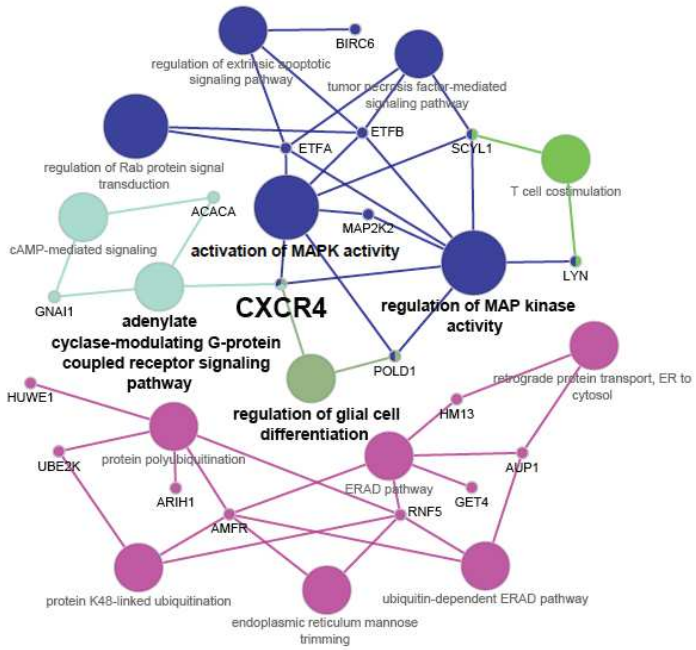

Figure 4. Biological processes statistically overrepresented in the CXCR4-associated complex.

Functional gene ontologies (GO) overrepresented among the 79 CXCR4-interacting proteins were analysed using the Cytoscappe Plugin with Cluego (v2.5.2), using all proteins identified in the interactomics screen as reference protein list. All evidences but the inferred from electronic associations (IEA) were used. Statistical test used = Enrichment/Depletion (Two-sided hypergeometric test). Correction method used = Benjamini-Hochberg. Min GO level = 7. Max GO level = 15. Minimum number of genes = 2. Min percentage = 8.0. GO term grouping was performed based on the Cohen's kappa coefficient and it divided the GOs in five groups here defined in five colours. The leading term for each group was defined based on the highest significance and they are T cell costimulation (**light green**), adenylate cyclase-modulating G-protein coupled receptor signalling pathway (**green**), regulation of glial cell differentiation (**dark green**), protein K48-linked ubiquitination (**purple**) and activation of MAPK activity (**blue**). BIRC6, baculoviral IAP repeat-containing protein 6; ETFB, electron transfer flavoprotein subunit beta; ETFA, electron transfer flavoprotein subunit alpha; ACACA, Acetyl-CoA carboxylase 1; GNAI1, guanine nucleotide-binding protein G(i) subunit alpha-1; LYN, tyrosine-protein kinase Lyn; POLD1, DNA polymerase delta catalytic subunit; HUWE1, E3 ubiquitin-protein ligase HUWE1; UBE2K, Ubiquitin-conjugating enzyme E2 K; ARIH1, E3 ubiquitin-protein ligase ARIH1; AMFR, E3 ubiquitin-protein ligase AMFR; RNF5, E3 ubiquitin-protein ligase RNF5; GET4, Golgi to ER traffic protein 4 homolog; AUP1, ancient ubiquitous protein 1; HM13, Minor histocompatibility antigen H13.

References

Alampour-Rajabi S, El Bounkari O, Rot a., Muller-Newen G, Bachelerie F, Gawaz M, Weber C, Schober a., and Bernhagen J (2015) MIF interacts with CXCR7 to promote receptor internalization, ERK1/2 and ZAP-70 signaling, and lymphocyte chemotaxis. *FASEB J* 1–15.

Alonso V, and Friedman PA (2013) Minireview: Ubiquitination-regulated G Protein-Coupled Receptor Signaling and Trafficking. *Mol Endocrinol* **27**:558–572.

Auwerx J, Isacsson O, Söderlund J, Balzarini J, Johansson M, and Lundberg M (2009) Human glutaredoxin-1 catalyzes the reduction of HIV-1 gp120 and CD4 disulfides and its inhibition reduces HIV-1 replication. *Int J Biochem Cell Biol* **41**:1269–75.

Balabanian K, Lagane B, Infantino S, Chow KYC, Harriague J, Moepps B, Arenzana-Seisdedos F, Thelen M, and Bachelerie F (2005) The chemokine SDF-1/CXCL12 binds to and signals through the orphan receptor RDC1 in T lymphocytes. *J Biol Chem* **280**:35760–35766.

Balabanian K, Levoye A, Klemm L, Lagane B, Hermine O, Harriague J, Baleux F, Arenzana-Seisdedos F, and Bachelerie F (2008) Leukocyte analysis from WHIM syndrome patients reveals a pivotal role for GRK3 in CXCR4 signaling. *J Clin Invest* **118**:1074–1084.

Banisadr G, Fontanges P, Haour F, Kitabgi P, Rostène W, and Mélik Parsadaniantz S (2002) Neuroanatomical distribution of CXCR4 in adult rat brain and its localization in cholinergic and dopaminergic neurons. *Eur J Neurosci* **16**:1661–71.

Banisadr G, Podojil JR, Miller SD, and Miller RJ (2016) Pattern of CXCR7 Gene Expression in Mouse Brain Under Normal and Inflammatory Conditions. *J Neuroimmune Pharmacol* **11**:26–35.

Barker BL, and Benovic JL (2011) G Protein-Coupled Receptor Kinase 5 Phosphorylation of Hip Regulates Internalization of the Chemokine Receptor CXCR4. *Biochemistry* **50**:6933–6941.

Benredjem B, Girard M, Rhainds D, St-Onge G, and Heveker N (2016) Mutational Analysis of Atypical Chemokine Receptor 3 (ACKR3/CXCR7) Interaction with its Chemokine Ligands CXCL11 and CXCL12. *J Biol Chem* **3**:jbc.M116.762252.

Berahovich RD, Zabel BA, Lewén S, Walters MJ, Ebsworth K, Wang Y, Jaen JC, and Schall TJ (2014) Endothelial expression of CXCR7 and the regulation of systemic CXCL12 levels. *Immunology* **141**:111–122.

Bhandari D, Robia SL, and Marchese A (2009) The E3 ubiquitin ligase atrophin interacting protein 4 binds directly to the chemokine receptor CXCR4 via a novel WW domain-mediated interaction. *Mol Biol Cell* **20**:1324–39.

Billard MJ, Fitzhugh DJ, Parker JS, Brozowski JM, McGinnis MW, Timoshchenko RG, Serafin DS, Lininger R, Klauber-Demore N, Sahagian G, Truong YK, Sassano MF, Serody JS, and Tarrant TK (2016) G Protein Coupled Receptor Kinase 3 Regulates Breast Cancer Migration, Invasion, and Metastasis. *PLoS One* **11**:e0152856.

Bockaert J, Dumuis A, Fagni L, and Marin P (2004) GPCR-GIP networks: a first step in the discovery of new therapeutic drugs? *Curr Opin Drug Discov Devel* **7**:649–57.

Boudot A, Kerdivel G, Lecomte S, Flouriot G, Desille M, Godey F, Leveque J, Tas P, Le Dréan Y, and Pakdel F (2014) COUP-TFI modifies CXCL12 and CXCR4 expression by activating EGF signaling and stimulates breast cancer cell migration. *BMC Cancer* **14**:407.

Brault L, Rovó A, Decker S, Dierks C, Tzankov A, and Schwaller J (2014) CXCR4-SERINE339 regulates cellular adhesion, retention and mobilization and is a marker for poor prognosis in acute myeloid leukemia. *Leukemia* **28**:566–576.

Busillo JM, Armando S, Sengupta R, Meucci O, Bouvier M, and Benovic JL (2010) Site-specific phosphorylation of CXCR4 is dynamically regulated by multiple kinases and results in differential modulation of CXCR4 signaling. *J Biol Chem* **285**:7805–7817.

Busillo JM, and Benovic JL (2007) Regulation of CXCR4 signaling. *Biochim Biophys Acta - Biomembr* **1768**:952–963.

Cai Z, Chehab NH, and Pavletich NP (2009) Structure and Activation Mechanism of the CHK2 DNA Damage Checkpoint Kinase. *Mol Cell* **35**:818–829.

Canals M, Scholten DJ, de Munnik S, Han MKL, Smit MJ, and Leurs R (2012) Ubiquitination of CXCR7 controls receptor trafficking. *PLoS One* **7**:e34192.

Chen Y-J, Oldfield S, Butcher AJ, Tobin AB, Saxena K, Gurevich V V., Benovic JL, Henderson G, and Kelly E (2013) Identification of phosphorylation sites in the COOH-terminal tail of the μ-opioid receptor. *J Neurochem* **124**:189–199.

Clegg RM (1995) Fluorescence resonance energy transfer. *Curr Opin Biotechnol* **6**:103–10.

Daulat AM, Maurice P, Froment C, Guillaume J-L, Broussard C, Monsarrat B, Delagrange P, and Jockers R (2007) Purification and Identification of G Protein-coupled Receptor Protein Complexes under Native Conditions. *Mol Cell Proteomics* **6**:835–844.

Dela Paz NG, Melchior B, Shayo FY, and Frangos JA (2014) Heparan sulfates mediate the interaction between platelet endothelial cell adhesion molecule-1 (PECAM-1) and the Galpha q/11 subunits of heterotrimeric G proteins. *J Biol Chem* **289**:7413–7424.

Dephoure N, Gould KL, Gygi SP, and Kellogg DR (2013) Mapping and analysis of phosphorylation sites: a quick guide for cell biologists. *Mol Biol Cell* **24**:535–542, American Society for Cell Biology.

Dores MR, and Trejo J (2012) Ubiquitination of G Protein-Coupled Receptors: Functional Implications and Drug Discovery. *Mol Pharmacol* **82**:563–570.

Ferguson SS, Barak LS, Zhang J, and Caron MG (1996) G-protein-coupled receptor regulation: role of G-protein-coupled receptor kinases and arrestins. *Can J Physiol Pharmacol* **74**:1095–110.

Ferguson SS, Downey WE, Colapietro AM, Barak LS, Ménard L, and Caron MG (1996) Role of beta-arrestin in mediating agonist-promoted G protein-coupled receptor internalization. *Science* **271**:363–6.

Ferré S, Casadó V, Devi LA, Filizola M, Jockers R, Lohse MJ, Milligan G, Pin J-P, and Guitart X (2014) G protein-coupled receptor oligomerization revisited: functional and pharmacological perspectives. *Pharmacol Rev* **66**:413–34, American Society for Pharmacology and Experimental Therapeutics.

Fields S, and Song O (1989) A novel genetic system to detect protein-protein interactions. [Yeast two hybrid]. *Nature* **340**:245–246.

Fong AM, Premont RT, Richardson RM, Yu Y-RA, Lefkowitz RJ, and Patel DD

(2002) Defective lymphocyte chemotaxis in β-arrestin2- and GRK6-deficient mice. *Proc Natl Acad Sci U S A* **99**:7478–83.

Forde S, Tye BJ, Newey SE, Roubelakis M, Smythe J, McGuckin CP, Pettengell R, and Watt SM (2007) Endolyn (CD164) modulates the CXCL12-mediated migration of umbilical cord blood CD133+ cells. *Blood* **109**:1825–33.

Fredriksson S, Gullberg M, Jarvius J, Olsson C, Pietras K, Gústafsdóttir SM, Östman A, and Landegren U (2002) Protein detection using proximity-dependent DNA ligation assays. *Nat Biotechnol* **20**:473–477.

Gerber SA, Rush J, Stemman O, Kirschner MW, and Gygi SP (2003) Absolute quantification of proteins and phosphoproteins from cell lysates by tandem MS. *Proc Natl Acad Sci* **100**:6940–6945.

Gómez-Moutón C, Fischer T, Peregil RM, Jiménez-Baranda S, Stossel TP, Nakamura F, and Mañes S (2015) Filamin A interaction with the CXCR4 third intracellular loop regulates endocytosis and signaling of WT and WHIM-like receptors. *Blood* **125**:1116–25.

Gordón-Alonso M, Rocha-Perugini V, Álvarez S, Ursa Á, Izquierdo-Useros N, Martinez-Picado J, Muñoz-Fernández MA, and Sánchez-Madrid F (2013) Actin-binding protein drebrin regulates HIV-1-triggered actin polymerization and viral infection. *J Biol Chem* **288**:28382–28397.

Hajishengallis G, Wang M, Liang S, Triantafilou M, and Triantafilou K (2008) Pathogen induction of CXCR4/TLR2 cross-talk impairs host defense function. *Proc Natl Acad Sci* **105**:13532–13537.

Hein MY, Hubner NC, Poser I, Cox J, Nagaraj N, Toyoda Y, Gak IA, Weisswange I, Mansfeld J, Buchholz F, Hyman AA, and Mann M (2015) A human interactome in three quantitative dimensions organized by stoichiometries and abundances. *Cell* **163**:712–23.

Helbig G, Christopherson KW, Bhat-Nakshatri P, Kumar S, Kishimoto H, Miller KD, Broxmeyer HE, and Nakshatri H (2003) NF-κ B Promotes Breast Cancer Cell Migration and Metastasis by Inducing the Expression of the Chemokine Receptor CXCR4. *J Biol Chem* **278**:21631–21638.

Hoffmann F, Müller W, Schütz D, Penfold ME, Wong YH, Schulz S, and Stumm R (2012) Rapid uptake and degradation of CXCL12 depend on CXCR7 carboxyl-

terminal serine/threonine residues. *J Biol Chem* **287**:28362–28377.

Hu C-D, Chinenov Y, and Kerppola TK (2002) Visualization of interactions among bZIP and Rel family proteins in living cells using bimolecular fluorescence complementation. *Mol Cell* **9**:789–98.

Huang A-F, Chen M-W, Huang S-M, Kao C-L, Lai H-C, and Chan JY-H (2013) CD164 regulates the tumorigenesis of ovarian surface epithelial cells through the SDF-1α/CXCR4 axis. *Mol Cancer* **12**:115.

Kallifatidis G, Munoz D, Singh RK, Salazar N, Hoy JJ, and Lokeshwar BL (2016) -Arrestin-2 Counters CXCR7-Mediated EGFR Transactivation and Proliferation. *Mol Cancer Res* **14**:493–503.

Konoplev S, Jorgensen JL, Thomas DA, Lin E, Burger J, Kantarjian HM, Andreeff M, Medeiros LJ, and Konopleva M (2011) Phosphorylated CXCR4 is associated with poor survival in adults with B-acute lymphoblastic leukemia. *Cancer* **117**:4689–4695.

Krupnick JG, and Benovic JL (1998) The role of receptor kinases and areestins in G protein-coupled receptor regulation. *Annu Rev Pharmacol Toxicol* **38**:289–319.

Kumar A, Kremer KN, Dominguez D, Tadi M, and Hedin KE (2011) G 13 and Rho Mediate Endosomal Trafficking of CXCR4 into Rab11+ Vesicles upon Stromal Cell-Derived Factor-1 Stimulation. *J Immunol* **186**:951–958.

Lefkowitz RJ (1993) G protein-coupled receptor kinases. *Cell* **74**:409–12.

Lefkowitz RJ (2004) Historical review: A brief history and personal retrospective of seven-transmembrane receptors. *Trends Pharmacol Sci* **25**:413–422.

Levoye A, Balabanian K, Baleux F, Bachelerie F, and Lagane B (2009) CXCR7 heterodimerizes with CXCR4 and regulates CXCL12-mediated G protein signaling. *Blood* **113**:6085–93, AMER SOC HEMATOLOGY, 1900 M STREET. NW SUITE 200, WASHINGTON, DC 20036 USA.

Li H, Liang R, Lu Y, Wang M, and Li Z (2016) RTN3 Regulates the Expression Level of Chemokine Receptor CXCR4 and is Required for Migration of Primordial Germ Cells. *Int J Mol Sci* **17**:382.

Lievens S, Gerlo S, Lemmens I, De Clercq DJH, Risseeuw MDP, Vanderroost N, De Smet A-S, Ruyssinck E, Chevet E, Van Calenbergh S, and Tavernier J (2014)

Kinase Substrate Sensor (KISS), a mammalian in situ protein interaction sensor. *Mol Cell Proteomics* **13**:3332–42.

Lipfert J, Ödemis V, and Engele J (2013) Grk2 is an essential regulator of CXCR7 signalling in astrocytes. *Cell Mol Neurobiol* **33**:111–118.

Lu Q, Sun EE, Klein RS, and Flanagan JG (2001) Ephrin-B reverse signaling is mediated by a novel PDZ-RGS protein and selectively inhibits G protein-coupled chemoattraction. *Cell* **105**:69–79.

Luker KE, Gupta M, Steele JM, Foerster BR, and Luker GD (2009) Imaging ligand-dependent activation of CXCR7. *Neoplasia* **11**:1022–35.

Luo J, Busillo JM, Stumm R, and Benovic JL (2017) G Protein-Coupled Receptor Kinase 3 and Protein Kinase C Phosphorylate the Distal C-Terminal Tail of the Chemokine Receptor CXCR4 and Mediate Recruitment of *β* -Arrestin. *Mol Pharmacol* **91**:554–566.

Magalhaes AC, Dunn H, and Ferguson SSG (2012) Regulation of GPCR activity, trafficking and localization by GPCR-interacting proteins. *Br J Pharmacol* **165**:1717–1736.

Marchese A, and Benovic JL (2001) Agonist-promoted Ubiquitination of the G Protein-coupled Receptor CXCR4 Mediates Lysosomal Sorting. *J Biol Chem* **276**:45509–45512.

Maurice P, Guillaume J-L, Benleulmi-Chaachoua A, Daulat AM, Kamal M, and Jockers R (2011) GPCR-Interacting Proteins, Major Players of GPCR Function, in *Advances in pharmacology (San Diego, Calif.)* pp 349–380.

Meisenhelder J, Hunter T, and van der Geer P (2001) Phosphopeptide mapping and identification of phosphorylation sites. *Curr Protoc Protein Sci* **Chapter 13**:Unit13.9, John Wiley & Sons, Inc., Hoboken, NJ, USA.

Meuris F, Carthagena L, Jaracz-Ros A, Gaudin F, Cutolo P, Deback C, Xue Y, Thierry F, Doorbar J, and Bachelerie F (2016) The CXCL12/CXCR4 Signaling Pathway: A New Susceptibility Factor in Human Papillomavirus Pathogenesis. *PLOS Pathog* **12**:e1006039.

Mueller W, Schütz D, Nagel F, Schulz S, and Stumm R (2013) Hierarchical organization of multi-site phosphorylation at the CXCR4 C terminus. *PLoS One*

8:e64975.

Nakata Y, Tomkowicz B, Gewirtz AM, and Ptasznik A (2006) Integrin inhibition through Lyn-dependent cross talk from CXCR4 chemokine receptors in normal human CD34+ marrow cells. *Blood* **107**:4234–4239.

Nazari A, Khorramdelazad H, and Hassanshahi G (2017) Biological/pathological functions of the CXCL12/CXCR4/CXCR7 axes in the pathogenesis of bladder cancer. *Int J Clin Oncol* **22**:991–1000.

Nogués L, Palacios-García J, Reglero C, Rivas V, Neves M, Ribas C, Penela P, and Mayor F (2018) G protein-coupled receptor kinases (GRKs) in tumorigenesis and cancer progression: GPCR regulators and signaling hubs. *Semin Cancer Biol* **48**:78–90.

Nogués L, Reglero C, Rivas V, Salcedo A, Lafarga V, Neves M, Ramos P, Mendiola M, Berjón A, Stamatakis K, Zhou XZ, Lu KP, Hardisson D, Mayor F, and Penela P (2016) G Protein-coupled Receptor Kinase 2 (GRK2) Promotes Breast Tumorigenesis Through a HDAC6-Pin1 Axis. *EBioMedicine* **13**:132–145.

Oakley RH, Laporte SA, Holt JA, Caron MG, and Barak LS (2000) Differential Affinities of Visual Arrestin, βArrestin1, and βArrestin2 for G Protein-coupled Receptors Delineate Two Major Classes of Receptors. *J Biol Chem* **275**:17201–17210.

Odemis V, Boosmann K, Heinen A, Küry P, and Engele J (2010) CXCR7 is an active component of SDF-1 signalling in astrocytes and Schwann cells. *J Cell Sci* **123**:1081–1088.

Okamoto Y, and Shikano S (2017) Differential phosphorylation signals control endocytosis of GPR15. *Mol Biol Cell* **28**:2267–2281.

Patel JR, McCandless EE, Dorsey D, and Klein RS (2010) CXCR4 promotes differentiation of oligodendrocyte progenitors and remyelination. *Proc Natl Acad Sci U S A* **107**:11062–7, National Academy of Sciences.

Penela P, Murga C, Ribas C, Lafarga V, Mayor F, and Jr (2010) The complex G protein-coupled receptor kinase 2 (GRK2) interactome unveils new physiopathological targets. *Br J Pharmacol* **160**:821–32, Wiley-Blackwell.

Penela P, Rivas V, Salcedo A, and Mayor F (2010) G protein-coupled receptor

kinase 2 (GRK2) modulation and cell cycle progression. *Proc Natl Acad Sci* **107**:1118–1123.

Pérez-Martínez M, Gordón-Alonso M, Cabrero JR, Barrero-Villar M, Rey M, Mittelbrunn M, Lamana A, Morlino G, Calabia C, Yamazaki H, Shirao T, Vázquez J, González-Amaro R, Veiga E, and Sánchez-Madrid F (2010) F-actin-binding protein drebrin regulates CXCR4 recruitment to the immune synapse. *J Cell Sci* **123**:1160–70.

Peterson YK, and Luttrell LM (2017) The Diverse Roles of Arrestin Scaffolds in G Protein-Coupled Receptor Signaling. *Pharmacol Rev* **69**:256–297.

Petschnigg J, Groisman B, Kotlyar M, Taipale M, Zheng Y, Kurat CF, Sayad A, Sierra JR, Usaj MM, Snider J, Nachman A, Krykbaeva I, Tsao M-S, Moffat J, Pawson T, Lindquist S, Jurisica I, and Stagljar I (2014) The mammalian-membrane two-hybrid assay (MaMTH) for probing membrane-protein interactions in human cells. *Nat Methods* **11**:585–592, Nature Publishing Group.

Ptasznik A, Urbanowska E, Chinta S, Costa MA, Katz BA, Stanislaus MA, Demir G, Linnekin D, Pan ZK, and Gewirtz AM (2002) Crosstalk between BCR/ABL oncoprotein and CXCR4 signaling through a Src family kinase in human leukemia cells. *J Exp Med* **196**:667–78.

Puig O, Caspary F, Rigaut G, Rutz B, Bouveret E, Bragado-Nilsson E, Wilm M, and Séraphin B (2001) The Tandem Affinity Purification (TAP) Method: A General Procedure of Protein Complex Purification. *Methods* **24**:218–229.

Rajagopal S, Kim J, Ahn S, Craig S, Lam CM, Gerard NP, Gerard C, and Lefkowitz RJ (2010) Beta-arrestin- but not G protein-mediated signaling by the “decoy” receptor CXCR7. *Proc Natl Acad Sci U S A* **107**:628–32.

Rath D, Chatterjee M, Borst O, Müller K, Langer H, Mack AF, Schwab M, Winter S, Gawaz M, and Geisler T (2015) Platelet surface expression of stromal cell-derived factor-1 receptors CXCR4 and CXCR7 is associated with clinical outcomes in patients with coronary artery disease. *J Thromb Haemost* **13**:719–728.

Ray P, Mihalko LA, Coggins NL, Moudgil P, Ehrlich A, Luker KE, and Luker GD (2012) Carboxy-terminus of CXCR7 regulates receptor localization and function. *Int J Biochem Cell Biol* **44**:669–678, Elsevier Ltd.

Reiser K, François KO, Schols D, Bergman T, Jörnvall H, Balzarini J, Karlsson A, and Lundberg M (2012) Thioredoxin-1 and protein disulfide isomerase catalyze the reduction of similar disulfides in HIV gp120. *Int J Biochem Cell Biol* **44**:556–62.

Rey M, Vicente-Manzanares M, Viedma F, Yáñez-Mó M, Urzainqui A, Barreiro O, Vázquez J, and Sánchez-Madrid F (2002) Cutting edge: association of the motor protein nonmuscle myosin heavy chain-IIA with the C terminus of the chemokine receptor CXCR4 in T lymphocytes. *J Immunol* **169**:5410–4.

Ribas C, Penela P, Murga C, Salcedo A, García-Hoz C, Jurado-Pueyo M, Aymerich I, and Mayor F (2007) The G protein-coupled receptor kinase (GRK) interactome: Role of GRKs in GPCR regulation and signaling. *Biochim Biophys Acta - Biomembr* **1768**:913–922.

Ritter SL, and Hall RA (2009) Fine-tuning of GPCR activity by receptor-interacting proteins. *Nat Rev Mol Cell Biol* **10**:819–30, NIH Public Access.

Roland J, Murphy BJ, Ahr B, Robert-Hebmann V, Delauzun V, Nye KE, Devaux C, and Biard-Piechaczyk M (2003) Role of the intracellular domains of CXCR4 in SDF-1-mediated signaling. *Blood* **101**:399–406.

Roux KJ, Kim DI, and Burke B (2013) BioID: A Screen for Protein-Protein Interactions, in *Current Protocols in Protein Science* p 19.23.1-19.23.14, John Wiley & Sons, Inc., Hoboken, NJ, USA.

Salazar N, Muñoz D, Kallifatidis G, Singh RK, Jordà M, and Lokeshwar BL (2014) The chemokine receptor CXCR7 interacts with EGFR to promote breast cancer cell proliferation. *Mol Cancer* **13**:198.

Salvucci O, Basik M, Bouchard A, Bianchi R, and Tosato G (2005) *Crosstalk between the CXCR4/SDF1 axis and Ephrin B2/ephrin B1 receptors in human endothelial cells*, Waverly Press.

Sánchez-Alcañiz JA, Haege S, Mueller W, Pla R, Mackay F, Schulz S, López-Bendito G, Stumm R, and Marín O (2011) Cxcr7 Controls Neuronal Migration by Regulating Chemokine Responsiveness. *Neuron* **69**:77–90.

Schmid MC, Avraamides CJ, Dippold HC, Franco I, Foubert P, Ellies LG, Acevedo LM, Manglicmot JRE, Song X, Wrasidlo W, Blair SL, Ginsberg MH, Cheresh DA, Hirsch E, Field SJ, and Varner JA (2011) Receptor tyrosine kinases and

TLR/IL1Rs unexpectedly activate myeloid cell PI3kγ, a single convergent point promoting tumor inflammation and progression. *Cancer Cell* **19**:715–27.

Schwartz V, Lue H, Kraemer S, Korbiel J, Krohn R, Ohl K, Bucala R, Weber C, and Bernhagen J (2009) A functional heteromeric MIF receptor formed by CD74 and CXCR4. *FEBS Lett* **583**:2749–2757, Federation of European Biochemical Societies.

Shenoy SK (2007) Seven-Transmembrane Receptors and Ubiquitination. *Circ Res* **100**:1142–1154.

Shenoy SK, and Lefkowitz RJ (2011) β-arrestin-mediated receptor trafficking and signal transduction. *Trends Pharmacol Sci* **32**:521–533.

Singh RK, and Lokeshwar BL (2011) The IL-8-regulated chemokine receptor CXCR7 stimulates EGFR signaling to promote prostate cancer growth. *Cancer Res* **71**:3268–3277.

Smith JS, and Rajagopal S (2016) The β-Arrestins: Multifunctional regulators of G protein-coupled receptors. *J Biol Chem* **291**:8969–8977.

Soede RD, Zeelenberg IS, Wijnands YM, Kamp M, and Roos E (2001) Stromal cell-derived factor-1-induced LFA-1 activation during in vivo migration of T cell hybridoma cells requires Gq/11, RhoA, and myosin, as well as Gi and Cdc42. *J Immunol* **166**:4293–301.

Sosa MS, Lopez-Haber C, Yang C, Wang H, Lemmon MA, Busillo JM, Luo J, Benovic JL, Klein-Szanto A, Yagi H, Gutkind JS, Parsons RE, and Kazanietz MG (2010) Identification of the Rac-GEF P-Rex1 as an essential mediator of ErbB signaling in breast cancer. *Mol Cell* **40**:877–92.

Stagljar I, Korostensky C, Johnsson N, and te Heesen S (1998) A genetic system based on split-ubiquitin for the analysis of interactions between membrane proteins in vivo. *Proc Natl Acad Sci U S A* **95**:5187–92.

Sun X, Cheng G, Hao M, Zheng J, Zhou X, Zhang J, Taichman RS, Pienta KJ, and Wang J (2010) CXCL12 / CXCR4 / CXCR7 chemokine axis and cancer progression. *Cancer Metastasis Rev* **29**:709–722.

Sun Y, Cheng Z, Ma L, and Pei G (2002) Beta-arrestin2 is critically involved in CXCR4-mediated chemotaxis, and this is mediated by its enhancement of p38

MAPK activation. *J Biol Chem* **277**:49212–9, American Society for Biochemistry and Molecular Biology.

Thomas RM, Kim J, Revelo-Penafiel MP, Angel R, Dawson DW, and Lowy AM (2008) The chemokine receptor CXCR4 is expressed in pancreatic intraepithelial neoplasia. *Gut* **57**:1555–60.

Tobin AB (2008) G-protein-coupled receptor phosphorylation: where, when and by whom. *Br J Pharmacol* **153 Suppl 1**:S167-76, Wiley-Blackwell.

Triantafilou M, Lepper PM, Briault CD, Ahmed MAE, Dmochowski JM, Schumann C, and Triantafilou K (2008) Chemokine receptor 4 (CXCR4) is part of the lipopolysaccharide "sensing apparatus". *Eur J Immunol* **38**:192–203.

Uhle S, Medalia O, Waldron R, Dumdey R, Henklein P, Bech-Otschir D, Huang X, Berse M, Sperling J, Schade R, and Dubiel W (2003) Protein kinase CK2 and protein kinase D are associated with the COP9 signalosome. *EMBO J* **22**:1302–1312.

Ulvmar MH, Hub E, and Rot A (2011) Atypical chemokine receptors. *Exp Cell Res* **317**:556–68.

Usenovic M, Knight AL, Ray A, Wong V, Brown KR, Caldwell GA, Caldwell KA, Stagljar I, and Krainc D (2012) Identification of novel ATP13A2 interactors and their role in α-synuclein misfolding and toxicity. *Hum Mol Genet* **21**:3785–94.

Volin M V., Joseph L, Shockley MS, and Davies PF (1998) Chemokine Receptor CXCR4 Expression in Endothelium. *Biochem Biophys Res Commun* **242**:46–53.

Vroon A, Heijnen CJ, Raatgever R, Touw IP, Ploemacher RE, Premont RT, and Kavelaars A (2004) GRK6 deficiency is associated with enhanced CXCR4-mediated neutrophil chemotaxis in vitro and impaired responsiveness to G-CSF in vivo. *J Leukoc Biol* **75**:698–704.

Wang J, Huo K, Ma L, Tang L, Li D, Huang X, Yuan Y, Li C, Wang W, Guan W, Chen H, Jin C, Wei J, Zhang W, Yang Y, Liu Q, Zhou Y, Zhang C, Wu Z, Xu W, Zhang Y, Liu T, Yu D, Zhang Y, Chen L, Zhu D, Zhong X, Kang L, Gan X, Yu X, Ma Q, Yan J, Zhou L, Liu Z, Zhu Y, Zhou T, He F, and Yang X (2014) Toward an understanding of the protein interaction network of the human liver. *Mol Syst Biol* **7**:536–536.

Woerner BM, Luo J, Brown KR, Jackson E, Dahiya SM, Mischel P, Benovic JL, Piwnica-Worms D, and Rubin JB (2012) Suppression of G-protein-Coupled Receptor Kinase 3 Expression Is a Feature of Classical GBM That Is Required for Maximal Growth. *Mol Cancer Res* **10**:156–166.

Woerner BM, Warrington NM, Kung AL, Perry A, and Rubin JB (2005) Widespread CXCR4 Activation in Astrocytomas Revealed by Phospho-CXCR4-Specific Antibodies. *Cancer Res* **65**:11392–11399.

Wu R, Haas W, Dephoure N, Huttlin EL, Zhai B, Sowa ME, and Gygi SP (2011) A large-scale method to measure absolute protein phosphorylation stoichiometries. *Nat Methods* **8**:677–683.

Wyse MM, Goicoechea S, Garcia-Mata R, Nestor-Kalinoski AL, and Eisenmann KM (2017) mDia2 and CXCL12/CXCR4 chemokine signaling intersect to drive tumor cell amoeboid morphological transitions. *Biochem Biophys Res Commun* **484**:255–261.

Xu Y, Harder KW, Huntington ND, Hibbs ML, and Tarlinton DM (2005) Lyn tyrosine kinase: Accentuating the positive and the negative.

Xu Y, Piston DW, and Johnson CH (1999) A bioluminescence resonance energy transfer (BRET) system: application to interacting circadian clock proteins. *Proc Natl Acad Sci U S A* **96**:151–6.

Yuan Y, Kan H, Fang Q, Chen F, and Finkel MS (2008) CXCR4 receptor antagonist blocks cardiac myocyte p38 MAP kinase phosphorylation by HIV gp120. *Cardiovasc Toxicol* **8**:173–80.

Zhao H, Guo L, Zhao H, Zhao J, Weng H, and Zhao B (2015) CXCR4 over-expression and survival in cancer: A system review and meta-analysis. *Oncotarget* **6**:5022–40.

Zheng Y, Wang Q, Li T, Qian J, Lu Y, Li Y, Bi E, Reu F, Qin Y, Drazba J, Hsi E, Yang J, Cai Z, and Yi Q (2016) Role of Myeloma-Derived MIF in Myeloma Cell Adhesion to Bone Marrow and Chemotherapy Response. *J Natl Cancer Inst* **108**:djw131.

Zhong J, Liao J, Liu X, Wang P, Liu J, Hou W, Zhu B, Yao L, Wang J, Li J, Stark JM, Xie Y, and Xu X (2011) Protein phosphatase PP6 is required for homology-directed repair of DNA double-strand breaks. *Cell Cycle* **10**:1411–1419.

Ziembik MA, Bender TP, Larner JM, and Brautigan DL (2017) Functions of protein phosphatase-6 in NF-κB signaling and in lymphocytes. *Biochem Soc Trans* **45**:693–701.

AUTHOR: Amos FUMAGALLI

TITLE: Deciphering CXCR4 and ACKR3 interactomes reveals an influence of ACKR3 upon Gap Junctional Intercellular Communication

THESES DIRECTION: Philippe MARIN and Séverine CHAUMONT-DUBEL

GENERAL PUBLIC SUMMARY: Chemokines constitute a large family of extracellular messenger molecules that govern important biological and pathological processes, such as the immune response and cancer. They act on their target cells by activating cell surface receptors that transmit the message delivered by the chemokine to the cell. Amongst these chemokine receptors we focused on ACKR3 because it is often found in various cancer types but we still do not know how it works and what happen inside the cell after its activation. In this thesis we identified Connexin 43 as a new player helping ACKR3 to exert its functions. Connexin 43 is a protein that forms channels connecting two adjacent cells and ensuring direct cell-cell communication. We discovered that ACKR3 directly inhibits cell-cell communication by reducing the number of functional channels formed by Connexin 43. This discovery improves our knowledge of the cellular effects of ACKR3 and might open new vista for the treatment of brain tumours.

RÉSUMÉ GRAND PUBLIC: Les chimiokines constituent une grande famille de messagers extracellulaires impliqués dans des processus physiologiques et pathologiques importants comme la réponse immunitaire et le cancer. Elles agissent sur leurs cellules cibles en activant des récepteurs localisés à la surface cellulaire qui transfèrent dans la cellule le message délivré par les chimiokines. Parmi les récepteurs des chimiokines, mon travail de thèse s'est focalisé sur le récepteur ACKR3 qui est surexprimé dans de nombreux cancers mais dont on connaît très mal le mécanisme d'action. J'ai montré que la connexine 43 (Cx43) était un acteur important des effets cellulaires du récepteur ACKR3. La Cx43 est une protéine constituant des canaux connectant deux cellules adjacentes et assurant ainsi une communication directe entre ces cellules. J'ai découvert que le récepteur ACKR3 inhibait cette communication directe entre les cellules en réduisant la quantité de canaux fonctionnels constitués de la Cx43. Cette découverte permet de mieux comprendre les fonctions du récepteur ACKR3 et ouvre de nouvelles perspectives thérapeutiques pour le traitement des tumeurs du cerveau.